frontiers | Research Topics

Community series in advances in pathogenesis and therapies of gout, volume II

Edited by
Jixin Zhong, Lihua Duan, Ye Yang, Xiaoxia Zhu and Yuan Liu

Published in
Frontiers in Immunology

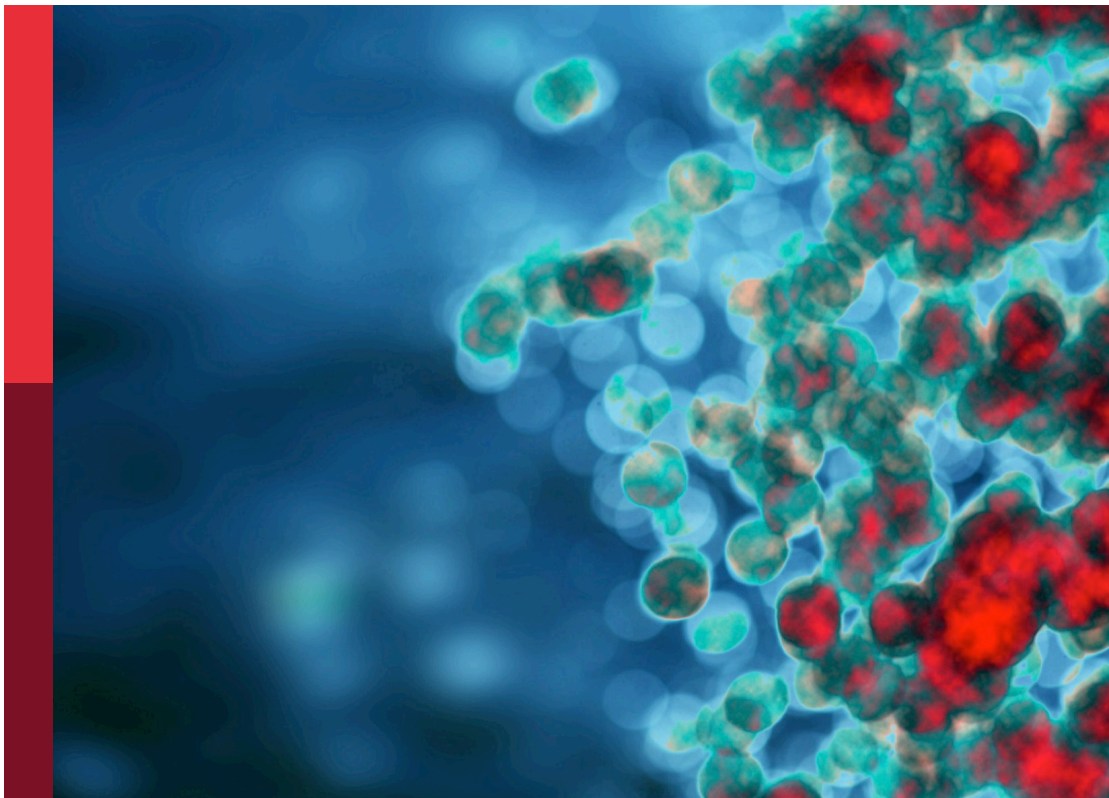

ISSN 1664-8714
ISBN 978-2-8325-6006-8
DOI 10.3389/978-2-8325-6006-8

About Frontiers

Frontiers is more than just an open access publisher of scholarly articles: it is a pioneering approach to the world of academia, radically improving the way scholarly research is managed. The grand vision of Frontiers is a world where all people have an equal opportunity to seek, share and generate knowledge. Frontiers provides immediate and permanent online open access to all its publications, but this alone is not enough to realize our grand goals.

Frontiers journal series

The Frontiers journal series is a multi-tier and interdisciplinary set of open-access, online journals, promising a paradigm shift from the current review, selection and dissemination processes in academic publishing. All Frontiers journals are driven by researchers for researchers; therefore, they constitute a service to the scholarly community. At the same time, the *Frontiers journal series* operates on a revolutionary invention, the tiered publishing system, initially addressing specific communities of scholars, and gradually climbing up to broader public understanding, thus serving the interests of the lay society, too.

Dedication to quality

Each Frontiers article is a landmark of the highest quality, thanks to genuinely collaborative interactions between authors and review editors, who include some of the world's best academicians. Research must be certified by peers before entering a stream of knowledge that may eventually reach the public - and shape society; therefore, Frontiers only applies the most rigorous and unbiased reviews. Frontiers revolutionizes research publishing by freely delivering the most outstanding research, evaluated with no bias from both the academic and social point of view. By applying the most advanced information technologies, Frontiers is catapulting scholarly publishing into a new generation.

What are Frontiers Research Topics?

Frontiers Research Topics are very popular trademarks of the *Frontiers journals series*: they are collections of at least ten articles, all centered on a particular subject. With their unique mix of varied contributions from Original Research to Review Articles, Frontiers Research Topics unify the most influential researchers, the latest key findings and historical advances in a hot research area.

Find out more on how to host your own Frontiers Research Topic or contribute to one as an author by contacting the Frontiers editorial office: frontiersin.org/about/contact

Community series in advances in pathogenesis and therapies of gout, volume II

Topic editors

Jixin Zhong — Huazhong University of Science and Technology, China
Lihua Duan — Jiangxi Provincial People's Hospital, China
Ye Yang — University of Florida, United States
Xiaoxia Zhu — Fudan University, China
Yuan Liu — First Affiliated Hospital of Xiamen University, China

Citation

Zhong, J., Duan, L., Yang, Y., Zhu, X., Liu, Y., eds. (2025). *Community series in advances in pathogenesis and therapies of gout, volume II*.
Lausanne: Frontiers Media SA. doi: 10.3389/978-2-8325-6006-8

Table of contents

frontiers | Frontiers in Immunology

TYPE Editorial
PUBLISHED 04 February 2025
DOI 10.3389/fimmu.2025.1556844

OPEN ACCESS

EDITED AND REVIEWED BY
Betty Diamond,
Feinstein Institute for Medical Research,
United States

*CORRESPONDENCE
Lihua Duan
lh-duan@163.com

RECEIVED 07 January 2025
ACCEPTED 13 January 2025
PUBLISHED 04 February 2025

CITATION
Duan L, Zhong J, Yang Y, Liu Y and Zhu X (2025) Editorial: Community series in advances in pathogenesis and therapies of gout, volume II. *Front. Immunol.* 16:1556844. doi: 10.3389/fimmu.2025.1556844

Editorial: Community series in advances in pathogenesis and therapies of gout, volume II

Lihua Duan[1]*, Jixin Zhong[2], Ye Yang[3], Yuan Liu[4] and Xiaoxia Zhu[5]

[1]Department of Rheumatology and Clinical Immunology, Jiangxi Provincial People's Hospital, The First Affiliated Hospital of Nanchang Medical College, Nanchang, China, [2]Department of Rheumatology and Immunology, Tongji Hospital, Tongji Medical College, Huazhong University of Science and Technology, Wuhan, China, [3]Department of Medicine, University of Florida, Gainesville, FL, United States, [4]Department of Rheumatology and Clinical Immunology, the First Affiliated Hospital of Xiamen University, Xiamen, China, [5]Division of Rheumatology, Huashan Hospital, Fudan University, Shanghai, China

KEYWORDS

gout, inflammasome, hyperuricemia, monosodium urate (MSU) crystal, cardiovascular disease

Editorial on the Research Topic
Community series in advances in pathogenesis and therapies of gout, volume II

Gout is a common sterile inflammatory disease caused by abnormal purine metabolism (1). Uric acid is the final product of purine metabolism in the human body. The pathogenesis of gout involves the formation and deposition of monosodium urate (MSU) crystals in tissues due to elevated serum uric acid. MSU is recognized and phagocytic by macrophages, and subsequently activates the inflammasome NOD-like receptor thermal protein domain associated protein 3 (NLRP3), produces interleukin (IL)-1β and promotes the release of other pro-inflammatory factors and the aggregation of neutrophils, thereby triggering local or even systemic inflammatory responses (2). With the improvement of living standards and the increase in purine intake, the incidence of hyperuricemia and gout is increasing annually (3). It is worth noting that hyperuricemia has become an independent risk factor for various systemic diseases, especially cardiovascular diseases and chronic kidney diseases (4, 5). To further identify new strategies for the prevention and improvement of hyperuricemia as well as gout, this Research Topic exhibits a number of original research articles on the topic of advances in diagnosis, genetic involvement, pathogenesis, and comorbidities of hyperuricemia and gout.

In this Research Topic, He et al. explored the relationship between the Oxidative Balance Score (OBS, composed of scores for 20 dietary and lifestyle factors) and hyperuricemia/gout. Among adult participants in the National Health and Nutrition Examination Survey (NHANES) spanning from 2009 to 2018, higher OBS was found to be associated with a decreased risk of developing hyperuricemia/gout, underscoring its potential in the prevention and management of these conditions. Life's Essential 8 (LE8) is a comprehensive measure of cardiovascular health promoted by the American Heart

Association, and Wang et al. suggested that higher LE8 scores are robustly associated with lower odds of hyperuricemia.

Recent reports have suggested that the intestine may play a crucial role in the excretion of uric acid outside the kidneys (6). Yang et al. performed a large Taiwanese population study to examine the risk factors for self-reported peptic ulcer disease (PUD), and found that hyperuricemia was associated with low prevalence of self-reported PUD in males, but not in females. Gouty nephropathy (GN) is a renal condition caused by precipitation of MSU in the kidney tubules (7). Li et al. introduced a new approach for the induction of GN by intrarenal injection of MSU, which may potentially serve as an experimental groundwork for future studies on the pathogenesis and prevention strategies of GN. Uric acid excretion in the intestine and kidney is closely related to the polymorphism of ABCG2 gene. Many common variants associated with gout have been reported, e.g., rs22331142 in *ABCG2* in a Taiwanese population (8). Nevertheless, Tseng et al. identified the rare variants rs559954634, rs186763678, and 13-85340782-G-A for the first time to be associated with gout in Taiwanese male, and the mechanism of these rare variants is worthy of further study.

The above-mentioned excessive intake of purine and the excretion disorder of uric acid lead to the formation of MSU, which participate in pyroptosis, to activate NLRP3 inflammasome of innate immune cells. IL-38 is a newly discovered anti-inflammatory cytokine, and a cardiovascular study highlighted that IL-38 inhibits the activation of the NLRP3 inflammasome (9). Huang et al. reported in this Research Topic that the serum levels of IL-38 were reduced in patients with gout compared to that in negative controls, suggesting that IL-38 may have immunomodulatory effects on gout inflammation and possesses clinical application value. In addition, Absent in melanoma 2 (AIM2) inflammasome stimulates apoptosis-associated speck-like protein containing a CARD (ASC) to facilitate the oligomerization and subsequent proteolytic maturation of pro-caspase-1 (10). Chu et al. investigated the action of AIM2 in the inflammatory processes of acute gouty arthritis (AGA) and asymptomatic hyperuricemia (AHU), which provide new insights into the involvement of the AIM2 mediated pyroptosis pathway in the development of AGA and strategies for treating gout.

In addition to inflammasomes, there are more biomarkers involved in the pathogenesis of gout. Using the gout-associated transcriptome dataset GSE160170, Wang et al. found that there were significant differences in the expression levels of CXCL8, CXCL1, and CXCL2 between the gouty group and the healthy group, and they also predicted 10 chemicals related to these proteins. Utilizing a high-quality, high-throughput proteomic analysis technique, Huang et al. identified differentially expressed proteins in the serum and synovial fluid of gout patients in comparison to that of healthy controls and osteoarthritis. These discoveries are potential biomarkers for diagnostic purposes and are believed to have critical roles as pathogenic factors in the pathophysiology of gout.

Overall, the original research articles in this Research Topic cover a series of important aspects in the field of potential biomarkers, influencing factors and clinical management of gout, which may provide new insights into the diagnosis and intervention of gout and hyperuricemia.

Author contributions

LD: Writing – original draft, Writing – review & editing. JZ: Writing – original draft, Writing – review & editing. YY: Writing – review & editing. XZ: Writing – original draft, Writing – review & editing. YL: Writing – review & editing.

Funding

The author(s) declare financial support was received for the research, authorship, and/or publication of this article. It was supported by National Natural Science Foundation of China (82371773, 62363028), Jiangxi Province Key Laboratory of Immunology and Inflammation (No. 2024SSY06251), Key R&D Program of Jiangxi Province, China (20232BBG70026), Jiangxi Provincial Health Technology Key Project (2024ZD003).

Conflict of interest

The authors declare that the research was conducted in the absence of any commercial or financial relationships that could be construed as a potential conflict of interest.

The author(s) declared that they were an editorial board member of Frontiers, at the time of submission. This had no impact on the peer review process and the final decision.

Publisher's note

References

1. Dalbeth N, Gosling AL, Gaffo A, Abhishek A. Gout. *Lancet*. (2021) 397:1843–55. doi: 10.1016/S0140-6736(21)00569-9

2. So AK, Martinon F. Inflammation in gout: mechanisms and therapeutic targets. *Nat Rev Rheumatol*. (2017) 13:639–47. doi: 10.1038/nrrheum.2017.155

3. Dehlin M, Jacobsson L, Roddy E. Global epidemiology of gout: prevalence, incidence, treatment patterns and risk factors. *Nat Rev Rheumatol*. (2020) 16:380–90. doi: 10.1038/s41584-020-0441-1

4. Borghi C, Agabiti-Rosei E, Johnson RJ, Kielstein JT, Lurbe E, Mancia G, et al. Hyperuricaemia and gout in cardiovascular, metabolic and kidney disease. *Eur J Intern Med*. (2020) 80:1–11. doi: 10.1016/j.ejim.2020.07.006

5. Chiu TH, Wu PY, Huang JC, Su HM, Chen SC, Chang JM, et al. hyperuricemia is associated with left ventricular dysfunction and inappropriate left ventricular mass in chronic kidney disease. *Diagnostics (Basel)*. (2020) 10:514. doi: 10.3390/diagnostics10080514

6. Yin H, Liu N, Chen J. The role of the intestine in the development of hyperuricemia. *Front Immunol*. (2022) 13:845684. doi: 10.3389/fimmu.2022.845684

7. Stamp LK, Farquhar H, Pisaniello HL, Vargas-Santos AB, Fisher M, Mount DB, et al. Management of gout in chronic kidney disease: a G-CAN Consensus Statement on the research priorities. *Nat Rev Rheumatol*. (2021) 17:633–41. doi: 10.1038/s41584-021-00657-4

8. Chen CJ, Tseng CC, Yen JH, Chang JG, Chou WC, Chu HW, et al. ABCG2 contributes to the development of gout and hyperuricemia in a genome-wide association study. *Sci Rep*. (2018) 8:3137. doi: 10.1038/s41598-018-21425-7

9. The E, de Graaf DM, Zhai Y, Yao Q, Ao L, Fullerton DA, et al. Interleukin 38 alleviates aortic valve calcification by inhibition of NLRP3. *Proc Natl Acad Sci United States Am*. (2022) 119:e2202577119. doi: 10.1073/pnas.2202577119

10. Hornung V, Ablasser A, Charrel-Dennis M, Bauernfeind F, Horvath G, Caffrey DR, et al. AIM2 recognizes cytosolic dsDNA and forms a caspase-1-activating inflammasome with ASC. *Nature*. (2009) 458:514–8. doi: 10.1038/nature07725

frontiers | Frontiers in Immunology

TYPE Original Research
PUBLISHED 15 April 2024
DOI 10.3389/fimmu.2024.1367019

OPEN ACCESS

EDITED BY
Jixin Zhong,
Huazhong University of Science and Technology, China

REVIEWED BY
Hongrui Li,
University of North Carolina at Chapel Hill, United States
Peiyan Wang,
University of Michigan, United States

*CORRESPONDENCE
Xi Yang
yangxi@sr.gxmu.edu.cn

†These authors have contributed equally to this work and share first authorship

RECEIVED 08 January 2024
ACCEPTED 28 March 2024
PUBLISHED 15 April 2024

CITATION
Wang X, Yang B, Xiong T, Qiu Y, Qin Y, Liang X, Lu D and Yang X (2024) Identification of potential biomarkers of gout through weighted gene correlation network analysis. *Front. Immunol.* 15:1367019. doi: 10.3389/fimmu.2024.1367019

Identification of potential biomarkers of gout through weighted gene correlation network analysis

Xinyi Wang[1†], Bing Yang[2†], Tian Xiong[2†], Yu Qiu[2], Yingfen Qin[1], Xinghuan Liang[1], Decheng Lu[3] and Xi Yang[2,4,5*]

[1]Department of Endocrinology, First Affiliated Hospital, Guangxi Medical University, Nanning, China, [2]Department of Geriatric Endocrinology and Metabolism, First Affiliated Hospital, Guangxi Medical University, Nanning, China, [3]Department of Endocrinology, Wuming Hospital, Guangxi Medical University, Nanning, China, [4]Guangxi Key Laboratory of Precision Medicine in Cardio-cerebrovascular Diseases Control and Prevention, Nanning, China, [5]Guangxi Clinical Research Center for Cardio-cerebrovascular Diseases, Nanning, China

Background: Although hyperuricemia is not always associated with acute gouty arthritis, uric acid is a significant risk factor for gout. Therefore, we investigated the specific mechanism of uric acid activity.

Methods: Using the gout-associated transcriptome dataset GSE160170, we conducted differential expression analysis to identify differentially expressed genes (DEGs). Moreover, we discovered highly linked gene modules using weighted gene coexpression network analysis (WGCNA) and evaluated their intersection. Subsequently, we screened for relevant biomarkers using the cytoHubba and Mcode algorithms in the STRING database, investigated their connection to immune cells and constructed a competitive endogenous RNA (ceRNA) network to identify upstream miRNAs and lncRNAs. We also collected PBMCs from acute gouty arthritis patients and healthy individuals and constructed a THP-1 cell gout inflammatory model, RT–qPCR and western blotting (WB) were used to detect the expression of C-X-C motif ligand 8 (CXCL8), C-X-C motif ligand 2 (CXCL2), and C-X-C motif ligand 1 (CXCL1). Finally, we predicted relevant drug targets through hub genes, hoping to find better treatments.

Results: According to differential expression analysis, there were 76 upregulated and 28 downregulated mRNAs in GSE160170. Additionally, WGCNA showed that the turquoise module was most strongly correlated with primary gout; 86 hub genes were eventually obtained upon intersection. IL1β, IL6, CXCL8, CXCL1, and CXCL2 are the principal hub genes of the protein–protein interaction (PPI) network. Using RT–qPCR and WB, we found that there were significant differences in the expression levels of CXCL8, CXCL1, and CXCL2 between the gouty group and the healthy group, and we also predicted 10 chemicals related to these proteins.

Conclusion: In this study, we screened and validated essential genes using a variety of bioinformatics tools to generate novel ideas for the diagnosis and treatment of gout.

KEYWORDS

gout, CXCL8, CXCL2, CXCL1, WGCNA

1 Introduction

Gout is a common type of arthritis that heals on its own. The prevalence of gout varies greatly between races and geographical areas, with rates ranging from less than 1% to 6.8% (1). The latest projections indicate that gout mortality may increase by 55% in 2060 (2), and the frequency and incidence of this disease have increased globally (3–5). Monosodium urate crystals accumulate in joints, tendons, and other tissues because of persistently high serum urate levels, which causes gout and recurrent episodes of severe, acute, painful arthritis. Gout is more common in older people than in younger people and is related to more risk factors, such as obesity, chronic kidney disease (CKD), and cardiovascular disease (CVD), all of which have a negative effect on patients (6, 7). There are four phases of gout: persistent hyperuricemia, acute inflammation generated by monosodium urate (MSU) crystal activation of immune cells, deposition of MSU crystals, and chronic gouty bone deterioration (8, 9).

MSU is an injury-related molecule whose accumulation in the joint does not always result in inflammation. Initially, MSU stimulates NF-κB via TLR4 and TLR2 and synthesizes pro-IL-1β and NLRP3. Second, MSU crystals also lead to the assembly of NLRP3 and the activation of caspase-1, the proteolytic hydrolysis of which results in the maturation of IL-1β. Ultimately, neutrophils and other cells are transported to the site of crystal deposition, and innate stimulatory immune pathways are activated when IL-1β interacts with IL-1β-interacting receptors, initiating a downstream signaling cascade that includes proinflammatory cytokines and chemokines (9, 10). A reduction in joint inflammation is an essential component of gout treatment. Oral prednisolone, nonsteroidal anti-inflammatory medications, and low-dose colchicine are the most used clinical treatments for gout flare control. However, these oral medicines have diverse modes of action and can cause side effects (10–13). As a result, biomarkers capable of guiding the prevention and treatment of acute gouty arthritis, as well as specific medications, are urgently needed.

Bioinformatics, which includes genomics, proteomics, gene regulation, biological networks, and other fields, employs computer technology to analyze and process enormous amounts of biological data to help researchers obtain a better understanding of disease mechanisms. Weighted gene coexpression network analysis (WGCNA) is a widely used bioinformatics method (14, 15) that clusters highly correlated genes into the same module to reveal functional associations between genes, reflect the biological processes or functions in which these genes are involved, and assess the correlations between gene features and clinical characteristics to discover potential biomarkers or new therapeutic targets. The AGA transcriptome dataset GSE160170 was used in our study to screen for differentially expressed genes (DEGs), and WGCNA was used to identify the most relevant modules for gout. Next, we screened for genes that overlapped between DEGs and the most relevant modules, analyzed these overlapping genes using GO and KEGG functional enrichment analyses, and constructed a protein–protein interaction (PPI) network. Finally, we identified hub genes and validated them using population blood samples and a THP-1 cell model. Using these hub genes, we investigated the connections between immune cells, generated competing endogenous RNA (ceRNA) networks, and predicted target drugs. Through the identification of biomarkers indicative of acute gouty arthritis diagnosis and treatment, we hope to identify new therapeutic options for this disease.

2 Materials and methods

2.1 Dataset collection

The NCBI-GEO database (https://www.ncbi.nlm.nih.gov/geo) is a free microarray/gene profile database. Gout-related noncoding RNAs, comprising differentially expressed lncRNAs and mRNAs, were obtained from the GEO database GSE160170. After screening the differentially expressed mRNAs using the "Limma" package in R 3.6.1, a P value< 0.05 and a |log2-fold change (FC)| >2 was used. The "ggplot2" package was used to visualize volcanic activity. The flowchart of our study design is shown in Figure 1.

2.2 Weighted gene correlation network analysis

The "WGCNA" package, a rigorous biological strategy that uncovers highly synergistic mRNAs by establishing scale-free networks and combining them with clinical data, was used to identify the most relevant gout genes.

2.3 Enrichment analysis

GO and KEGG functional enrichment analyses were subsequently used to investigate the biological activities and important pathways associated with the significant enrichment of

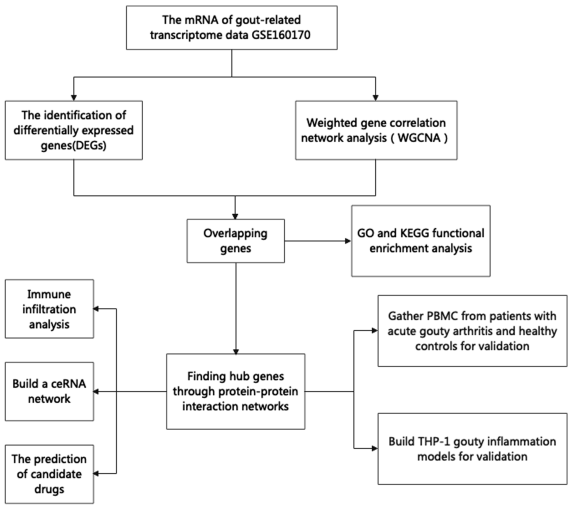

FIGURE 1
The flowchart of our research.

DEGs. Based on the "clusterProfiler" package, functional enrichment analysis was carried out, and the "ggplot2" package was used to visualize the results. The standard was established at a p value<0.05.

2.4 Protein–protein interaction (PPI) network

The STRING database (http://string.embl.de/) is a biological database used to retrieve protein interactions. PPIs of DEGs were constructed with a confidence score of ≥0.7 based on the STRING web tool. Afterward, the Mcode and cytoHubba plugins in Cytoscape 3.5.1 software were used to screen and visualize the hub genes of the PPI network.

2.5 Immune cell infiltration analysis

The "GSVA" package was used to conduct ssGSEA on the GSE160170 dataset. Three files were used for GSVA: the transcriptome matrix, the immune cell type list, and the grouping data. Grouping box plots were created to show the differences in immune cells between the two groups. Heatmap was utilized to show the link between hub genes and immune cells.

2.6 Construction of the ceRNA network

The "MultiMir" package was used to search the MIRTARBASE database for potential upstream miRNAs. Then, miRNA–lncRNA data were downloaded from the STARBASE database (STARBASEV3_HG19_CLIP-SEQ_LNCRNA_ALL) with Pancancernum>10 and Clipexpnum>5, and Cytoscape 3.5.1 software was used to visualize the ceRNA network.

2.7 Patient samples

Twelve healthy control individuals and male patients with primary gout were recruited from Guangxi Medical University's First Affiliated Hospital. Our research was approved by the First Affiliated Hospital of Guangxi Medical University's Ethics Committee[2023-E710-01]. The gout diagnosis satisfied the 2015 American College of Rheumatology/European League Against Rheumatism gout classification criteria (16). We evaluated each patient by determining their sex, age, serum urate (SUA), white blood cell count (WBC), neutrophil granulocyte counts (NEU), lymphocyte counts (LYM), monocyte counts (MONO), total cholesterol (TC), triglycerides (TG), high density lipoprotein cholesterol (HDL-C), low density lipoprotein cholesterol (LDL-C) and blood glucose (GLU) (Table 1).

2.8 THP-1 gout inflammatory model

THP-1 cells (Procell, Wuhan, China) were cultured in RPMI-1640 medium (Procell, Wuhan, China) supplemented with 10% FBS (Gibco, USA), 0.05 mM β-mercaptoethanol (Solarbio, Beijing, China), and 1% P/S (Solarbio, Beijing, China). THP-1 cells were stimulated for 24 hours to produce macrophages using 100 ng/L phenol 12-myristate 13-acetate (PMA; Sigma–Aldrich USA) (17–19).

PMA-treated THP-1 cells were stimulated with 0 μg/ml, 50 μg/ml, 100 μg/ml, or 200 μg/ml MSU crystals, and the optimal stimulation concentration was selected by CCK8 (NCM, Suzhou, China) to establish the gout inflammation model.

$$\text{Cell viability (\%)} = [A(\text{spiked}) - A(\text{blank})]/[A(0\ \text{spiked}) - A(\text{blank})] \times 100$$

2.9 RT–qPCR

All primer sequences are shown in Table 2, and GAPDH was used as an internal reference. RNA was extracted from peripheral blood mononuclear cells (PBMCs) from human blood and THP-1 cells using TRIzol reagent (Takara, Japan), and cDNA was produced by reverse transcription using HiScript®III RT SuperMix for qPCR (+gDNA wiper) (Vazyme, Nanjing, China). The target genes were amplified and detected via Stepone Plus (Thermo Fisher Scientific, USA) using ChamQ Universal SYBR qPCR Master Mix (Vazyme, Nanjing, China), and the relative mRNA expression of the hub genes was calculated via the $^{2-\Delta\Delta Ct}$ method.

2.10 Western blot

RIPA high-efficiency tissue cell lysates and 1% PMSF proteinase inhibitor (Solarbio, Beijing, China) were used to lyse the THP-1 cells. A bicinchoninic acid (BCA) kit (Beyotime, Shanghai, China) was used to measure the protein concentration. After being

TABLE 1 The clinical data of gout patients.

	HC	GA	p
Sex (F/M)	0/12	0/12	
Age (year)	44 ± 5.8	45 ± 13	0.886
SUA (μmol/L)	391 [66]	519 [121]	0.001 **
WBC ($\times10^9$/L)	6.3 [1.8]	9 [5.9]	0.024 *
NEU ($\times10^9$/L)	3.2 [0.93]	6.1 [5.2]	0.002 **
LYM ($\times10^9$/L)	2.2 ± 0.46	1.6 ± 0.77	0.0347 *
MONO ($\times10^9$/L)	0.43 [0.17]	0.91 [0.36]	0.006 **
TC (mmol/L)	5.3 ± 0.82	5.9 ± 1.3	0.18
TG (mmol/L)	1.6 [0.87]	1.7 [1]	0.603
HDL-C (mmol/L)	1 [0.25]	1.1 [0.14]	0.603
LDL-C (mmol/L)	3.2 [1]	3.9 [0.81]	0.133
GLU (mmol/L)	4.9 [0.36]	5.4 [1.9]	0.453

* P<0.05, ** P<0.01.

TABLE 2 The primer sequences of different genes.

gene name	sequence (5′-3′)
GAPDH-F	AATCAAGTGGGGCGATGCTG
GAPDH-R	GCAAATGAGCCCCAGCCTTC
CXCL8-F	ACTGAGAGTGATTGAGAGTGGAC
CXCL8-R	AACCCTCTGCACCCAGTTTTC
CXCL2-F	CTCAAGAACATCCAAAGTGTG
CXCL2-R	ATTCTTGAGTGTGGCTATGAC
CXCL1-F	GCCCAAACCGAAGTCATAGCC
CXCL1-R	ATCCGCCAGCCTCTATCACA
IL1β-F	GTTCCCTGCCCACAGACCT
IL1β-R	TGGACCAGACATCACCAAGC

separated via 15% sodium dodecyl sulfate–polyacrylamide gel electrophoresis (SDS–PAGE), the proteins were transferred to a polyvinylidene difluoride (PVDF) membrane. The PVDF membranes were blocked with 5% skim milk containing Tris-buffered saline/Tween 20 (TBST) for 1 hour before being incubated at 4°C for 18 hours with antibodies against CXCL8 (1:800; Proteintech, Wuhan, China), CXCL2 (1:800; Bioss, China), and CXCL1 (1:800; Proteintech, Wuhan, China). The membrane was incubated with secondary antibody at room temperature for one hour (anti-rabbit immunoglobulin G, 1:12,000; Absin). Enhanced chemiluminescence (ECL) (Biosharp, China) was used in an imaging device (iBright FL1000, Thermo Fisher Scientific, USA) to visualize the bands.

2.11 ELISA

Following the manufacturer's instructions, an ELISA kit (Solarbio, Beijing, China) was used to measure IL-1β secretion into the serum by THP-1 cells.

2.12 Prediction of potential drugs

With the use of the Enrichr platform (https://amp.pharm.mssm.edu/Enrichr/), we were able to access the Drug Signature Database (DSigDB), which contains a variety of publicly available drug-related gene expression data, and the candidate drugs we obtained were sorted from smallest to largest based on adjusted p values.

2.13 Statistical analysis

Ordinary one-way ANOVA was utilized for multiple group comparisons. When two groups were compared, the independent Student's t test was used for normally distributed variables, and the Mann–Whitney U test was used for nonnormal variables. The median was used to represent nonnormal distributions, and the mean ± standard deviation was used to express data that approximated a normal distribution. SPSS26 was used for all the statistical tests, and P values less than 0.05 were regarded as statistically significant. *** P<0.001, ** P<0.01, * P<0.05, ns insignificance.

3 Results

3.1 Screening and identification of DEGs

We applied the only microarray dataset for human primary gout in the GEO dataset, GSE160170 (https://www.ncbi.nlm.nih.gov/geo/query/acc.cgi?acc=GSE160170), and the GPL21827 data platform (https://www.ncbi.nlm.nih.gov/geo/query/acc.cgi?acc=GPL21827), to screen the DEGs. We then analyzed the microarray data of mRNAs using the "Limma" package, visualizing DEGs (Figure 2A) with volcano plots based on P<0.05 and |log fc|>2. Each point on the plot represents a separate gene. Red represents upregulated genes, green represents downregulated genes, and black represents nondifferentially expressed genes. The GSE160170 dataset included 28 downregulated and 76 upregulated mRNAs.

3.2 Identifying the most relevant module

Using the WGCNA algorithm, we constructed a coexpression network and modules for the GSE160170 dataset. We set the soft threshold power β to 15 (R^2 = 0.8) to construct a scale-free network (Figure 2B). Following that, a clustering dendrogram demonstrating the arrangement of the genes within the module (Figure 2C). After the acquisition of seven functional modules (Figure 2D), the turquoise module showed positive correlations between module membership and gene importance (Figure 2E) and was the most strongly connected and statistically significant module linked to primary gout (Figure 2D). Eighty-six hub genes were ultimately obtained by intersecting the turquoise module with the DEGs (Figure 2F).

3.3 GO and KEGG enrichment analyses of the hub genes

We were able to explore the main pathways enriched by the hub genes using the "clusterProfiler" package. The DEGs were divided into three categories according to their GO annotations (Figure 3A): molecular function (MF), cellular composition (CC), and biological process (BP). The top 8 pathways were chosen for further evaluation based on the number of enriched genes and P value. For the biological process (BP) category, DEGs were associated mainly with cell chemotaxis. For the cellular component (CC) category, the main pathway was on the external side of the plasma membrane. For the molecular function (MF) category, DEGs were involved mainly in receptor ligand activity and signaling receptor activator activity. KEGG

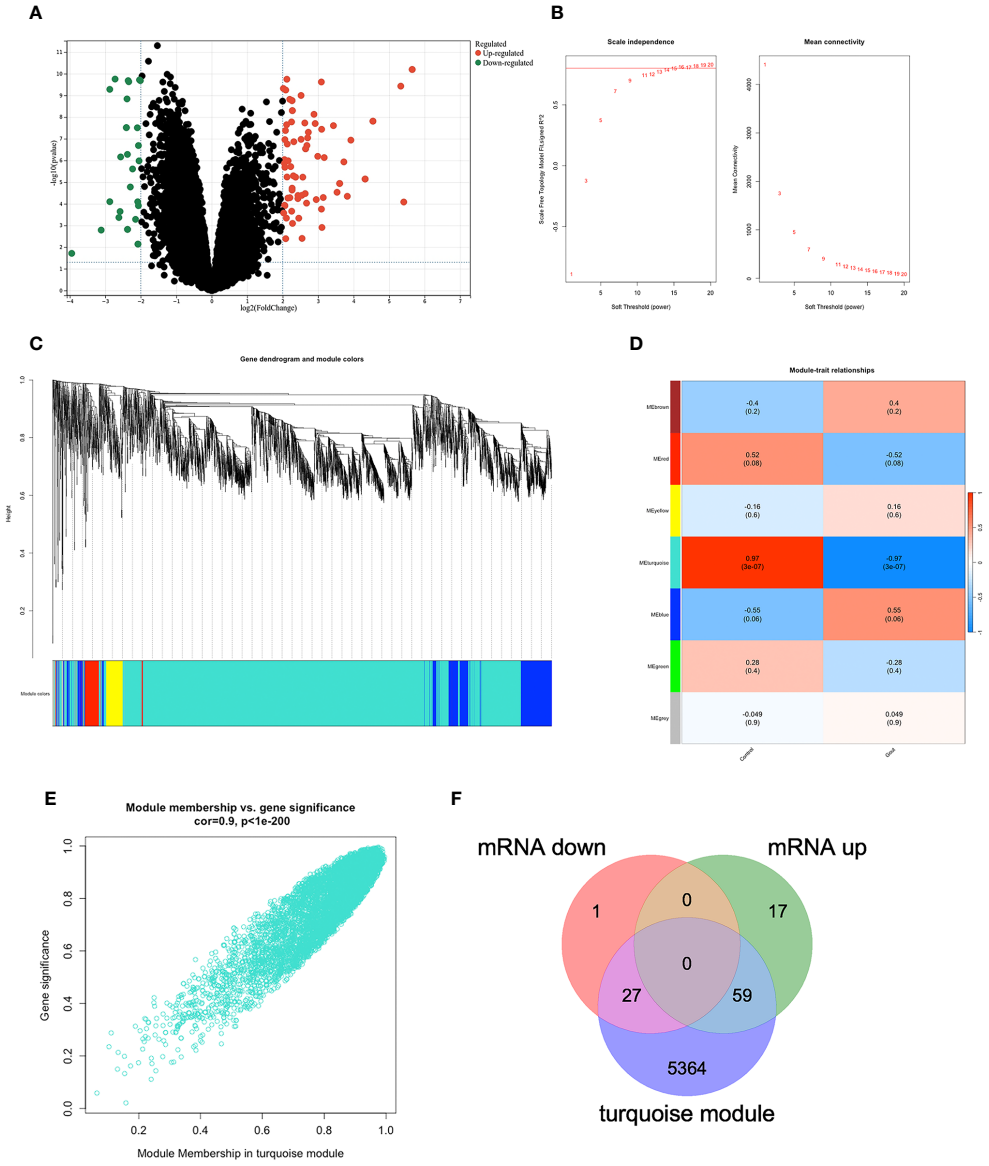

FIGURE 2
DEGs in GSE160170. **(A)**Volcano map of GSE160170, P<0.05 and |log fc|>2, with red indicating high expression, green indicating low expression, and black indicating no difference. **(B)** β=15 was selected to establish a scale-free network. **(C)** The correlations between gene module and clinical features, each module contains the corresponding correlation coefficient and p-value. Turquoise module has the highest correlation with gout. **(D)** A clustering dendrogram that illustrates how the genes are grouped within the module. **(E)** The correlation in turquoise module. **(F)** 27 mRNA were down-regulated, and 59 mRNA were up-regulated between DEGs and turquoise module.

analysis (Figure 3B) revealed that the DEGs were associated mainly with cytokine–cytokine receptor interactions.

3.4 PPI network analysis of the hub genes

To identify important key genes, we entered 86 hub genes into the STRING database (Figure 3C). The minimum required interaction score was a high confidence interval of 0.700. Eventually, we obtained a PPI network with 73 nodes and 86 edges. The average node degree was 2.36, and the average local clustering coefficient was 0.379. The PPI concentration p value was less than 1.0e-16. The results were imported into Cytoscape for network visualization and analysis via the cytoHubba_MCC algorithm (Figure 3E). We chose the 5 most highly expressed genes—CXCL8, CXCL1, CXCL2, IL1β, and IL6—for the following study. We also performed a module analysis using the Mcode plugin (Figure 3D) and ultimately discovered that these 5 key genes were found in the most crucial modules.

3.5 Immune cell infiltration analysis

We used the ssGSEA algorithm to assess the association between immune cell infiltration and patients with primary gout. The results of our study indicate that (Figure 4A) patients with

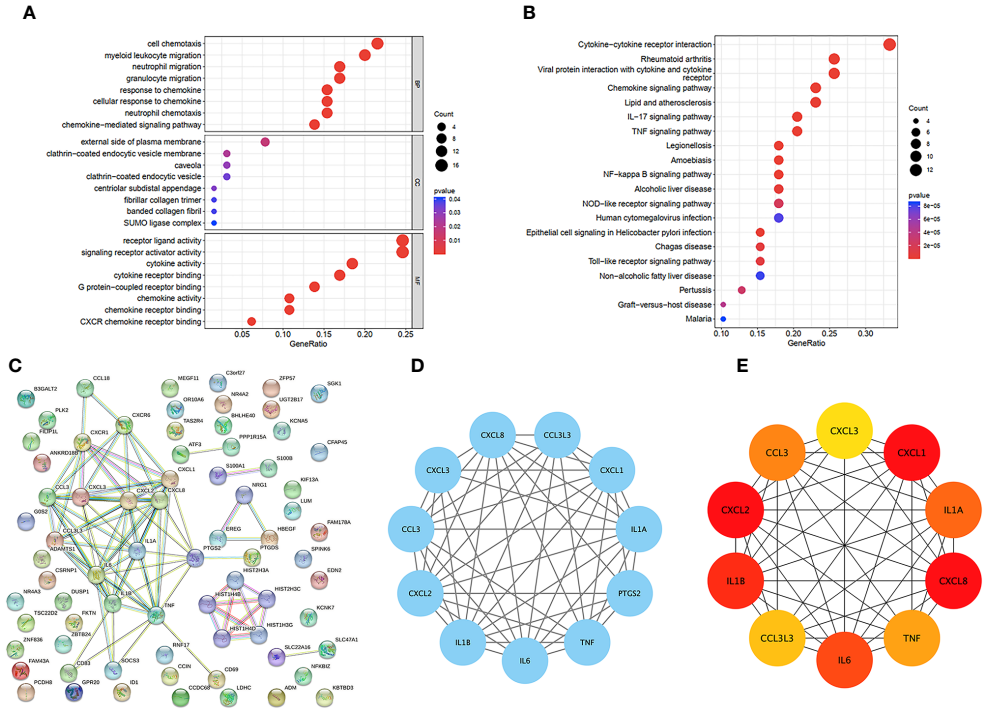

FIGURE 3
GO and KEGG functional enrichment analysis of DEGs in GSE160170. **(A)** Bubble diagram of GO enrichment in biological process terms, cellular component terms, and molecular function terms. **(B)** Bubble diagram of KEGG enriched terms. **(C)** The PPI network which contained 73 nodes and 86 edges, an average node degree of 2.36, an average local clustering coefficient of 0.379, and a PPI enrichment p-value of<1.0e-16, was visualized in STRING. **(D)** The densest connected region in the PPI network was identified using MCODE. **(E)** Top 10 genes with the highest degree values were found using CytoHubba_MCC and the depth of the color correspond to the weighted score.

primary gout exhibited greater levels of CD56dim natural killer cells, eosinophils, gamma delta T cells, immature B cells, immature dendritic cells, macrophages, mast cells, memory B cells, natural killer cells, plasmacytoid dendritic cells, regulatory T cells, T follicular helper cells and type 17 T helper cells; however, patients with primary gout also exhibited lower levels of activated CD8 T cells, CD56bright natural killer cells, central memory CD4 T cells, central memory CD8 T cells, effector memory CD4 T cells, effector memory CD8 T cells, MDSCs, monocytes, natural killer T cells, neutrophils, type 1 T helper cells, and type 2 T helper cells. We also found that (Figure 4B) these hub genes were positively correlated with immune cells such as activated CD4 T cells, immature B cells, CD56dim natural killer cells, Eosinophils and T follicular helper cells, and negatively correlated with immune cells such as effector memory CD4 T cells, monocytes, type 1 T helper cells, CD56bright natural killer cells, type 2 T helper cells, effector memory CD8 T cells, activated CD8 T cells and central memory CD4 T cells. These findings may also suggest a potential target for immunotherapy.

3.6 Construction of the ceRNA network

CeRNAs were found to be related to mRNAs, lncRNAs, and microRNAs, and we found 53 miRNAs and 18 lncRNAs that correlated with our hub genes (Figure 4C). Cytoscape was subsequently used to display the network.

3.7 Building a model of gouty inflammation

MSU crystals (0 μg/ml, 50 μg/ml, 100 μg/ml, and 200 μg/ml) were added after THP-1 cells were induced into macrophages. The CCK-8 assay results indicated that the viability of THP-1 cells decreased with increasing MSU concentration (Figure 5A), and 100 μg/ml MSU crystals were chosen for the generation of a gouty inflammation model in THP-1 cells. Compared with those in the group not treated with MSU crystals, RT–qPCR ($p=0.0001$) and ELISA ($p<0.0001$) showed that the expression of IL1β was significantly greater and that our gout inflammatory model was successfully established (Figures 5B, C).

3.8 The expression of hub genes in the population and in THP-1 cells

After PBMCs were harvested from five healthy individuals and six patients suffering from acute gouty arthritis, RT–qPCR revealed that patients with AGA expressed significantly more CXCL8 ($p = 0.0173$), CXCL2 ($p = 0.0087$), and CXCL1 ($p = 0.0303$) than healthy control individuals did (Figures 5D–F). After further validation of the expression of CXCL8, CXCL2, and CXCL1 in the THP-1 gouty inflammation model, MSU crystal stimulation was found to increase the expression of CXCL8, CXCL2, and CXCL1 compared

10.3389/fimmu.2024.1367019

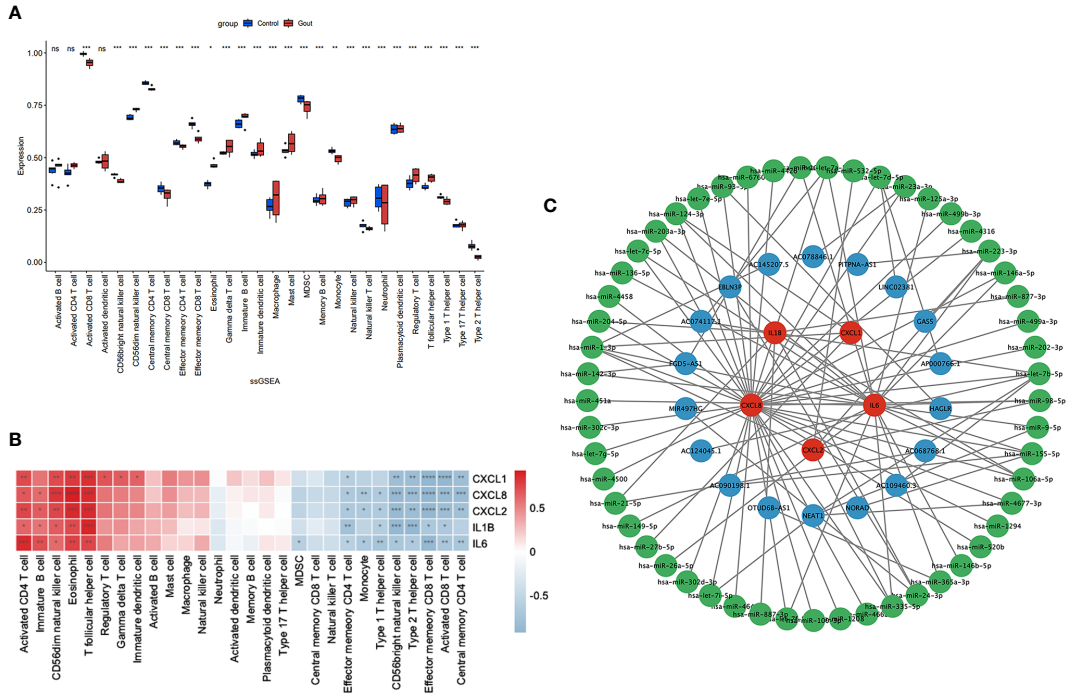

FIGURE 4
Immune infiltration analysis and CERNA networks. The distribution of 28 types of immune cells in GSE160170 are shown in the boxplot **(A)** and heatmap **(B)** show the relationship between hub genes and immune cells. **(C)** CERNA networks associated to hub genes have been built. Green denotes microRNA, blue denotes lncRNA, and red denotes mRNA. **** P < 0.0001, *** P < 0.001, ** P 0.01, * P < 0.05, ns insignificance.

to that in the group not stimulated with MSU crystals according to the RT–qPCR (Figure 5G) and WB (Figures 5H–K) results.

3.9 The prediction of candidate drugs

To anticipate potentially useful medications, we employed the Enrichr platform, which is based on the DSigDB database. The top ten candidate compounds were chosen based on their adjusted p values (Table 3).

4 Discussion

Gout is a prevalent kind of metabolic arthritis in which urate crystals accumulate in joints and nonjoint tissues. The consumption of seafood, red meats and shellfish, fructose, sugar-containing soft drinks, and alcoholic beverages, particularly beer, increases the risk of gout (1). Acute arthritis, particularly in the big toe joints, is the most common sign of gout. Patients may experience excruciating pain at night along with joint swelling, redness, and burning. Other joints, such as the knees and ankles, may also become affected as the illness progresses. The identification of effective therapies is crucial for managing and preventing gout. The transcriptome sequencing dataset GSE160170 was used for analysis, and we concentrated on mRNAs. By identifying genes with differential expression, building a WGCNA network to identify gout-related mRNAs, and inputting these overlapping mRNAs into the STRING database to construct a protein interaction network, the Mcode module analysis and the cytoHubba_MCC algorithm identified CXCL8, CXCL1, CXCL2, IL-1β, and IL6 as important biomarkers. Since IL-1β and IL6 have been linked to gout in numerous studies (20–23), our main focus was on the connection between CXCL8, CXCL1, and CXCL2 and acute gouty arthritis.

Chemokines are typically intimately linked to the migration and distribution of white blood cells within the immune system. Immune cells respond to infection or injury by releasing chemokines, which instruct other immune cells to migrate toward the site of infection or injury to carry out their defensive role. The majority of chemokines are currently categorized as inflammatory since they are essential for regulating leukocyte recruitment during the inflammatory response (24). CXCL8, also known as interleukin-8 (IL8), was the first chemokine discovered (25) and is secreted by numerous cells, including monocytes, endothelial cells, and macrophages, in response to suitable stimulation to trigger an endogenous or external inflammatory response (26). In a study by Anna Scanu et al. (27), synovial fluids were collected from a range of patients with untreated arthritis. The authors reported the highest expression of IL-1β, IL-8, and IL-6 in gouty synovial fluid. Additionally, other researchers have shown that the IL-8 rs4073 T allele is linked to a significantly greater risk of primary gouty arthritis. These findings imply that CXCL8 may be a unique biomarker for gout. Several cohort studies have shown that higher CXCL8 levels in gout patients increase the risk of CVD and type 2 diabetes (28, 29). As a result, CXCL8 might be a crucial target for the management and prevention of gout patients with diabetes

10.3389/fimmu.2024.1367019

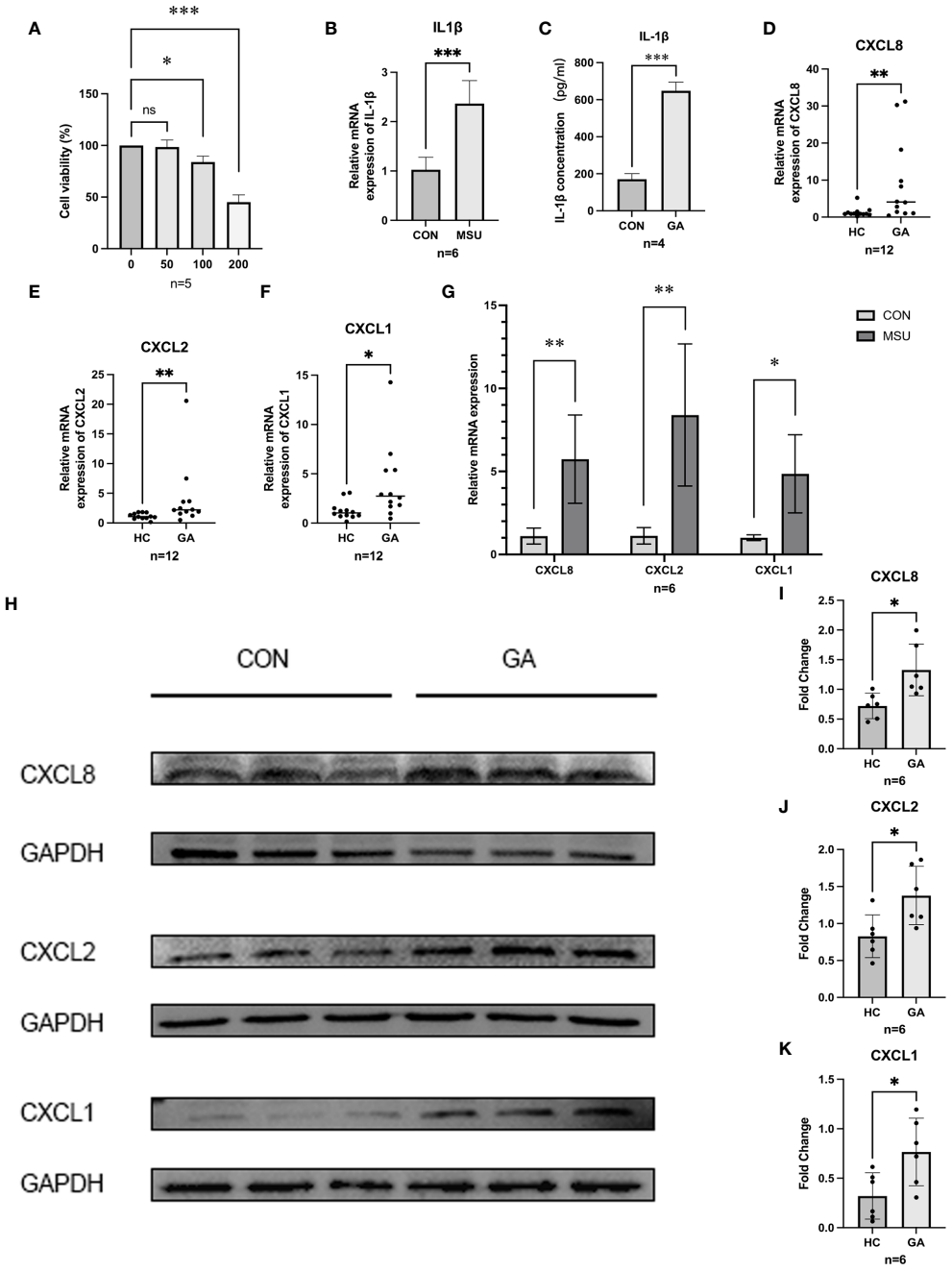

FIGURE 5
Gene expression and validation. **(A)** CCK8 was used to detect the proliferation of MSU on THP-1 cell activity. **(B,C)** ELISA and RT-qPCR were used to detect the release of IL-1β in THP-1 cells. **(D–F)** The relative mRNA expression of CXCL1, CXCL2, and CXCL8 in crowds. **(G)** The relative mRNA expression of hub genes in THP-1. **(H–K)** Protein level expression of hub genes. *** P < 0.001, ** P < 0.01, * P < 0.05, ns insignificance.

mellitus or CVD. Studies on the role of CXCL2 in gout are rare, although CXCL2 has a chemotactic effect on neutrophils during MSU crystal-induced neutrophil migration (30). CXCL1 is an essential chemokine that can be activated by activating the NF-κB signaling pathway (31). Numerous researchers were able to alleviate gout by reducing the expression of CXCL1 (32–34). Kyle Jablonski et al. reported that (35) regular, moderate physical activity prevents acute inflammation in a gout model through the downregulation of circulating neutrophils by TLR2 and the inhibition of serum CXCL1. Ouratea spectabilis, especially ouratein D, acts as an antigout drug by reducing the migration of total inflammatory cells, monocytes and neutrophils and reducing the levels of IL-1β and CXCL1 in synovial tissue (36).

THP-1 cells are human monocytes that may be induced into macrophages by PMA. PMA-treated THP-1 cells are common cellular models for investigating the mechanism of gout because they replicate the release of inflammatory cytokines by MSU-stimulated macrophages *in vitro*. We observed that the expression of CXCL8, CXCL1, and CXCL2 increased after PMA-treated THP-1 cells were exposed to MSU. These findings are consistent with the

TABLE 3 Drug prediction of the hub genes.

Term	Odds Ratio	Combined Score	P value	Adjusted P value
Profenamine PC3 UP	99640	2817407.04	5.25E-13	8.13E-10
CP-690334-01 PC3 DOWN	4994.75	131568.84	3.63E-12	2.81E-09
Muramyl Dipeptide CTD 00005307	4439.33	115109.77	5.48E-12	2.83E-09
Promethazine PC3 UP	2662	64109.21	3.47E-11	1.35E-08
CROTONALDEHYDE CTD 00000669	99080	2328114.32	6.24E-11	1.93E-08
Acetovanillone CTD 00002374	1995.5	45915.33	1.02E-10	2.63E-08
Pizotifen PC3 UP	1813.73	41080.14	1.46E-10	3.02E-08
PHENCYCLIDINE CTD 00005881	98870	2220526.04	1.76E-10	3.02E-08
Suloctidil PC3 UP	1662.25	37100.52	2.03E-10	3.02E-08
1-NITROPYRENE CTD 00001569	98830	2202286.26	2.10E-10	3.02E-08

findings in gout patients and healthy individuals, suggesting that CXCL8, CXCL1, and CXCL2 may be the keys to preventing and controlling gout. Furthermore, we discovered ten related therapeutic targets using the Enrichr platform, and a strong and statistically significant link between profenamine and hub genes was found. Profenamine, had sedative properties, is mainly used to treat Parkinson's disease (37). At present, there are few studies related to Profenamine, numerous additional tests are still required to confirm the follow-up.

Although we used multiple methods to validate the data above, there are still some limitations. Our findings could lead to the development of new approaches for the treatment of gout; however, the precise regulatory mechanisms of CXCL8, CXCL1, and CXCL2 in gout remain unclear. Additionally, the sample sizes we obtained were too small, and the pharmacological therapeutic targets we identified have not yet been verified in animal models. Furthermore, we investigated the alterations in immune cells associated with gout. The ability of the ceRNA network to predict miRNAs and lncRNAs upstream of CXCL8, CXCL1, CXCL2, IL-1β, and IL6 may lead to the use of a novel diagnostic and prognostic marker for gout. In summary, CXCL8, CXCL1, and CXCL2 may be gout biomarkers, and this research may lead to novel approaches for the clinical management of individuals with gouty arthritis.

Data availability statement

The datasets presented in this study can be found in online repositories. The names of the repository/repositories and accession number(s) can be found in the article/supplementary material.

Ethics statement

The studies involving humans were approved by the First Affiliated Hospital of Guangxi Medical University's Ethics Committee. The studies were conducted in accordance with the local legislation and institutional requirements. The ethics committee/institutional review board waived the requirement of written informed consent for participation from the participants or the participants' legal guardians/next of kin because our samples were obtained in the past clinical diagnosis and treatment.

Author contributions

XW: Conceptualization, Data curation, Methodology, Writing – original draft, Writing – review & editing. BY: Conceptualization, Investigation, Methodology, Project administration, Supervision, Writing – review & editing. TX: Data curation, Formal analysis, Investigation, Methodology, Writing – review & editing. YQ: Writing – review & editing, Data curation, Supervision, Formal analysis. YFQ: Conceptualization, Investigation, Methodology, Project administration, Resources, Supervision, Validation, Writing – review & editing. XL: Methodology, Project administration, Resources, Supervision, Validation, Visualization, Writing – review & editing. DL: Formal analysis, Methodology, Supervision, Writing – review & editing. XY: Funding acquisition, Methodology, Project administration, Resources, Supervision, Writing – review & editing.

Funding

The author(s) declare financial support was received for the research, authorship, and/or publication of this article. This work was supported by the Science and Technology Plan Project of Qingxiu District, Nanning City [grant no. 2019024] and National Natural Science Foundation of China [grant no.82360179].

Conflict of interest

The authors declare that the research was conducted in the absence of any commercial or financial relationships that could be construed as a potential conflict of interest.

Publisher's note

References

1. Dehlin M, Jacobsson L, Roddy E. Global epidemiology of gout: prevalence, incidence, treatment patterns and risk factors. *Nat Rev Rheumatol*. (2020) 16:380–90. doi: 10.1038/s41584-020-0441-1

2. Mattiuzzi C, Lippi G. Recent updates on worldwide gout epidemiology. *Clin Rheumatol*. (2020) 39:1061–3. doi: 10.1007/s10067-019-04868-9

3. Jeong YJ, Park S, Yon DK, Lee SW, Tizaoui K, Koyanagi A, et al. Global burden of gout in 1990-2019: A systematic analysis of the Global Burden of Disease study 2019. *Eur J Clin Invest*. (2023) 53:e13937. doi: 10.1111/eci.13937

4. Chen Y, Tang Z, Huang Z, Zhou W, Li Z, Li X, et al. The prevalence of gout in mainland China from 2000 to 2016: a systematic review and meta-analysis. *J Public Health*. (2017) 25:521–9. doi: 10.1007/s10389-017-0812-5

5. Elfishawi MM, Zleik N, Kvrgic Z, Michet CJ, Crowson CS, Matteson EL, et al. The rising incidence of gout and the increasing burden of comorbidities: A population-based study over 20 years. *J Rheumatol*. (2018) 45:574–9. doi: 10.3899/jrheum.170806

6. Cipolletta E, Tata LJ, Nakafero G, Avery AJ, Mamas MA, Abhishek A. Association between gout flare and subsequent cardiovascular events among patients with gout. *JAMA*. (2022) 328:440–50. doi: 10.1001/jama.2022.11390

7. Borghi C, Agabiti-Rosei E, Johnson RJ, Kielstein JT, Lurbe E, Mancia G, et al. Hyperuricaemia and gout in cardiovascular, metabolic and kidney disease. *Eur J Intern Med*. (2020) 80:1–11. doi: 10.1016/j.ejim.2020.07.006

8. Dalbeth N, Stamp L. Hyperuricaemia and gout: time for a new staging system? *Ann Rheum Dis*. (2014) 73:1598–600. doi: 10.1136/annrheumdis-2014-205304

9. Dalbeth N, Gosling AL, Gaffo A, Abhishek A. Gout. *Lancet*. (2021) 397:1843–55. doi: 10.1016/S0140-6736(21)00569-9

10. So AK, Martinon F. Inflammation in gout: mechanisms and therapeutic targets. *Nat Rev Rheumatol*. (2017) 13:639–47. doi: 10.1038/nrrheum.2017.155

11. Janssens HJEM, Janssen M, van de Lisdonk EH, van Riel PLCM, van Weel C. Use of oral prednisolone or naproxen for the treatment of gout arthritis: a double-blind, randomised equivalence trial. *Lancet*. (2008) 371:1854–60. doi: 10.1016/S0140-6736(08)60799-0

12. Parperis K. Open-label randomised pragmatic trial (CONTACT) comparing naproxen and low-dose colchicine for the treatment of gout flares in primary care. *Ann Rheum Dis*. (2021) 80:e202. doi: 10.1136/annrheumdis-2019-216643

13. Man CY, Cheung ITF, Cameron PA, Rainer TH. Comparison of oral prednisolone/paracetamol and oral indomethacin/paracetamol combination therapy in the treatment of acute goutlike arthritis: a double-blind, randomized, controlled trial. *Ann Emerg Med*. (2007) 49:670–7. doi: 10.1016/j.annemergmed.2006.11.014

14. Zhang B, Horvath S. A general framework for weighted gene co-expression network analysis. *Stat Appl Genet Mol Biol*. (2005) 4:Article17. doi: 10.2202/1544-6115.1128

15. Langfelder P, Horvath S. WGCNA: an R package for weighted correlation network analysis. *BMC Bioinf*. (2008) 9:559. doi: 10.1186/1471-2105-9-559

16. Neogi T, Jansen TLTA, Dalbeth N, Fransen J, Schumacher HR, Berendsen D, et al. 2015 Gout classification criteria: an American College of Rheumatology/European League Against Rheumatism collaborative initiative. *Ann Rheum Dis*. (2015) 74:1789–98. doi: 10.1136/annrheumdis-2015-208237

17. Yan Y, Yu L, Chen B, Cao C, Zhao H, Wang Q, et al. Mastoparan M suppressed NLRP3 inflammasome activation by inhibiting MAPK/NF-κB and oxidative stress in gouty arthritis. *J Inflamm Res*. (2023) 16:6179–93. doi: 10.2147/JIR.S434587

18. Popov D, Jain L, Alhilali M, Dalbeth N, Poulsen RC. Monosodium urate crystals alter the circadian clock in macrophages leading to loss of NLRP3 inflammasome repression: Implications for timing of the gout flare. *FASEB J*. (2023) 37:e22940. doi: 10.1096/fj.202202035R

19. Jhang J-J, Cheng Y-T, Ho C-Y, Yen G-C. Monosodium urate crystals trigger Nrf2- and heme oxygenase-1-dependent inflammation in THP-1 cells. *Cell Mol Immunol*. (2015) 12:424–34. doi: 10.1038/cmi.2014.65

20. Yu H, Xue W, Yu H, Gu H, Qin L, Peng A. Joint application of multiple inflammatory cytokines in diagnosis of gout flare. *J Inflamm Res*. (2023) 16:1771–82. doi: 10.2147/JIR.S408929

21. Jansen TL, Berendsen D, Crisan TO, Cleophas MCP, Janssen MCH, Joosten LAB. New gout test: enhanced ex vivo cytokine production from PBMCS in common gout patients and a gout patient with Kearns-Sayre syndrome. *Clin Rheumatol*. (2014) 33:1341–6. doi: 10.1007/s10067-014-2620-4

22. Bertazzo A, Punzi L, Bertazzolo N, Pianon M, Pozzuoli A, Costa CV, et al. Tryptophan catabolism in synovial fluid of various arthropathies and its relationship with inflammatory cytokines. *Adv Exp Med Biol*. (1999) 467:565–70. doi: 10.1007/978-1-4615-4709-9_70

23. Guerne PA, Terkeltaub R, Zuraw B, Lotz M. Inflammatory microcrystals stimulate interleukin-6 production and secretion by human monocytes and synoviocytes. *Arthritis Rheum*. (1989) 32:1443–52. doi: 10.1002/anr.1780321114

24. Zlotnik A, Yoshie O. The chemokine superfamily revisited. *Immunity*. (2012) 36:705–16. doi: 10.1016/j.immuni.2012.05.008

25. Zlotnik A, Yoshie O. Chemokines: a new classification system and their role in immunity. *Immunity*. (2000) 12:121–7. doi: 10.1016/s1074-7613(00)80165-x

26. Russo RC, Garcia CC, Teixeira MM, Amaral FA. The CXCL8/IL-8 chemokine family and its receptors in inflammatory diseases. *Expert Rev Clin Immunol*. (2014) 10:593–619. doi: 10.1586/1744666X.2014.894886

27. Chen C-J, Kono H, Golenbock D, Reed G, Akira S, Rock KL. Identification of a key pathway required for the sterile inflammatory response triggered by dying cells. *Nat Med*. (2007) 13:851–6. doi: 10.1038/nm1603

28. Kienhorst LBE, van Lochem E, Kievit W, Dalbeth N, Merriman ME, Phipps-Green A, et al. Gout is a chronic inflammatory disease in which high levels of interleukin-8 (CXCL8), myeloid-related protein 8/myeloid-related protein 14 complex, and an altered proteome are associated with diabetes mellitus and cardiovascular disease. *Arthritis Rheumatol*. (2015) 67:3303–13. doi: 10.1002/art.39318

29. Kienhorst L, Janssens H, Radstake T, van Riel P, Jacobs J, van Koolwijk E, et al. A pilot study of CXCL8 levels in crystal proven gout patients during allopurinol treatment and their association with cardiovascular disease. *Joint Bone Spine*. (2017) 84:709–13. doi: 10.1016/j.jbspin.2016.10.013

30. Ryckman C, McColl SR, Vandal K, de Médicis R, Lussier A, Poubelle PE, et al. Role of S100A8 and S100A9 in neutrophil recruitment in response to monosodium urate monohydrate crystals in the air-pouch model of acute gouty arthritis. *Arthritis Rheum*. (2003) 48:2310–20. doi: 10.1002/art.11079

31. Shinjo T, Onizuka S, Zaitsu Y, Ishikado A, Park K, Li Q, et al. Dysregulation of CXCL1 Expression and Neutrophil Recruitment in Insulin Resistance and Diabetes-Related Periodontitis in Male Mice. *Diabetes*. (2023) 72:986–98. doi: 10.2337/db22-1014

32. Galvão I, Vago JP, Barroso LC, Tavares LP, Queiroz-Junior CM, Costa VV, et al. Annexin A1 promotes timely resolution of inflammation in murine gout. *Eur J Immunol*. (2017) 47:585–96. doi: 10.1002/eji.201646551

33. Vieira AT, Galvão I, Amaral FA, Teixeira MM, Nicoli JR, Martins FS. Oral treatment with Bifidobacterium longum 51A reduced inflammation in a murine experimental model of gout. *Benef Microbes*. (2015) 6:799–806. doi: 10.3920/BM2015.0015

34. Batista NV, Barbagallo M, Oliveira VLS, Castro-Gomes T, Oliveira RDR, Louzada-Junior P, et al. The long pentraxin 3 contributes to joint inflammation in gout by facilitating the phagocytosis of monosodium urate crystals. *J Immunol*. (2019) 202:1807–14. doi: 10.4049/jimmunol.1701531

35. Jablonski K, Young NA, Henry C, Caution K, Kalyanasundaram A, Okafor I, et al. Physical activity prevents acute inflammation in a gout model by downregulation of TLR2 on circulating neutrophils as well as inhibition of serum CXCL1 and is associated with decreased pain and inflammation in gout patients. *PloS One*. (2020) 15:e0237520. doi: 10.1371/journal.pone.0237520

36. Rocha MP, Oliveira DP, de Oliveira VLS, Zaidan I, Grossi LC, Campana PRV, et al. Ouratea spectabilis and its Biflavanone Ouratein D Exert Potent Anti-inflammatory Activity in MSU Crystal-induced Gout in Mice. *Planta Med*. (2023) 89:718–28. doi: 10.1055/a-2009-9809

37. Goldschmidt PL, Savary L, Simon P. Comparison of the stimulatory effects of eight antiparkinsonian drugs. *Prog Neuropsychopharmacol Biol Psychiatry*. (1984) 8:257–61. doi: 10.1016/0278-5846(84)90162-3

frontiers | Frontiers in Medicine

TYPE Original Research
PUBLISHED 10 June 2024
DOI 10.3389/fmed.2024.1383290

OPEN ACCESS

EDITED BY
Lihua Duan,
Jiangxi Provincial People's Hospital, China

REVIEWED BY
Alessandro Maloberti,
University of Milano-Bicocca, Italy
Chih-Chung Shiao,
Saint Mary's Hospital Luodong, Taiwan

*CORRESPONDENCE
Szu-Chia Chen
✉ scarchenone@yahoo.com.tw
Chao-Hung Kuo
✉ kjh88kmu@gmail.com

RECEIVED 07 February 2024
ACCEPTED 29 May 2024
PUBLISHED 10 June 2024

CITATION
Yang C-S, Geng J-H, Wu P-Y, Huang J-C, Hu H-M, Chen S-C and Kuo C-H (2024) Sex difference in the associations among hyperuricemia with self-reported peptic ulcer disease in a large Taiwanese population study.
Front. Med. 11:1383290.
doi: 10.3389/fmed.2024.1383290

Sex difference in the associations among hyperuricemia with self-reported peptic ulcer disease in a large Taiwanese population study

Chi-Sheng Yang[1,2], Jiun-Hung Geng[3,4], Pei-Yu Wu[5,6,7], Jiun-Chi Huang[5,6,7], Huang-Ming Hu[2,7], Szu-Chia Chen[5,6,7]* and Chao-Hung Kuo[2,5,7]*

[1]Department of Internal Medicine, Kaohsiung Medical University Hospital, Kaohsiung Medical University, Kaohsiung, Taiwan, [2]Division of Gastroenterology, Department of Internal Medicine, Kaohsiung Medical University Hospital, Kaohsiung Medical University, Kaohsiung, Taiwan, [3]Department of Urology, Kaohsiung Municipal Siaogang Hospital, Kaohsiung Medical University Hospital, Kaohsiung Medical University, Kaohsiung, Taiwan, [4]Department of Urology, Kaohsiung Medical University Hospital, Kaohsiung Medical University, Kaohsiung, Taiwan, [5]Department of Internal Medicine, Kaohsiung Municipal Siaogang Hospital, Kaohsiung Medical University Hospital, Kaohsiung Medical University, Kaohsiung, Taiwan, [6]Division of Nephrology, Department of Internal Medicine, Kaohsiung Medical University Hospital, Kaohsiung Medical University, Kaohsiung, Taiwan, [7]Faculty of Medicine, College of Medicine, Kaohsiung Medical University, Kaohsiung, Taiwan

Background: Hyperuricemia may play a role in various systemic diseases. However, few studies have investigated the relationship between hyperuricemia and the risk of peptic ulcer disease (PUD). Therefore, in this population-based study, we enrolled over 120,000 participants from the Taiwan Biobank (TWB) and examined the risk factors for self-reported PUD. In addition, we investigated sex differences in the association between hyperuricemia and self-reported PUD.

Methods: Data of 121,583 participants were obtained from the TWB. Male participants with a serum uric acid level >7 mg/dl and female participants with a serum uric acid level >6 mg/dl were classified as having hyperuricemia. Details of self-reported PUD were obtained by questionnaire. The association between hyperuricemia and self-reported PUD in the male and female participants was examined using multivariable logistic regression analysis.

Results: The overall prevalence of self-reported PUD was 14.6%, with a higher incidence in males (16.5%) compared to females (13.5%). After multivariable adjustment, male sex [vs. female sex; odds ratio (OR) = 1.139; 95% confidence interval (CI) = 1.084–1.198; $p < 0.001$], and hyperuricemia (OR = 0.919; 95% CI = 0.879–0.961; $p < 0.001$) were significantly associated with self-reported PUD. Further, a significant interaction was found between sex and hyperuricemia on self-reported PUD ($p = 0.004$). Hyperuricemia was associated with a low risk of self-reported PUD in males (OR = 0.890; 95% CI = 0.837–0.947; $p < 0.001$) but not in females ($p = 0.139$).

Conclusion: The prevalence of self-reported PUD was higher in the male participants than in the female participants. Hyperuricemia was associated with low prevalence of self-reported PUD in males, but not in females. Further studies are needed to clarify the mechanisms behind these observations and verify the potential protective role of hyperuricemia on the development of self-reported PUD.

KEYWORDS

sex difference, hyperuricemia, self-reported peptic ulcer disease, Taiwan Biobank, Risk factors

Introduction

Peptic ulcer disease (PUD) is defined as a mucosa defect greater than 3–5 mm extending through the muscularis mucosa over the gastrointestinal tract, although it usually presents in the stomach and proximal duodenum (1). A 2020 study, which analyzed PUD burden according to the Global Burden of Disease, Injuries and Risk Factors Study, estimated that there were 8.09 million prevalent cases in 2019 globally (2). A 2004 prospective study in Taiwan of 6,457 subjects who underwent esophagogastroduodenoscopy during a health examination found that two-thirds of the patients diagnosed with PUD endoscopically were asymptomatic (3). PUD is associated with Helicobacter pylori infection (4) and the use of nonsteroidal anti-inflammatory drugs (NSAIDs) (5), and additional risk factors include advanced age, smoking, and alcoholism (6, 7). These factors may influence various aspects of gastrointestinal physiology, such as gastric acid secretion and mucosal defense mechanisms, ultimately contributing to the development of PUD (8). Sex differences have been observed in many diseases, including cancer, liver and cardiovascular diseases, and these differences can have an essential influence on the clinical presentation, disease progression, and response to treatment (9). While PUD was predominantly observed in males in the past, there has been a shift from a male-dominated pattern in Western countries to a nearly equal prevalence between males and females (10). PUD can lead to serious complications such as acute upper gastrointestinal bleeding, perforation, gastric outlet obstruction, and even mortality (11). Therefore, identifying risk factors which may be associated with PUD is important to decrease healthcare system burden and prompt the development of new treatment strategies for improving patient care.

Hyperuricemia is a chronic disease caused by high levels of uric acid due to conditions including dysfunctional purine metabolism and a reduction in the excretion of uric acid (12, 13). Purine metabolism to uric acid occurs through the catalyzation of hypoxanthine to xanthine by xanthine oxidase (14). Moreover, the reactive oxygen species generated during this process have been shown to contribute to metabolic dysfunction (14). These mechanisms imply that hyperuricemia may play a role in various systemic diseases. Associations between hyperuricemia and a higher risk of gout (15) and cardiovascular issue such as hypertension, low left ventricular ejection fraction, and high left atrial diameter have been reported (16, 17), along with dyslipidemia, thyroid dysfunction, chronic kidney disease, and metabolic syndrome (15, 16, 18, 19). However, several studies have suggested that hyperuricemia or gout might act as a protective factor against neurodegenerative diseases such as Alzheimer's disease or neurological functional outcomes after an acute ischemic stroke (20–22). Nevertheless, some studies have reported conflicting results (23), and the same debate has arisen in the context of osteoporosis and hyperuricemia. Some studies have indicated that individuals with normal or elevated levels of uric acid were associated with a decrease in bone mineral density and lower risk of bone fractures (24). Other studies have demonstrated that elevated levels of serum uric acid were linked to increased bone mass, reduced bone turnover, and a lower incidence of vertebral fractures in postmenopausal women (25). Recent studies have reported that the intestine may play a crucial role in the excretion of uric acid outside the kidneys (26). However, few studies have investigated the relationship between hyperuricemia and the risk of PUD. Therefore, in this population-based study, we enrolled over 120,000 participants from the Taiwan Biobank (TWB) and examined the risk factors for self-reported PUD. In addition, we investigated sex differences in the association between hyperuricemia and self-reported PUD.

Materials and methods

TWB

To enhance biomedical and epidemiological research and address the aging population in Taiwan, the TWB is an ongoing prospective study launched by the Ministry of Health and Welfare in 2012 of community-dwelling cancer-free women and men (27, 28). Ethical approval for the TWB was given by the Ethics and Governance Council of the TWB and Institutional Review Board on Biomedical Science Research, Academia Sinica, Taiwan.

The TWB contains medical, genomic and lifestyle factor data, including age, weight, height, and diagnoses of hypertension and diabetes mellitus (DM). In addition, laboratory tests on fasting serum samples (Roche Diagnostics GmbH, D-68298 Mannheim COBAS Integra 400) are conducted to collect data on glucose, hemoglobin, triglycerides, total cholesterol, high- and low-density lipoprotein cholesterol (HDL-C/LDL-C), and uric acid. Estimated

glomerular filtration rate (eGFR) and serum creatinine levels were calculated as reported in previous studies (29).

The average of three blood pressure measurements was used for analysis, with each measurement being performed in the absence of caffeine, nicotine and exercise by a nurse using an electronic monitor. Regular exercise was defined according to the "Physical Fitness 333 Plan" in Taiwan as at least three sessions of exercise per week with each session lasting at least 30 min (30). This study complies with the Declaration of Helsinki and was performed according to institutional review board approval (KMUHIRB-E(I)-20210058).

Sample population and sample size

The TWB enrolls cancer-free members of the community aged 30–70 years, and includes data on medical, genetic, and lifestyle factors. We collected 121,583 enrollees in the TWB. These participants were then classified into those with and without hyperuricemia based on a serum uric acid concentration of >7.0 and >6.0 mg/dl in males and females, respectively (31) (**Figure 1**).

Definitions of self-reported PUD

A history of self-reported PUD was recorded using self-reported questionnaires. The presence of self-reported PUD was defined by asking the participants whether they a history of PUD.

Statistical analysis

The statistical analyses in this study were performed using SPSS version 19.0 for Windows (IBM Inc., Armonk, NY, USA). Continuous variables were expressed as mean ± standard deviation, and between-group differences were analyzed using the independent *t*-test. Categorical variables were presented as frequencies and percentages, and between-group differences were analyzed using the Chi-square test. Associations between hyperuricemia and self-reported PUD in the male and female participants were examined using multivariable logistic regression analysis, which included significant variables in univariable analysis. An interaction *p* in logistic analysis: Model disease (y) = x1 + x2 + x1 × x2 + covariates. x1 × x2 was the interaction term, in which y = self-reported PUD; x1 = sex; x2 = hyperuricemia; covariates = age, sex, DM, hypertension, smoking and alcohol history, regular exercise habit, systolic blood pressure (SBP), body mass index (BMI), hyperuricemia, fasting glucose, hemoglobin, triglycerides, total cholesterol, LDL-cholesterol, and eGFR. A two-tailed p-value < 0.05 was considered statistically significant.

Results

Of the 121,583 participants, 43,698 were male and 77,885 were female, with a mean age of 49.9 ± 11.0 years. The overall prevalence of self-reported PUD in the study cohort was 14.6%, and the difference between the male and female participants was significant (16.5% vs. 13.5%, $p < 0.001$).

Comparison of the participants with and without self-reported PUD

Table 1 shows the comparisons of the participants with and without self-reported PUD. The participants in the self-reported PUD group were older, predominantly female, and had higher rates of DM, hypertension, smoking and alcohol consumption, regular exercise, and higher SBP, uric acid, hemoglobin, triglycerides, total cholesterol, and LDL-C, and lower BMI, eGFR and fasting glucose compared to those without self-reported PUD (**Table 1**).

Factors associated with self-reported PUD

Table 2 shows the factors associated with self-reported PUD. The results of multivariable logistic regression analysis with adjustments for the covariates listed in section "Statistical analysis" showed that older age ($p < 0.001$), male sex [vs. female sex; odds ratio (OR) = 1.139, 95% confidence interval (CI) = 1.084–1.198, $p < 0.001$], DM ($p = 0.001$), hypertension ($p < 0.001$), smoking history ($p < 0.001$), alcohol history ($p < 0.001$), without regular exercise habits ($p < 0.001$), low SBP ($p < 0.001$), low BMI ($p < 0.001$), without hyperuricemia (OR = 0.919; 95% CI = 0.879–0.961, $p < 0.001$), low fasting glucose ($p < 0.001$), and high hemoglobin ($p = 0.019$) were significantly associated with self-reported PUD (**Table 2**).

Comparisons of the male and female participants with and without self-reported PUD

Table 3 shows the comparisons of the male and female participants with and without self-reported PUD. The male participants with self-reported PUD were older and had higher rates of DM, hypertension, smoking and alcohol consumption, regular exercise, and higher HDL-C, and lower diastolic blood pressure, BMI, uric acid, hyperuricemia prevalence, hemoglobin, triglycerides, LDL-C, and eGFR than those without self-reported PUD (**Table 3**). The female participants with self-reported PUD were older and had higher prevalence rates of DM, hypertension, alcohol and smoking consumption, regular exercise, and higher SBP, uric acid, fasting glucose, hemoglobin, triglyceride, total cholesterol, and LDL-C, and lower BMI and eGFR than those without self-reported PUD (**Table 1**).

Association and interaction of hyperuricemia with self-reported PUD in the male and female participants

Table 4 shows the association and interaction of hyperuricemia with self-reported PUD in the male and female participants. The results of multivariable logistic regression analysis with adjustments for the covariates listed in section "Statistical analysis" except sex

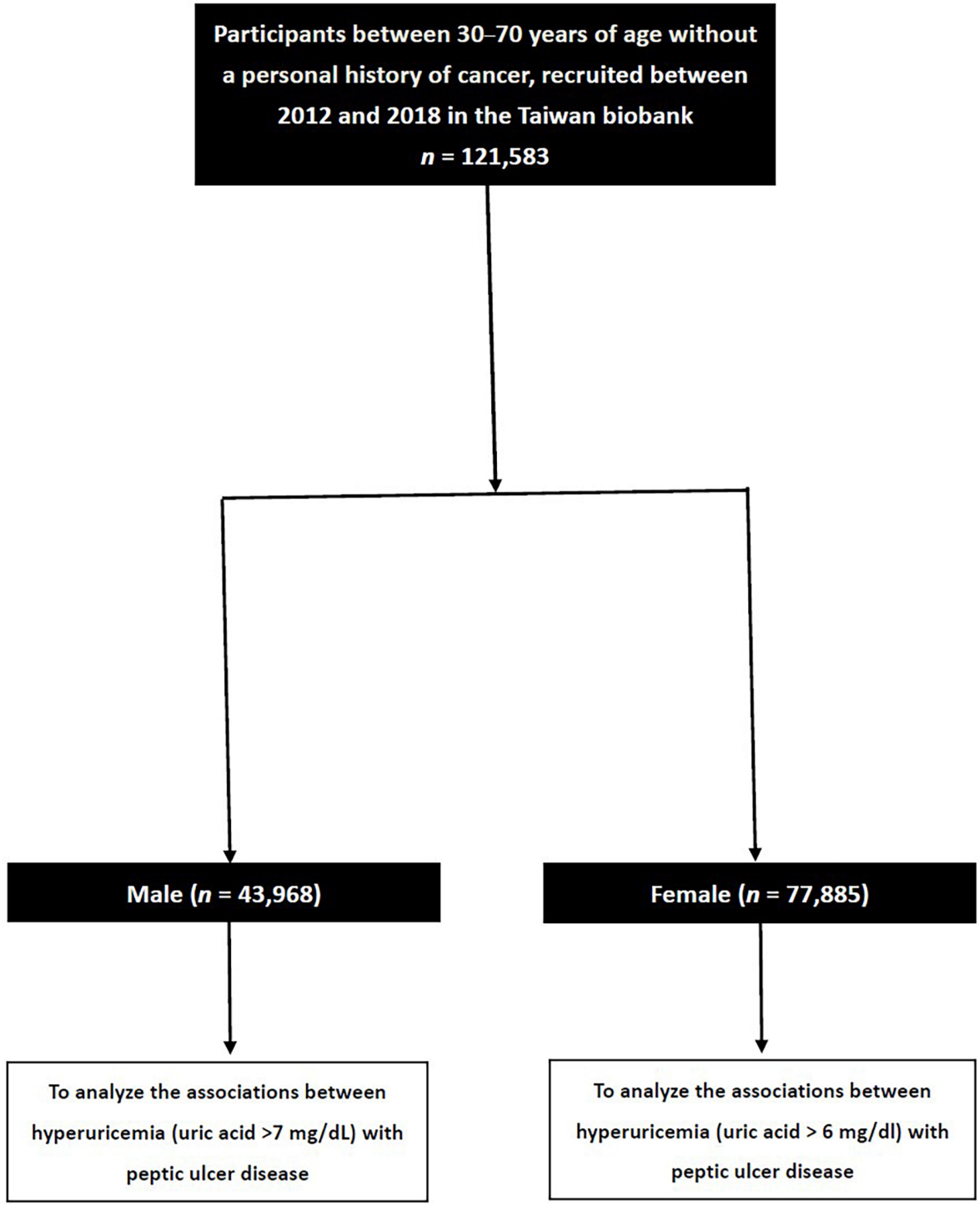

FIGURE 1
Flowchart of study population.

showed that hyperuricemia was associated with a lower risk of self-reported PUD (OR = 0.890; 95% CI = 0.837–0.947; $p < 0.001$) in the male participants, but that hyperuricemia was not associated with self-reported PUD (OR = 0.952; 95% CI = 0.893–1.016; $p = 0.139$) in the female participants. In addition, a significant interaction was found between sex and hyperuricemia on self-reported PUD ($p = 0.004$) (Table 4).

Discussion

In this large Taiwanese population-based study, we examined the risk factors for self-reported PUD and sex differences in the association between hyperuricemia and self-reported PUD. Our results showed that compared to the female participants, the male participants had a higher prevalence of self-reported PUD. Further,

TABLE 1 Clinical characteristics of the study participants classified by the presence of self-reported PUD.

Characteristics	Self-reported PUD (n = 121,583)		
	Self-reported PUD (−) (n = 103,887)	Self-reported PUD (+) (n = 17,696)	p
Age (year)	49.3 ± 11.0	53.2 ± 1.01	<0.001
Male sex (%)	35.1	40.7	<0.001
DM (%)	4.9	6.7	<0.001
Hypertension (%)	11.7	15.6	<0.001
Smoking history (%)	26.4	32.6	<0.001
Alcohol history (%)	8.2	10.3	<0.001
Regular exercise habits (%)	39.9	44.5	<0.001
Systolic BP (mmHg)	120.3 ± 18.7	121.1 ± 18.3	<0.001
Diastolic BP (mmHg)	73.8 ± 11.4	73.9 ± 11.1	0.076
BMI (kg/m^2)	24.2 ± 3.8	24.1 ± 3.7	<0.001
Laboratory parameters			
Uric acid (mg/dl)	5.42 ± 1.43	5.46 ± 1.40	<0.001
Hyperuricemia (%)	19.5%	19.0%	0.199
Fasting glucose (mg/dl)	95.8 ± 20.8	86.8 ± 19.9	<0.001
Hemoglobin (g/dl)	13.7 ± 1.6	13.9 ± 1.6	<0.001
Triglyceride (mg/dl)	115.2 ± 94.8	117.8 ± 89.0	0.001
Total cholesterol (mg/dl)	195.5 ± 35.9	196.6 ± 35.6	<0.001
HDL-C (mg/dl)	54.6 ± 13.4	54.4 ± 13.7	0.111
LDL-C (mg/dl)	120.8 ± 31.8	121.5 ± 31.6	0.007
eGFR (ml/min/1.73 m^2)	103.8 ± 23.9	100.4 ± 23.6	<0.001

Hyperuricemia was defined as serum uric acid concentration greater than 7.0 and 6.0 mg/dl in the male and female participants, respectively. PUD, peptic ulcer disease; DM, diabetes mellitus; BP, blood pressure; BMI, body mass index; HDL-C, high-density lipoprotein cholesterol; LDL-C, low-density lipoprotein cholesterol; eGFR, estimated glomerular filtration rate.

a significant interaction was found between sex and hyperuricemia on self-reported PUD, and hyperuricemia was associated with a low prevalence of self-reported PUD in the male participants, but not in the female participants.

Our finding of a higher prevalence of self-reported PUD in males compared to females (16.5% vs. 13.5%, $p < 0.001$), male sex (vs. female sex; OR = 1.139; 95% CI = 1.084–1.198; $p < 0.001$) was significantly associated with self-reported PUD, which is similar to a large-scale, multicenter trial involving over 2,000 patients taking NSAIDs (32). The trial aimed to assess the effectiveness of omeprazole compared to other agents including misoprostol and ranitidine in healing and preventing NSAID-induced ulcers, and the results showed that the incidence of these lesions tended to be higher in in men (62%) compared to women (50%) (32). In addition, duodenal ulcers were more prevalent in men (26%) than in women (8%) (32). In a population-based study involving 204 countries, males had a higher incidence and prevalence of PUD, along with higher mortality and disability-adjusted life years associated with PUD than women in all years from 1990 to 2019 (2). In 2019, there were 3.92 million prevalent cases of PUD in females compared to 4.17 million in males, and the proportion of prevalent cases between males and females was 1:0.94 (2). Possible reasons for the higher prevalence of PUD in males may involve biological and physiological differences between males and females, such as hormonal differences (i.e., the protective effects of estrogen in women) affecting the development of ulcers (33–35).

Another interesting finding is that hyperuricemia was associated with a low prevalence of self-reported PUD in the male participants (OR = 0.890; 95% CI = 0.837–0.947; $p < 0.001$). This finding provides evidence supporting the protective effect of hyperuricemia against PUD in males. Previous studies have reported a link between hyperuricemia with an increased risk of several systemic diseases, notably gout and various cardiovascular issues (such as hypertension, heart structure and function), dyslipidemia, chronic kidney disease, thyroid disorders, and metabolic syndrome (15–19). Whereas, another study discussing the relationship between uric acid and osteoporosis suggested that hyperuricemia could have a protective effect against neurodegenerative diseases and may reduce the risk of bone fractures by affecting bone mineral density (24). In the narrative review by Otani et al. (36), the authors investigate the complex role of uric acid in neurological disorders. It details how uric acid's antioxidant properties might confer neuroprotection by scavenging free radicals and inhibiting lipid peroxidation (36). Notably, the review presents evidence indicating that higher uric acid levels might be linked to a decreased risk and slower progression of Parkinson's disease (36). High uric acid levels might have contributed to the development of higher intelligence and better neurological health in humans by providing significant

TABLE 2 Determinants for self-reported PUD using multivariable logistic regression analysis.

Variables	Multivariable (self-reported PUD)	
	Odds ratio (95% CI)	*p*
Age (per 1 year)	1.038 (1.036–1.040)	<0.001
Male (vs. female)	1.139 (1.084–1.198)	<0.001
DM	1.142 (1.058–1.273)	0.001
Hypertension	1.160 (1.103–1.220)	<0.001
Smoking history	1.286 (1.232–1.342)	<0.001
Alcohol history	1.113 (1.051–1.179)	<0.001
Regular exercise habits	0.939 (0.907–0.972)	<0.001
Systolic BP (per 1 mmHg)	0.993 (0.992–0.994)	<0.001
BMI (per 1 kg/m^2)	0.982 (0.977–0.987)	<0.001
Laboratory parameters		
Hyperuricemia	0.919 (0.879–0.961)	<0.001
Fasting glucose (per 1 mg/dl)	0.998 (0.997–0.999)	<0.001
Hemoglobin (per 1 g/dl)	1.016 (1.003–1.030)	0.019
Triglyceride (per 10 mg/dl)	1.002 (1.000–1.004)	0.109
Total cholesterol (per 10 mg/dl)	0.993 (0.982–1.004)	0.191
LDL-C (per 1 mg/dl)	1.001 (1.000–1.002)	0.143
eGFR (per 1 ml/min/1.73 m^2)	0.999 (0.999–1.000)	0.099

Values expressed as odds ratio and 95% confidence interval (CI). Abbreviations are the same as in Table 1. Adjusted for age, sex, DM and hypertension, smoking and alcohol history, regular exercise habit, systolic BP, BMI, uric acid, fasting glucose, hemoglobin, triglyceride, total cholesterol, LDL-cholesterol, and eGFR. Hyperuricemia was defined as serum uric acid concentration greater than 7.0 and 6.0 mg/dl in the male and female participants, respectively.

antioxidant capacity (36, 37). In a randomized, double-blind, placebo-controlled study involving 24 participants, the effects of intravenously administered uric acid on endothelial function were explored (38). Each participant received 1,000 mg of uric acid, vitamin C, vehicle alone, or saline across separate sessions. Forearm blood flow responses to acetylcholine and sodium nitroprusside were measured using venous occlusion plethysmography. The study found that uric acid, like vitamin C, improved endothelial responses to acetylcholine in diabetics and smokers, suggesting that high levels of uric acid could have protective cardiovascular effects in conditions associated with increased oxidative stress (38). In addition, a study conducted in Taiwan of 1,166 patients hospitalized for ischemic stroke found that higher serum uric acid levels were correlated with better neurological outcomes in male patients but not in female patients, especially in those with the large-artery atherosclerosis stroke subtype (22). The study suggested that serum uric acid level might have a neuroprotective role due to its antioxidant properties, which could be particularly beneficial in the context of oxidative stress during acute ischemic stroke (22). In addition, an animal study observed a relationship between the intestinal tract in mice and uric acid (39). In that study, mice were given inosinic acid to create high and moderate levels of serum uric acid. When the mice were given indomethacin, a medication that typically causes enteropathy, those with higher uric acid levels showed less damage and reduced intestinal reactive oxygen species. The authors concluded that elevated levels of uric acid in the mice seemed to protect their intestines from damage (39). It is also mentioned that uric acid significantly influences gut microbiota composition, which plays a key role in its protective effects against enteropathy. Studies have demonstrated that mice with elevated uric acid levels exhibit richer α-diversity and distinct β-diversity in their gut microbiota compared to controls. This more diverse microbiota potentially enhances the gut's defense against pathogenic bacteria and supports intestinal integrity (39). Hyperuricemia might reduce the risk of PUD due to its strong antioxidant properties, which can mitigate oxidative stress—an underlying factor in the pathogenesis of PUD (39). Oxidative stress can damage gastric mucosal linings (39), and the antioxidant capability of uric acid may help protect against this damage. The study by Wada et al. (39) provides significant insights into the potential protective mechanisms of uric acid against indomethacin-induced enteropathy, particularly focusing on its role within the intestinal lumen. Their findings suggest that luminal uric acid may protect against gastrointestinal damage through antioxidant properties of uric acid and modulation of gut microbiota. Furthermore, the transplantation of fecal microbiota from mice with high uric acid levels into other mice ameliorated indomethacin-induced enteropathy, underscoring the significant role of microbiota in mediating uric acid's protective effects (39). These findings may partially explain our finding that hyperuricemia was associated with a low prevalence of self-reported PUD in the male participants.

We also found that hyperuricemia was associated with a low prevalence of self-reported PUD in the male participants (OR = 0.890; 95% CI = 0.837–0.947; $p < 0.001$), whereas this association was not found in the female participants ($p = 0.139$). The absence of a relationship between high uric acid levels and PUD in women might be due to sex differences in uric acid metabolism and its biological effects (40). Sex differences have been observed in many diseases, including cancer, cardiovascular and liver diseases, and these differences can have a major influence on the clinical presentation, disease progression, and response to treatment (9). The mechanism behind sex differences and sexual dimorphism is considered to be linked to sex hormones (41). Another possible reason may be that women have larger subcutaneous fat stores than men, providing better lipid storage and starvation resistance. Female mitochondria exhibit higher functional capacity and resistance to oxidative damage, reducing the transmission of metabolic disorders (42). Sex differences have also been noted in immune responses, with females exhibiting stronger T cell and humoral immune responses compared to males in adaptive immunity (43). Hormonal differences, especially the role of estrogen, may influence how uric acid affects the body (44), potentially altering the risk and severity of PUD. Moreover, women typically have lower uric acid levels than men due to hormonal regulation and renal excretion, which could account for the lack of association (45). Further research is required to delineate these mechanisms more clearly.

The key strength of this population-based investigation is that we included a large study cohort of adults living in the

TABLE 3 Clinical characteristics of the study participants classified by the presence of different sex and self-reported PUD.

Characteristics	Male (*n* = 43,698)			Female (*n* = 77,885)		
	Self-reported PUD (−) (*n* = 36,494)	Self-reported PUD (+) (*n* = 7,204)	*p*	Self-reported PUD (−) (*n* = 67,393)	Self-reported PUD (+) (*n* = 10,492)	*p*
Age (year)	49.1 ± 11.4	53.8 ± 10.2	<0.001	49.4 ± 10.8	52.7 ± 9.9	<0.001
DM (%)	6.5	8.4	<0.001	4.0	5.6	<0.001
Hypertension (%)	16.0	21.1	<0.001	9.3	11.9	<0.001
Smoking history (%)	56.3	62.8	<0.001	10.1	11.8	<0.001
Alcohol history (%)	18.2	21.4	<0.001	2.8	3.2	0.017
Regular exercise habits (%)	41.5	46.6	<0.001	39.0	43.1	<0.001
Systolic BP (mmHg)	126.3 ± 17.3	126.7 ± 17.2	0.098	117.1 ± 18.6	117.5 ± 18.1	0.017
Diastolic BP (mmHg)	78.5 ± 11.1	78.2 ± 10.7	0.024	71.2 ± 10.8	71.0 ± 10.4	0.069
BMI (kg/m^2)	25.5 ± 3.6	24.9 ± 3.5	<0.001	23.6 ± 3.8	23.5 ± 3.7	0.028
Laboratory parameters						
Uric acid (mg/dl)	6.45 ± 1.37	6.28 ± 1.35	<0.001	4.86 ± 1.12	4.90 ± 1.13	0.002
Hyperuricemia (%)	30.5	26.2	<0.001	13.5	14.2	0.051
Fasting glucose (mg/dl)	99.3 ± 23.6	99.8 ± 22.2	0.064	93.9 ± 18.9	94.8 ± 17.9	<0.001
Hemoglobin (g/dl)	15.1 ± 1.2	15.0 ± 1.3	<0.001	13.0 ± 1.3	13.1 ± 1.2	<0.001
Triglyceride (mg/dl)	138.8 ± 121.4	133.0 ± 97.7	<0.001	102.5 ± 73.6	107.3 ± 80.8	<0.001
Total cholesterol (mg/dl)	192.0 ± 35.2	191.2 ± 34.5	0.080	197.4 ± 36.1	200.2 ± 35.8	<0.001
HDL-C (mg/dl)	47.9 ± 11.1	48.5 ± 11.3	<0.001	58.2 ± 13.2	58.5 ± 13.7	0.093
LDL-C (mg/dl)	121.9 ± 31.5	120.9 ± 31.4	0.020	120.3 ± 31.9	121.9 ± 31.7	<0.001
eGFR (ml/min/1.73 m^2)	94.1 ± 19.3	92.0 ± 20.0	<0.001	109.0 ± 24.5	106.2 ± 24.1	<0.001

Abbreviations are the same as in Table 1. Hyperuricemia was defined as serum uric acid concentration greater than 7.0 and 6.0 mg/dl in the male and female participants, respectively.

TABLE 4 Association of factors with self-reported PUD in different sex using multivariable logistic regression analysis.

Characteristics	Male (*n* = 43,698)			Female (*n* = 77,885)		
	OR	95% CI	*p*	OR	95% CI	*p*
Age (per 1 year)	1.039	1.036–1.042	<0.001	1.037	1.034–1.039	<0.001
DM	1.047	0.938–1.170	0.414	1.237	1.112–1.376	<0.001
Hypertension	1.183	1.102–1.270	<0.001	1.140	1.060–1.225	<0.001
Smoking history	1.226	1.161–1.295	<0.001	1.387	1.296–1.483	<0.001
Alcohol history	1.135	1.062–1.212	<0.001	1.084	0.959–1.225	0.197
Regular exercise habits	0.928	0.879–0.980	0.008	0.949	0.907–0.992	0.022
Systolic BP (per 1 mmHg)	0.995	0.993–0.996	<0.001	0.993	0.991–0.994	<0.001
BMI (per 1 kg/m^2)	0.968	0.960–0.977	<0.001	0.990	0.984–0.997	0.004
Laboratory parameters						
Hyperuricemia (%)	0.890	0.837–0.947	<0.001	0.952	0.893–1.016	0.139
Fasting glucose (per 1 mg/dl)	0.998	0.997–0.999	0.005	0.998	0.997–0.999	0.005
Hemoglobin (per 1 g/dl)	1.007	0.984–1.029	0.565	1.026	1.008–1.044	0.004
Triglyceride (per 10 mg/dl)	1.000	0.997–1.003	0.911	1.004	1.001–1007	0.005
Total cholesterol (per 10 mg/dl)	0.995	0.976–1.014	0.624	0.995	0.981–1.008	0.432
LDL-C (per 1 mg/dl)	1.001	0.999–1.003	0.451	1.001	0.999–1.002	0.468
eGFR (per 1 ml/min/1.73 m^2)	0.999	0.998–1.001	0.435	0.999	0.998–1.000	0.123

Values expressed as odds ratio (OR) and 95% confidence interval (CI). Abbreviations are the same as in Table 1. Adjusted for age, DM and hypertension, smoking and alcohol history, regular exercise habit, systolic BP, BMI, hyperuricemia, fasting glucose, hemoglobin, triglyceride, total cholesterol, LDL-cholesterol, and eGFR. Hyperuricemia was defined as serum uric acid concentration greater than 7.0 and 6.0 mg/dl in the male and female participants, respectively.

community. Several limitations should also be mentioned. First, as this was a cross-sectional study, we were unable to evaluate the duration of illness, and consequently we were unable to evaluate causal relationships between hyperuricemia and PUD. Longitudinal studies to evaluate the risk of incident PUD are warranted. Second, the presence of PUD was assessed using self-reported questionnaires, and therefore the severity and type of PUD were unknown. Nevertheless, Wu et al. (46) reported a moderate concordance between claims records and self-reported renal diseases in Taiwan. Third, some medications may influence the value of uric acid, and result in PUD were lacking in TWB, which may influence our analysis. Finally, the Chinese ethnicity of our participants may limit the applicability of our findings to other groups.

Conclusion

In conclusion, we identified a higher prevalence of self-reported PUD in the male participants than in the female participants. Furthermore, we found a significant interaction between sex and hyperuricemia on self-reported PUD. Hyperuricemia was associated with a low prevalence of self-reported PUD in the male participants but not in the female participants in this large Taiwanese population study. Further studies are needed to clarify the mechanisms behind these observations and verify the potential protective role of hyperuricemia on the development of PUD.

Data availability statement

The raw data supporting the conclusions of this article will be made available by the authors, without undue reservation.

Ethics statement

The studies involving humans were approved by the Institutional Review Board of Kaohsiung Medical University Hospital (protocol code KMU-HIRB-E(I)-20210058 and 8 April 2021 approval). The studies were conducted in accordance with the local legislation and institutional requirements. The participants provided their written informed consent to participate in this study.

Author contributions

C-SY: Writing – original draft. J-HG: Conceptualization, Data curation, Methodology, Writing – review & editing. P-YW: Conceptualization, Data curation, Writing – review & editing. J-CH: Conceptualization, Data curation, Writing – review & editing. H-MH: Conceptualization, Data curation, Writing – review & editing. S-CC: Conceptualization, Data curation, Formal analysis, Methodology, Writing – review & editing. C-HK: Conceptualization, Data curation, Supervision, Writing – review & editing.

Funding

The author(s) declare that no financial support was received for the research, authorship, and/or publication of this article.

Conflict of interest

The authors declare that the research was conducted in the absence of any commercial or financial relationships that could be construed as a potential conflict of interest.

Publisher's note

References

1. Malik TF, Gnanapandithan K, Singh K. *Peptic ulcer disease*. Treasure Island, FL: StatPearls (2022).

2. Xie X, Ren K, Zhou Z, Dang C, Zhang H. The global, regional and national burden of peptic ulcer disease from 1990 to 2019: A population-based study. *BMC Gastroenterol.* (2022) 22:58. doi: 10.1186/s12876-022-02130-2

3. Lu CL, Chang SS, Wang SS, Chang FY, Lee SD. Silent peptic ulcer disease: Frequency, factors leading to "silence," and implications regarding the pathogenesis of visceral symptoms. *Gastrointest Endosc.* (2004) 60:34–8. doi: 10.1016/s0016-5107(04)01311-2

4. Prescrire International. *Helicobacter pylori* and gastric or duodenal ulcer. *Prescrire Int.* (2016) 25:18–23.

5. Melcarne L, Garcia-Iglesias P, Calvet X. Management of NSAID-associated peptic ulcer disease. *Expert Rev Gastroenterol Hepatol.* (2016) 10:723–33.

6. Lau JY, Sung J, Hill C, Henderson C, Howden CW, Metz DC. Systematic review of the epidemiology of complicated peptic ulcer disease: Incidence, recurrence, risk factors and mortality. *Digestion.* (2011) 84:102–13.

7. Lee SP, Sung IK, Kim JH, Lee SY, Park HS, Shim CS. Risk factors for the presence of symptoms in peptic ulcer disease. *Clin Endosc.* (2017) 50:578–84.

8. Hooi JKY, Lai WY, Ng WK, Suen MMY, Underwood FE, Tanyingoh D, et al. Global prevalence of *Helicobacter pylori* infection: Systematic review and meta-analysis. *Gastroenterology.* (2017) 153:420–9.

9. Mauvais-Jarvis F, Bairey Merz N, Barnes PJ, Brinton RD, Carrero JJ, DeMeo DL, et al. Sex and gender: Modifiers of health, disease, and medicine. *Lancet.* (2020) 396:565–82.

10. Lin KJ, Garcia Rodriguez LA, Hernandez-Diaz S. Systematic review of peptic ulcer disease incidence rates: Do studies without validation provide reliable estimates? *Pharmacoepidemiol Drug Saf.* (2011) 20:718–28. doi: 10.1002/pds.2153

11. Chmiela M, Kupcinskas J. Review: Pathogenesis of *Helicobacter pylori* infection. *Helicobacter.* (2019) 24:e12638.

12. Benn CL, Dua P, Gurrell R, Loudon P, Pike A, Storer RI, et al. Physiology of hyperuricemia and urate-lowering treatments. *Front Med (Lausanne).* (2018) 5:160. doi: 10.3389/fmed.2018.00160

13. Si K, Wei C, Xu L, Zhou Y, Lv W, Dong B, et al. Hyperuricemia and the risk of heart failure: Pathophysiology and therapeutic implications. *Front Endocrinol (Lausanne).* (2021) 12:770815. doi: 10.3389/fendo.2021.770815

14. Kanellis J, Feig DI, Johnson RJ. Does asymptomatic hyperuricaemia contribute to the development of renal and cardiovascular disease? An old controversy renewed. *Nephrology (Carlton).* (2004) 9:394–9. doi: 10.1111/j.1440-1797.2004.00336.x

15. Yu KH, Chen DY, Chen JH, Chen SY, Chen SM, Cheng TT, et al. Management of gout and hyperuricemia: Multidisciplinary consensus in Taiwan. *Int J Rheum Dis.* (2018) 21:772–87. doi: 10.1111/1756-185X.13266

16. Chiu TH, Wu PY, Huang JC, Su HM, Chen SC, Chang JM, et al. hyperuricemia is associated with left ventricular dysfunction and inappropriate left ventricular mass in chronic kidney disease. *Diagnostics (Basel).* (2020) 10:514. doi: 10.3390/diagnostics10080514

17. Maloberti A, Mengozzi A, Russo E, Cicero AFG, Angeli F, Agabiti Rosei E, et al. Cardiovascular risk of the italian society of, the results of the urrah (uric acid right for heart health) project: A focus on hyperuricemia in relation to cardiovascular and kidney disease and its role in metabolic dysregulation. *High Blood Press Cardiovasc Prev.* (2023) 30:411–25. doi: 10.1007/s40292-023-00602-4

18. Wei CY, Sun CC, Wei JC, Tai HC, Sun CA, Chung CF, et al. Association between hyperuricemia and metabolic syndrome: An epidemiological study of a labor force population in Taiwan. *Biomed Res Int.* (2015) 2015:369179. doi: 10.1155/2015/369179

19. Segura J, Campo C, Ruilope L. How relevant and frequent is the presence of mild renal insufficiency in essential hypertension? *J Clin Hypertens.* (2002) 4:332–6. doi: 10.1111/j.1524-6175.2002.01003.x

20. Latourte A, Dumurgier J, Paquet C, Richette P. Hyperuricemia, gout, and the brain-an update. *Curr Rheumatol Rep.* (2021) 23:82. doi: 10.1007/s11926-021-01050-6

21. Wang L, Tan Z, Wang FY, Wu WP, Wu JC. Gout/hyperuricemia reduces the risk of Alzheimer's disease: A meta-analysis based on latest evidence. *Brain Behav.* (2023) 13:e3207.

22. Wang YF, Li JX, Sun XS, Lai R, Sheng WL. High serum uric acid levels are a protective factor against unfavourable neurological functional outcome in patients with ischaemic stroke. *J Int Med Res.* (2018) 46:1826–38. doi: 10.1177/0300060517752996

23. Tang X, Song ZH, Cardoso MA, Zhou JB, Simo R. The relationship between uric acid and brain health from observational studies. *Metab Brain Dis.* (2022) 37:1989–2003. doi: 10.1007/s11011-022-01016-2

24. Lin KM, Lu CL, Hung KC, Wu PC, Pan CF, Wu CJ, et al. The paradoxical role of uric acid in osteoporosis. *Nutrients.* (2019) 11:2111.

25. Ahn SH, Lee SH, Kim BJ, Lim KH, Bae SJ, Kim EH, et al. Higher serum uric acid is associated with higher bone mass, lower bone turnover, and lower prevalence of vertebral fracture in healthy postmenopausal women. *Osteoporos Int.* (2013) 24:2961–70. doi: 10.1007/s00198-013-2377-7

26. Yin H, Liu N, Chen J. The role of the intestine in the development of hyperuricemia. *Front Immunol.* (2022) 13:845684. doi: 10.3389/fimmu.2022.845684

27. Chen CH, Yang JH, Chiang CWK, Hsiung CN, Wu PE, Chang LC, et al. Population structure of Han Chinese in the modern Taiwanese population based on 10,000 participants in the Taiwan Biobank project. *Hum Mol Genet.* (2016) 25:5321–31. doi: 10.1093/hmg/ddw346

28. Fan CT, Hung TH, Yeh CK. Taiwan regulation of biobanks. *J Law Med Ethics.* (2015) 43:816–26.

29. Vickery S, Stevens PE, Dalton RN, van Lente F, Lamb EJ. Does the ID-MS traceable MDRD equation work and is it suitable for use with compensated Jaffe and enzymatic creatinine assays? *Nephrol Dial Transplant.* (2006) 21:2439–45. doi: 10.1093/ndt/gfl249

30. Ministry of Education. *Physical fitness 333 plan*. Taipei: Ministry of Education (1999).

31. Lee JW, Kwon BC, Choi HG. Analyses of the relationship between hyperuricemia and osteoporosis. *Sci Rep*. (2021) 11:12080.

32. Hawkey CJ, Wilson I, Naesdal J, Langstrom G, Swannell AJ, Yeomans ND. Influence of sex and *Helicobacter pylori* on development and healing of gastroduodenal lesions in non-steroidal anti-inflammatory drug users. *Gut.* (2002) 51:344–50. doi: 10.1136/gut.51.3.344

33. Truelove SC. Stilboestrol, phenobarbitone, and diet in chronic duodenal ulcer. A factorial therapeutic trial. *Br Med J.* (1960) 2:559–66. doi: 10.1136/bmj.2.5198.559

34. Shorrock CJ, Langman MJ. Nonsteroidal anti-inflammatory drug-induced gastric damage: Epidemiology. *Dig Dis.* (1995) 13:3–8.

35. Kurata JH, Haile BM, Elashoff JD. Sex differences in peptic ulcer disease. *Gastroenterology.* (1985) 88:96–100.

36. Otani N, Hoshiyama E, Ouchi M, Takekawa H, Suzuki K. Uric acid and neurological disease: A narrative review. *Front Neurol.* (2023) 14:1164756. doi: 10.3389/fneur.2023.1164756

37. Alvarez-Lario B, Macarron-Vicente J. Uric acid and evolution. *Rheumatology.* (2010) 49:2010–5.

38. Waring WS, McKnight JA, Webb DJ, Maxwell SR. Uric acid restores endothelial function in patients with type 1 diabetes and regular smokers. *Diabetes.* (2006) 55:3127–32. doi: 10.2337/db06-0283

39. Wada A, Higashiyama M, Kurihara C, Ito S, Tanemoto R, Mizoguchi A, et al. Protective effect of luminal uric acid against indomethacin-induced enteropathy: role of antioxidant effect and gut microbiota. *Dig Dis Sci.* (2022) 67:121–33. doi: 10.1007/s10620-021-06848-z

40. Qian T, Sun H, Xu Q, Hou X, Hu W, Zhang G, et al. Hyperuricemia is independently associated with hypertension in men under 60 years in a general Chinese population. *J Hum Hypertens.* (2021) 35:1020–8. doi: 10.1038/s41371-020-00455-7

41. Mittendorfer B. Insulin resistance: Sex matters. *Curr Opin Clin Nutr Metab Care.* (2005) 8:367–72.

42. Mauvais-Jarvis F. Sex differences in energy metabolism: Natural selection, mechanisms and consequences. *Nat Rev Nephrol.* (2024) 20:56–69.

43. Klein SL, Flanagan KL. Sex differences in immune responses. *Nat Rev Immunol.* (2016) 16:626–38.

44. Eun Y, Kim IY, Han K, Lee KN, Lee DY, Shin DW, et al. Association between female reproductive factors and gout: A nationwide population-based cohort study of 1 million postmenopausal women. *Arthritis Res Ther.* (2021) 23:304. doi: 10.1186/s13075-021-02701-w

45. Anton FM, Garcia Puig J, Ramos T, Gonzalez P, Ordas J. Sex differences in uric acid metabolism in adults: Evidence for a lack of influence of estradiol-17 beta (E2) on the renal handling of urate. *Metabolism.* (1986) 35:343–8. doi: 10.1016/0026-0495(86)90152-6

46. Wu CS, Lai MS, Gau SS, Wang SC, Tsai HJ. Concordance between patient self-reports and claims data on clinical diagnoses, medication use, and health system utilization in Taiwan. *PLoS One.* (2014) 9:e112257. doi: 10.1371/journal.pone.0112257

frontiers | Frontiers in Endocrinology

TYPE Original Research
PUBLISHED 01 July 2024
DOI 10.3389/fendo.2024.1416996

OPEN ACCESS

EDITED BY
Lihua Duan,
Jiangxi Provincial People's Hospital, China

REVIEWED BY
Asim Kumar Mandal,
Brigham and Women's Hospital and Harvard Medical School, United States
Jie Lu,
The Affiliated Hospital of Qingdao University, China

*CORRESPONDENCE
Chuang Li
lichuang@gzucm.edu.cn
Wei Mao
maowei@gzucm.edu.cn

†These authors have contributed equally to this work

RECEIVED 13 April 2024
ACCEPTED 10 June 2024
PUBLISHED 01 July 2024

CITATION
Li D, Li Y, Chen X, Ouyang J, Lin D, Wu Q, Fu X, Quan H, Wang X, Wu S, Yuan S, Liu A, Zhao J, Liu X, Zhu G, Li C and Mao W (2024) The pathogenic mechanism of monosodium urate crystal-induced kidney injury in a rat model.
Front. Endocrinol. 15:1416996.
doi: 10.3389/fendo.2024.1416996

The pathogenic mechanism of monosodium urate crystal-induced kidney injury in a rat model

Delun Li[1,2,3,4†], Yimeng Li[1,2,3,4†], Xuesheng Chen[1,2,3,4], Jianting Ouyang[1,2,3,4], Danyao Lin[1,2,3,4], Qiaoru Wu[1,2,3,4], Xinwen Fu[1,2,3,4], Haohao Quan[1,2,3,4], Xiaowan Wang[1,2,3,4], Shouhai Wu[1,2,3,4], Siyu Yuan[5,6,7], Anqi Liu[8], Jiaxiong Zhao[1,2], Xiaowu Liu[1,2], Gangxing Zhu[1,2], Chuang Li[1,2,3,4*] and Wei Mao[1,2,3,4*]

[1]State Key Laboratory of Dampness Syndrome of Chinese Medicine, The Second Affiliated Hospital of Guangzhou University of Chinese Medicine, The Second Clinical College of Guangzhou University of Chinese Medicine, Guangzhou, China, [2]Department of Nephrology, The Second Affiliated Hospital of Guangzhou University of ChineseMedicine (Guangdong Provincial Hospital of Chinese Medicine), Guangzhou, China, [3]State Key Laboratory of Dampness Syndrome of Chinese Medicine, The Second Affiliated Hospital of Guangzhou University of Chinese Medicine, Guangzhou, China, [4]Nephrology Institute of Guangdong Provincial Academy of Chinese Medical Sciences (NIGH-CM), Guangzhou, China, [5]Ministry of Education Key Laboratory of Pharmacology of Traditional Chinese Medical Formulae, Tianjin University of Traditional Chinese Medicine, Tianjin, China, [6]School of Chinese Materia Medica, Tianjin University of Traditional Chinese Medicine, Tianjin, China, [7]State Key Laboratory of Component-based Chinese Medicine, Tianjin University of Traditional Chinese Medicine, Tianjin, China, [8]Cadre Department, Guizhou Provincial People's Hospital, Guizhou, China

Objective: (MSU) crystals usually in the kidney tubules especially collecting ducts in the medulla. Previous animal models have not fully reproduced the impact of MSU on kidneys under non-hyperuricemic conditions.

Methods: In the group treated with MSU, the upper pole of the rat kidney was injected intrarenally with 50 mg/kg of MSU, while the lower pole was injected with an equivalent volume of PBS solution. The body weight and kidney mass of the rats were observed and counted. H&E staining was used to observe the pathological damage of the kidney and to count the number of inflammatory cells. Masoon staining was used to observe the interstitial fibrosis in the kidneys of the rat model. Flow cytometric analysis was used for counting inflammatory cells in rats. ElISA was used to measure the concentration of serum and urine uric acid, creatinine and urea nitrogen in rats.

Results: At the MSU injection site, a significantly higher infiltration of inflammatory cells and a substantial increase in the area of interstitial fibrosis compared to the control group and the site of PBS injection were observed. The serum creatinine level was significantly increased in the MSU group. However, there were no significant differences in the rats' general conditions or blood inflammatory cell counts when compared to the control group.

Conclusion: The injection of urate crystals into the kidney compromised renal function, caused local pathological damage, and increased inflammatory cell infiltration and interstitial fibrosis. Intrarenal injection of MSU crystals may result in urate nephropathy. The method of intrarenal injection did not induce surgical infection or systemic inflammatory response.

KEYWORDS

MSU crystal, uric acid, gouty nephropathy, hyperuricemic nephropathy, model

Introduction

Gouty nephropathy (GN) is a renal condition caused by precipitation of monosodium urate (MSU) crystals in the kidney tubules especially collecting ducts in the medulla (1). Hyperuricemia is prevalent in China, with a notable prevalence of 13.3% (2). The persistent presence of supersaturated level of uric acid (UA) in biological fluids causes the formation of MSU crystals in the kidneys. A subnormal pH also promotes precipitation of MSU crystals as the first pKa value of uric acid is about 5.6 (3, 4). Mechanistically, following phagocytosis, intracellular MSU crystals via activation of the NLRP3 inflammasome complex in monocytes/macrophages stimulates the secretion of IL-1β, IL-18 etc. into the extracellular space that cause recruitment of leucocytes from the bloodstream into the inflamed site of the tissue (3, 5, 6). MSU crystals were also shown to directly activate neutrophils (7).

Generally, it was believed that asymptomatic hyperuricemia is less likely to cause kidney injury. However, recent research indicates that asymptomatic hyperuricemia can actually induce inflammation and consequently lead to kidney injury (7, 8). This new finding suggests that animal models previously used for understanding the cause of GN were likely simulating hyperuricemic nephropathy (HN) instead of GN. The majority of these prior models employed various methodologies to elevate blood uric acid levels, such as raising blood uric acid, by inhibiting uric acid excretion (9), and inhibiting hepatic uricase that converts uric acid into more soluble allantoin (10). Rat models elicited by these methods were primarily used to simulate renal injuries caused by hyperuricemia. Although lengthening the modeling period may result in MSU deposition in the kidneys, which could cause injury, it is unclear whether the causal factors are hyperuricemia, MSU, or a combination of both. Therefore, in these models, it is impossible to know the impact of only deposited MSU on kidneys under the condition of normal blood urate level.

In this study, we have introduced a new approach that involves the intrarenal injection of MSU to induce GN. The aim is to elucidate the pathological impact of MSU on the kidney. This approach could potentially serve as an experimental groundwork for future research on the pathogenesis and prevention strategies of GN.

Materials and methods

Animals

The use of animals in this study was approved by the Animal Policy and Welfare Committee of Guangdong Academy of Chinese Medicine (Approval Document No. 2022051) and all animal experiments were conducted in accordance with the guidelines of the National Institutes of Health (NIH). The experiments were also performed in accordance with NIH guidelines. Male SD (Sprague Dawley rat) rats were purchased from Charles River and placed in an SPF(Specific-pathogen-free)-grade environment (SPF) with a relative humidity of 40% to 70%, an ambient temperature of 20–25° C, and a photoperiod of 12/12 h.

Experimental grouping

After one week of acclimatization, the rats were randomly divided into a control group, a GN group (MSU group), a HN group(UA group), and a Joint GN and HN modelling group (UA +MSU group). Each group was further divided into two observation time points, at the third and fourth weeks, respectively. Each group consisted of eight rats. GN was induced in the rats by injecting urate crystals into their kidneys. HN was induced by intragastric administration 750 mg/kg potassium oxonate (PO; a competitive inhibitor of uricase) (Cat # 2207–75-2, Sigma-Aldrich) and 300 mg/kg uric acid (Cat # A8626 Sigma-Aldrich). For combined GN and HN model group MSU crystals were injected into kidneys the day before gavage of a mixture of PO and uric acid. The administrationof PO and uric acic was continued for 3 or 4 weeks (Figure 1A). To anesthetize the rats, chloral hydrate (350 mg/kg, i.p) was administered intraperitoneally. The hair on the rats' backs below the sternum was removed and disinfected with iodophor. The rats were considered suitably anesthetized when they exhibited general weakness or responses. The rats were positioned supine on a sterile operating table. The epidermis and muscle layers were incised using surgical scissors, and the abdomen was gently compressed to extrude the kidney from the abdominal cavity through the dorsal surgical opening. The MSU crystals were

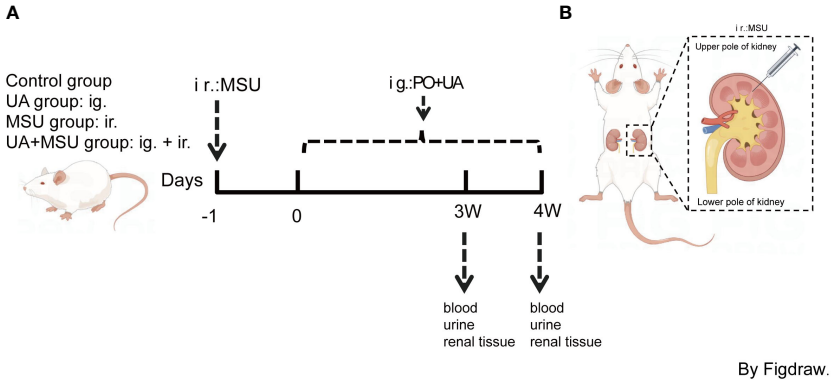

FIGURE 1
Flowchart of strategic study design in animal model (rat). **(A)** Control, uric acid (UA), MSU and UA+MSU groups: For the UA group, the 8-week-old male rats were gavaged (intragastric; ig) with 750 mg/kg potassium oxonate (PO) and 300 mg/kg uric acid once daily. For the MSU group, the suspension of MSU crystals (10 mg/100 µl/kidney) was injected (intrarenal; ir) with an injection needle into the renal cortico-medullary junction at the upper pole of the kidneys of the 8-week-old male rats. An equal volume (100 µl) of PBS (pH 7.4) was injected into the lower pole of the kidney for site-specific control of the MSU-injected kidney. For the UA+MSU group, the suspension of MSU crystals (10 mg/100 µl/kidney) was injected (ir) into the renal cortico-medullary junction at the upper pole of the kidneys of the 8-week-old male rats that were gavaged (ig) with PO + UA as described above on the first day after the MSU injection. An equal volume (100 µl) of PBS (pH 7.4) was injected into the lower pole of the kidney for site-specific control for UA+MSU effect. Urine samples, blood samples and kidney tissues were collected three or four weeks (3W/4W) after injection. **(B)** MSU suspension was injected into the upper pole of the kidney as shown in the figure. MSU, monosodium urate crystal.

administered with an injection needle at the renal cortico-medullary junction at the upper pole (suprarenal pole) of the rat kidney, approximately 1.3–2/3 of the width of the rat kidney (i.e. 5–10 mm). The injection volume was 100 µl (0.1 mg/µl) per kidney, and the needle was removed after the injection. An equal volume of Phosphate buffered saline (PBS) (AR0032, Bosterbio Biotechnologies) was injected into the lower pole (infrarenal pole) of the kidney. The kidneys were replaced in the abdominal cavity and replenished with 1 ml of saline. Finally, the muscle and epidermal layers of the rats were closed using sutures. After suturing, the wounds were cleaned with saline cotton pads to remove any blood. The rats were then placed on a heating plate and returned to their cage once they had awoken. The rat model of GN induced by MSU was successfully obtained.

Preparation of MSU crystals for injection

Uric acid was dissolved in pure water with the help of 3M NaOH added dropwise until complete dissolution. The pH was adjusted to 8.9 using NaOH and glacial acetic acid. The uric acid was then left to crystallize for 2 days at room temperature. The crystals were collected on filter paper, washed 3 times with 70% ethanol, allowing to dry at 37–45°C. MSU crystals were collected in centrifuge tubes and autoclaved at 120°C and 15 psi for about 30 min. A sterile PBS solution was used to prepare the MSU crystal suspension.

H&E staining

The kidneys were fixed in a 4% paraformaldehyde solution and trimmed to a suitable shape using a scalpel. Subsequently, the tissue was dehydrated using alcohol of increasing concentration. The dehydrated tissue was then dipped in wax to get paraffinembedded tissue blocks. The chilled paraffin-embedded tissue blocks are sectioned into 4 µm thin sections. The paraffin sections of rat kidneys on glass slides were dewaxed in Xylene, dehydrated by washing in absolute ethanol and then washed in water for 3–5 minutes. After deparaffinization, dehydration and subsequent hydration, slides were immersed in water and stained with the H&E Staining Kit (HEC005M, Beyotime). The slides containing hydrated tissue sections were completely submerge in hematoxylin staining solution for 15–20 min until the nuclei were clearly stained. The sections were then washed in PBS buffer with sufficient swirling and stained with Eosin. The extent of the staining was observed under the microscope. Finally, the tissue sections were allowed to dry and sealed with a neutral resin before observing and photographing the morphological changes in the rat kidney under a light microscope. We randomly selected 10 fields of view for the sections of whole rat kidneys in the control group, and 5 fields of view each for the sections of upper and lower poles of the kidney of rats in the GN group.

Masson's Trichrome staining

The Masson (Trichrome) staining (used primarily to demonstrate connective tissue elements, collagen and muscle fibers) of the kidney sections, involves fixing, dehydrating, embedding, and sectioning in order before staining using the Masson staining kit (DC0033, Leagene Biotechnology). After staining, collagen becomes colored blue, muscle fibers, cytoplasm and keratin in red and the nuclei blue/black. The staining of the tissue sections was performed in the order of Bouin's solution (an excellent fixative for preserving soft and delicate structures), azurite blue staining solution, hematoxylin staining solution (to stain

nuclei), color separation solution, and Rejuvenate red staining solution. Phosphomolybdic acid solution was used for staining connective tissue fibers to Aniline Blue. Finally, the sections were dried and sealed with resin. The level of fibrosis in rat kidney tissue was observed and photographed under a microscope. In the control group, 10 random fields of view were selected from the entire kidney tissue, while in the GN group, 5 random fields of view were selected from each of the suprarenal and infrarenal poles. The positive area was counted by analyzing the collected fields of view using Image J software.

Immunohistochemistry

Kidney sections were formalin fixed, dehydrated, sectioned into 4μm thickness and then embedded on glass slides. For heat induced antigen retrieval, tissue sections fixed on slides were dipped in 10mM sodium citrate solution (pH 6.0) (AR0024,Bosterbio Biotechnologies) and heated in a pressure cooker for 4 minutes. Endogenous peroxidase enzymes in the tissue sections were inhibited by dipping the tissue-embedded slides in 3% H202 solution for 15 minutes. The slides were then blocked with 5% BSA (bovine serum albumin) in PBS (phosphate-buffered saline)solution (180728, Genxion Biotechnologies) for 1 h at room temperature to minimize non-specific binding of primary and secondary antibodies before incubating with the appropriate primary antibody (diluted in 1% BSA in PBS) for twelve hours at 4°C. The tissue sections embedded on slides were washed three times with PBS and stained appropriate secondary antibody (KIT-5020, MXB Biotechnologies) for one hour at 25°C. The tissue sections were then washed with PBS to remove non-specifically adhering the secondary antibodies and then stained using 3,3'-diaminobenzidine (DAB) (DAB 2031, MXB Biotechnologies) to develop dark-brown color by hydrogen peroxide in the presence of HRP-linked secondary antibody attached to the primary antibody which is bound to the antigen. After drying the sections, we used neutral resin to seal them before observing and photographing the morphological changes in the rat kidney under a light microscope. We randomly selected 10 fields of view for the sections of whole rat kidneys in the control group, and 5 fields of view each for the sections of upper and lower poles of the kidney of rats in the GN group.

To identify crystal deposits in the kidneys, paraffin sections of kidneys from mice on the day 28 were stained with hematoxylin and eosin (H&E) and UA crystal deposits were visualized under polarized light.

Multiplex fluorescence immunohistochemistry was conducted in accordance with the instructions provided in the staining kit (G1236–50T, ServiceBio), utilizing paraffin sections of rat kidneys and TSA-488 dye-conjugated NLRP3 antibody, TSA-555 dye-conjugated F4/80 antibody, and TSA-647 dye-conjugated CD11b antibody. The stained sections were then subjected to tissue panoramic scanning using a tissue panoramic scanner(VS200,PanoView).

Antibody: Anti-α-smooth muscle actin antibody (a-SMA)(Cat # ab124964, abcam); anti-Vimentin antibody (Cat # ab92547, abcam) for cytoskeleton detection; anti-NLRP3 antibody (Cat # T55651, Abmart), anti-integrin αM/CD11b antibody (Cat # sc-1186, Santa Cruz); anti-F4/80 antibody (Cat # ab300421, abcam) for macrophage detection.

Uric acid dissolution test

A 50X solution (50 mM, pH 9.0) of ethylenediaminetetraacetic acid (EDTA; P0084, Beyotime) was diluted to 1X (1 mM, pH 9.0) using ultrapure water. One milligram of uric acid oxidoreductase (S10175, Yuanye Bio) was volumized to 1 ml of 1X EDTA solution to formulate a uric acid oxidase (UOX) solution at a concentration of 37.87 u/ml. The prepared MSU crystals were placed on slides and the UOX solution or EDTA solution (as a negative control) was added dropwise. Following the dropwise addition of the solutions, observations were conducted under a microscope at 200x magnification at 0, 5, 10, 20 and 30 minutes.

Analysis of circulating inflammatory cell counts

The rats were anesthetized with chloral hydrate (350 mg/kg, i.p) and confirmed the depth of anesthesia suitable for surgery by monitoring their heart rate, respiratory rate, blood pressure, weakness and unresponsiveness. The abdominal cavity was then opened to expose the abdominal aorta and blood was drawn using a blood collection needle and collected in vial containing heparin (EDTAK2,SANLI CHINA) and sent to the the Laboratory Department of Guangdong Provincial Hospital of Traditional Chinese Medicine, University Town Branch, for testing. The blood was analyzed using a fully automated blood cell analyzer (Myriad, BC-6000Plus).

Test of renal functioning

Glomerular filtration rate (GFR) is the best overall index of kidney function. The value of GFR is calculated from the concentration of creatinine and blood urea nitrogen (BUN) in serum and in urine, respectively. Therefore, urine was collected from each rat in a metabolic cage for 24 hours prior to observation. Blood samples were collected as described above, centrifuged, and the upper serum layer was separated. The levels of uric acid (Cat # C012–2-1, Nanjing Jiancheng Bioengineering Insitute), creatinine (Cat # C011–2-1,Nanjing Jiancheng Bioengineering Insitute), and blood urea nitrogen (BUN) (Cat # C013–2-1, Nanjing Jiancheng Bioengineering Insitute) in both serum and urine were measured following supplied protocols of the respective appropriate kits.

10.3389/fendo.2024.1416996

ELISA

The concentration of IL-1β in the serum was measured using the ELISA kit for rat IL-1β (Cat # CSB-E08055r, Cusabio) following manufacturer's supplied protocol. The absorbances (Optical Density, OD) of ELISA tests were read at 450 nm.

Statistical analysis

Statistical analysis was conducted using GraphPad Prism 8.0 (GraphPad Software Inc., San Diego, CA, USA). The data were presented as mean ± SEM. The normality of the data (relative value of the SD with respect to mean) was confirmed, and group comparisons were assessed using either one-way ANOVA or Student's t-test. A p-value of less than 0.05 was considered statistically significant. The symbol" * " is employed to indicate statistical differences from the control group, the symbol " # " is employed to indicate statistical differences between any two groups, with the exception of the control group.

Results

Intrarenal administration of MSU crystal suspension shows no impact on the whole body weight and kidney mass of rats

The outward appearance of the rat kidneys and the mass were compared across two different groups post-injection. The results

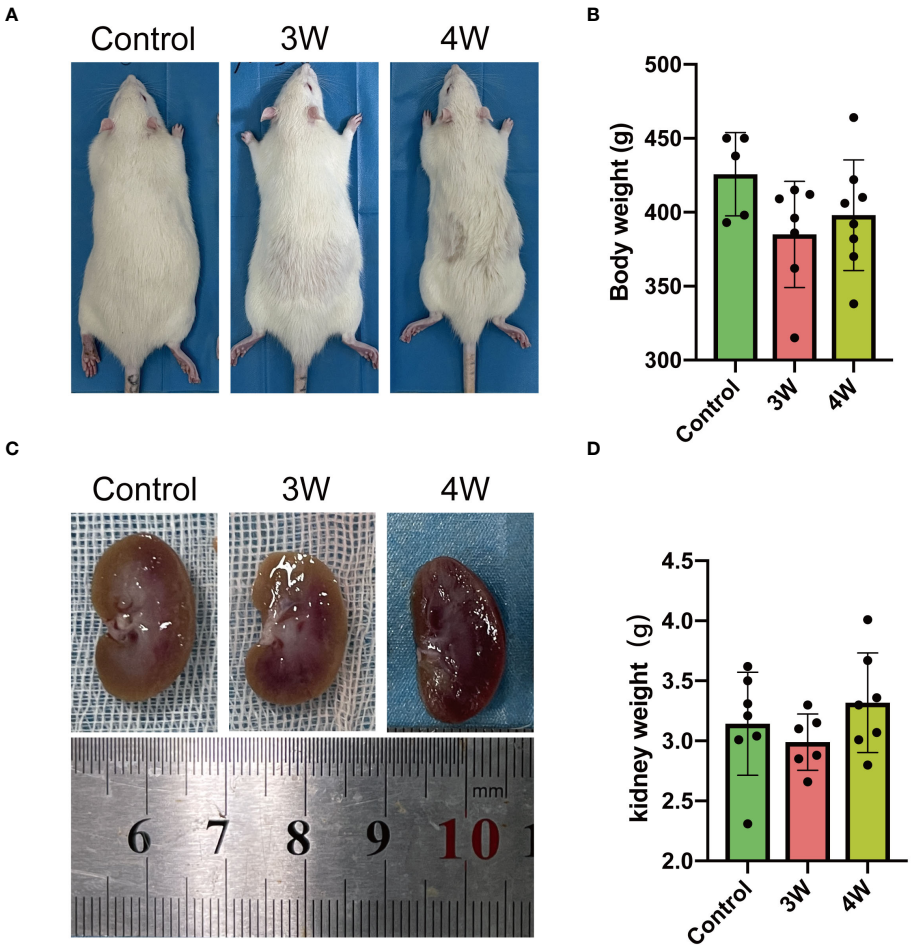

FIGURE 2
Intrarenal administration of MSU crystals appears to have no significant effect on physical appearance of the animals (rats), whole body weight and outward appearance and mass of kidney. **(A)** The pictures of the rats were taken at three or four weeks (3W/4W) after injection of suspension of MSU crystals. **(B)** The whole body weight (g) of rats were measured three or four weeks after injection of suspension of MSU crystals. **(C)** The pictures of the physical appearance of rat kidneys taken at three or four weeks after injection of suspension of MSU crystals. **(D)** The weight (g) of rat kidneys was measured at three or four weeks after injection of suspension of MSU crystals.

10.3389/fendo.2024.1416996

show that intrarenal injection of MSU crystals did not significantly alter the physical appearance (Figure 2A), whole body weight (Figure 2B) and overall appearance (Figure 2C) or weight (Figure 2D) of the kidneys compared to controls during the third and fourth weeks after the injections. Thus, intrarenal injection of MSU crystals seems did not affect the overall health conditions of rats in the third and fourth weeks post-procedure.

Intrarenal MSU injection caused localized renal tubular damage and an increase in inflammatory cell infiltration

To examine the impact of intrarenal MSU crystals on renal pathology, we conducted Hematoxylin and Eosin (H&E) staining of renal tissue sections. The results revealed the presence of uratoma at the upper pole of the kidneys injected with MSU crystals by the end of third and fourth weeks post-injection (Figure 3A). The MSU crystals exhibited significant damage to the peripheral renal tubules, characterized by tubular dilatation and vacuolar degeneration (White arrows and black arrows). In contrast, the lower renal pole injected with PBS revealed no significant pathological changes like the control group, with no discernible damage at weeks three and four (Figure 3A). MSU crystals were shown to provoke pathological damage at its location by inducing innate immunity (11). To know the mechanism of how MSU crystals induce renal tissue inflammation, we measured the number of infiltrated inflammatory cells (cellular components of innate immunity) into the interstitium of renal tissues (Figure 3B). The results of panoramic scanning of slides of kidney sections stained for multiplex fluorescence immunohistochemistry with TSA-488 dye conjugated NLRP3 antibody, TSA-555 dye conjugated F4/80 antibody (for labeling matured macrophages), and TSA-647 dye

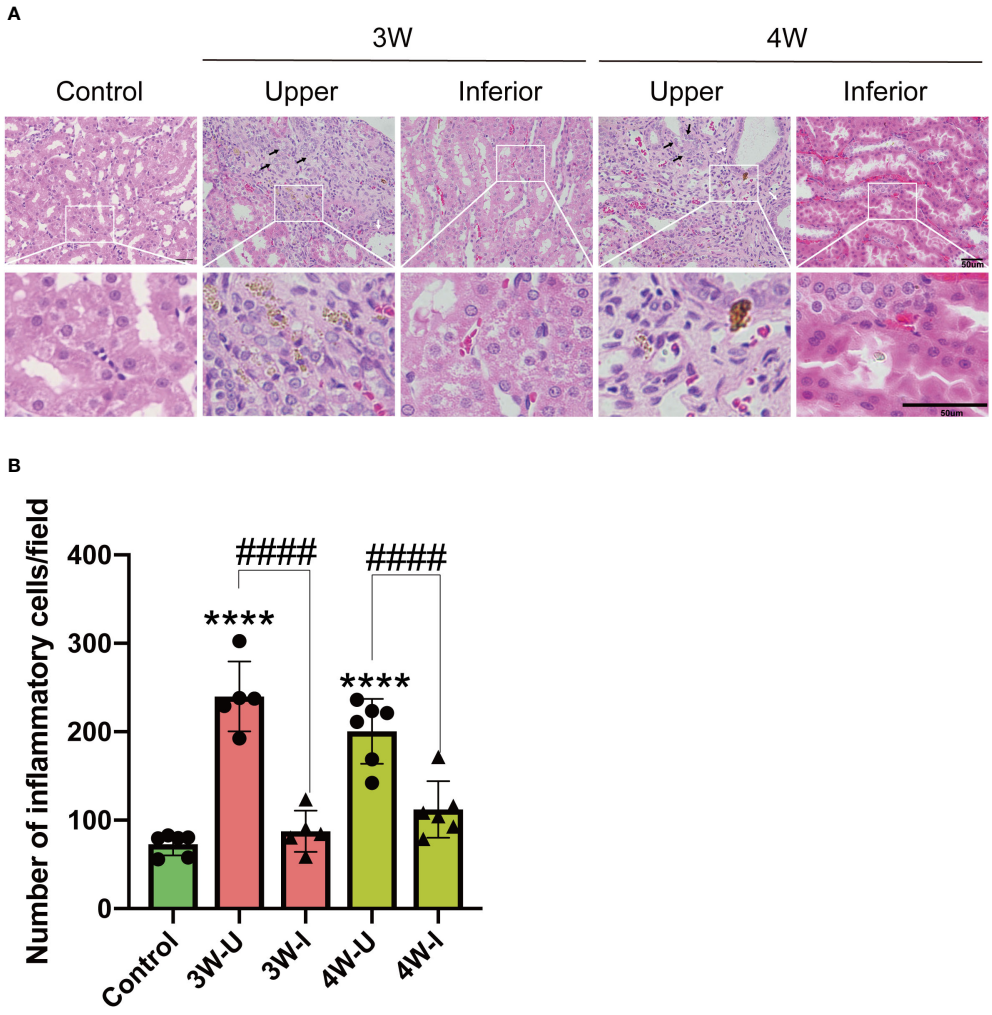

FIGURE 3
Intrarenal administration of MSU crystals exhibited significant damage to the peripheral renal tubules; characterized by tubular dilatation,vacuolar degeneration and substantial infiltration of inflammatory cells into the renal interstitium. **(A)** The Hematoxylin and Eosin (H&E) staining of a representative of the kidney sections (n = 6; mean ± SEM) of the MSU crystals injected upper pole and PBS injected lower pole. Scale bar = 50 µm. Arrow sign (→) on the picture shows damage to the peripheral renal tubules, the white arrow indicates tubular dilatation, while the black arrow denotes vacuolar degeneration. **(B)** Inflammatory cell count infiltrated into the interstitium of rat kidneys three or four weeks (3W/4W) after injection of suspension of MSU crystals in the upper pole (3W-U/4W-U) and PBS injection in the lower pole (3W-I/4W-I) of the rat kidney. (n = 5–6; mean ± SEM). **** $P < 0.0001$. #### $P < 0.0001$.

10.3389/fendo.2024.1416996

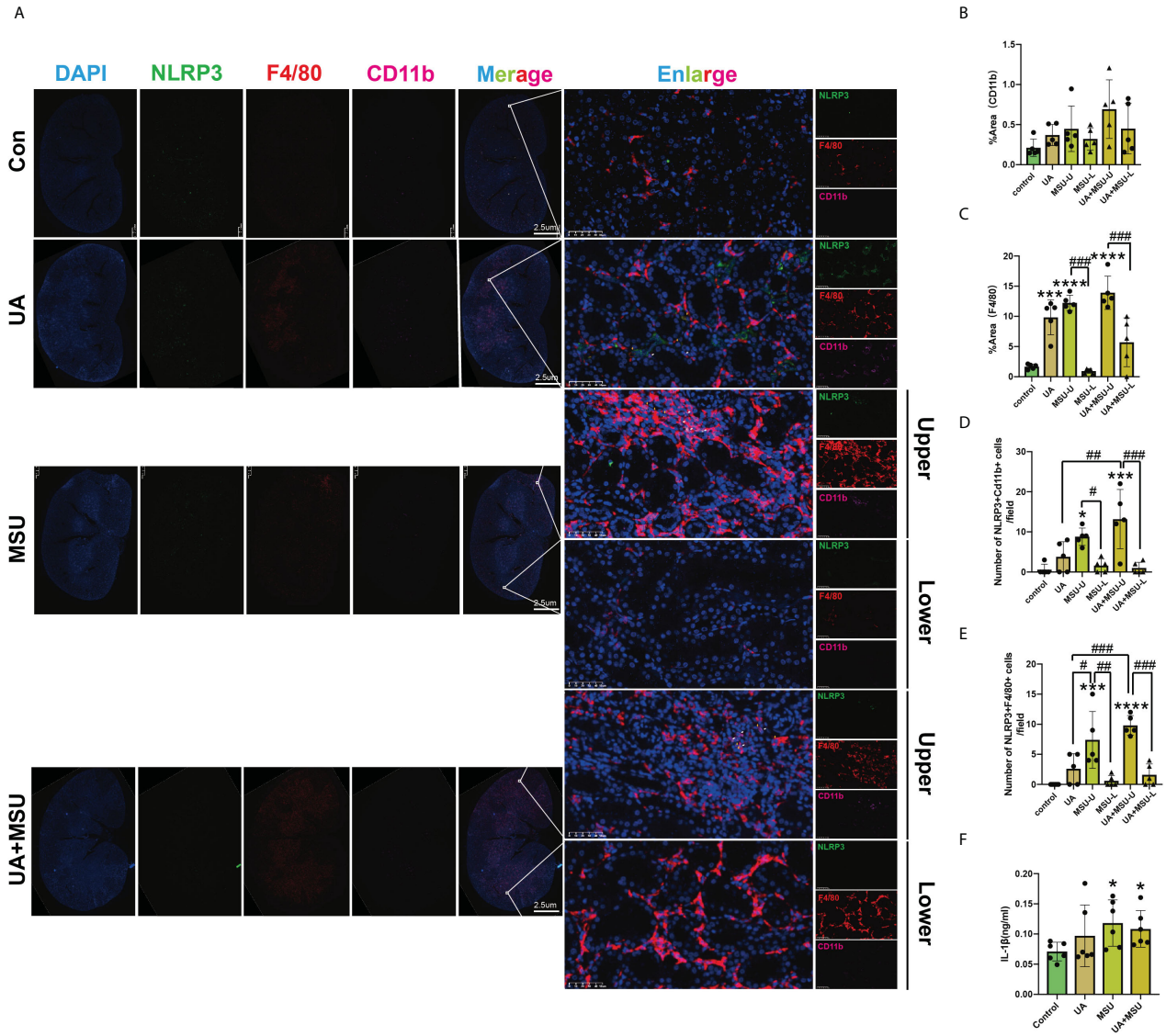

FIGURE 4
Intrarenal injection of MSU crystals into the kidneys of normal rats or PO-induced hyperuricemic rats induces the activation of NLRP3 inflammasome protein complexes in renal monocytes and macrophages and elevate serum IL-1β levels. **(A)** Representative images of kidney sections of control rat, PO-induced hyperuricemic rat (UA group), MSU crystals-injected rat (MSU group), and MSU crystals-injected PO-induced hyperuricemic rat (UA +MSU group) at 28 days of after MSU injection/gavage that were stained using TSA-488 dye-conjugated NLRP3 antibody, TSA-555 dye-conjugated F4/80 antibody, and TSA-647 dye-conjugated CD11b antibody for Multiplex immunohistochemical staining. Green fluorescence represents NLRP3, red fluorescence represents F4/80, and pink fluorescence represents CD11b. White arrows represent double-positive cells (macrophages and monocytes) for NLRP3+CD11b+; yellow arrows represent double-positive cells (macrophages) for NLRP3+F4/80+. Scale bars = 2.5 μm and 50 μm. **(B)** Quantification of the pink area immune-stained for CD11b (n = 5; mean ± SEM). **(C)** Quantification of the read area immune-stained for F4/80 (n = 5; mean ± SEM). **(D)** The relative number of double-positive cells for NLRP3+CD11b+ per view (n = 5; mean ± SEM). **(E)** The relative number of double-positive cells for NLRP3+F4/80+ per view (n = 5; mean ± SEM). **(F)** The concentrations of IL-β in the sera of all four groups of rats (n = 5; mean ± SEM). Rat kidneys were sectioned four weeks (4W) after MSU injection/gavage. Blood samples from all four groups of rats (for sera) were collected four weeks after MSU injection/gavage. *, # <0.05; **, ## P < 0.01; ***, ### P < 0.001; ****, P < 0.0001 The panoramic scanning of slides of kidney sections stained for multiplex fluorescence immunohistochemistry with TSA-488 dye conjugated NLRP3 antibody, TSA-555 dye conjugated F4/80 antibody (for labeling matured macrophages), and TSA-647 dye conjugated CD11b antibody (for labeling monocytes, activated lymphocytes, macrophages) was used for counting the number of infiltrated inflammatory cells.

conjugated CD11b antibody (for labeling monocytes, activated lymphocytes, macrophages) revealed a significant increase in inflammatory cell infiltration at the upper renal pole injected with MSU crystals during weeks four, compared to the PBS-injected and control kidneys (Figures 3B, 4A–C). We did not find any significant increase in infiltration of inflammatory cells in the PBS-injected lower renal pole compared to the control kidneys during these time periods.

Intrarenal injection of MSU crystals did not induce systemic inflammatory response in rats

To know the impact of intrarenal injection with MSU crystals on systemic inflammatory response we conducted a thorough analysis of inflammatory cell types in rat blood samples. The

10.3389/fendo.2024.1416996

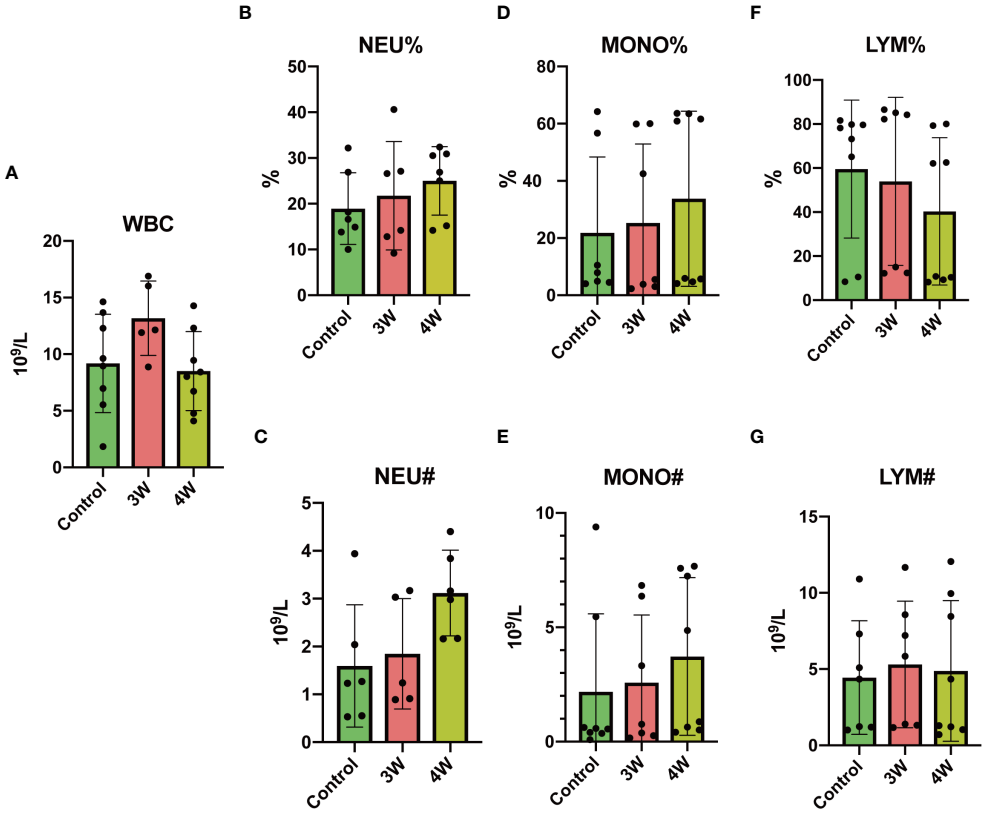

FIGURE 5
Intrarenal administration of MSU crystals did not induce a systemic inflammatory response in rats. The percentage and total number of inflammatory cells per liter in the blood of rat was analyzed using a fully automated blood cell analyzer. **(A)** Blood leukocyte (WBC) count (109/L). **(B)** Blood neutrophil (NEU) percentage (%). **(C)** Blood neutrophil count(109/L). **(D)** Blood monocyte (MONO) percentage (%). **(E)** Blood monocyte count (109/L). **(F)** Blood lymphocyte (LYM) percentage (%). **(G)** Blood lymphocyte count (109/L). Blood samples from rata were collected three or four weeks (3W/4W) after injection of suspension of MSU crystals in the upper pole and after injection of PBS in the lower pole of the rat kidney.

results of flow cytometry analyses revealed almost no significant differences in counts or proportions of leukocyte, neutrophil, lymphocyte, and monocyte in the circulation during the third and fourth weeks post-injection compared to the control group (Figure 5). The results suggest that the intrarenal injection of MSU crystals did not cause any infection or induce systemic inflammatory response in the rats.

Intrarenal Injection of MSU crystals induces focal renal interstitial fibrosis

The MSU crystal-induced nephropathy was previously shown as the result of stimulation of renal inflammation and fibrosis through activation of the cytosolic Nod-like receptor protein 3 (NLRP3) inflammasome (12). We assessed the effect of intrarenal MSU crystal injection on renal fibrosis by Masson's Trichrome staining of connective tissue fibers and collagen in renal tissue sections and measured the positively stained (blue) area. The results show a significant increase in fibrosis in the renal interstitium at the upper pole of kidneys injected with MSU crystals during the third and fourth weeks, compared to the lower pole injected with PBS and control rat kidneys. We did not find any significant increase in fibrosis at the PBS-injected lower pole of the kidneys at weeks 3 and 4 compared to the control rats (Figure 6). The results are indicative of the effect of MSU crystals on localized induction of interstitial fibrosis only at the site of MSU crystal injection in kidney during the third and fourth weeks.

Intrarenal injection of MSU crystals results in renal impairment in rats without influencing blood uric acid levels

To assess the effect of intrarenal injection of MSU crystals on rat kidney function, we measured the levels of uric acid, creatinine, and urea nitrogen in urine and serum. Comparative analysis revealed no significant differences in uric acid and urea nitrogen levels in rat serum and urine three and four weeks after MSU injection compared to control rats (Figures 7A, B, E, F). However, the serum creatinine levels showed a significant increase four weeks after the MSU injection compared to the control group, while no noticeable changes were observed in urine creatinine (Figures 7C, D). These results indicate that the intrarenal injection of MSU crystals did not interfere with the renal function related to uric acid transport (reabsorption/secretion) or metabolism. However, the

10.3389/fendo.2024.1416996

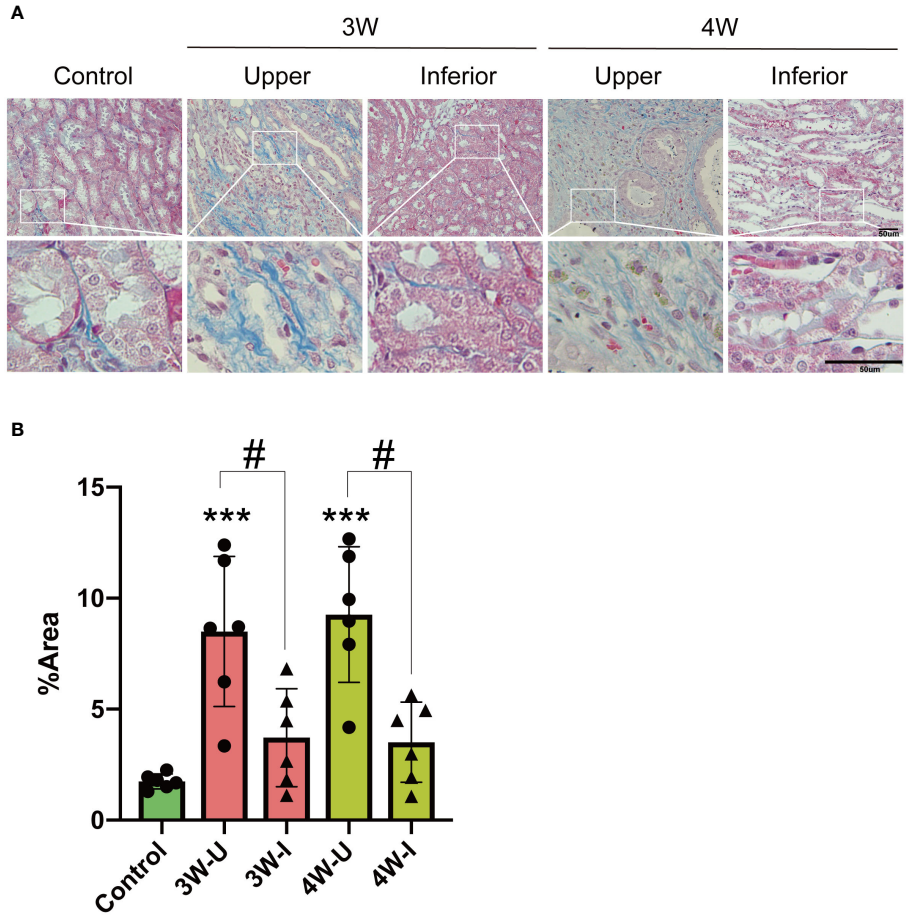

FIGURE 6
Intrarenal injection of MSU crystals induces focal renal interstitial fibrosis as revealed by Masson (Trichrome) staining of rat kidney sections. **(A)** Masson (Trichrome)staining of connective tissue fibers and collagen in the kidney sections as shown by positively stained (blue) area of rat kidney sections (n = 6; mean ± SEM). Scale bar = 50 μm. **(B)** Quantification of the area of Masson (Trichrome) stained blue region (n = 5–6; mean ± SEM). Rat kidneys were sectioned three or four weeks (3W/4W) after injection of suspension of MSU crystals in the upper pole (3W-U/4W-U) and PBS injection in the lower pole (3W-I/4W-I) of the rat kidney. # $P < 0.05$, *** $P < 0.001$.

injection of MSU crystals significantly increased serum creatinine (a waste product of the muscles) indicating MSU crystals might have triggered renal dysfunction in rats by the fourth week post-injection.

Both MSU crystals and soluble UA results in renal impairment, pathological damage and fibrosis

To know the difference in the impacts of MSU crystals (MSU group) and soluble UA on renal injury, we induced hyperuricemia in rats by gavaging potassium oxonate (PO) and UA (UA group) to simulate the effect of soluble UA on the kidney. We also used rats with hyperuricemia (by gavaging PO and UA) after intrarenal injection of MSU crystals (UA+MSU group) to simulate the effects on the kidney when MSU crystals and soluble uric acid are present in the kidney at the same time (Figures 1A, B). The outward appearance of the rat kidneys and the mass were compared across four different groups. The results demonstrate that the UA, MSU, and UA+MSU groups exhibited no significant differences in physical appearance (Figure 8A), whole body weight (Figure 8B), or overall appearance (Figure 8C) or weight (Figure 8D) of the kidneys compared to controls during the third and fourth weeks. Thus, in the presence of MSU crystals, soluble UA and both in the kidney, the overall health conditions of rats did not change after the third and fourth weeks post-procedure. A comparative analysis of kidney function indicators revealed that at the third and fourth weeks of modelling, there was no significant difference in serum UA (sUA) levels between the MSU and control groups. Nevertheless, sUA levels were found to be significantly elevated in the UA and UA +MSU groups in comparison to the control and MSU groups. Furthermore, at the fourth week, sUA levels were found to be significantly higher in the UA+MSU group than in the UA group (Figure 8E). There was no significant difference in serum creatinine (sCr) levels between the UA group and the control group at week four. However, sCr levels were significantly higher in the MSU group and the UA+MSU group (Figure 8G). The modelling groups exhibited no significant differences in urine UA (uUA), urine creatinine (uCr), serum urea nitrogen (sUN) and urine urea

10.3389/fendo.2024.1416996

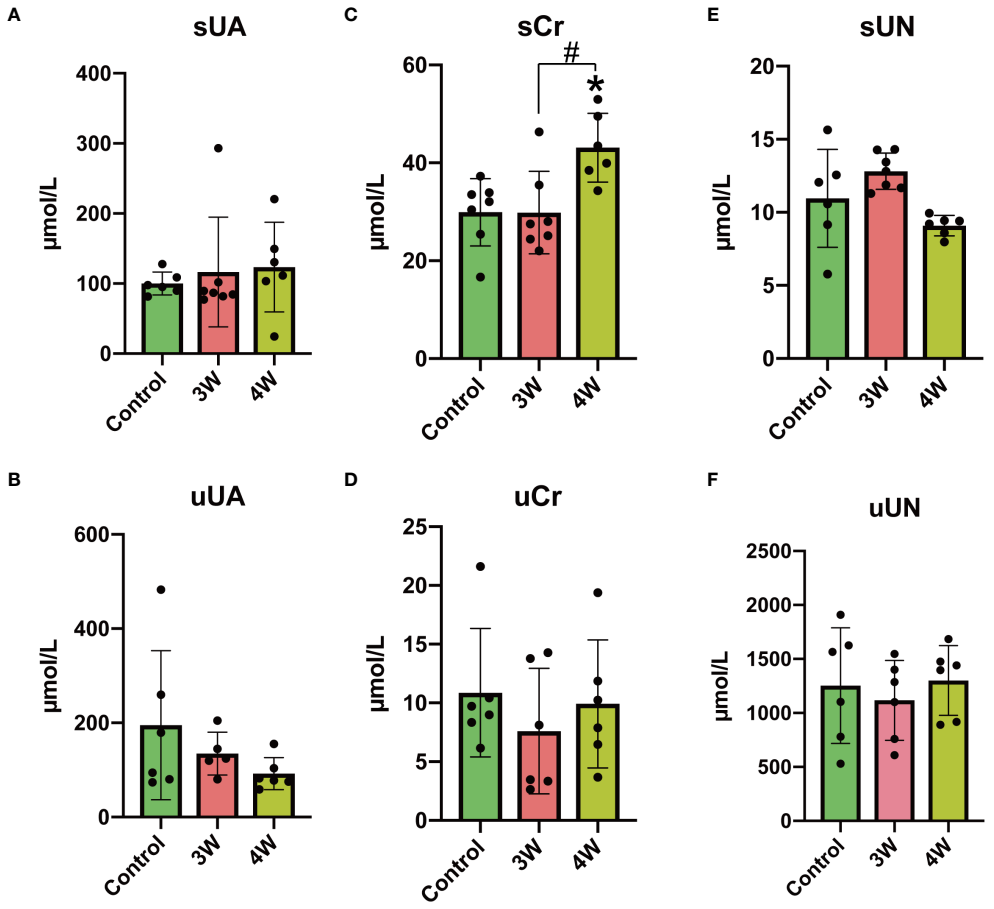

FIGURE 7
Effect of intrarenal injection of MSU crystals on serum and urinary indices of renal function in rats. **(A)** Serum urate (sUA) (ummol/L). **(B)** Urinary uric acid (uUA) (ummol/L). **(C)** Serum creatinine (sCr) (ummol/L). **(D)** Urinary creatinine (uCr)(ummol/L). **(E)** Serum urea nitrogen (sUN) (ummol/L). **(F)** Urinary urea nitrogen (uUN) (ummol/L).*, # $P < 0.05$.

nitrogen (uUN) compared to the control group at weeks three and four (Figures 8F, H–J). The results indicate that the administration of PO and UA by gavage may affect renal function related to uric acid transport (reabsorption/secretion) or metabolism. Furthermore, the presence of MSU crystals in the kidney appears to exacerbate this effect. Concurrently, the injection of MSU crystals into the kidneys of PO and UA gavaged rats resulted in a significant elevation in serum creatinine (a byproduct of muscle), indicating that MSU crystals may be the primary contributor to renal dysfunction in rats during the fourth week following injection, rather than soluble UA.

The results of hematoxylin and eosin (H&E) staining show that the UA group, UA+MSU group, and the upper pole of the kidney in MSU groups suffered significant damage, as evidenced by tubular dilatation and vacuolar degeneration (shown by the arrows in the Figure 8K). In contrast, the lower pole of the kidney in the MSU group did not exhibit any significant pathological changes or damages compared to the control group after third and fourth weeks of the procedures. It is noteworthy that pathological damage in the MSU group was present only in the vicinity of the MSU crystals. In contrast, pathological damage in the UA and UA+MSU groups was observed diffused throughout the renal tissue (Figure 8K). To know the mechanism how MSU crystals and soluble UA induce pathological changes in the renal tissue, the number of inflammatory cells infiltrating the interstitium of renal tissue was quantified (Figure 8L). The results show a significant increase in the infiltration of inflammatory cells in the third and fourth weeks after procedures in the kidneys of UA group, UA +MSU group, and the upper pole of the kidney in the MSU groups compared with control group. Furthermore, the number of inflammatory cells was significantly increased in the upper pole of the kidney in the MSU group and the UA+MSU group in the presence of MSU crystals compared to the lower pole of the kidney injected with PBS.

To demonstrate that intrarenal injection of MSU crystals results in kidney damage, we employed uric acid oxidase (UOX)to dissolve the intrarenally injected MSU and used polarized light microscopy to observe the kidney tissue after injection. The results indicated that uricase could dissolve the intrarenally injected MSU and within 30 minutes, while the dissolution reagent without UOX was ineffective (Figure 8M). Interestingly, the results of polarized light microscopy of rat kidney sections also showed the increased growth/size/number of the injected MSU crystals in the kidney of UA+MSU group of rats (Figure 8N). This indicates that under

10.3389/fendo.2024.1416996

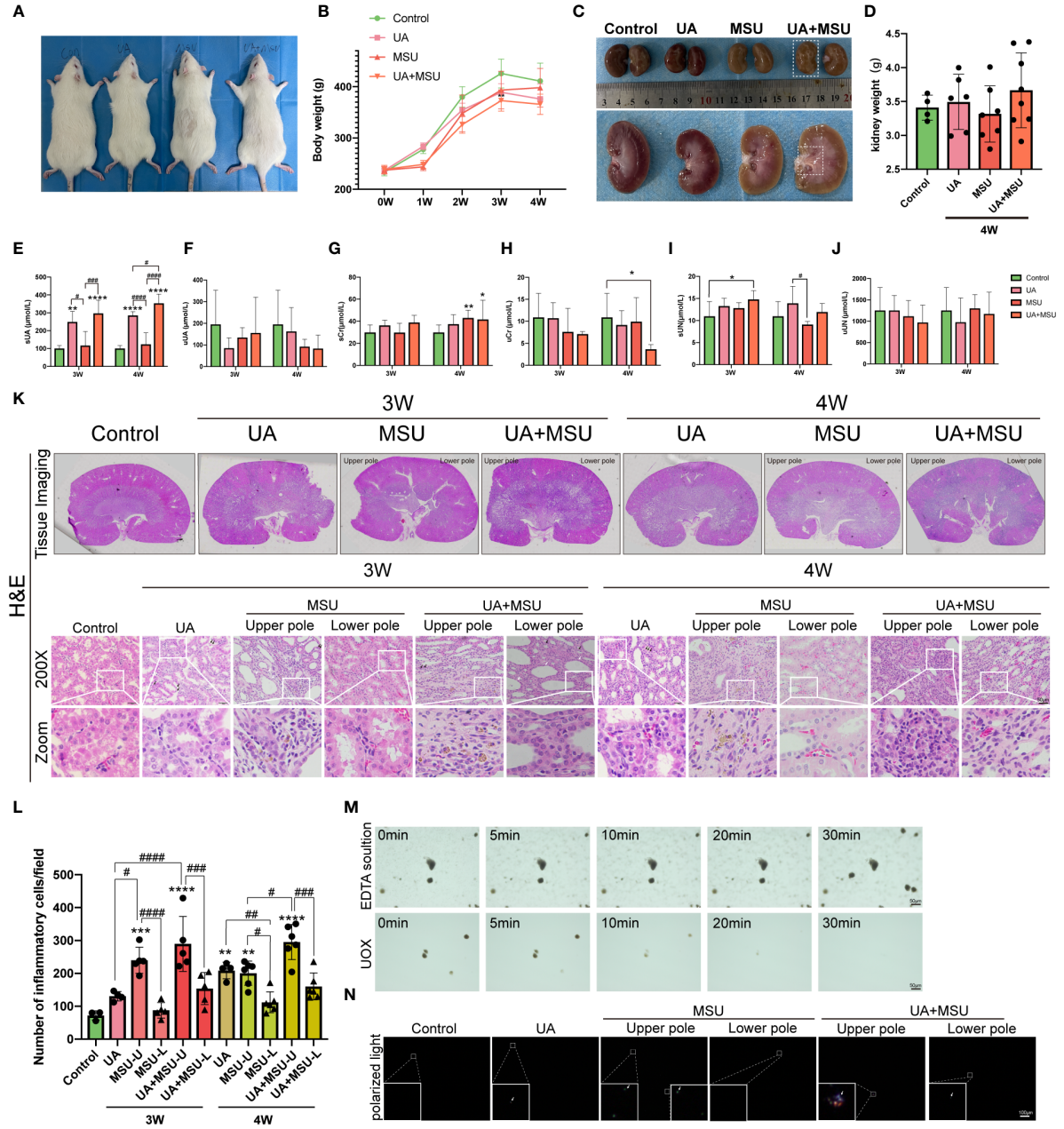

FIGURE 8
Intrarenal injection of MSU crystals into the kidneys of normal rats or PO-induced hyperuricemic rats triggers renal impairment, pathological damage and inflammatory cell infiltration. **(A)** The pictures of rats from left to right are the representative control rat, PO-induced hyperuricemic rat (of UA group), MSU crystals-injected rat (of MSU group), and MSU crystals-injected PO-induced hyperuricemic rat (of UA+MSU group). These pictures were taken four weeks (4W) after injection of suspension of MSU crystals (MSU group). The PO-induced group of hyperuricemic rats (UA group) was generated by intragastric gavage of 750 mg/kg of PO and 300 mg/kg of UA. The UA+MSU group of rats was generated by intragastric gavage of 750 mg/kg of PO and 300 mg/kg of UA after intrarenal injection of MSU crystals. **(B)** Whole body weight (g) of rats of the control, UA, MSU, and UA+MSU groups were measured from zero to four weeks after MSU injection/gavage. **(C)** The pictures show the physical appearance of rat kidneys in the control, UA, MSU and UA+MSU groups taken at four weeks after after MSU injection/gavage. **(D)** The weight (in grams) of the kidneys of the rats was measured four weeks after MSU injection/gavage. **(E)** Serum urate (sUA) (ummol/L); **(F)** Urinary uric acid (uUA) (ummol/L); **(G)** Serum creatinine (sCr) (ummol/L); **(H)** Urinary creatinine (uCr)(ummol/L); **(I)** Serum urea nitrogen (sUN) (ummol/L) and **(J)** Urinary urea nitrogen (uUN) (ummol/L). **(K)** Hematoxylin and Eosin (H&E) staining of a representative of the kidney sections (n = 5–8; mean ± SEM) of control, UA, MSU and UA+MSU groups. Tissue Imaging and 200x field of view. Scale bar = 2μm, 50 μm. Arrow sign (→) on the picture shows damage to the peripheral renal tubules; the white arrow indicates tubular dilatation, while the black arrow denotes vacuolar degeneration. **(L)** Inflammatory cell count infiltrated into the interstitium of rat kidneys three or four weeks (3W/4W) after MSU injection/gavage. (n = 5–6; mean ± SEM). The panoramic scanning of slides of kidney sections stained for multiplex fluorescence immunohistochemistry with TSA-488 dye conjugated NLRP3 antibody, TSA-555 dye conjugated F4/80 antibody (for labeling matured macrophages), and TSA-647 dye conjugated CD11b antibody (for labeling monocytes, activated lymphocytes, macrophages) was used for counting the number of infiltrated inflammatory cells. **(M)** The intrarenally accumulated MSU crystals were shown getting dissolved by UOX (urate oxidas'uricase) treatment for about 10–30 min. The EDTA solution used to make UOX solution had no effect in dissolving MSU crystals at the site of injection. The picture was taken at 200X magnification. Scale bar, 50μm. **(N)** The photograph of rat kidney sections was taken using a polarized light microscope. Scale bar,100μm. The white arrow symbol (→) shows the presence of MSU Crystals.
*, # <0.05; **, ##P < 0.01; ***, ###P < 0.001; ****, ####P < 0.0001.

condition of hyperuricemia, intrarenally injected smaller MSU crystals acted like seeding crystals to accelerate the growth of the injected smaller MSU crystals that ultimately results in more damages to the kidney.

Next, we stepped forward to know the differences in the impacts of intrarenal MSU crystals, soluble UA, and UA+MSU on the degree of renal fibrosis through evaluation of the fibrosis marker proteins α-SMA and vimentin proteins of connective tissue fibers in renal tissue sections using Masson's trichrome staining and immunohistochemical staining. The results show significant degree of fibrosis, in the renal tissues of the UA and UA+MSU groups, as well as in the upper pole of the kidneys in the MSU group at the location of MSU crystal injection (Figures 9A–F). Quantitative analyses reveal that the UA group, the UA+MSU group, and the upper pole of the kidney in the MSU group exhibits significantly higher level of Vimentin and α-SMA than the control group (Figures 9G–I). In contrast, no significant difference was observed in the positive area of the three indicators in the lower pole of the kidney in the MSU group compared to the control group (Figures 9G–I). The results thus indicate that MSU crystals, soluble UA, and their combination can induce interstitial fibrosis during the third and fourth weeks.

MSU crystals induce NLRP3 activation in renal tissue monocytes and macrophages and elevate serum IL-1β levels

MSU crystals have been demonstrated to release inflammatory factors by activating the Nod-like receptor protein 3 (NLRP3) in monocytes and macrophages, thereby exacerbating the tissue inflammatory response (12). In order to ascertain the role of MSU crystals and soluble UA in the regulation of inflammatory factors in renal tissues, kidney tissue sections were stained using multiplex immunohistochemical staining. Green signals represented NLRP3, red signals represented F4/80 (a marker for macrophages) and pink signals represented CD11b (a marker for monocytes). The results demonstrated that there was no significant difference in the CD11b-positive area between the UA, MSU and UA+MSU groups (Figures 4A, B). The F4/80-positive area was significantly greater in the UA group, MSU group and UA+MSU group compared to the control group. Furthermore, the F4/80-positive area of the upper pole of the kidney injected with MSU crystals was significantly greater than that of the lower pole injected with PBS in the MSU group and UA+MSU group (Figures 4A, C). The number of cells that were positive for both NLRP3 and CD11b or F4/80 was counted. The results reveal a remarkable increase in the number of NLRP3, CD11b and F4/80-positive cells in the MSU and UA+MSU groups in comparison to the control group. A significant increase in the number of CD11b and F4/80-positive cells was also observed in the PBS-injected lower pole of the kidney in the UA+MSU group compared to the PBS-injected lower pole of the kidney of MSU group of rats (Figures 4A–E). Since, NLRP3 activation in macrophages and monocytes was reported to increase IL-1β secretion (12), we examined the level of IL-1β in the blood of all these experimental groups of rats. The results show that the level of IL-1β in the blood of UA group, MSU group and the UA+MSU group was significantly increased compared to that of the control group. (Figure 4F) The results thus indicate that the intrarenal injection of MSU crystals may be the causal factor to the observed increase in IL-1β expression.

Discussion

GN is caused by the precipitation of MSU crystals in the kidney tubules, usually collecting ducts with tubular injury (1). Patients suffering from acute GN usually have severe hyperuricemia, gout and kidney failure and/or impaired kidney function with renal fibrosis (1, 2). In this study, we found that direct administration of the suspension of MSU crystals into the rat kidney caused significant infiltration of inflammatory cells and interstitial fibrosis at the site of injection, while the other uninjected sites or sites injected with PBS remained almost normal. However, we can't rule out the impact of MSU crystals on other sites of kidney over longer periods of time.

Previous studies on GN have mainly relied on models that had elevated levels of serum urate (11, 13). In contrast, this study design aimed to explore the localized effect of MSU crystals in the rat kidney compared with the other parts of the kidney. We monitored the presence of MSU crystals at the site of injection directly by light microscopy to confirm direct effect of MSU crystals on infiltration of inflammatory cells and fibrosis. However, in other previous studies, confirming the presence of MSU crystals at the site of infiltration of inflammatory cells and fibrosis was a challenging issue to prove that the symptoms of GN was caused directly by MSU crystals, not by circulating higher level of urate (11).

To assess the role of only the MSU crystals on the pathogenesis of GN, it is important to exclude the interference caused by elevated levels of circulating uric acid, which can be very challenging. In this study, renal inflammation, fibrosis and tubular injury was induced by the MSU crystals (detectable at the site of injection directly by light microscopy) while keeping the serum urate at normal level during the study period. Furthermore, by comparing this study model of GN with the GN model having elevated uric acid levels, it might be possible to simulate renal injury in patients with clinically comorbid hyperuricemia and gout. The use of this study approach can be helpful to understand the differences between the pathogenic mechanisms of HN and GN.

GN is characterized by the presence of mostly MSU crystals in the renal tubules usually collecting ducts with tubular injury1 and/or interstitium, with infiltrating inflammatory cells such as macrophages, lymphocytes, and granulocytes in the interstitium of kidneys (2, 14) accompanied by fibrosis. The results of this study confirm that the presence of MSU crystals at the site of injection in the rat kidney caused profound infiltration of inflammatory cells accompanied by fibrosis without affecting other areas of kidney injected with PBS. In this study, serum urate levels remained almost unaffected in both serum and urine in the MSU crystals injected rats like the control group. Thus, the induction of GN symptoms and renal injury by MSU crystals in this study, unlike that in the HUA model, was under the conditions of normal serum urate levels.

10.3389/fendo.2024.1416996

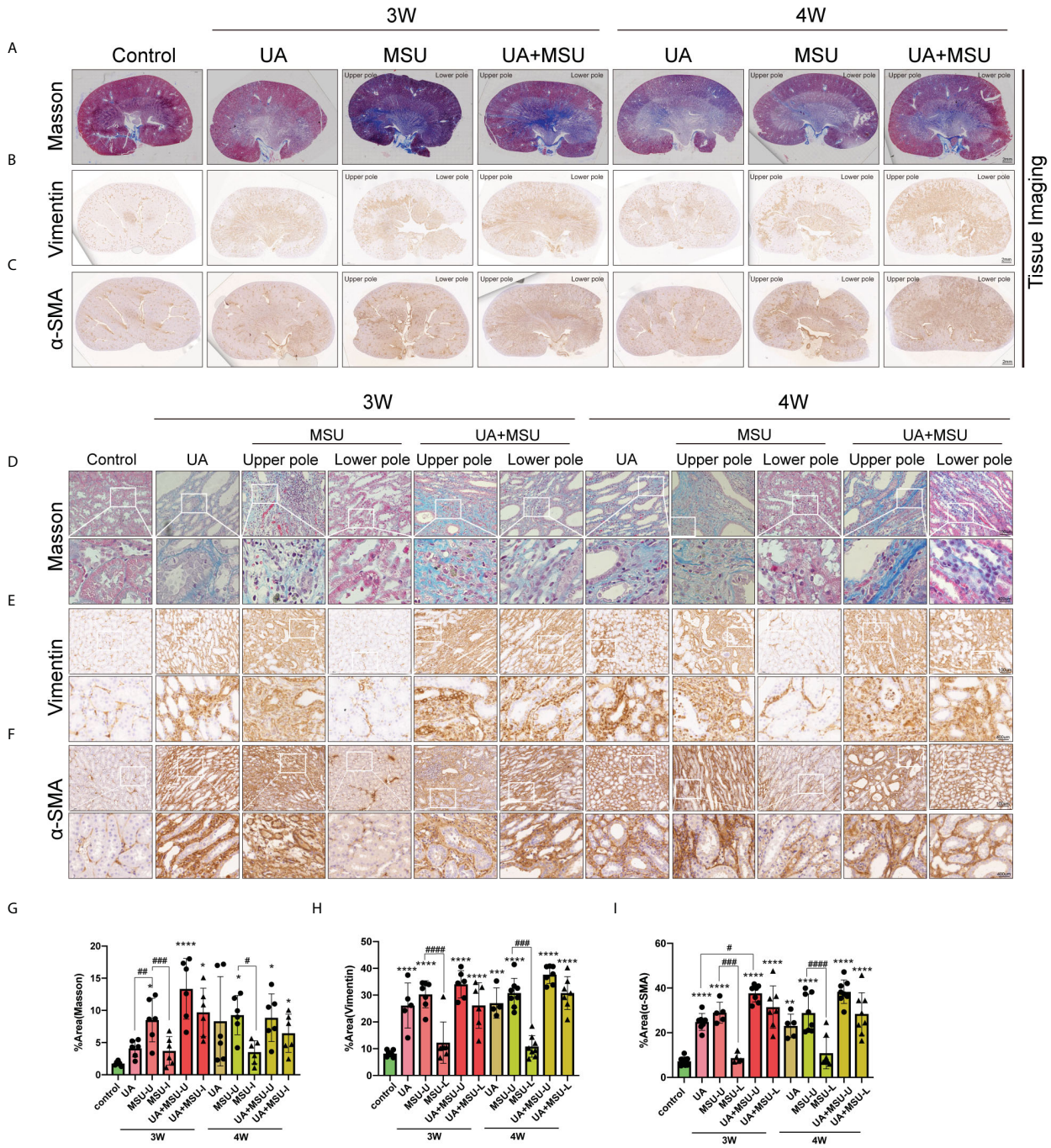

FIGURE 9
Intrarenal injection of MSU crystals into the kidneys of normal rats or PO-induced hyperuricemic rats induces renal interstitial fibrosis, as evidenced by Masson's trichrome staining (for detection of the extent of collagen fibers deposition indicative of fibrosis) and immune-staining of α-SMA (α-smooth muscle actin, a marker of fibrosis) and vimentin (a cytoskeletal protein, a marker of fibrosis) in rat kidney sections. **(A)** Images of kidney sections taken after Masson's trichrome staining. Scale bar = 2μm. Muscle fibers are stained red and collagens are stained blue. **(B)** Images of kidney sections taken after immune staining using anti-Vimentin antibody, HRP-linked secondary antibody and DAB+ [3,3'-diaminobenzidine (DAB+) substratechromogen which results in a brown-colored precipitate at the antigen site. Scale bar = 2μm. **(C)** Images of kidney sections taken after immune staining using anti-α-SMA antibody, HRP-linked secondary antibody and the above-mentioned substrate-chromogen. Scale bar = 2μm. **(D)** Representative images of kidney sections taken after Masson's trichrome staining of connective tissue fibers particularly collagen (blue) (n = 5–8; mean ± SEM). Scale bar = 50 μm. **(E)** Representative images of kidney sections taken after immune-staining using anti-vimentin antibody (brown) (n = 5–8; mean ± SEM). Scale bar = 50 μm. **(F)** Representative images of kidney sections taken after immune-staining using anti-α-SMA antibody (brown) (n = 5–8; mean ± SEM). Scale bar = 50 μm. **(G)** Quantification of the Masson's trichrome stained blue region (for collagen fibers deposition) (n = 5–8; mean ± SEM). **(H)** Quantification of the of brown-stained area for Vimentin expression (n = 5–8; mean ± SEM). **(I)** Quantification of the brown-stained area for α-SMA expression (n = 5–8; mean ± SEM). Rat kidneys were sectioned three or four weeks (3W/4W) after MSU injection/gavage. *, # <0.05; **, ## P < 0.01; ***, ### P < 0.001; ****, #### P < 0.0001.

Regrettably, our study was not designed for a longer observation period to determine the pathological development of rat kidney tissue after MSU crystal injection at 4 weeks. Therefore, extending the observation time after injection might bring some data valuable for the mechanism of pathological progression of disease.

A comparison of renal function indexes, pathological damage and fibrosis in rats subjected to different modelling methods revealed that both MSU crystals and soluble UA in the kidneys are associated with renal impairment, pathological damage and fibrosis. Furthermore, these factors appear to act in a synergistic manner, contributing to the pathogenesis of renal disease. However, the indexes of renal impairment were not identical. MSU crystals primarily affected the excretion or production of sCr, whereas PO and UA gavage primarily affected the excretion or production of sUA, resulting in elevated sUA levels. This is attributed to the fact that PO is a selective competitive inhibitor of uricase/urate oxidase (EC 1.7. 3.3) that causes hyperuricemia by blocking the conversion of uric acid to more soluble allantoin (10). Furthermore, the renal pathology and fibrosis induced by MSU injection only at a specific site of kidney differ from that induced by PO. MSU crystals induce tissue damage, inflammatory cell infiltration, and fibrosis at the site of their action, whereas in PO-induced hyperuricemia, soluble UA induces tissue damage, inflammatory cell infiltration, and fibrosis in all over the kidney KO can cause hyperkalemia which may cause unexpected animal death due to heart failure (15, 16). It is noteworthy that the combined intrarenal injection of MSU and gavage feeding of PO approach resulted in further exacerbation of some renal function parameters, renal pathology and fibrosis. Our results are consistent with recent findings suggesting that soluble UA can trigger renal injury as well as MSU crystals (7, 8). In our study, we administered 750 mg/kg PO and 300 mg/kg UA by gavage, resulting in sUA levels of approximately 250–280 umol/L at weeks 3 and 4. This indicates that this concentration of soluble UA may act as a pro-inflammatory or pathologically damaging agent.

It is believed that the activation of immune cells, primarily macrophages and monocytes, is the primary cause of the inflammatory response induced by MSU crystals (5). The results of our investigation indicate that the intrarenal injection of MSU crystals can result in the infiltration of macrophages into renal tissues and the activation of NLRP3 in macrophages and monocytes. In this study, we did not find any significant effect of injected intrarenal MSU crystals on infiltration of monocytes, which could be due to the imperfect choice of CD11b as the proper marker of the monocytes in renal tissues at this stage of the disease. It has been demonstrated in the literature that monocytes exhibit distinct subtypes of expression at different stages of gout (17), suggesting that future study with appropriate selection markers for staining of different populations of monocytes might give us better conclusive results. Activation of NLRP3 in macrophages and monocytes releases IL-1β (12), which amplifies the inflammatory response. The results indicate that blood levels of IL-1β may be elevated following intrarenal MSU crystal deposition. However, further validation is necessary to ascertain whether the increased IL-1β originates from activated macrophages and monocytes. Furthermore, MSU crystals have been observed to influence the activity of a range of immune cells, thus, the present study might act as the basis for further detailed study identifying and associating which population of infiltrating inflammatory cells in the renal interstitium, are the major players of crystal-induced renal injury and what kind of proinflammatory cytokines they secrete into the extracellular space.

In conclusion, we were able to induce the symptoms of gouty nephropathy in a rat model by intrarenal injection of the suspension of MSU crystals. We verified that the stable presence of MSU crystals (in absence of hyperuricemia) in renal tissue caused infiltration of inflammatory cells accompanied by interstitial fibrosis and tubular injury localized at the site of injection without affecting the other areas of the kidney injected with PBS. Renal impairment was observed four weeks after MSU crystal injection. This strategic study design is effective for studying gouty nephropathy triggered by MSU crystals only, as it isolates from the impact of elevated level of circulating urate.

Data availability statement

The original contributions presented in the study are included in the article/supplementary material. Further inquiries can be directed to the corresponding authors.

Ethics statement

The animal study was approved by Welfare Committee of Guangdong Academy of Chinese Medicine (Approval Document No. 2022051). The study was conducted in accordance with the local legislation and institutional requirements.

Author contributions

DLL: Conceptualization, Data curation, Visualization, Writing – original draft, Writing – review & editing. YL: Validation, Visualization, Writing – review & editing. XC: Visualization, Writing – review & editing. JO: Visualization, Writing – review & editing. DYL: Validation, Writing – review & editing. QW: Validation, Writing – review & editing. XF: Writing – review & editing. HQ: Validation, Writing – review & editing. XW: Writing – review & editing. SW: Writing – review & editing. SY: Writing – review & editing. AL: Writing – review & editing. JZ: Writing – review & editing. XL: Writing – review & editing. GZ: Writing – review & editing. CL: Funding acquisition, Writing – review & editing. WM: Funding acquisition, Writing – review & editing.

Funding

The author(s) declare financial support was received for the research, authorship, and/or publication of this article. This work was supported by National Natural Science Foundation of China 82074376 and 82374388, the Specific Fund of State Key Laboratory of Dampness Syndrome of Chinese Medicine SZ2021ZZ50.

Guangdong Provincial Science and Technology Project 2022A1515012051.

Conflict of interest

The authors declare that the research was conducted in the absence of any commercial or financial relationships that could be construed as a potential conflict of interest.

Publisher's note

References

1. Stamp LK, Farquhar H, Pisaniello HL, Vargas-Santos AB, Fisher M, Mount DB, et al. Management of gout in chronic kidney disease: a G-CAN Consensus Statement on the research priorities. *Nat Rev Rheumatol*. (2021) 17:633–41. doi: 10.1038/s41584-021-00657-4

2. Mei Y, Dong B, Geng Z, Xu L. Excess uric acid induces gouty nephropathy through crystal formation: A review of recent insights. *Front Endocrinol (Lausanne)*. (2022) 13:911968. doi: 10.3389/fendo.2022.911968

3. Wang L, Zhang X, Shen J, Wei Y, Zhao T, Xiao N, et al. Models of gouty nephropathy: exploring disease mechanisms and identifying potential therapeutic targets. *Front Med (Lausanne)*. (2024) 11:1305431. doi: 10.3389/fmed.2024.1305431

4. Sakhaee K. Epidemiology and clinical pathophysiology of uric acid kidney stones. *J Nephrol*. (2014) 27:241–5. doi: 10.1007/s40620-013-0034-z

5. Martinon F, Pétrilli V, Mayor A, Tardivel A, Tschopp J. Gout-associated uric acid crystals activate the NALP3 inflammasome. *Nature*. (2006) 440:237–41. doi: 10.1038/nature04516

6. So AK, Martinon F. Inflammation in gout: mechanisms and therapeutic targets. *Nat Rev Rheumatol*. (2017) 13:639–47. doi: 10.1038/nrrheum.2017.155

7. Anders HJ, Li Q, Steiger S. Asymptomatic hyperuricaemia in chronic kidney disease: mechanisms and clinical implications. *Clin Kidney J*. (2023) 16:928–38. doi: 10.1093/ckj/sfad006

8. Joosten LAB, Crişan TO, Bjornstad P, Johnson RJ. Asymptomatic hyperuricaemia: a silent activator of the innate immune system. *Nat Rev Rheumatol*. (2020) 16:75–86. doi: 10.1038/s41584-019-0334-3

9. Hori T, Ouchi M, Otani N, Nohara M, Morita A, Otsuka Y, et al. The uricosuric effects of dihydropyridine calcium channel blockers in *vivo* using urate under-excretion animal models. *J Pharmacol Sci*. (2018) 136:196–202. doi: 10.1016/j.jphs.2017.11.011

10. Wen S, Wang D, Yu H, Liu M, Chen Q, Bao R, et al. The time-feature of uric acid excretion in hyperuricemia mice induced by potassium oxonate and adenine. *Int J Mol Sci*. (2020) 21:5178. doi: 10.3390/ijms21155178

11. Sellmayr M, Hernandez Petzsche MR, Ma Q, Krüger N, Liapis H, Brink A, et al. Only Hyperuricemia with Crystalluria, but not Asymptomatic Hyperuricemia, Drives Progression of Chronic Kidney Disease. *J Am Soc Nephrol*. (2020) 31:2773–92. doi: 10.1681/ASN.2020040523

12. Bakker PJ, Butter LM, Kors L, Teske GJ, Aten J, Sutterwala FS, et al. Nlrp3 is a key modulator of diet-induced nephropathy and renal cholesterol accumulation. *Kidney Int*. (2014) 85:1112–22. doi: 10.1038/ki.2013.503

13. Shi X, Zhuang L, Zhai Z, He Y, Sun E. Polydatin protects against gouty nephropathy by inhibiting renal tubular cell pyroptosis. *Int J Rheum Dis*. (2023) 26:116–23. doi: 10.1111/1756-185X.14463

14. Lusco MA, Fogo AB, Najafian B, Alpers CE. AJKD atlas of renal pathology: gouty nephropathy. *Am J Kidney Dis*. (2017) 69:e5–6. doi: 10.1053/j.ajkd.2016.11.006

15. Gralla EJ, Crelin ES. Oxonic acid and fetal development: I. Embryotoxicity in mice. *Toxicology*. (1976) 6:289–97. doi: 10.1016/0300-483x(76)90032-9

16. Lin C, Zheng Q, Li Y, Wu T, Luo J, Jiang Y, et al. Assessment of the influence on left ventricle by potassium oxonate and hypoxanthine-induced chronic hyperuricemia. *Exp Biol Med (Maywood)*. (2023) 248:165–74. doi: 10.1177/15353702221120113

17. Gu H, Yu H, Qin L, Yu H, Song Y, Chen G, et al. MSU crystal deposition contributes to inflammation and immune responses in gout remission. *Cell Rep*. (2023) 42:113139. doi: 10.1016/j.celrep.2023.113139

frontiers | Frontiers in Immunology

TYPE Original Research
PUBLISHED 19 July 2024
DOI 10.3389/fimmu.2024.1386939

OPEN ACCESS

EDITED BY
Jixin Zhong,
Huazhong University of Science and Technology, China

REVIEWED BY
Jiaqian Luo,
Cornell University, United States
Min Zhang,
University of Kentucky, United States

*CORRESPONDENCE
Ping Li
graceli008@sohu.com

†These authors have contributed equally to this work

RECEIVED 16 February 2024
ACCEPTED 05 July 2024
PUBLISHED 19 July 2024

CITATION
Chu J, Tian J, Li P, Fu D, Guo L and Sun R (2024) The impact of AIM2 inflammasome-induced pyroptosis on acute gouty arthritis and asymptomatic hyperuricemia patients. *Front. Immunol.* 15:1386939. doi: 10.3389/fimmu.2024.1386939

The impact of AIM2 inflammasome-induced pyroptosis on acute gouty arthritis and asymptomatic hyperuricemia patients

Jiyan Chu[1,2†], Jing Tian[3†], Ping Li[1*], Diyu Fu[1,2], Lin Guo[1] and Rui Sun[1]

[1]Department of Rheumatology, General Hospital of Northern Theater Command, Shenyang, Liaoning, China, [2]Graduate School, Dalian Medical University, Dalian, Liaoning, China, [3]Department of Orthopedics, General Hospital of Northern Theater Command, Shenyang, Liaoning, China

Objective: This study aimed to evaluate the role of absent in melanoma 2 (AIM2) inflammasome-mediated pyroptosis in the pathogenesis of acute gouty arthritis (AGA) and asymptomatic hyperuricemia(AHU).

Methods: A cohort of 30 AGA patients, 30 AHU individuals, and 30 healthy controls (HC) was assembled. Demographic and biochemical data, along with blood samples, were collected. Serum double-stranded DNA (dsDNA) levels were quantified using a fluorescent assay. Transcriptomic and proteomic analysis of AIM2, Caspase-1, GSDMD, IL-1β, and IL-18 in peripheral blood mononuclear cells was performed using qRT-PCR and Western blot. Enzyme-linked immunosorbent assay (ELISA) was employed to measure serum IL-1β and IL-18. Spearman correlation analysis was utilized to assess relationships between variables.

Results: Both AGA and AHU groups demonstrated elevated metabolic indicators and serum levels of dsDNA, IL-1β, and IL-18 compared to the HC group. AGA patients exhibited higher inflammatory markers than the AHU group. In the AGA group, there was a significant increase in the mRNA and protein levels of AIM2, Caspase-1, GSDMD, IL-1β, and IL-18 ($P<0.05$ to $P<0.001$). The AHU group showed higher AIM2, Caspase-1, GSDMD, and IL-18 mRNA levels than the HC group ($P<0.001$ to $P<0.01$), with a non-significant increase in AIM2, GSDMD, and IL-1β proteins ($P>0.05$). In contrast, Caspase-1 and IL-18 proteins were significantly higher in the AHU group ($P<0.05$). Notable correlations were observed between AIM2 protein expression and levels of Caspase-1 and GSDMD in both AGA and AHU groups. In the AGA group, AIM2 protein correlated with IL-1β, but not in the AHU group. The AIM2 protein in the AHU

Abbreviations: AGA, acute gouty arthritis; AHU, asymptomatic hyperuricemia; HC, healthy control; dsDNA, double strand DNA; PBMCs, Peripheral blood mononuclear cells; PRR, pattern recognition receptor; AIM2, Absent in melanoma 2; GSDMD, Gasdermin D; IL-1β, interleukin-1β; ELISA, enzyme-linked immunosorbent assay; UA, uric acid; TC, total cholesterol; TG, triglycerides; Scr, serum creatinine; Ccr, creatinine clearance rate; WBC, white blood cells; ESR, erythrocyte sedimentation rate; CRP, C-reactive protein; BG, blood glucose; ALT, alanine aminotransferase; AST, aspartate aminotransferase; BUN, blood urea nitrogen; NETs, neutrophil extracellular traps.

group was positively associated with IL-18, with no such correlation in the AGA group.

Conclusion: AIM2 inflammasome may play a role in the inflammatory processes of AGA and AHU and that its activation may be related to the pyroptosis pathway.

KEYWORDS

absent in melanoma 2(AIM2), pyroptosis, caspase-1, gasdermin D (GSDMD), acute gouty arthritis, asymptomatic hyperuricemia

Introduction

Gout and asymptomatic hyperuricemia (AHU) are impacting individuals worldwide, with a growing prevalence among younger people (1, 2). Acute gout arthritis (AGA) is an inflammatory disorder characterized by hyperuricemia and the deposition of monosodium urate (MSU) crystals in joints and tissues (3). Patients with AGA have episodes of severe inflammation, swelling, and pain. Without appropriate treatment, chronic gout can lead to cardiovascular disease and renal impairment (1, 3). In hyperuricemia, serum uric acid levels exceed the saturation threshold. The condition is known as asymptomatic hyperuricemia when it occurs in the absence of inflammation caused by monosodium urate crystals (4, 5). Asymptomatic hyperuricemia, traditionally considered a metabolic abnormality linked to gout and kidney stones, is now recognized as a significant risk factor for hypertension, adiposity, diabetes mellitus, hepatic steatosis, chronic nephropathy, and cardiometabolic diseases (5, 6). As safe and effective medications for AGA treatment are lacking, and the necessity of urate-lowering therapy for individuals with asymptomatic hyperuricemia is debatable, there is an urgent need to investigate the etiology of AGA and silent hyperuricemia.

Pyroptosis is a type of inflammatory programmed cell death, first proposed by Brennan and Cookson in 2001 (7). Unlike necrosis and apoptosis, it induces cellular membrane disruption and the secretion of pro-inflammatory cytokines, which amplify the inflammatory response (8). In individuals suffering from gout, the body activates innate immune cells by recognizing MSU through endogenous damage associated molecular patterns (DAMPs), which participate in pyroptosis (9). Pyroptosis is known to occur through three main pathways: the canonical pathway, the non-canonical pathway, and the Caspase-3 mediated pathway (10). The canonical pathway is mediated by inflammasomes and Caspase-1. Upon stimulation by PAMPs or DAMPs, the inflammasomes activate Caspase-1, promoting the maturation and release of pro-inflammatory cytokines like interleukin-1β (IL-1β) and IL-18, as well as the activation of gasdermin D (GSDMD). The activated effector molecule GSDMD forms non-selective pores on the cell membrane, leading to the loss of its integrity (11). Various inflammatory factors are released through these pores, while extracellular substances enter the cell, accelerating cell swelling and organelle damage, ultimately resulting in cell rupture.

Inflammasomes, composed of pattern recognition receptors (PRRs), apoptosis-associated speck-like protein containing a CARD (ASC), and inactive pro-caspase-1, are multiprotein complexes found in the cytoplasm (12). They can only function after they are activated. PRRs serve as the initial signal to induce transcription and synthesis of inactive pro-IL-1β and pro-IL-18. Inflammasomes then act as the second signal to convert pro-caspase-1 to active Caspase-1 (13). The PRRs of inflammasomes mainly include members of the nucleotide-binding oligomerization domain-like receptor (NLR) family and the absent in melanoma 2 (AIM2)-like receptor (ALR) family (14).

Absent in melanoma 2 (AIM2) constitutes a component of the AIM-like receptor (ALR) family, which contains an N-terminal pyrin domain (PYD) and a C-terminal domain that belongs to a group known as hematopoietic, interferon-inducible, nuclear proteins with a 200-amino-acid repeat (HIN-200). This receptor helps recognize cytosolic DNA via its HIN-200 region, which stimulates the adaptor protein ASC to facilitate the oligomerization and subsequent proteolytic maturation of pro-caspase-1 (15, 16). AIM2 is an intracellular DNA sensor that identifies genomic material originating from several sources, such as pathogenic bacteria, viral entities, genotoxic stress from ionizing radiation, and endogenously derived DNA disseminated via exosomal mechanisms (17–21). Researchers have found through experiments that the oligomeric assembly kinetics of the AIM2 inflammasome depends on the chain length of double-stranded DNA (dsDNA). The oligomerization is optimally induced by dsDNA that is 80–200 base pairs in length (22, 23). In the context of autoimmune diseases, such as systemic lupus erythematosus (SLE), rheumatoid arthritis (RA), and Sjögren's syndrome (SS), dysregulated hyperactivation of the AIM2 inflammasome pathway may occur due to the continuous accumulation of self-derived DNA substrates (24–26). However, only a few studies have investigated the role of the AIM2 inflammasome in AGA. Therefore, in this study, we evaluated the expression of AIM2, Caspase 1, and GSDMD in PBMCs of patients diagnosed with AGA and AHU, estimated the levels of the

inflammatory cytokines IL-1β and IL-18 in serum, hope to provide new insights into the involvement of the AIM2 mediated pyroptosis pathway in the development of AGA and strategies for treating gout.

Materials and methods

Participants and samples

Data were collected from patients attending outpatient clinics at the General Hospital of Northern Theater Command between December 2021 and August 2022. The study included 90 male participants aged between 18 and 70 years. Among them, 30 individuals were diagnosed with acute gouty arthritis based on the 2015 ACR/EULAR gout classification criteria and assigned to the AGA group (27). Another 30 individuals were diagnosed with asymptomatic hyperuricemia based on the hyperuricemia criteria (4) and assigned to the AHU group. Finally, 30 healthy participants who visited the medical examination center for a physical examination were assigned to the control group. Care was taken to match the age and gender distribution among the three groups.

The study excluded the following patients: (1) individuals with acute purulent arthritis, traumatic arthritis, and rheumatoid arthritis; (2) those with other crystal-related diseases like calcium pyrophosphate deposition disease; (3) patients with mental disorders, abnormal liver and kidney function, and cardiovascular and cerebrovascular diseases; (4) individuals with secondary gout; (5) pregnant women or those with malignancy.

All procedures used in the study were approved by the Medical Ethics Committee of the General Hospital of Northern Theater Command. Written informed consent was obtained from each participant. Total RNA and protein were extracted from blood samples stored at −80°C for subsequent analyses.

Hematology analysis and determination of biochemical parameters

Peripheral venous blood (8 mL) was collected from the participants and processed by a hematology analyzer to quantify the white blood cell (WBC) count, hemoglobin (Hb) level, and platelet count (PLT). An automated biochemical analyzer was used to determine the levels of fasting blood glucose (FBG), uric acid (UA), triglycerides (TG), total cholesterol (TC), alanine aminotransferase (ALT), aspartate aminotransferase (AST), serum creatinine (Scr), blood urea nitrogen (BUN), erythrocyte sedimentation rate (ESR), and C-reactive protein (CRP). Creatinine clearance rate (Ccr) was calculated using the equation Ccr = (140-age) × body weight (kg)/72×Scr (mg/dL).

Fluorescent quantification for determining serum dsDNA levels

The serum dsDNA was quantified using the Quant-iT PicoGreen dsDNA Kit (Invitrogen, USA), following the manufacturer's instructions. Briefly, 90 μL of TE buffer was added to each well of a 96-well plate, followed by 10 μL of serum. Next, 100 μL of PicoGreen solution diluted 200 times with TE buffer was added to each well. The samples were incubated at room temperature for 10 min in the dark. A BioTek Synergy2 multifunctional microplate reader was used to detect and calculate the concentration of dsDNA under the excitation light at 480 nm and emission light at 520 nm.

Total RNA isolation and real-time PCR analysis

Blood samples were processed using the Whole Blood Total RNA Kit (IVDSHOW, China) to extract total RNA according to the manufacturer's instructions. The RNA was then used to synthesize cDNA using a reverse transcription kit (TaKaRa, Japan). Next, 1uL of the synthesized cDNA was used to measure the mRNA expressions of *AIM2*, *Caspase-1*, and *GSDMD* with specific primers as templates. The primers used in the amplification of the target mRNAs are shown below: *AIM2*: forward: 5′-AGCAA GATATTATCGGCACAGTG-3′, reverse: 5′-GTTCAGCGGGACA TTAACCTT-3′; *Capase-1*: forward: 5′-TTTCCGCAAGGTTCG ATTTTCA-3′, reverse: 5′-GGCATCTGCGCTCTACCATC-3′.

TACCATC-3′; *GSDMD*: forward: 5′-GTGTGTCAACCTGTCT ATCAAGG-3′, reverse: 5′-CATGGCATCGTAGAAGTGGAAG-3′.

CATCGTAGAAGTGGAAG-3′; *IL-18*: forward: 5′-TTCAAGA CCAGCCTGACCAAC-3′, reverse: 5′-GCTCACCACAACCTCTA CCTCC-3′; *IL-1β*: forward: 5′-TGAGCTCGCCAGTGAAATGAT-3′, reverse: 5′-TGCTGTAGTGGTGGTCGGAG-3′; *GAPDH*: forward: 5′-ACAACTTTGGTATCGTGGAAGG-3′.

AAGG-3′, reverse: 5′-GCCATCACGCCACAGTTTC-3′. The analysis was performed using the Applied Biosystems 7500 Real-Time PCR system (Applied Biosystems, USA). The conditions used for thermal cycling were heating at 95°C for 5 min, followed by 40 cycles of denaturation at 95°C for 15s, and annealing at 60°C for 34s. The expression levels of *AIM2*, *Caspase-1*, and *GSDMD* mRNA were analyzed using the 2−ΔΔCT method after normalized by the expression of glyceraldehyde-3-phosphate dehydrogenase (*GAPDH*).

Western blotting

PBMCs from various groups were lysed using a specific lysis buffer for Western blotting and immunoprecipitation. Protein concentrations were measured by the BCA assay kit (abs9232, Absin, China) and normalized. Next, proteins were separated by SDS-PAGE on either 10% or 12% gels (PG112 and PG113, Epizyme Scientific, China) according to their molecular weight and transferred to a 0.45 μm PVDF membrane. The proteins on the membrane were blocked with 5% non-fat milk for two hours at room temperature, then rinsed three times with tris-buffer saline tween (TBST) for 5 min. After rinsing, the protein on the membrane was incubated with primary antibodies against AIM2 (abs125828, rabbit polyclonal, 1:500, Absin, China), Caspase-1

(#3866, rabbit monoclonal, 1:1000, cell signaling technology, Danvers, MA), GSDMD (P57764, rabbit polyclonal, 1:500, Bioss, China), IL-1β (#12703, rabbit monoclonal, 1:1000, cell signaling technology, Danvers, MA), IL-18 (#54943, rabbit monoclonal, 1:1000, cell signaling technology, Danvers, MA), or GAPDH (GB15004, rabbit monoclonal, 1:2000, Servicebio, China) at 4°C on a shaker overnight. After thoroughly washing with TBST, the protein on the membranes was incubated with HRP-conjugated goat anti-rabbit IgG antibodies (GB23303, 1:3,000, Servicebio, China) at room temperature for 2 hours. The protein bands were visualized using an ECL chemiluminescence kit (abs920, Absin, China) and imaged with a GE AI 680 ultra-sensitive multifunctional imaging system. Image J software was used to analyze band intensities and calculate relative protein expression levels.

ELISA

The concentrations of IL-18 and IL-1β in the cell supernatants were quantified using a human enzyme-linked immunosorbent assay kit (No:0139H1, Meimian, China; No: 0181H1, Meimian, China), following the manufacturer's instructions. Duplicate samples were analyzed. The optical density (OD) values of the participants' peripheral blood serum at 450 nm were measured using a Rayto RT-6100 microplate reader. Standard curves were generated by plotting the absorbance values against the graded concentrations of the standards provided with the kits. Positive and negative controls were simultaneously analyzed on the same plate.

Statistical analysis

SPSS 23.0 was used for statistical analysis, and GraphPad Prism 10.1.2 was employed to generate graphs. Quantitative data following a normal distribution were presented as mean ± standard deviation ($\bar{x}$ ± s), and intergroup differences were assessed using Student's t-test. Quantitative data not conforming to a normal distribution were presented as Median (*P*25, *P*75), and intergroup differences were evaluated using the non-parametric Mann-Whitney U test. Intergroup differences were determined using one-way ANOVA followed by Tukey's *post-hoc* test. Spearman correlation analyses were conducted to assess the relationship between variables. A statistically significant difference was defined as $P < 0.05$.

Results

Clinical characteristics and laboratory indices of the three groups

The clinical and laboratory characteristics of the three groups are summarized in Table 1. In contrast to the HC group, both the AGA and AHU groups exhibited significantly elevated levels of body mass index (BMI), uric acid (UA), total cholesterol (TC), triglyceride (TG), and platelet count(PLT). There were no statistically significant distinctions between the AGA and AHU groups. These findings suggest that gout/hyperuricemia is a contributory factor to metabolic syndrome, often accompanied by obesity, hyperlipidemia, and an inflammatory state. The AGA group exhibited significantly higher levels of white blood cells (WBC), erythrocyte sedimentation rate (ESR), and C-reactive protein (CRP) compared to the AHU group, aligning with the characteristic features of an acute gout attack. There were no significant differences in age, blood glucose (BG), alanine aminotransferase (ALT), aspartate aminotransferase (AST), and blood urea nitrogen (BUN) among the three groups. The level of creatinine clearance (Ccr) was higher in both the AGA and AHU groups than the healthy control group, indicating gout/hyperuricemia associated with increased renal blood flow, perfusion, and compensatory renal function.

TABLE 1 Clinical characteristics and laboratory indices of the three groups.

Items	AGA Group (n = 30)	AHU Group (n = 30)	HC Group (n = 30)
Age (year)	33.00 (26.00,39.00)	33.50 (30.50,37.25)	34.50 (28.75,46.50)
BMI (kg/m^2)	28.18 ±2.93$^{\#\#}$	27.40 (25.63,28.40)$^{\#\#}$	23.89 ±2.27
WBC (×10^9/L)	8.85 ±1.74$^{\#\#}$**	6.68 ±1.63	5.80 ±1.21
PLT (×10^9/L)	276.03 ±50.67$^{\#\#}$	247.53 ±43.30$^{\#}$	226.17 ±46.58
ESR (mm/h)	17.70 ±10.94$^{\#\#}$**	3.00 (2.00,6.25)	2.00 (2.00,2.00)
CRP (mg/L)	14.35 (6.85,28.40)$^{\#\#}$**	2.90 (2.90,2.90)	2.90 (2.90,2.90)
UA (μmol/L)	535.37 ±97.02$^{\#\#}$	498.50 (466.00,549.25)$^{\#\#}$	355.10 ±38.35
FBG (mmol/L)	5.31 (5.00,5.66)	5.37 (5.16,5.53)	5.21 ±0.39
TC (mmol/L)	5.29 ±0.86$^{\#\#}$	4.90 (4.59,5.51)$^{\#\#}$	3.67 (3.36,4.48)
TG (mmol/L)	1.83 (1.41,2.76)$^{\#\#}$	2.01 (1.09,3.30)$^{\#\#}$	0.76 (0.65,1.41)
ALT (U/L)	28.50 (21.75,59.25)	26.50 (18.75,37.75)	25.50 (16.75,29.25)
AST (U/L)	22.00 (18.00,34.00)	20.50 (16.75,27.25)	20.50 (18.75,24.25)
BUN (mmol/L)	4.00 (4.00,5.00)	5.00 (4.38,6.00)	5.00 (4.83,6.00)
Scr (μmol/L)	92.53 ±17.00$^{\#\#}$*	84.10 ±9.42	82.83 ±9.19
Ccr (mL/min)	125.89 ±31.22$^{\#}$	127.81 (109.72,140.92)$^{\#}$	109.34 ±18.32

$^{\#}$P<0.05, $^{\#\#}$P<0.01 vs. HC group; *P<0.05, **P<0.01 vs. AHU group.

Serum dsDNA levels of the participants

The serum dsDNA level was significantly higher in the AGA group compared to both the AHU and HC groups, with a highly significant statistical difference ($P < 0.001$). In addition, the AHU group demonstrated a modest elevation in serum dsDNA concentration compared to the HC group, showing a statistically significant variance ($P < 0.05$), as illustrated in Figure 1.

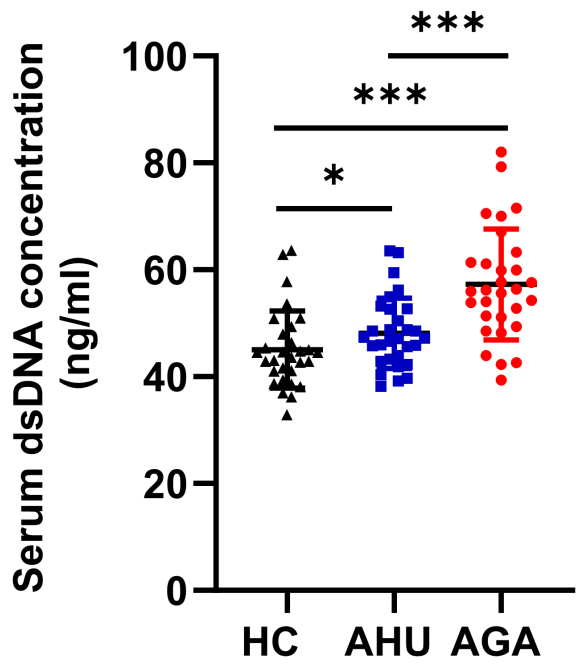

FIGURE 1
Serum dsDNA concentration of the three groups. Each cohort comprised 30 specimens. Serum levels of dsDNA detected by fluorescent quantification were most elevated in the AGA group, succeeded by the AHU group, with both groups exhibiting higher concentrations than the healthy control group. Comparative analyses between groups demonstrated statistically significant variances. *$P < 0.05$, ***$P < 0.001$.

Relative level of expression of the mRNAs of *AIM2*, *Caspase 1*, *GSDMD*, *IL-1β*, and *IL-18* in PBMCs of the three groups

As shown in Figure 2, compared with the HC group, the levels of *AIM2*, *Caspase-1*, *GSDMD*, *IL-1β*, and *IL-18* mRNAs expression were higher in the AGA group, and the difference was statistically significant ($P<0.05$, $P<0.01$, $P<0.001$, $P<0.01$, $P<0.001$). The levels of *AIM2*, *Caspase-1*, *GSDMD*, and *IL-18* mRNA expression were higher in the AHU group than in the HC group, with significant differences ($P<0.001$, $P<0.01$, $P<0.01$, $P<0.01$). The relative mRNA expression levels of *IL-1β* was also slightly higher in the AHU group than in the HC group, however, without statistically significant difference ($P>0.05$). The level of *Caspase-1* mRNA expression was higher in the AGA group than that in the AHU group, while *AIM2* mRNA expression in the AHU group higher than that in the AGA group, and the differences were all significant($P<0.05$ for both).

Relative level of proteins expression of AIM2, caspase 1, GSDMD, IL-1β, and IL-18 in the PBMCs of the three groups

Figure 3 demonstrates that in PBMCs, the levels of proteins such as AIM2, Caspase-1, GSDMD, IL-1β, and IL-18 were markedly elevated in the AGA group when compared to the HC group, with statistical significance ($P<0.05$ for AIM2 and Caspase-1; $P<0.01$ for GSDMD; $P<0.001$ for IL-1β and IL-18). Moreover, the AGA group also displayed a substantial increase in the proteins AIM2, IL-1β, and IL-18 relative to the AHU group, which was statistically significant ($P<0.05$ for each). Conversely, the AHU group showed only a marginal rise in the proteins AIM2, GSDMD, and IL-1β compared to the HC group, which was not statistically significant ($P>0.05$ for all). Nonetheless, the proteins Caspase-1 and IL-18 were present at significantly higher levels in the AHU group compared to the HC group with significant differences ($P<0.05$ for both).

The concentration of IL-18 and IL-1β in the serum of the three groups

Figure 4 indicates that the concentrations of IL-18 in the serum for participants in the AGA and AHU cohorts were markedly elevated compared with the HC group, with the difference being statistically significant ($P < 0.001$ for both). Additionally, the same figure shows that the concentrations of IL-1β in the AGA and AHU groups were significantly greater than in the HC group ($P < 0.001$, $P < 0.05$). However, there was no statistical significance in the concentrations of IL-18 or IL-1β when comparing the AGA group to the AHU group ($P > 0.05$ for both).

Correlation analysis of the level between dsDNA with Clinical characteristics and laboratory indices

Analysis revealed a moderate correlation between dsDNA concentrations and levels of BMI ($r = 0.353$, $P = 0.001$), TG ($r = 0.311$, $P = 0.003$), UA ($r = 0.371$, $P = 0.000$), WBC ($r = 0.360$, $P = 0.000$), ESR ($r = 0.414$, $P = 0.000$) and CRP ($r = 0.427$, $P = 0.000$), and a weak correlation with PLT ($r = 0.277$, $P = 0.008$), TC ($r = 0.242$, $P = 0.022$), serum IL-1β ($r = 0.271$, $P = 0.010$), and serum creatine ($r = 0.252$, $P = 0.017$) in this research (shown in Table 2).

Correlation analysis between AIM2 protein and the inflammasome components

The analysis depicted in Figure 5 indicated a significant correlation between the expression of AIM2 protein and the levels of Caspase-1 and GSDMD proteins in the AHU ($R = 0.517$, $P = 0.016$; $R = 0.761$, $P = 0.000$) and AGA groups ($R = 0.572$, $P = 0.000$; $R = 0.665$, $P = 0.000$). The expression of AIM2 protein correlated with IL-1β protein in the AGA group ($R = 0.304$, $P = 0.026$). However, the expression of AIM2 protein didn't correlate with IL-1β protein in the AHU group ($R = 0.064$, $P = 0.820$). In the AHU group, the AIM2 protein demonstrated a statistically significant positive correlation with IL-18 ($R = 0.478$, $P = 0.028$). Conversely, in the AGA group, there was no observed correlation between AIM2 protein and IL-18 ($R = -0.348$, $P = 0.122$).

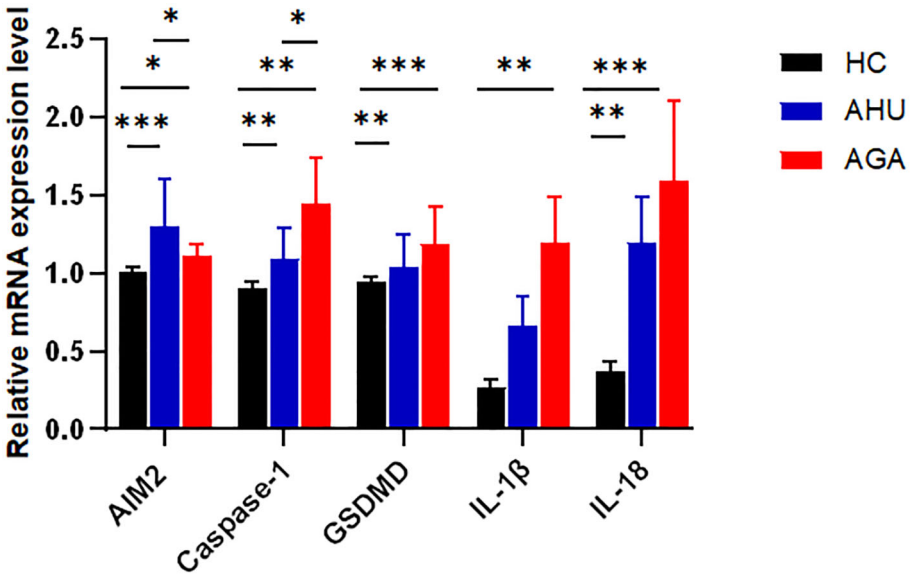

FIGURE 2
The mRNA expression levels of *AIM2, Caspase-1, GSDMD, IL-1β,* and *IL-18* relative to *GAPDH* in PBMCs were determined by real-time PCR in the three groups. Compared with the HC group(n=26), the AGA group (n=26) demonstrated elevated mRNA expression levels of *AIM2, Caspase-1, GSDMD, IL-1β,* and *IL-18*; similarly, the AHU group (n=26) exhibited increased expression levels of *AIM2, Caspase-1, GSDMD*, and *IL-18* mRNAs when compared to the HC group; the level of *AIM2* in the AHU group is higher than the AGA group, and all these differences were statistically significant. **P*<0.05, ***P* < 0.01, ****P* < 0.001.

Discussion

Double-stranded DNA is the sole ligand of the AIM2 inflammasome. To assess the feasibility of this study, we first measured the plasma levels of double-stranded DNA in the healthy control (HC), AHU, and AGA groups. Plasma DNA is non-cellular DNA circulating in the blood, which can exist as DNA-protein complexes or as free DNA fragments. Due to the release of DNA from a small number of necrotic or apoptotic cells during metabolism, the generation and clearance of DNA are in dynamic equilibrium, resulting in a relatively stable low concentration of free DNA in the blood of healthy individuals. Our findings underscore the impact of obesity on chronic low-grade inflammation (see Table 1, Figure 4), which may precipitate DNA damage and impair DNA repair mechanisms, as suggested by previous studies (28, 29). The accumulation of DNA damage, particularly in response to high-fat diets (30, 31), is further supported by the presence of γH2AX foci, an early indicator of DNA double-strand breaks (32). Additionally, the correlation between overweight status in adolescents and lymphocytic DNA damage (33) and the association of obesity with various DNA lesions, including double-strand breaks and oxidative base damage, which are

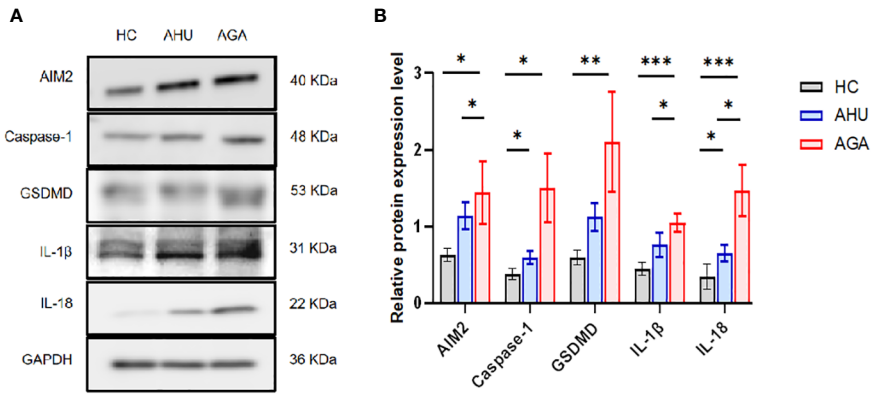

FIGURE 3
The relative expression levels of AIM2, Caspase-1, GSDMD, IL-1β, and IL-18 protein in the PBMCs of the three groups. **(A)** Western blot analysis was conducted to measure the protein expression of AIM2, Caspase-1, GSDMD, IL-1β, and IL-18 relative to GAPDH. **(B)** Statistical analysis was performed to compare relative protein levels of AIM2, Caspase-1, GSDMD, IL-1β, and IL-18 in PBMCs from healthy controls (n=8, n=5, n=6, n=6, n=6), asymptomatic hyperuricemia patients (n=8, n=7, n=7, n=5, n=7), and acute gouty arthritis patients (n=8, n=7, n=7, n=5, n=8). *P<0.05, **P < 0.01, ***P < 0.001.

10.3389/fimmu.2024.1386939

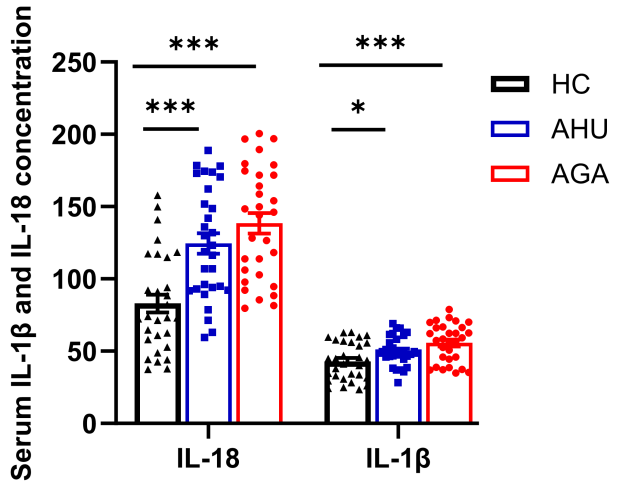

FIGURE 4
The concentration of IL-1β and IL-18 in serum was assessed by ELISA. There were 30 samples in each group. *P<0.05, ***P < 0.001.

reflective of BMI and DNA damage indices (29), align with our observations. In the AHU group, significantly elevated dsDNA levels were observed compared to the HC group (see Figure 1), which is consistent with the metabolic syndrome phenotype characterized by obesity, dyslipidemia, and mild inflammation (see Table 1, Figure 4). Moreover, the AGA group exhibited even higher dsDNA levels (see Figure 1), suggesting a more pronounced inflammatory state. Despite no significant differences in metabolic factors between the AGA and AHU groups, the AGA group displayed significantly higher levels of inflammatory markers, such as platelets, ESR, and CRP (see Table 1). The moderate correlation between dsDNA levels and these inflammatory markers indicates a potential role for acute inflammation in the elevated dsDNA levels observed in AGA patients (refer to Table 2). AGA is recognized as a disease involving a complex interplay within the "metabolic-immune-inflammatory" network, where various inflammatory factors contribute to disease onset and progression (34). The aggregation of neutrophils at crystal deposition sites in AGA and their subsequent release of inflammatory mediators, such as IL-1β and IL-18, initiate a local acute inflammatory response. The activation of IL-1β further stimulates the secretion of neutrophil extracellular traps (NETs), composed of DNA, histones, and granules, which, when in excess or not promptly cleared, can induce the release of damage-associated molecular patterns (DAMPs) and trigger inflammatory responses (35). The detection of dsDNA in the synovial fluid of gout patients (36) and the association of acute gout attacks with increased oxidative stress and mitochondrial dysfunction, leading to the release of mitochondrial DNA into the circulation, further support the role of dsDNA in inflammatory processes. Additionally, the recent discovery that pyroptosis can lead to the loss of membrane integrity and leakage of intracellular contents, potentially contributing to increased dsDNA levels, highlights the complexity of dsDNA dynamics in disease states. In conclusion, the clearance of plasma dsDNA fragments emerges as a promising therapeutic target for AGA.

AIM2 is the sole inflammasome capable of detecting double-stranded DNA. Recent studies using gene-silenced cells and gene-knockout animal models have shown that AIM2 recruits ASC to form an inflammatory complex upon sensing dsDNA fragments of 80-200bp, which in turn activates Caspase-1 and facilitates the maturation and release of inflammatory cytokines such as IL-1β and IL-18 (9, 37). Our understanding of the AIM2 inflammasome's role in pathogenesis has been furthered by observations of its upregulated expression, alongside that of ASC and Caspase-1, in PBMCs and neutrophils of rheumatoid arthritis patients. This increase correlates with the severity of the disease (25). Additionally, impaired DNase1 activity in the ductal tissues of Sjögren's syndrome patients and non-tumor salivary gland epithelial cell lines has been implicated in the insufficient degradation of cytoplasmic DNA, leading to the persistent activation of AIM2 (26). Notably, diminished AIM2 expression in a murine lupus model corresponded to improvement in lupus symptoms (38). Discrepancies may exist, however, between the immune mechanisms of AIM2 inflammasome observed under artificial conditions and those in human physiology. Prior studies have reported elevated dsDNA levels in the peripheral blood of systemic lupus erythematosus (SLE) patients, alongside heightened *AIM2* mRNA expression in PBMCs. These findings were associated with kidney involvement and disease activity (24). Su X and colleagues extended this research by examining AIM2 inflammasome expression in Chinese patients with acute and chronic brucellosis (39). Their findings indicate a disease-stage-specific modulation of AIM2 inflammasome components. Acute brucellosis patients exhibit higher AIM2 and lower ASC expression, while chronic brucellosis patients show the opposite pattern.

TABLE 2 Correlation analysis of the level between dsDNA with Clinical characteristics and laboratory indices.

		BMI	WBC	Hb	PLT	ESR	CRP	FBG	TC
dsDNA	r	0.353**	0.360**	0.113	0.277**	0.414**	0.427**	-0.007	0.242*
	P	0.001	0.000	0.290	0.008	0.000	0.000	0.946	0.022
		TG	UA	ALT	Scr	BUN	Ccr	Serum IL-1β	Serum IL-18
	r	0.311**	0.371**	0.075	0.252*	-0.102	0.118	0.271**	0.149
	P	0.003	0.000	0.484	0.017	0.337	0.267	0.010	0.160

*P<0.05, **P<0.01.

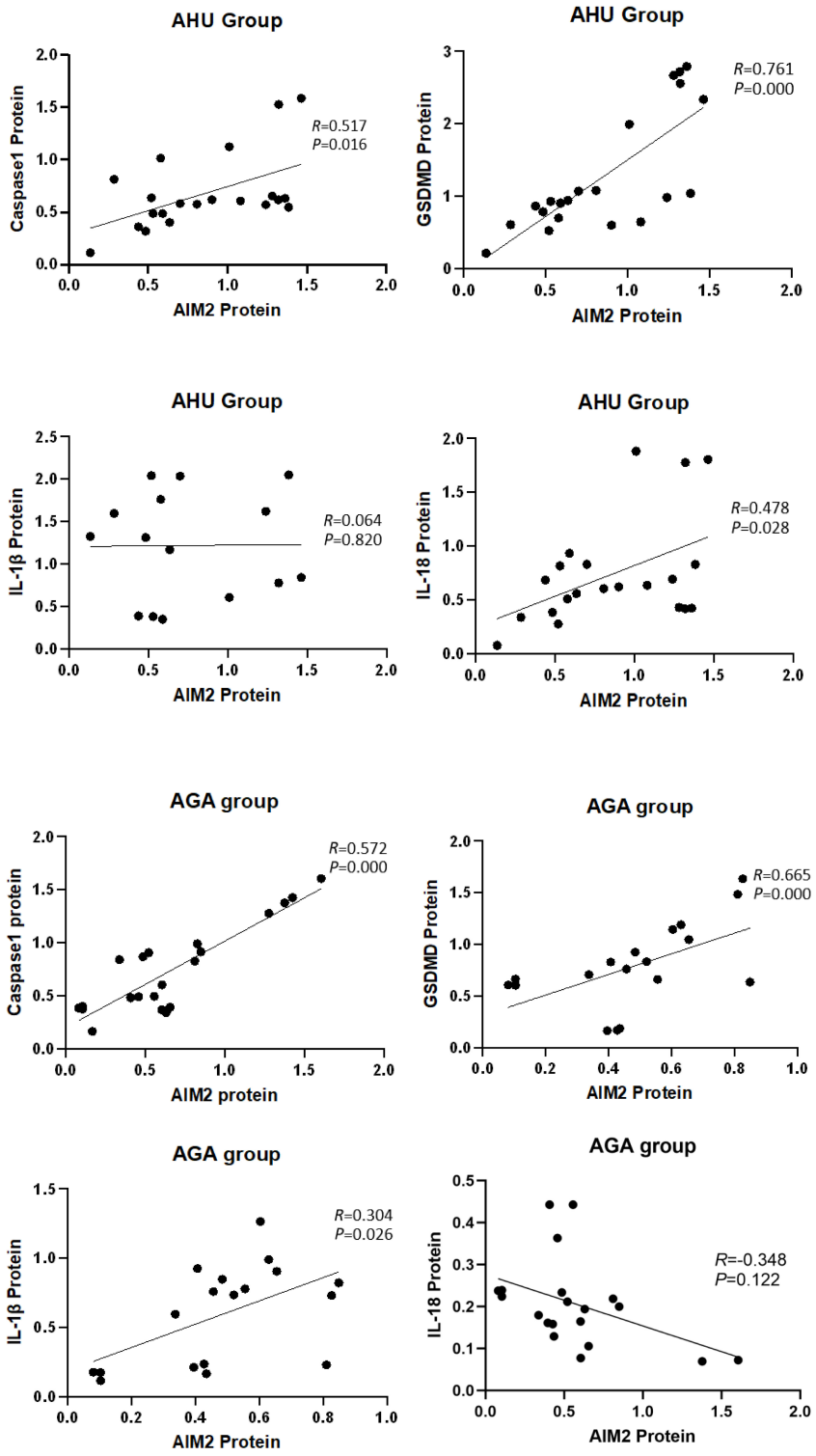

FIGURE 5
Correlation analysis of the AIM2 protein with inflammasome components and inflammatory factors.

Furthermore, acute brucellosis was associated with significantly higher serum IL-18 levels (39). In our study, we document a pronounced upregulation of *AIM2* mRNA and protein in PBMCs from individuals with AGA and AHU, in contrast to healthy controls (as shown in Figures 2, 3). The AHU group displayed a statistically significant higher concentration of AIM2 mRNA compared to the AGA group (indicated in Figure 2). Conversely, the AGA group presented with markedly elevated AIM2 protein levels compared to the AHU group, as shown in Figure 3. These findings suggest a nuanced role of AIM2 in the pathogenesis of gout

and asymptomic hyperuricemia. NLRP3 is a widely recognized inflammasome and identified as playing a crucial role in the innate immune response associated with gout. Both NLRP3 and AIM2 mediated the canonical pyroptotic pathway. The regulation of NLRP3 and AIM2, as well as the release of pro-IL-1β are associated with NF-κB activation through various receptors, culminating in the transcription of pro-inflammatory cytokine genes and the attraction of inflammatory cells to the joint. Mild-to-moderate pyroptosis can be beneficial, but severe pyroptosis can harm the organism by increasing cell death (40). Our findings suggest that the AIM2 inflammasome responds differently in different states, and the influence of AIM2 on patients with AGA and AHU may be biphasic regulation to protect the host. It deserves more attention to investigate further to clarify the impact of AIM2 inflammasome on AHU and AGA. The interplay of NLRP3 and AIM2 in cellular inflammatory dialogues is an area that requires further investigation.

Caspase-1 as one of the members of the caspase family, functions as the principal effector in the canonical pyroptotic pathway. The canonical pyroptotic pathway, also known as the caspase 1-dependent pathway, involves the activation of inflammasomes such as NLRP3, NLRC4, AIM2, Pyrin, etc. In the molecular pathways of MSU-triggered inflammation, the NLRP3 inflammasome plays a crucial role in the innate immune response associated with gout. The NLRP3 inflammasome depends on a two-signal initiation system, which avoids unregulated activation that would damage the host. The first signal stimulates NF-κB via TLR4 and TLR2, leading to the production of pro-IL-1β, pro-caspase-1, and inflammasome components (41). In the cytoplasm, pro-caspase-1 exists as an inactive zymogen. Monosodium urate crystals act as the second activation signal, causing the assembly of inflammasome and activation of Caspase-1 (42). After activation, pro-caspase-1 is cleaved and separated into its subunits, p20 and p10. These subunits combine to form a functional p20/p10 heterodimeric enzyme, which functions as the activated form of Caspase-1, which proteolyzes pro-IL-1β to mature IL-1β (43). IL-1β then interacts with the IL-1β receptor to trigger a downstream signaling cascade involving proinflammatory cytokines and chemokines, resulting in the recruitment of neutrophils and other cells to the site of crystal deposition. Several regulatory mechanisms are involved in NLRP3 inflammasome activation by MSU crystals, such as NETosis, mitochondrial ROS generation, ATP, K+ efflux, etc (41). Many researches besides our previous investigation revealed a significant upregulation of NLRP3 and Caspase-1 expression in the PBMCs of individuals with AGA and the synovial tissues of rodent AGA analogs (44). AIM2 inflammasome is the first non-NLR family member and belongs to the Caspase-1-dependent canonical pyroptotic pathway. In previous studies, elevated expression of AIM2 and Caspase-1 has been observed in rheumatoid arthritis (25), systemic lupus erythematosus (45), Sjogren's syndrome (26), and psoriasis (46). AIM2 mRNA or protein expression is associated with Caspase-1 mRNA or protein expression and is related to disease severity. In this study, we observed an increase in the levels of *Caspase-1* mRNA and protein expression not only in the PBMCs of individuals with AGA but also in those with AHU (see Figures 2, 3). Moreover, the expression levels of the Caspase-1 protein positively correlated with the AIM2 protein (as shown in Figure 5). These findings suggest a synergistic effect between Caspase-1 expression and AIM2 inflammasome activation in the pathogenesis of AGA. Both NLRP3 and AIM2, as components of the canonical pyroptosis pathways, can activate Caspase-1. What relationship do they have in acute gout attacks and asymptomatic hyperuricemia? Further investigation is warranted.

GSDMD and GSDME are members of the Gasdermin superfamily and are closely associated with the process of pyroptosis (47, 48). GSDMD acts as a substrate of Caspase-1 and participates in inflammatory responses (49). Cleaved by Caspase-1, GSDMD converted into C-terminal and N-terminal domains during pyroptosis. The N-terminal domain can initiate pyroptosis, whereas the C-terminal domain inhibits pyroptosis by binding to the N-terminal domain. Caspase-1 can release GSDMD-N from the inhibitory state of GSDMD-C, which leads to the formation of pores on the cell membrane that are 10–20 nm in diameter. Intracellular substances flow out, and water flows in through these pores, leading to an increase in the osmotic pressure, which causes cell membrane rupture and cell pyroptosis (37, 50). Studies have shown that GSDMD-deficient cells cannot undergo pyroptosis upon stimulation, resulting in a significantly reduced mortality rate post-stimulation, indicating that GSDMD plays a crucial role in pyroptosis (51). Previous studies have also documented similar findings, albeit with the involvement of the NLRP3 inflammasome (52, 53). Accompanied by the inhibition of pyroptosis and reduced IL-1β release, the expression of NLRP3 inflammasome was suppressed both *in vivo* and *in vitro* through knockdown of GSDMD (54). In mice with AGA induced by MSU, GSDMD inhibition via siRNA markedly reduced ankle swelling and inflammation, verified by histopathological analysis (54). In this study, the mRNA and protein levels of the *GSDMD* increased significantly in the AGA group compared with the HC group (see Figures 2, 3). *GSDMD* mRNA and protein levels increased in the AHU group compared to the HC group, but only the mRNA level exhibited significance (see Figures 2, 3). GSDMD protein slightly increased without statistically significant, aligning with the AHU group's characteristics. There were significantly positive correlations between the protein levels of GSDMD and AIM2 in both AGA and AHU groups. These findings suggested that GSDMD may be involved in AIM2 inflammasome-mediated pyroptosis in patients with AGA and AHU.

The cytokines IL-1β and IL-18 are common pro-inflammatory factors in the IL-1 family. IL-1β is primarily secreted by activated macrophages, which trigger downstream pro-inflammatory cytokines and chemokines by binding to IL-1β receptors. This interaction stimulates the accumulation of neutrophils and other cells at the site of crystal deposition, thus initiating and exacerbating local inflammatory reactions. IL-18 is found in monocytes in the blood of healthy individuals and epithelial cells throughout the gastrointestinal tract. Its secretion is mainly related to Caspase-1, thereby playing a critical role in inflammation and immune regulation (55). Some studies have found that the concentrations of uric acid in the serum of AGA patients and the synovium of model mice positively correlated with the levels of IL-1β and IL-18 (56, 57). Moreover, IL-1β blockers can significantly improve the symptoms of

acute gouty arthritis (56, 57). In this study, we found that the levels of IL-1β and IL-18 increased significantly in the sera and PBMCs of patients with AGA, and slightly increased in the patients with AHU compared with healthy volunteers (see Figures 2–4). The expression of AIM2 protein correlated with IL-1β protein in the AGA group, on the contrary, unrelated to IL-1β protein in the AHU group (as depicted in Figure 5). AIM2 protein exhibited a positive correlation with IL-18 in the AHU group and no correlation was observed in the AGA groups (as illustrated in Figure 5). This distinction is congruent with the distinct immunopathological characteristics of asymptomatic hyperuricemia and a tendency for acute gouty arthritis spontaneous remission.

To summarize, AGA is a complex disorder characterized by metabolic, immunologic, and inflammatory dysregulation. The AIM2-mediated canonical pathway plays a significant role in the onset and development of AGA and AHU. The modulation of AIM2 inflammasome expression might be a promising target for AGA therapy. Our research has certain limitations, such as a limited sample size, a single-site design, potential selection bias, and neglecting the impact of NLRP3. Therefore, further investigations involving cultivated gene-silenced cells and gene knockout animal models are warranted to elucidate the precise contribution of the AIM2 inflammasome-mediated pyroptosis pathway in AGA and asymptomatic hyperuricemia.

Data availability statement

The original contributions presented in the study are included in the article/supplementary material. Further inquiries can be directed to the corresponding author.

Ethics statement

The studies involving humans were approved by Medical Ethics Committee of the General Hospital of Northern Theater Command. The studies were conducted in accordance with the local legislation and institutional requirements. The participants provided their written informed consent to participate in this study.

Author contributions

JC: Formal analysis, Investigation, Methodology, Software, Writing – original draft. JT: Funding acquisition, Supervision, Writing – review & editing. PL: Conceptualization, Formal analysis, Project administration, Resources, Supervision, Writing – original draft, Writing – review & editing. DF: Data curation, Investigation, Software, Visualization, Writing – original draft. LG: Data curation, Resources, Validation, Visualization, Writing – review & editing. RS: Data curation, Investigation, Validation, Writing – review & editing.

Funding

The author(s) declare financial support was received for the research, authorship, and/or publication of this article. This study was financed by the Natural Science Foundation of Liaoning Province (2019-MS-350).

Conflict of interest

The authors declare that the research was conducted in the absence of any commercial or financial relationships that could be construed as a potential conflict of interest.

Publisher's note

References

1. Liu R, Han C, Wu D, Xia XH, Gu JQ, Guan HX, et al. Prevalence of hyperuricemia and gout in mainland China from 2000 to 2014:A systematic review and meta-analysis. *Biomed Res Int.* (2015) 2015:762820. doi: 10.1155/2015/762820

2. Dehlin M, Jacobsson L, Roddy E. Global epidemiology of gout: prevalence, incidence, treatment patterns and risk factors. *Nat Rev Rheumatol.* (2020) 16:380–90. doi: 10.1038/s41584-020-0441-1

3. Dalbeth N, Gosling AL, Gaffo A, Abhishek A. Gout. *Lancet.* (2021) 397:1843–55. doi: 10.1016/S0140-6736(21)00569-9

4. Bursill D, Taylor W, Terkeltaub R, Kuwabara M, Merriman TR, Grainger R, et al. Gout, hyperuricemia, and crystal-associated disease network consensus statement regarding labels and definitions for disease elements in gout. *Arthritis Care Res.* (2019) 71:427–34. doi: 10.1002/acr.23607

5. Joosten LAB, Crişan TO, Bjornstad P, Johnson RJ. Asymptomatic hyperuricaemia: a silent activator of the innate immune system. *Nat Rev Rheumatol.* (2020) 16:75–86. doi: 10.1038/s41584-019-0334-3

6. Johnson RJ, Bakris GL, Borghi C, Chonchol MB, Feldman D, Lanaspa MA, et al. Hyperuricemia, acute and chronic kidney disease, hypertension, and cardiovascular disease: report of a scientific workshop organized by the National Kidney Foundation. *Am J Kidney Dis.* (2018) 71:851–65. doi: 10.1053/j.ajkd.2017.12.009

7. Cookson BT, Brennan MA. Pro-inflammatory programmed cell death. *Trends Microbiol.* (2001) 9:113–4. doi: 10.1016/S0966-842X(00)01936-3

8. Man SM, Karki R, Kanneganti TD. Molecular mechanisms and functions of pyroptosis, inflammatory caspases, and inflammasomes in infectious diseases. *Immunol Rev.* (2017) 277:61–75. doi: 10.1111/imr.12534

9. Sharma BR, Karki R, Kanneganti TD. Role of AIM2 inflammasome in inflammatory diseases, cancer and infection. *Eur J Immunol.* (2019) 49:1998–2011. doi: 10.1002/eji.201848070

10. Chai R, Li Y, Shui L, Ni L, Zhang A. The role of pyroptosis in inflammatory diseases. *Front Cell Dev Biol.* (2023) 11:1173235. doi: 10.3389/fcell.2023.1173235

11. Gaidt MM, Hornung V. Pore formation by GSDMD is the effector mechanism of pyroptosis. *EMBO J.* (2016) 35:2167–9. doi: 10.15252/embj.201695415

12. Lu A, Magupalli VG, Ruan J, Yin Q, Atianand MK, Vos MR, et al. Unified polymerization mechanism for the assembly of ASC-dependent inflammasomes. *Cell.* (2014) 156:1193–206. doi: 10.1016/j.cell.2014.02.008

13. Broz P, Dixit VM. Inflammasomes: mechanism of assembly, regulation, and signaling. *Nat Rev Immunol*. (2016) 16:407–20. doi: 10.1038/nri.2016.58

14. Man SM, Kanneganti TD. Regulation of inflammasome activation. *Immunol Rev*. (2015) 265:6–21. doi: 10.1111/imr.12296

15. Fernandes-Alnemri T, Yu JW, Datta P, Wu J, Alnemri ES. AIM2 activates the inflammasome and cell death in response to cytoplasmic DNA. *Nature*. (2009) 458:509–13. doi: 10.1038/nature07710

16. Hornung V, Ablasser A, Charrel-Dennis M, Bauernfeind F, Horvath G, Caffrey DR, et al. AIM2 recognizes cytosolic dsDNA and forms a caspase-1-activating inflammasome with ASC. *Nature*. (2009) 458:514–8. doi: 10.1038/nature07725

17. Hu B, Jin C, Li HB, Tong J, Ouyang X, Cetinbas NM, et al. The DNA-sensing AIM2 inflammasome controls radiation-induced cell death and tissue injury. *Science*. (2016) 354:765–8. doi: 10.1126/science.aaf7532

18. Lian Q, Xu J, Yan S, Huang M, Ding H, Sun X, et al. Chemotherapy-induced intestinal Inflammatory Responses are Mediated by Exosome Secretion of Double-Strand DNA via AIM2 Inflammasome Activation. *Cell Res*. (2017) 27:784–800. doi: 10.1038/cr.2017.54

19. Yogarajah T, Ong KC, Perera D, Wong KT. AIM2 inflammasome-mediated pyroptosis in enterovirus A71-infected neuronal cells restricts viral replication. *Sci Rep*. (2017) 7:5845. doi: 10.1038/s41598-017-05589-2

20. Lugrin J, Martinon F. The AIM2 inflammasome: sensor of pathogens and cellular perturbations. *Immunol Rev*. (2018) 281:99–114. doi: 10.1111/imr.12618

21. Moriyama M, Nagai M, Maruzuru Y, Koshiba T, Kawaguchi Y, Ichinohe T. Influenza virus-induced oxidized DNA activates inflammasomes. *iScience*. (2020) 23:101270. doi: 10.1016/j.isci.2020.101270

22. Jin T, Perry A, Jiang J, Smith P, Curry JA, Unterholzner L, et al. Structures of the HIN domain: DNA complexes reveal ligand binding and activation mechanisms of the AIM2 inflammasome and IFI16 receptor. *Immunity*. (2012) 36:561–71. doi: 10.1016/j.immuni.2012.02.014

23. Matyszewski M, Morrone SR, Sohn J. Digital signaling network drives the assembly of the AIM2-ASC inflammasome. *Proc Natl Acad Sci USA*. (2018) 115:E1963–e1972. doi: 10.1073/pnas.1712860115

24. Choubey D, Panchanathan R. Absent in melanoma 2 proteins in SLE. *Clin Immunol*. (2017) 176:42–8. doi: 10.1016/j.clim.2016.12.011

25. Mendez-Frausto G, Medina-Rosales MN, Uresti-Rivera EE, Baranda-Cándido L, Zapata-Zúñiga M, Bastián Y, et al. Expression and activity of AIM2-inflammasome in rheumatoid arthritis patients. *Immunobiology*. (2020) 225:151880. doi: 10.1016/j.imbio.2019.11.015

26. Vakrakou AG, Svolaki IP, Evangelou K, Gorgoulis VG, Manoussakis MN. Cell-autonomous epithelial activation of AIM2 (Absent in melanoma-2) inflammasome by cytoplasmic DNA accumulations in primary sjögren's syndrome. *J Autoimmun*. (2020) . 108:102381. doi: 10.1016/j.jaut.2019.102381

27. Neogi T, Jansen TL, Dalbeth N, Fransen J, Schumacher HR, Berendsen D, et al. 2015 Gout classification criteria: an American College of Rheumatology/European League Against Rheumatism collaborative initiative. *Ann Rheum Dis*. (2015) 74:1789–98. doi: 10.1136/annrheumdis-2015-208237

28. Kay J, Thadhani E, Samson L, Engelward B. Inflammation-induced DNA damage, mutations and cancer. *DNA Repair (Amst)*. (2019) 83:102673. doi: 10.1016/j.dnarep.2019.102673

29. Wlodarczyk M, Nowicka G. Obesity, DNA damage, and development of obesity-related diseases. *Int J Mol Sci*. (2019) 20:1146. doi: 10.3390/ijms20051146

30. Zwamborn RA, Slieker RC, Mulder PC, Zoetemelk I, Verschuren L, Suchiman HE, et al. Prolonged high-fat diet induces gradual and fat depot-specific DNA methylation changes in adult mice. *Sci Rep*. (2017) 7:43261. doi: 10.1038/srep43261

31. Keleher MR, Zaidi R, Hicks L, Shah S, Xing XY, Li DF, et al. A high-fat diet alters genome-wide DNA methylation and gene expression in SM/J mice. *BMC Genomics*. (2018) 19:888. doi: 10.1186/s12864-018-5327-0

32. Redon CE, Nakamura AJ, Martin OA, Parekh PR, Weyemi US, Bonner WM. Recent developments in the use of γ-H2AX as a quantitative DNA double strand break biomarker. *Aging (Albany NY)*. (2011) 3:168–74. doi: 10.18632/aging.v3i2

33. Usman M, Woloshynowych M, Britto JC, Bilkevic I, Glassar B, Chapman S, et al. Obesity, oxidative DNA damage and vitamin D as predictors of genomic instability in children and adolescents. *Int J Obes (Lond)*. (2021) 45:2095–107. doi: 10.1038/s41366-021-00879-2

34. Bodofsky S, Merriman TR, Thomas TJ, Schlesinger N. Advances in our understanding of gout as an auto-inflammatory disease. *Semin Arthritis Rheum*. (2020) 50:1089–100. doi: 10.1016/j.semarthrit.2020.06.015

35. Vedder D, Gerritsen M, Duvvuri B, van Vollenhoven RF, Nurmohamed MT, Lood C. Neutrophil activation identifies patients with active polyarticular gout. *Arthritis Res Ther*. (2020) 22:148. doi: 10.1186/s13075-020-02244-6

36. Mitroulis I, Kambas K, Ritis K. Neutrophils, IL- 1β, and gout: is there a link? *Semin Immunopathol*. (2013) 35:501–12. doi: 10.1007/s00281-013-0361-0

37. Broz P, Pelegrin P, Shao F. The gasdermins are a protein family executing cell death and inflammation. *Nat Rev Immunol*. (2020) 20:143–57. doi: 10.1038/s41577-019-0228-2

38. Yang M, Long D, Hu L, Zhao Z, Li Q, Guo Y, et al. AIM2 deficiency in B cells ameliorates systemic lupus erythematosus by regulating Blimp-1-Bcl-6 axis-mediated B-cell differentiation. *Signal Transduct Target Ther*. (2021) 6:341. doi: 10.1038/s41392-021-00725-x

39. Su X, Zhao SG, Song YJ. Expression of NLRP3 and AIM2 inflammasome in Peripheral blood in Chinese patients with acute and chronic brucellosis. *Sci Rep*. (2022) 12:15123. doi: 10.1038/s41598-022-19398-9

40. Lu F, Lan Z, Xin Z, He C, Guo Z, Xia X, et al. Emerging insights into molecular mechanisms underlying pyroptosis and functions of inflammasomes in diseases. *J Cell Physiol*. (2020) 235:3207–21. doi: 10.1002/jcp.29268

41. He Y, Hara H, Núñez G. Mechanism and regulation of NLRP3 inflammasome activation. *Trends Biochem Sci*. (2016) 41:1012–21. doi: 10.1016/j.tibs.2016.09.002

42. So AK, Martinon F. Inflammation in gout: mechanisms and therapeutic targets. *Nat Rev Rheumatol*. (2017) 13:639–47. doi: 10.1038/nrrheum.2017.155

43. Boucher D, Monteleone M, Coll RC, Chen KW, Ross CM, Teo JL, et al. Caspase-1 self-cleavage is an intrinsic mechanism to terminate inflammasome activity. *J Exp Med*. (2018) 215:827–40. doi: 10.1084/jem.20172222

44. Tian J, Wang BC, Xie B, Liu X, Zhou D, Hou X, et al. Pyroptosis inhibition alleviates potassium oxonate- and monosodium urate-induced gouty arthritis in mice. *Mod Rheumatol*. (2022) 32:221–30. doi: 10.1080/14397595.2021.1899569

45. Shin JI, Lee KH, Joo YH, Lee JM, Jeon J, Jung HJ, et al. Inflammasomes and autoimmune and rheumatic diseases: A comprehensive review. *J Autoimmun*. (2019) .103:102299. doi: 10.1016/j.jaut.2019.06.010

46. Dombrowski Y, Peric M, Koglin S, Kammerbauer C, Göß C, Anz D, et al. Cytosolic DNA triggers inflammasome activation in keratinocytes in psoriatic lesions. *Sci Transl Med*. (2011) 3:82ra38. doi: 10.1126/scitranslmed.3002001

47. Qiu S, Liu J, Xing F. 'Hints'in the killer protein gasdermin D: unveiling the secrets of gasdermins driving cell death. *Cell Death Differ*. (2017) 24:588–96. doi: 10.1038/cdd.2017.24.2020.02.002

48. Fischer FA, Chen KW, Bezbradica JS. Posttranslational and therapeutic control of gasdermin-mediated pyroptosis and inflammation. *Front Immunol*. (2021) 12:661162. doi: 10.3389/fimmu.2021.661162

49. Shi J, Zhao Y, Wang K, Shi X, Wang Y, Huang H, et al. Cleavage of GSDMD by inflammatory caspases determines pyroptotic cell death. *Nature*. (2015) 526:660–5. doi: 10.1038/nature15514

50. Wang K, Sun Q, Zhong X, Zeng M, Zeng H, Shi X, et al. Structural mechanism for GSDMD targeting by autoprocessed caspases in pyroptosis. *Cell*. (2020) 180:941–55. doi: 10.1016/j.cell

51. Bergsbaken T, Fink SL, Cookson BT. Pyroptosis: host cell death and inflammation. *Nat Rev Microbiol*. (2009) 7:99–109. doi: 10.1038/nrmicro2070

52. Martinon F, Petrilli V, Mayor A, Tardivel A, Tschopp J. Gout-associated uric acid crystals activate the NALP3 inflammasome. *Nature*. (2006) 440:237–41. doi: 10.1038/nature04516

53. Hao K, Jiang W, Zhou M, Li H, Chen Y, Jiang F, et al. Targeting BRD4 prevents acute gouty arthritis by regulating pyroptosis. *Int J Biol Sci*. (2020) 16:3163–73. doi: 10.7150/ijbs.46153

54. Ye SM, Zhou MZ, Jiang WJ, Liu CX, Zhou ZW, Sun MJ, et al. Silencing of Gasdermin D by siRNA-Loaded PEI-Chol Lipopolymers Potently Relieves Acute Gouty Arthritis through Inhibiting Pyroptosis. *Mol Pharm*. (2021) 18:667–78. doi: 10.1021/acs.molpharmaceut.0c00229

55. Kaplanski G. Interleukin-18: Biological properties and role in disease pathogenesis. *Immunol Rev*. (2018) 281:138–53. doi: 10.1111/imr.12616

56. Han W, Chao H, Xie J, Yang C, Zhao Y, Guo Y, et al. Doliroside A attenuates monosodium urate crystal-induced inflammation by targeting NLRP3 inflammasome. *Eur J Pharmacol*. (2014) 740:321–8. doi: 10.1016/j.ejphar.2014.07.023

57. Tian J, Zhou D, Xiang L, Liu X, Zhang H, Wang B, et al. miR-223–3p inhibits inflammation and pyroptosis in monosodium urate-induced rats and fibroblast-like synoviocytes by targeting NLRP3. *Clin Exp Immunol*. (2021) 204:396–410. doi: 10.1111/cei.13587

frontiers | Frontiers in Genetics

TYPE Brief Research Report
PUBLISHED 25 September 2024
DOI 10.3389/fgene.2024.1423714

OPEN ACCESS

EDITED BY
Jing Chen,
Cincinnati Children's Hospital Medical Center, United States

REVIEWED BY
Qing Li,
Vanderbilt University Medical Center, United States
Xinping Cui,
University of California, Riverside, United States

*CORRESPONDENCE
Jan-Gowth Chang,
jgchang99@gmail.com
Grace S. Shieh,
gshieh@stat.sinica.edu.tw

†These authors have contributed equally to this work

‡PRESENT ADDRESS
Ya-Sian Chang,
Precision and Cell Center, Show Chwan Memorial Hospital, Changhua, Taiwan
Jan-Gowth Chang,
Office of Superintendent, Hualien Tzu Chi Hospital, Hualien, Taiwan

RECEIVED 26 April 2024
ACCEPTED 28 August 2024
PUBLISHED 25 September 2024

CITATION
Tseng Y-P, Chang Y-S, Mekala VR, Liu T-Y, Chang J-G and Shieh GS (2024) Whole-genome sequencing reveals rare variants associated with gout in Taiwanese males. *Front. Genet.* 15:1423714.
doi: 10.3389/fgene.2024.1423714

Whole-genome sequencing reveals rare variants associated with gout in Taiwanese males

Yu-Ping Tseng[1†], Ya-Sian Chang[2†‡], Venugopala R. Mekala[1], Ting-Yuan Liu[3], Jan-Gowth Chang[4*‡] and Grace S. Shieh[1,5,6,7*]

[1]Institute of Statistical Science, Academia Sinica, Taipei, Taiwan, [2]Department of Pathology, Chung Shan Medical University Hospital, Taichung, Taiwan, [3]Department of Medical Research, China Medical University Hospital, Taichung, Taiwan, [4]Department of Laboratory Medicine, China Medical University Hospital, Taichung, Taiwan, [5]Bioinformatics Program, Taiwan International Graduate Program, Academia Sinica, Taipei, Taiwan, [6]Data Science Degree Program, Academia Sinica and National Taiwan University, Taipei, Taiwan, [7]Genome and Systems Biology Degree Program, Academia Sinica and National Taiwan University, Taipei, Taiwan

To identify rare variants (RVs) of gout, we sequenced the whole genomes of 321 male gout patients and combined these with those of 64 male gout patients and 682 normal controls at Taiwan Biobank. We performed ACAT-O to identify 682 significant RVs ($p < 3.8 \times 10^{-8}$) clustered on chromosomes 1, 7, 10, 16, and 18. To prioritize causal variants effectively, we sifted them by Combined Annotation-Dependent Depletion score >10 or |effect size| ≥ 1.5 for those without CADD scores. In particular, to the best of our knowledge, we identified the rare variants rs559954634, rs186763678, and 13-85340782-G-A for the first time to be associated with gout in Taiwanese males. Importantly, the RV rs559954634 positively affects gout, and its neighboring gene *NPHS2* is involved in serum urate and expressed in kidney tissues. The kidneys play a major role in regulating uric acid levels. This suggests that rs559954634 may be involved in gout. Furthermore, rs186763678 is in the intron of *NFIA* that interacts with *SLC2A9,* which has the most significant effect on serum urate. Note that gene-gene interaction *NFIA-SLC2A9* is significantly associated with serum urate in the Italian MICROS population and a Croatian population. Moreover, 13-85340782-G-A significantly affects gout susceptibility (odds ratio 6.0; P = 0.038). The >1% carrier frequencies of these potentially pathogenic (protective) RVs in cases (controls) suggest the revealed associations may be true; these RVs deserve further studies for the mechanism. Finally, multivariate logistic regression analysis shows that the rare variants rs559954634 and 13-85340782-G-A jointly are significantly associated with gout susceptibility.

KEYWORDS

association study, CADD, gout, rare variant, serum urate, whole-genome sequencing

Introduction

Gout is a joint and excruciating inflammatory arthritis caused by hyperuricemia and inflammation dysregulation. Furthermore, gout and serum urate levels are heritable. Several genes reported to be associated with serum uric acid (SUA) or gout are involved in the renal urate transporter system, such as *SLC22A12* (Enomoto et al., 2002), *SLC2A9* (Matsuo et al., 2008; Dinour et al., 2010) and *ABCG2* (Matsuo et al., 2009; Higashino et al., 2017) that modulate uric acid levels (Reginato et al., 2012; Chen et al., 2018). However, the pathogenic mechanisms of hyperuricemia and gout differ. Furthermore, although many common

variants of gout have been discovered, they can not fully explain its susceptibility. Moreover, most of the 400 million detected variants from the ~53 K diverse human genomes are rare, and functional variants tend to be rare (Taliun et al., 2021). Thus, we aim to discover novel rare variants that may cause gout in this study.

Many common variants associated with gout have been reported, e.g., rs22331142 in *ABCG2* (Chen et al., 2018) in a Taiwanese population. Matsuo and colleagues sequenced *ABCG2* to reveal multiple common and rare variants in a Japanese population (Higashino et al., 2017). Nevertheless, most of the variants for gout identified thus far are common variants (MAF > 5%). In this study, we aim to identify rare variants (MAF < 1%) that are associated with gout in male Taiwanese, as rare variants can have much larger per-allele effect sizes than common variants (Cheng et al., 2022). We integrated whole genome sequencing (WGS) data of 321 male gout patients from China Medical University Hospital (CMUH), 64 male gout patients, and 682 normal controls from Taiwan Biobank (TWB), to reveal rare variants associated with gout disease.

As rare variants appear very infrequently in the population, set-based methods that jointly analyze variants in a set are much more powerful than the single-variant analysis applied to common variants in genome-wide association studies (GWASs). Thus, we applied ACAT-O (Liu et al., 2019), which combines the strength of the sequence kernel association test (SKAT; Wu et al., 2011), the burden test (Li and Leal, 2008; Madsen and Browning, 2009; Price et al., 2010) and ACAT-V test (Liu et al., 2019). The power of ACAT-O to detect rare variants is robust against the sparsity of causal variants and the directionality of effects. After the rare variants associated with gout are detected, we further sift these variants by their Combined Annotation-Dependent Depletion (CADD (Kircher et al., 2014; Rentzsch et al., 2019; van der Velde et al., 2015), scores. CADD is a widely used measure of variant deleteriousness, and it can prioritize causal variants in genetic analysis. Next, we compute the odds ratio and proportion test of the rare variants with CADD ≥10 or |effect size| ≥ 1.5 for those without CADD scores.

Materials and methods

Study population

This study aimed to identify genes and rare variants associated with gout in Taiwanese male patients. Because there were no normal controls at China Medical University Hospital(CMUH henceforth, Taichung, Taiwan), we integrated the WGS data from CMUH with those from the Taiwan Biobank (TWB henceforth, Taipei, Taiwan) database. There were 321 male gout patients recruited at CMUH; 64 male gout patients and 682 normal controls (with serum urate level <6 mg/dL; according to the 2012 guideline of the American College of Rheumatology) from TWB, which provided WGS data, age, gout annotation, and serum urate levels for each sample. The 746 WGS data from TWB were the total male subjects sequenced when we started this investigation. The clinical information of gout patients and normal control analyzed are in Supplementary Table S1.

TWB is a database established in 2012 for research, a prospective study of 200,000 individuals aged 30–70 recruited from Taiwan. TWB consists of individuals, predominantly of Han Chinese ancestry, whose genomic profiles were integrated with lifestyle patterns to study the relationships between diseases and genetics. All participants underwent biochemical tests with blood and urine specimens and physical examination; they all signed informed consent for genotyping. The phenotype of gout disease was the self-report of physician-diagnosed gout, which was reported to retain good reliability and sensitivity (McAdams et al., 2011).

The IRB-BM committee of Academia Sinica (AS-IRB02-113170) and the CMUH Institutional Review Board in Taiwan (CMUH108-REC1-091) approved this study. All data from human participants were obtained from CMUH and the Taiwan Biobank database, for which data sharing and data linkage were parts of the consent, so a waiver of consent was granted by the CMUH IRB. Both the Declaration of Helsinki and the Good Clinical Practice Guidelines were followed, and informed consent was signed by all participants.

Genotyping

The whole genomes of male gout patients at CMUH and participants of TWB were sequenced by the Illumina NovaSeq 6000 platform at least 30x depth, mapped to reference genome (hg38) by Dragon and BWA, and variant calling (.gvcf) performed by Dragon and GATK, respectively; both .gvcf files were annotated by VEP (McLaren et al., 2016). As we only assessed .vcf files from TWB, we combined the .bed files (converted by PLINK version 1.9) from the two sources. Because the batch effect of the union of the called variants from both sites could not be adjusted well even using 99 principle components (PCs), we intersected both sets of variants to result in the overlappings, and we called these SNPs CMUH_TWB data henceforth.

Quality control

The standard per-individual and per-marker quality control (Anderson, et al., 2010) were performed on the CMUH_TWB data using PLINK 1.9 software. We first adopted the procedure of per-individual quality control. Individuals were excluded if identification of 1) individuals with incorrectly recorded or missing sex status, 2) individuals with genotyping call rates below 90% or outlying heterozygosity rate, namely homozygosity rate out of the sample mean ±3 s.e. confidence bounds, 3) individuals of divergent ancestry, or 4) uric acid levels missing. Moreover, we implemented per-marker quality control procedures to remove SNPs if 1) genotyping call rate below 100% (i.e., no missing allowed) or significant deviation from Hardy-Weinberg equilibrium in the controls ($p < 0.001$ and MAF >1%).

Finally, SNPs with MAF <1% were called to result in 8,703,559 rare variants, which satisfied the above QC procedures, from 287 CMUH and 63 TWB male gout patients and 671 TWB male controls. Supplementary Figure S1 shows that all subjects from CMUH and TWB share the same genetic background.

Batch effect and population stratification correction by PCA

To adjust the effect that the integrated SNPs were from two resources and population stratification (different ethnic groups among Taiwanese, e.g. Fujian and Hakka), we performed PCA on SNPs with MAF >1% and satisfying the Hardy-Weinberg equilibrium QC. When plotted against PC9 and PC10, the SNPs of the two sites were finally mixed, so the first nine PCs were used for correction of the batch effects; PCA plots are in Supplementary Figure S2).

Uncovering significant rare variants by ACAT-O

We applied the aggregated Cauchy association test (ACAT-O (Liu, et al., 2019); in R software to identify significant rare variants. ACATO is a set-based test that is particularly powerful when sparse causal variants exist in a variant set (window). ACAT-O first transforms the *p*-value of the burden test (Li and Leal, 2008; Madsen and Browning, 2009; Price, et al., 2010), SKAT test (Wu, et al., 2011), and ACAT-V (Liu, et al., 2019), to Cauchy variables. Then ACAT-O combines the above variables, each with two choices of weights, as the test statistic and evaluates the significance. We used the default Beta (1, 25) and Beta (1, 1) for the above two weights.

We split the 8,703,559 rare variants into ~1.31 M windows of 4 kb with 2 kb overlaps in adjacent windows. In each window, we conducted ACAT-V, which implemented a logistic regression of gout status on all variants in the window conditional on covariates of age, uric acid levels, and the aforementioned nine PCs; similarly, the burden test and SKAT were also implemented. The significance threshold of ACAT-O was $p < 3.8 \times 10^{-8}$ after Bonferroni correction for multiple testing of ~1.31 million windows.

Statistical analysis

There are 682 rare variants (MAF < 1%) among the 61 windows uncovered to be significantly associated with gout susceptibility by ACAT-O ($P < 3.8 \times 10^{-8}$), and these RVs are deemed significant according to ACAT-O. For each significant rare variant, we computed the odds ratio and the associated 95% confidence interval, as well as the two-sample t-test for the equality of the proportion in cases and controls. Finally, logistic regression adjusted on serum urate levels was performed to evaluate the effects of rare variants on gout susceptibility.

Results

Study population

This study includes 350 male gout patients (287 from China Medical University Hospital (CMUH henceforth) and 63 from the Taiwan Biobank database (TWB henceforth)), whose data passed our QC procedures. In addition, it also included 671 male normal controls from TWB, which provided gout history, uric acid levels, demographic, and whole genome sequencing data. There were 40, 644, 135 and 42, 571, 357 SNPs called from the WGS data of CMUH and TWB, respectively. We intersected the SNP called from the two sites (CMUH_TWB) and subjected the 18, 426, 362 overlapping SNPs to quality check, of which 8,703,559 rare variants (MAF < 1%) satisfied the QC procedures; please see SNP genotyping and quality control in Materials and Methods for details.

The mean age of male gout patients and normal controls were 49.56 years (±15.99) and 49.69 years (±11.58), respectively, which was not significantly different ($P = 0.888$). There was too many mssing values of the covariate BMI for patients from CMUH, so BMI was not analyzed. However, uric acid of the two groups was significantly different ($P < 2.2 \times 10^{-16}$); see Supplementary Table S1 for details. In the subsequent analysis, serum urate was treated as a potential confounder of gout.

Results of rare variant association tests

The overall rare-variant analysis identified 61 windows significantly associated with gout disease ($p < 3.8 \times 10^{-8}$; ACAT-O), out of 1,314,794 windows analyzed. These windows consist of 682 distinct rare variants (Supplementary Table S2). The Manhattan plot depicted all *p*-values after the negative logarithm transformation of all ~8.7 million RVs that passed QC across 22 pairs of autosomal chromosomes; note all RVs in a window share the same *p*-value from ACAT-O (Figure 1A). We further used balls with sizes proportional to the number of significant rare variants in each window (Figure 1B), and found significant RVs are clustered on chromosomes 1, 7, 10, 16, and 18.

Of the 682 significant rare variants, we further sifted these by CADD scores (Kircher, et al., 2014; Rentzsch, et al., 2019; van der Velde, et al., 2015) greater than 10; CADD is a widely used measure for variant deleteriousness that can prioritize causal variants effectively in genetic analysis, in particular highly penetrate contributors to severe Mendelian disorders. CADD is an annotation integrated from >60 genomic features, such as surrounding sequence context and gene model annotations. For any given variant, all the features are integrated into a CADD score which is a phred-scale rank score for all ~9 billion potential single nucleotide variants (Rentzsch et al., 2019).

In particular, we identified rare variant rs559954634 ($p = 6.4 \times 10^{-9}$; ACAT-O; CADD = 13.5), and rs186763678 ($p = 3.2 \times 10^{-8}$; ACAT-O; CADD = 10.5) which is in intron of *NFIA*. *NFIA* is known to interact with *SLC2A9* that has the largest effect on serum urate levels. Gene-gene interaction *NFIA-SLC2A9* was reported to be significantly associated with serum urate in the Italian MICROS population (n = 1,201) and replicated in a Croatian population (n = 1772) (Wei, et al., 2011). The rare variant rs186763678 has an effect size of −1.79, odds ratio 0.24 ($P = 0.176$), and the proportion test of gout patients versus controls ($P = 0.075$) in this study.

The rare variant rs559954634 positively affects gout susceptibility (odds ratio = 4.85; $P = 0.060$); this is the first report. This variant has been annotated in dbSNP (Sherry, et al., 2001) but not in ClinVar (Landrum, et al., 2018) and GWAS

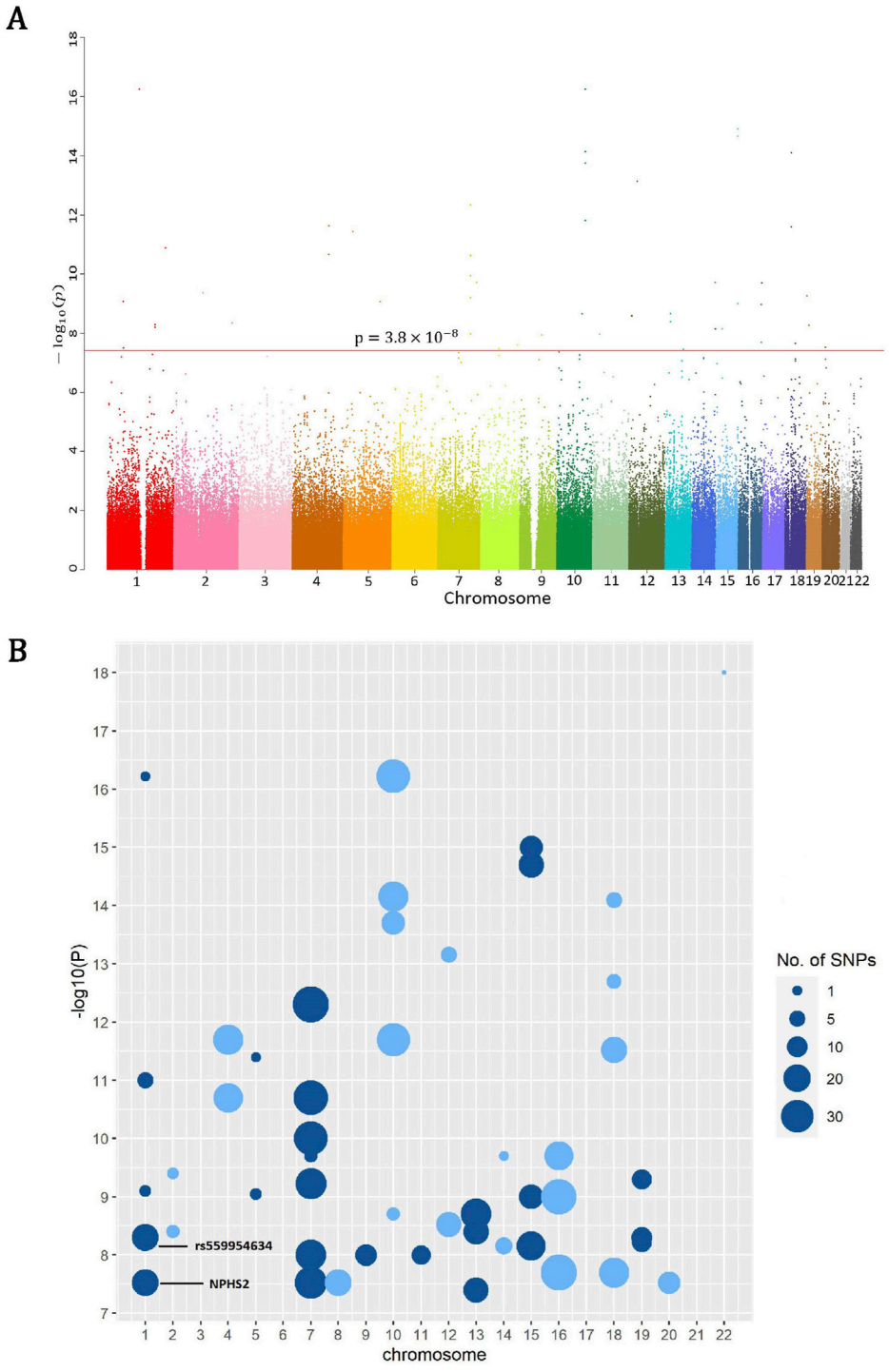

FIGURE 1
(A) The Manhattan plot depicted all *p*-values after the negative logarithm transformation of all ~8.7 million RVs which passed QC across 22 pairs of autosomal chromosomes, where the red line corresponds to the threshold 3.8×10^{-8} (ACAT-O) for significant rare variants. **(B)** The $\log_{10}$ (1/*P*) of rare variants significantly associated with gout susceptibility show clusters in chromosomes 1, 7, 10, 16 and 18, where larger balls denote more variants in the corresponding windows.

(Uffelmann, et al., 2021). Table 1 consists of significant rare variants ($p < 3.8 \times 10^{-8}$; ACAT-O) with CADD score >10 or without CADD scores but |effect size| > 1.5, as WGS may reveal unannotated rare variants, so we also report the latter. Supplementary Table S3-1 summarizes their effect sizes, odds ratios, *P* values (the proportion test of gout patients versus normal controls, and logistic regression adjusted on serum urate), and CADD phred scores.

Next, we merged adjacent significant windows of ACAT-O into larger ones and extended both edges of these windows upstream and downstream 1 Mb. Of these extended windows, the window of

TABLE 1 The significant rare variants with CADD ≥10 or without CADD score but |effect size| ≥ 1.5 found in this study.

SNP name	Locus	Chr	Position	HGVS.c[a]	HGVS.p	Allele			CADD score
						MAF	Case	Control	
rs765272850	*FAM92B*	16	85,110,461	c.G21-1C	n.G21-1C	0.001	1	1	32.00
rs199599166	*FAM92B*	16	85,108,054	c.G301A	p.G101A	0.002	3	1	25.40
rs753091695	*FAM92B*	16	85,110,392	c.C89T	p.S30L	0.004	3	5	23.20
rs746009560	*OR7D4* *OR7E24*	19	9,214,314	c.C524T	p.P175L	0.001	1	1	21.80
rs75755442	*LINC00687*	20	11,878,042	c.C176 + 212T	NA	0.007	7	8	18.73
rs375422213	*CELF4*[b]	18	39,025,897	NA	NA	0.001	1	2	18.03
rs1447484432	*CELF4*[b]	18	39,026,967	NA	NA	0.001	1	1	17.52
rs932402166	*AC015660.5*	15	99,475,249	c.G248-442T	NA	0.002	3	2	17.24
rs77675394	*CELF4*[b]	18	39,027,680	NA	NA	0.0005	1	0	17.10
rs144030951	*CELF4*[b]	18	39,025,679	NA	NA	0.0005	1	0	16.56
rs57012644	*CELF4*[b]	18	39,027,584	NA	NA	0.0005	1	0	16.06
rs1487893445	*SORCS1*[b]	10	1,06,218,086	NA	NA	0.001	2	0	15.59
rs1485225053	*CELF4*[b]	18	39,027,007	NA	NA	0.0005	1	0	15.41
rs1344344694	*LINC00687*	20	11,878,021	n.176 + 229_176 + 232del	NA	0.001	1	1	15.25
rs1258043800		12	10,489,523	NA	NA	0.001	0	3	14.68
rs541620279		12	10,492,869	NA	NA	0.001	1	1	14.44
rs950806939		18	39,027,469	NA	NA	0.001	1	1	14.30
rs559954634[c]		1	178,632,863	NA	NA	0.003	5	2	13.48
rs369183475	AC105362.1	4	135,809,425	NA	NA	0.004	3	6	13.45
rs1323073113		15	99,534,543	NA	NA	0.001	0	3	12.93
rs75734921	*PLA2G4D*	15	42,094,432	c.C28A	p.P10T	0.0005	1	0	12.89
rs531158543		12	10,493,640	NA	NA	0.001	0	2	12.53
rs181190277		10	1,06,217,544	NA	NA	0.0005	1	0	11.91
rs1359426229		13	37,067,584	NA	NA	0.001	2	1	11.47
rs1475570291		12	10,492,576	NA	NA	0.002	1	3	11.18
rs375254150	C16orf95	16	87,170,326	n.C111-29223T	NA	0.004	3	6	11.03
rs745657928	AL162726.3	9	82,527,931	n.T247 + 31073A	NA	0.0005	1	0	10.74
rs77904948		12	10,489,582	NA	NA	0.002	1	3	10.65
rs186763678[c]	*NFIA*	1	61,147,493	c.G559 + 58813T	n.G559 + 58813T	0.004	1	8	10.47
rs200909907		20	11,877,823	n.G176 + 431A	NA	0.001	1	1	10.25
rs148751159	*RALGPS2*	1	178,770,651	c.A-83-6031G	n.A-83-6031G	0.008	5	11	10.16
rs914948342		10	106,226,226	NA	NA	0.0005	1	0	10.01
—	*SLITRK6*[b]	13	85,340,105	NA	NA	0.002	0	5	—
—	*SLITRK6*[b]	13	85,340,778	NA	NA	0.003	6	1	—

(Continued on following page)

TABLE 1 (*Continued*) The significant rare variants with CADD ≥10 or without CADD score but |effect size| ≥ 1.5 found in this study.

SNP name	Locus	Chr	Position	HGVS.c[a]	HGVS.p	Allele			CADD score
						MAF	Case	Control	
—	*SLITRK6*[b]	**13**[c]	**85,340,782**[c]	NA	NA	0.006	11	1	—

[a]c. denotes coding DNA, reference sequence; n. denotes non-coding RNA, reference sequence. p denotes protein reference sequence; N + M denotes nucleotide M in the intron after (3′of) position N in the coding reference sequence; N-M denotes nucleotide M in the intron before (5′of) position N in the coding reference sequence; -N + M/-N-M denotes nucleotide in an intron in the 5′UTR; _ (underscore) denotes nucleotide numbering, used to indicate a range (e.g. in combination with a deletion, duplication, insertion, or variable sequence).
[b]Genes not mapped in the merged window of the rare variants, but they are in the extended windows.
[c]The novel RVs associated with gout in Taiwanese males revealed in this study.

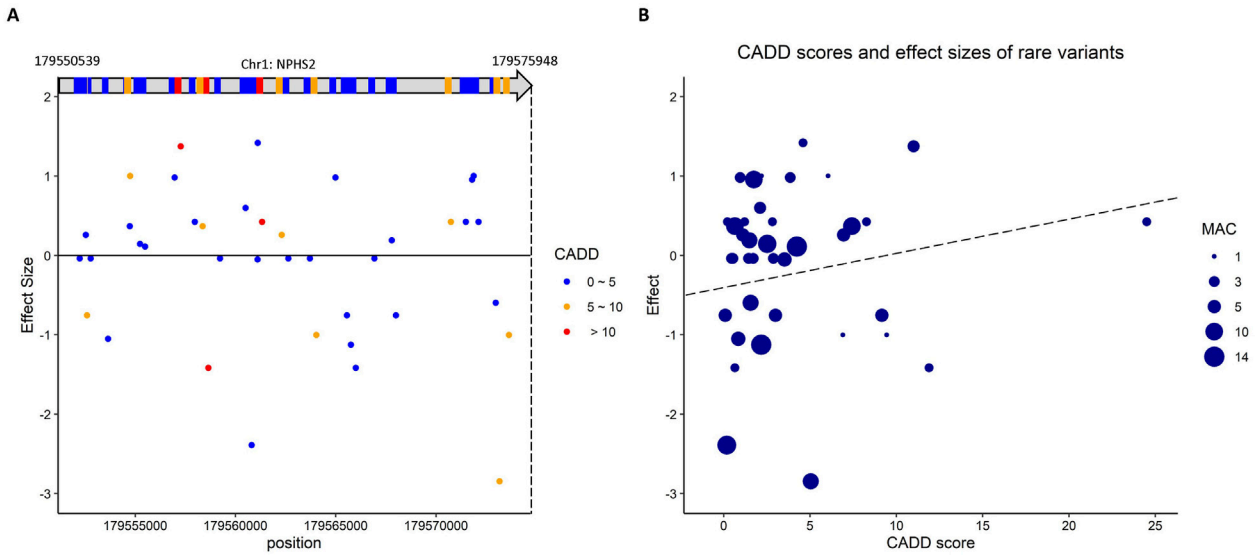

FIGURE 2
The putative rare variants in *NPHS2* which is involved in serum urate and indirectly linked to gout. **(A)** The scheme shows the positions of these variants in *NPHS2* and the corresponding effect sizes. **(B)** the rare variants of *NPHS2* with higher CADD scores are associated with larger positive effects on gout susceptibility.

rs559954634 intersected with *NPHS2,* which is involved in serum urate and indirectly linked to gout through hyperuricemia. Moreover, *NPHS2* expresses in kidney tissues (queried from GTEx portal), and the kidneys play a major role in regulating uric acid levels. This suggests rs559954634 may be involved in gout, though further research is warranted. All overlapping genes in the 1 Mb-extended windows of rs559954634 are summarized in Supplementary Table S3-2. Moreover, there are 39 genes in the 1-Mb extended window of rs186763678; however, none is related to gout or serum urate, so we summarize these 39 genes in Supplementary Table S3-3.

Prioritization of the rare variants in *NPHS2*

Gene *NPHS2* encodes podocin, which is directly involved with serum urate levels (hyperuricemia; (Romi et al., 2017). Of the rare variants that passed the QC checks, 39 distinct rare variants are in *NPHS2*; however, none is significant in ACAT-O. Among these rare variants, rs202036853 (effect size = 5.79) shows a nominal association with gout adjusted on serum urate (P = 0.038; logistic regression) and has a CADD score of 11.0. Figure 2A shows the positions of these variants and the corresponding effect sizes. Figure 2B depicts that the rare variants of *NPHS2* with higher CADD scores are associated with more significant positive effects on gout susceptibility. The effect size, proportion test, logistic regression, and CADD score of these variants in *NPHS2* are in Supplementary Table S3-4.

Another novel rare variant discovered

We also uncovered a novel rare variant 13-85340782-G-A (chr. 13; $P = 3.5 \times 10^{-8}$; ACAT-O), which has an odds ratio of 6.02 (P = 0.038) and is significant in the proportion test (P = 0.002). Two other RVs in the same window of 13-85340782-G-A also have |effect size| > 1.5, but their odds ratio for gout is insignificant (Supplementary Table S3-1). The RV 13-85340782-G-A is significantly associated with gout (P = 0.038; logistic regression), but the significance diminished when adjusted on serum urate (P = 0.124; logistic regression), which may indicate the association of this variant with gout is through serum urate. The 1 Mb-extended windows of this rare variant do not intersect with

TABLE 2 Logistic regression analysis of gout susceptibility on the three identified rare variants.

Univariate variable	$\hat{\beta}$	Odds ratio (95% CI)	*P* value
rs559954634	1.58	4.84 (1.04 – 33.97)	0.060
rs186763678	−1.44	0.24 (0.01 – 1.30)	0.176
13-85340782-G-A	1.80	6.02 (1.74 –89.68)	0.038
Multivariate Variable	$\hat{\beta}$	**Odds ratio (95% CI)**	***P* value**
rs559954634	1.60	4.93 (1.06 – 34.56)	0.057
13-85340782-G-A	1.80	6.06 (1.75 – 90.45)	0.037

any known gene involved in gout or serum urate. The genes in this 1 Mb-extended window are in Supplementary Table S3-5.

Rs559954634 and 13-85340782-G-A jointly are significantly associated with gout susceptibility

Recently, several genetic studies have reported that multiple rare variants play essential roles in complex genetic diseases, e.g., Alzheimer's disease (Cruchaga et al., 2014), which support the "Common Disease Multiple Rare Variants" (CDMRVs) or "Common Disease Rare Variants" (CDRV) hypothesis (Schork et al., 2009). CDMRV and CDRV hypotheses argue that multiple rare variants and a single rare variant, each with relatively high penetrance, are the major contributors to common diseases, respectively. In this section, we applied multivariate logistic regression analysis to evaluate the joint effect of the rare variant in *NFIA* rs186763678, rs559954634, and 13-85340782-G-A discovered by ACAT-O and CADD scores/or effect size. The results support the "CDMRVs" hypothesis at $P < 0.06$ (multiple logistic regression). Specifically, univariate logistic regression analysis reveals that rs559954634 and 13-85340782-G-A are significantly associated with gout susceptibility (Table 2). When analyzed jointly, 13-85340782-G-A (beta = 1.80, $P = 0.037$; OR = 6.06) and rs559954634 (beta = 1.60, $P = 0.057$; OR = 4.93) are significantly associated with gout susceptibility at $P < 0.06$; the result supports CDMRVs at a non-stringent criteria.

Rare variants in known gout-related genes *ABCG2, SLC2A9* and *SLC22A12*

This study found 16 (16, 3) rare variants in the known gout-related gene ABCG2 (SLC2A9, SLC22A12). However, none of these are significant in ACAT-O; the smallest *P* values of these variants in *ABCG2, SLC2A9,* and *SLC22A12* are 0.004, 0.012, and 0.122, respectively (Supplementary Table S4-1). This may be due to our samples and those in previous studies being of different ancestry or our sample size not being large (under budget constraints). The position, allele frequency, and CADD score of these variants are summarized in Supplementary Table S4-2.

In the following, we report the rare variants in these genes, which have CADD scores ≥10 and are significant in both the odds ratio and the proportion test. The rare variant rs199897813 in *ABCG2* has a CADD score of 28.3, an effect size of 1.96, and an odds ratio equal to 9.71 ($P = 0.038$), respectively, and its proportion test of patients versus controls has $P = 0.051$. Moreover, three rare variants identified in *ABCG2,* rs548254708, rs34678167, and rs149106245, were previously reported in a Japanese cohort (Higashino et al., 2017), but neither is significant in odds ratio and the proportion test in this study; this is reasonable as individuals of these two cohorts are of different ancestry. Of the rare variant revealed in *SLC2A9,* rs150391338 has a CADD score of 10.4, effect size of −2.37, odds ratio 0.25 ($P = 0.068$), and it is significant in the proportion test ($p = 0.018$); detailed information is summarized in Supplementary Table S4-3.

The rare variants in the remaining merged windows

We also computed the odds ratio and conducted the proportion test in the remaining merged windows of the significant rare variants ($P < 3.8 \times 10^{-8}$; ACAT-O). However, none of the rare variants therein satisfies both CADD ≥10 and is significant in odds ratio or the proportion test ($P < 0.10$).

Discussion

Rare variants often contribute to complex diseases with large effect sizes per allele; however, the power to detect these variants remains limited (Chen et al., 2022). This study integrated data from male gout patients from CMUH and TWB and normal controls of TWB to identify 682 significant rare variants by ACAT-O. We further sifted these variants by the measure of variant deleteriousness CADD >10 (|effect size| > 1.5) to find rs559954634 and rs186763678 (13-85340782-G-A). These variants have been identified for the first time as associated with gout susceptibility in Taiwanese males. The carrier frequency of potentially pathogenic rs559954634 and 13-85340782-G-A is higher in gout patients when compared to normal controls (1.4% versus 0.30%; $P = 0.046$, and 3.1% versus 0.15%; $P = 0.011$; the proportion test). Conversely, the carrier frequency of potentially protective variant rs186763678 is higher in controls than in patients (0.29% versus 1.2%; $P = 0.037$; the proportion test). The identified potentially pathogenic (protective) RVs with a prevalence >1% in cases (controls) indicate that these RVs may be associated with gout in this population. Nevertheless, further studies are warranted, as the inflation factor λ of the ~8.7 million QC-passed RVs is moderate (1.42).

In the neighborhood of rs559954634, we found *NPHS2* that encodes podocin, which is directly involved in hyperuricemia (Romi et al., 2017). Moreover, *NPHS2* is expressed in kidney tissues (queried from the GTEx portal), and the kidneys play a major role in regulating uric acid levels. This suggests that rs559954634 may be involved in gout, though further research is warranted. The rare variant rs186763678 is in the intron of *NFIA* which interacts with *SLC2A9,* while *SLC2A9* is known for lowering serum urate and protecting gout (Tin et al., 2018). The RV 13-85340782-G-A has an odds ratio of 6.06 ($P = 0.037$) and a large effect size (3.15).

We caution that these findings were statistically significant and prioritized by CADD scores, but the revealed RVs have not been verified biologically.

ACAT-O is a sliding-window-based method that uses the conventional 4 kb window size with 2 kb overlaps. Varying the window size to 5 kb (3 kb), we reran ACAT-O to yield the *p* value of rs559954634, rs186763678, and 13-85340782-G-A equal to 6.2×10^{-9}, 3.15×10^{-8}, and 3.4×10^{-8} (6.36×10^{-9}, 3.15×10^{-8}, and 3.40×10^{-8}), respectively; all the three RVs remain significant for the ACAT-O (with 5 kb-windows) cutoff 4.7×10^{-8} (resulted from ~1.06 million windows), but only rs559954634 is significant for the ACAT-O (with 3 kb-windows) cutoff 2.86×10^{-8} (resulted from ~1.78 million windows). As the number of windows increases, e.g., prespecifying 3 kb for window size, the Bonferroni correction for multiple testing becomes too conservative, leading to power loss. Furthermore, it is noted in Li et al. (2019) that the sliding window methods are likely to lose power if the pre-specified window size is too big because it might include too many neutral variants, or if the pre-specified window size is too small that it might exclude adjacent regions containing association signals. To circumvent the difficulty of specifying a window size *a priori*, Li and colleagues introduced a dynamic scan procedure (SCANG) to flexibly detect the sizes and locations of RV association regions of WGS studies. Thus, applying SCANG to our data to yield robust RVs of gout in Taiwanese males is an interesting future research. As the number of subjects in this study is moderate, it will be valuable to further sequence whole genomes of male gout patients in Taiwan or analyze an independent cohort, such as the UK Biobank, to confirm/compare these unraveled RVs. Moreover, the combination of individual variants into a polygenic risk score (PRS) has the potential to be a predictor for a disease (Elliott et al., 2020); it may be helpful for the diagnosis of gout, in addition to increasing statistical power to detect genetic associations. Therefore, deriving a PRS using the identified 682 rare variants and integrating our data with WGS data of individuals of other ancestry, e.g., the UK Biobank, are also promising future research directions for gout study.

Data availability statement

The datasets presented in this article are not readily available because the data of 64 male gout patients and normal controls from TWB belongs to the Taiwan Biobank and can be accessed upon application at: https://www.biobank.org.tw/. The data of 321 male gout patients at CMUH are under IRB restriction and thus are not publicly available. Requests to access the datasets should be directed to the corresponding authors and with permission of the CMUH. However, WGS summary statistics for the CMUH-TWB data are available at https://staff.stat.sinica.edu.tw/gshieh/WGS-data.htm and at GWAS catalog ID: GCST90432173.

Ethics statement

The IRB-BM committee of Academia Sinica (AS-IRB02-113170) approved this study. The studies involving humans were approved by The ethics committee of the China Medical University Hospital Institutional Review Board in Taiwan (CMUH108-REC1-091) approved this study. The studies were conducted in accordance with the local legislation and institutional requirements. The participants provided their written informed consent to participate in this study.

Author contributions

Y-PT: Writing–original draft, Formal Analysis, Software, Visualization. Y-SC: Data curation, Resources, Writing–review and editing. VM: Formal Analysis, Writing–review and editing. T-YL: Writing–review and editing, Data curation, Resources. J-GC: Writing–review and editing, Conceptualization, Funding acquisition, Methodology, Project administration, Supervision. GS: Conceptualization, Methodology, Supervision, Writing–review and editing, Funding acquisition, Project administration, Formal Analysis, Investigation, Writing–original draft.

Funding

The author(s) declare that financial support was received for the research, authorship, and/or publication of this article. This research was supported by Academia Sinica, Taiwan (Tukey and Group research Grant to GS.S); and National Science & Technology Council, Taiwan, Republic of China (111-2320-B-039-064 to J.G.C, and 111-2118-M-001-009-MY2 and 113-2118-M-001-002 to GS.S.).

Acknowledgments

We are grateful to the AE and two anomynous reviewers for constructive comments and suggestions that improved earlier versions of our manuscript. We thank Chia-Ni Hsiung at the Data Science Statistical Cooperation Center of Academia Sinica (AS-CFII-111-215) for statistical support, and Shi-Kai Chu and Yu-Jen Liang for discussions.

Conflict of interest

The authors declare that the research was conducted in the absence of any commercial or financial relationships that could be construed as a potential conflict of interest.

The author(s) declared that they were an editorial board member of Frontiers, at the time of submission. This had no impact on the peer review process and the final decision.

Publisher's note

Supplementary material

The Supplementary Material for this article can be found online at: https://www.frontiersin.org/articles/10.3389/fgene.2024.1423714/full#supplementary-material

References

Anderson, C. A., Pettersson, F. H., Clarke, G. M., Cardon, L. R., Morris, A. P., and Zondervan, K. T. (2010). Data quality control in genetic case-control association studies. *Nat. Protoc.* 5 (9), 1564–1573. doi:10.1038/nprot.2010.116

Chang, Y.-S., Lin, C.-Y., Liu, T.-Y., Huang, C.-M., Chung, C.-C., Chen, Y.-C., et al. (2022). Polygenic risk score trend and new variants on chromosome 1 are associated with male gout in genome-wide association study. *Arthritis Res. and Ther.* 24 (1), 229. doi:10.1186/s13075-022-02917-4

Chen, C.-J., Tseng, C.-C., Yen, J.-H., Chang, J.-G., Chou, W.-C., Chu, H.-W., et al. (2018). ABCG2 contributes to the development of gout and hyperuricemia in a genome-wide association study. *Sci. Rep.* 8 (1), 3137. doi:10.1038/s41598-018-21425-7

Chen, W., Coombes, B. J., and Larson, N. B. (2022). Recent advances and challenges of rare variant association analysis in the biobank sequencing era. *Front. Genet.* 13, 1014947. doi:10.3389/fgene.2022.1014947

Cruchaga, C., Karch, C. M., Jin, S. C., Benitez, B. A., Cai, Y., Guerreiro, R., et al. (2014). Rare coding variants in the phospholipase D3 gene confer risk for Alzheimer's disease. *Nature* 505 (7484), 550–554. doi:10.1038/nature12825

Dinour, D., Gray, N. K., Campbell, S., Shu, X., Sawyer, L., Richardson, W., et al. (2010). Homozygous SLC2A9 mutations cause severe renal hypouricemia. *J. Am. Soc. Nephrol. JASN* 21 (1), 64–72. doi:10.1681/ASN.2009040406

Elliott, J., Bodinier, B., Bond, T. A., Chadeau-Hyam, M., Evangelou, E., Moons, K. G., et al. (2020). Predictive accuracy of a polygenic risk score–enhanced prediction model vs a clinical risk score for coronary artery disease. *Jama* 323 (7), 636–645. doi:10.1001/jama.2019.22241

Enomoto, A., Kimura, H., Chairoungdua, A., Shigeta, Y., Jutabha, P., Ho Cha, S., et al. (2002). Molecular identification of a renal urate–anion exchanger that regulates blood urate levels. *Nature* 417 (6887), 447–452. doi:10.1038/nature742

Higashino, T., Takada, T., Nakaoka, H., Toyoda, Y., Stiburkova, B., Miyata, H., et al. (2017). Multiple common and rare variants of ABCG2 cause gout. *RMD open* 3 (2), e000464. doi:10.1136/rmdopen-2017-000464

Kircher, M., Witten, D. M., Jain, P., O'roak, B. J., Cooper, G. M., and Shendure, J. (2014). A general framework for estimating the relative pathogenicity of human genetic variants. *Nat. Genet.* 46 (3), 310–315. doi:10.1038/ng.2892

Landrum, M. J., Lee, J. M., Benson, M., Brown, G. R., Chao, C., Chitipiralla, S., et al. (2018). ClinVar: improving access to variant interpretations and supporting evidence. *Nucleic acids Res.* 46 (D1), D1062-D1067–D1067. doi:10.1093/nar/gkx1153

Li, B., and Leal, S. M. (2008). Methods for detecting associations with rare variants for common diseases: application to analysis of sequence data. *Am. J. Hum. Genet.* 83 (3), 311–321. doi:10.1016/j.ajhg.2008.06.024

Li, Z., Li, X., Liu, Y., Shen, J., Chen, H., Zhou, H., et al. (2019). Dynamic scan procedure for detecting rare-variant association regions in whole-genome sequencing studies. *Am. J. Hum. Genet.* 104 (5), 802–814. doi:10.1016/j.ajhg.2019.03.002

Liu, Y., Chen, S., Li, Z., Morrison, A. C., Boerwinkle, E., and Lin, X. (2019). ACAT: a fast and powerful p value combination method for rare-variant analysis in sequencing studies. *Am. J. Hum. Genet.* 104 (3), 410–421. doi:10.1016/j.ajhg.2019.01.002

Madsen, B. E., and Browning, S. R. (2009). A groupwise association test for rare mutations using a weighted sum statistic. *PLoS Genet.* 5 (2), e1000384. doi:10.1371/journal.pgen.1000384

Matsuo, H., Chiba, T., Nagamori, S., Nakayama, A., Domoto, H., Phetdee, K., et al. (2008). Mutations in glucose transporter 9 gene SLC2A9 cause renal hypouricemia. *Am. J. Hum. Genet.* 83 (6), 744–751. doi:10.1016/j.ajhg.2008.11.001

Matsuo, H., Takada, T., Ichida, K., Nakamura, T., Nakayama, A., Ikebuchi, Y., et al. (2009). Common defects of ABCG2, a high-capacity urate exporter, cause gout: a function-based genetic analysis in a Japanese population. *Sci. Transl. Med.* 1 (5), 5ra11–15ra11. doi:10.1126/scitranslmed.3000237

McAdams, M. A., Maynard, J. W., Baer, A. N., Köttgen, A., Clipp, S., Coresh, J., et al. (2011). Reliability and sensitivity of the self-report of physician-diagnosed gout in the campaign against cancer and heart disease and the atherosclerosis risk in the community cohorts. *J. rheumatology* 38 (1), 135–141. doi:10.3899/jrheum.100418

McLaren, W., Gil, L., Hunt, S. E., Riat, H. S., Ritchie, G. R., Thormann, A., et al. (2016). The ensembl variant effect predictor. *Genome Biol.* 17, 122. doi:10.1186/s13059-016-0974-4

Price, A. L., Kryukov, G. V., de Bakker, P. I., Purcell, S. M., Staples, J., Wei, L.-J., et al. (2010). Pooled association tests for rare variants in exon-resequencing studies. *Am. J. Hum. Genet.* 86 (6), 832–838. doi:10.1016/j.ajhg.2010.04.005

Reginato, A. M., Mount, D. B., Yang, I., and Choi, H. K. (2012). The genetics of hyperuricaemia and gout. *Nat. Rev. Rheumatol.* 8 (10), 610–621. doi:10.1038/nrrheum.2012.144

Rentzsch, P., Witten, D., Cooper, G. M., Shendure, J., and Kircher, M. (2019). CADD: predicting the deleteriousness of variants throughout the human genome. *Nucleic acids Res.* 47 (D1), D886-D894–D894. doi:10.1093/nar/gky1016

Romi, M. M., Arfian, N., Tranggono, U., Setyaningsih, W. A. W., and Sari, D. C. R. (2017). Uric acid causes kidney injury through inducing fibroblast expansion, Endothelin-1 expression, and inflammation. *BMC Nephrol.* 18, 326–328. doi:10.1186/s12882-017-0736-x

Schork, N. J., Murray, S. S., Frazer, K. A., and Topol, E. J. (2009). Common vs. rare allele hypotheses for complex diseases. *Curr. Opin. Genet. and Dev.* 19 (3), 212–219. doi:10.1016/j.gde.2009.04.010

Sherry, S. T., Ward, M.-H., Kholodov, M., Baker, J., Phan, L., Smigielski, E. M., et al. (2001). dbSNP: the NCBI database of genetic variation. *Nucleic acids Res.* 29 (1), 308–311. doi:10.1093/nar/29.1.308

Taliun, D., Harris, D. N., Kessler, M. D., Carlson, J., Szpiech, Z. A., Torres, R., et al. (2021). Sequencing of 53,831 diverse genomes from the NHLBI TOPMed Program. *Nature* 590 (7845), 290–299. doi:10.1038/s41586-021-03205-y

Tin, A., Li, Y., Brody, J. A., Nutile, T., Chu, A. Y., Huffman, J. E., et al. (2018). Large-scale whole-exome sequencing association studies identify rare functional variants influencing serum urate levels. *Nat. Commun.* 9 (1), 4228. doi:10.1038/s41467-018-06620-4

Uffelmann, E., Huang, Q. Q., Munung, N. S., De Vries, J., Okada, Y., Martin, A. R., et al. (2021). Genome-wide association studies. *Nat. Rev. Methods Prim.* 1 (1), 59. doi:10.1038/s43586-021-00056-9

van der Velde, K. J., Kuiper, J., Thompson, B. A., Plazzer, J. P., van Valkenhoef, G., de Haan, M., et al. (2015). Evaluation of CADD scores in curated mismatch repair gene variants yields a model for clinical validation and prioritization. *Hum. Mutat.* 36 (7), 712–719. doi:10.1002/humu.22798

Wei, W., Hemani, G., Hicks, A. A., Vitart, V., Cabrera-Cardenas, C., Navarro, P., et al. (2011). Characterisation of genome-wide association epistasis signals for serum uric acid in human population isolates. *PLoS One* 6 (8), e23836. doi:10.1371/journal.pone.0023836

Wu, M. C., Lee, S., Cai, T., Li, Y., Boehnke, M., and Lin, X. (2011). Rare-variant association testing for sequencing data with the sequence kernel association test. *Am. J. Hum. Genet.* 89 (1), 82–93. doi:10.1016/j.ajhg.2011.05.029

frontiers | Frontiers in Immunology

TYPE Original Research
PUBLISHED 17 October 2024
DOI 10.3389/fimmu.2024.1434738

OPEN ACCESS

EDITED BY
Lihua Duan,
Jiangxi Provincial People's Hospital, China

REVIEWED BY
Yoshitaka Kimura,
Teikyo University, Japan
Masanori A Murayama,
Kansai Medical University, Japan

*CORRESPONDENCE
Xiudi Wu
wuxiudinbey@163.com
Mingcai Li
mingcaili@126.com

RECEIVED 18 May 2024
ACCEPTED 30 September 2024
PUBLISHED 17 October 2024

CITATION
Huang H, Zhou Y, Li Y, Zhao H, Wu X and Li M (2024) The decreased serum levels of interleukin-38 in patients with gout and its clinical significance.
Front. Immunol. 15:1434738.
doi: 10.3389/fimmu.2024.1434738

The decreased serum levels of interleukin-38 in patients with gout and its clinical significance

Hua Huang[1], Yinxin Zhou[2], Yan Li[1,2], Hui Zhao[3], Xiudi Wu[1]* and Mingcai Li[1,2]*

[1]Department of Rheumatology and Immunology, The First Affiliated Hospital of Ningbo University, Ningbo, China, [2]School of Basic Medical Sciences, Health Science Center, Ningbo University, Ningbo, China, [3]Department of Clinical Laboratory, Ningbo No.6 Hospital Affiliated to Ningbo University, Ningbo, China

Background: Interleukin (IL)-38 is a newly discovered anti-inflammatory cytokine. However, its concentration and clinical significance in patients with gout remain unclear. This study aimed to investigate the levels of IL-38 in patients with gout and evaluate their clinical significance.

Methods: Thirty-two patients with active gout, 27 patients with inactive gout, and 20 negative controls (NCs) were included in the study. Clinical parameters, including white blood cell count, C-reactive protein, serum amyloid A, erythrocyte sedimentation rate, uric acid, urea, creatinine, alanine aminotransferase, aspartate aminotransferase, glutamyl transpeptidase, and glycoserated serum protein, were obtained from laboratory tests of blood samples. The serum concentration of IL-38 was determined using enzyme-linked immunosorbent assay. Spearman's correlation analysis and receiver operating characteristic curve assessments were used to investigate the role and diagnostic value of IL-38 in gout.

Results: Patients with active and inactive gout exhibited significantly lower serum IL-38 levels than NCs. No significant differences were observed between the two gout groups. A negative correlation was observed between IL-38 and white blood cell counts, whereas a positive correlation was found between IL-38 and creatinine levels. Furthermore, IL-38, either alone or in combination with uric acid, demonstrated substantial diagnostic potential.

Conclusion: The findings suggest that the decreased serum levels of IL-38 in patients with gout compared to that in NCs indicates that IL-38 may have immunomodulatory effects on gout inflammation and possesses clinical application value.

KEYWORDS

gout, interleukin-38, uric acid, inflammation, biomarker

1 Introduction

Gout is a common type of joint inflammation caused by abnormal purine metabolism (1, 2). The overall prevalence of gout in China is approximately 1% and continues to increase annually (3). Gout mainly affects men, and the incidence of gout in women does not increase significantly until menopause (2). Acute episodes of gout are often characterized by severe pain, redness, and limited joint movement that lasts from several hours to tens of hours (4, 5). The first acute episode in a person with gout is usually self-limiting, occurring within a week or two when the signs and symptoms of arthritis completely subsided (4). However, this reprieve is temporary, as without proper treatment, the arthritic symptoms of gout can recur, worsen, and even turn into chronic gout (4, 6).

Accumulation of monosodium urate (MSU) crystals in patients with gout stimulates an inflammatory response via two pathways. First, toll-like receptor 2 and 4 synthesize pro-interleukin (IL)-1β and inflammatory components in macrophages or monocytes via the nuclear transcription factor-κB signaling pathway. Subsequently, the MSU crystals stimulate the assembly of the inflammasome NOD-like receptor thermal protein domain associated protein 3 (NLRP3), activating the cysteinyl aspartate-specific proteinase-1, which cleaves pro-IL-1β into IL-1β. The inflammasome mediates the binding of IL-1β to IL-1β receptors, inducing acute inflammatory responses (2, 7). Uric acid-lowering therapy is a comprehensive strategy for the long-term management of gout. During acute flares, colchicine, non-steroidal anti-inflammatory drugs, and corticosteroids, are commonly administered in clinical treatment (4, 5). Furthermore, due to the vital role of IL-1 inflammation in gout pathogenesis (8), IL-1 inhibitors are also utilized in clinical treatment (7, 9).

First discovered in 2001, IL-38 is a novel cytokine belonging to the IL-1 family (IL-1F), also known as IL-1F10 (10). IL-38, originating from B-lymphocytes, peripheral blood mononuclear cells, and various immune cells, is expressed in multiple tissues, such as the skin, tonsils, spleen, and thymus (11, 12). IL-38 shares amino acid homology with IL-1 receptor antagonists (IL-1Ra) and IL-36Ra (13). In addition, IL-38 can bind to specific receptors, such as IL-36 receptor (IL-36R), IL-1R1, and IL-1 receptor accessory protein-like 1 (IL-1RAPL1), to exert its biological functions (12, 14). IL-38 regulates autoimmune diseases and exhibits anti-inflammatory effects in the inflammatory response (12, 15). The IL-36R pathway has been extensively studied, and its involvement in autoimmune diseases and inflammatory conditions, such as systemic lupus erythematosus (16), rheumatoid arthritis (17), ankylosing spondylitis (18), and asthma (19), has been reported. The presence of both the full-length and truncated forms of the recombinant IL-38 protein (20) is controversial regarding the activation of the IL-1R1 pathway (21). The IL-1RAPL1 pathway is highly associated with immune and tumor processes (21). The full-length and truncated recombinant IL-38 proteins can bind to IL-1RAPL1 to promote or inhibit inflammation, respectively (20). *IL-38* gene overexpression can modulate the balance between IL-1β and IL-1R, thereby controlling the inflammatory response (22). In addition, a cardiovascular study highlighted that IL-38 inhibits the activation of the NLRP3 inflammasome, inhibiting inflammation (23).

In summary, a potential association between IL-38 and gout exist, indicating that IL-38 controls the occurrence and development of gout by binding to specific receptors and inhibiting the inflammatory response. Therefore, we hypothesized that IL-38 can be a novel biomarker for gout and provide valuable insights into the diagnosis and treatment of this disease. This study aimed to investigate the effect of IL-38 on gout by measuring the serum levels of IL-38 in patients with active and inactive gout.

2 Materials and methods

2.1 Participants

Fifty-nine patients with gout and 20 negative controls (NCs) from the Ningbo No. 6 Hospital from June 2022 to November 2022, were included in the study. The detailed screening process is illustrated in Figure 1.

Due to the high prevalence of gout in men, male gout patients older than 18 years were included. The diagnosis of gout is confirmed by two or more rheumatologists using diagnostic criteria (24). On the other hand, hormone administration, infection, tumor, autoimmune disease, and other diseases were excluded, as well as gout related treatment prior to admission. Active and inactive gout were distinguished in 32 and 27 patients, respectively, depending on their gout episode and subjective feelings (25, 26). NCs were obtained from outpatient patients. Their inclusion and exclusion criteria are as follows. (1) No obvious signs of disease were found during routine examination; (2) Age over 18 years old; (3) Male; (4) Exclude hormone administration, infections, tumors, autoimmune diseases, and other diseases especially gout.

This study was approved by the Ethical Review Board of the relevant institutions and conducted in accordance with the Declaration of Helsinki. Informed consent was obtained from all participants.

2.2 Clinical data

The age and sex of all participants were recorded prior to inclusion in the study. Clinical data, including white blood cell (WBC) count, C-reactive protein (CRP), serum amyloid A (SAA), erythrocyte sedimentation rate (ESR), uric acid (UA), urea (UR), creatinine (CR), alanine aminotransferase (ALT), aspartate aminotransferase (AST), glutamyl transpeptidase (GGT), and glycoserated serum protein (GSP), total cholesterol (TC), and triglyceride (TG), were obtained from laboratory tests of blood samples. Blood samples were collected from the participants after fasting for 12 h. Blood samples were kept at room temperature (20–25°C) for 2 h. Subsequently, the samples were centrifuged at 1,000 *g* for 15 min at 2-8°C to separate the serum. Laboratory tests were

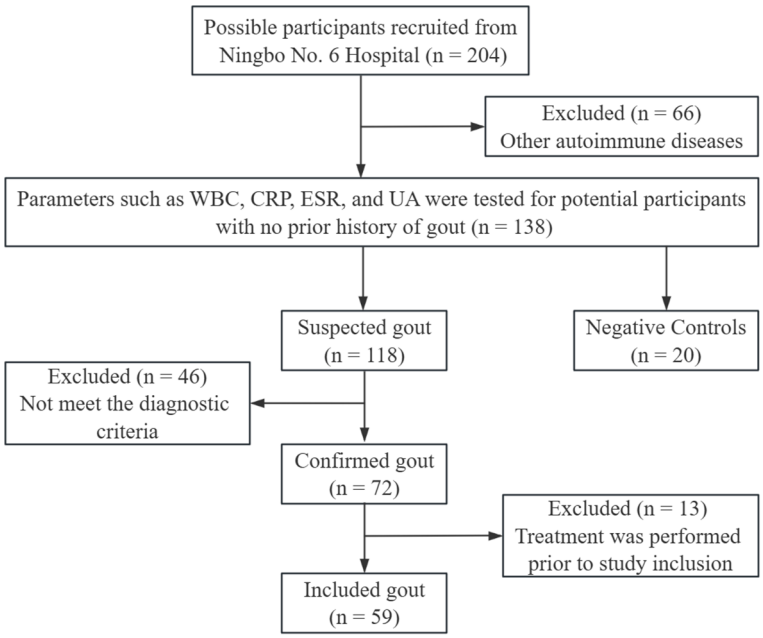

FIGURE 1
Participants screening process. WBC, white blood cell count; CRP, C-reactive protein; ESR, erythrocyte sedimentation rate; UA, uric acid.

performed using automated blood (BC-6800, Mindray) and biochemical (AU640, Olympus Corporation) analyzers.

2.3 Quantification of serum IL-38

The IL-38 concentration in the serum samples of the participants was determined using enzyme-linked immunosorbent assay (ELISA) kit (CSB-EL011615HU, Cusabio Technology, Wuhan, China) according to the manufacturer's instructions. The precision within an assay and between assays of the ELISA kits was less than 8% and 10%, respectively. The assay detection range was 31.25–2,000 pg/mL.

The experimental procedure is summarized as follows: melted serum and diluted standards were added to an enzymatic plate balanced at room temperature for 30 min. After incubating at 37 °C for 2 h, the supernatant was removed, and the biotin antibody and horseradish peroxidase avidin were added and incubated at 37°C for 1 h. Finally, after adding 3,3′,5,5′-tetramethylbenzidine (TMB) solution for 30 min in the dark, the reaction was ended using termination solution. Then, the absorbance was measured at 450 nm using a spectrophotometer (Multiskan GO; Thermo Fisher Scientific). A standard curve was constructed using equally diluted standard solutions.

2.4 Statistical analysis

All statistical analyses in this study were performed using GraphPad Prism 9.0 version. The measurement data were tested using the Shapiro–Wilk test for normal distribution. According to the distribution, the measurement data were presented as mean ± standard deviation (SD) or median and interquartile range (IQR). For the analysis of the three sets of data, one-way analysis of variance (ANOVA) or the Kruskal–Wallis test was used. In multiple comparisons between the three groups, the Dunn's *post-hoc* test was used. Correlations between clinical data were analyzed using rank correlations. The diagnostic value of the disease was demonstrated using receiver operating characteristic (ROC) curves. All tests were two-sided, with a test level of 0.05.

3 Results

3.1 Characteristics of participants

The ages of the participants in the three groups were comparable (P = 0.195). The levels of UR (P = 0.345) and GSP (P = 0.088) in serum did not differ among the participants. The pairwise comparison using Dunn's *post-hoc* test showed that all other indicators of patients with active gout were different from those of NCs. However, only SAA, UA, CR, and ALT levels were significantly different in patients with inactive gout. Detailed clinical data are presented in Table 1.

3.2 Serum IL-38 concentrations

Serum IL-38 concentrations of the participants are shown in Figure 2. The levels of IL-38 in active gout, inactive gout, and NCs were 113.45 (88.04, 126.75), 117.55 (90.48, 149.89), and 145.51 (113.12, 203.37) pg/mL, respectively. The nonparametric test

10.3389/fimmu.2024.1434738

TABLE 1 Characteristics of participants.

Variables	Active gout	Inactive gout	NCs	*P*-value
N	32	27	20	/
Sex (Male%)	100%	100%	100%	/
Age (y)	42.4 ± 12.8	39.7 ± 13.8	35.7 ± 11.5	0.195
WBC (10^9/L)	8.7 (7.6, 10.4)[a]	6.7 (5.5, 7.8)	5.7 (5.1, 6.9)	< 0.001
CRP (mg/L)	12.3 (5.6, 31.2)[a]	1.4 (0.6, 2.5)	1.3 (1.2, 1.5)	< 0.001
SAA (mg/L)	55.9 (6.9, 227.8)[a]	5.2 (2.6, 9.4)[b]	2.0 (1.6, 2.8)	< 0.001
ESR (mm/h)	26.5 (11.0, 39.3)[a]	8.0 (4.0, 16.0)	8.0 (4.2, 10.75)	< 0.001
UA (μmol/L)	445.5 (359.5, 566.5)[a]	442.0 (376.0, 580.0)[b]	345.5 (319.8, 378.5)	< 0.001
UR (mmol/L)	4.1 (3.6, 5.3)	4.7 (4.1, 5.6)	4.9 (3.6, 5.7)	0.345
CR (μmol/L)	85.4 (75.7, 91.8)[a]	82.9 (77.3, 86.9)[b]	72.5 (65.2, 78.7)	0.001
ALT (U/L)	40.5 (27.0, 64.8)[a]	38.0 (28.0, 54.0)[b]	25.5 (20.3, 30.8)	0.002
AST (U/L)	24.0 (19.0, 38.0)[a]	24.0 (20.0, 32.0)	19.5 (17.0, 23.0)	0.037
GGT (U/L)	43.5 (29.8, 92.8)[a]	33.0 (23.0, 72.0)	23.0 (16.5, 33.3)	0.007
GSP (mmol/L)	2.0 ± 0.3	1.9 ± 0.3	2.0 ± 0.2	0.088
TC (mmol/L)	5.0 (4.4, 5.4)	5.1 (4.4, 5.9)[b]	4.4 (3.9, 5.1)	0.031
TG (mmol/L)	2.0 (1.4, 2.5)a	2.7 (1.8, 3.7)[b]	1.1 (0.7, 1.4)	< 0.001

NCs, negative controls; WBC, white blood cell count; CRP, C-reactive protein; SAA, serum amyloid A; ESR, erythrocyte sedimentation rate; UA, uric acid; UR, urea; CR, creatinine; ALT, alanine aminotransferase; AST, aspartate aminotransferase; GGT, glutamyl transpeptidase; GSP, glycoserated serum protein; TC, total cholesterol; TG, triglyceride. Multiple group comparisons of age were made using one-way analysis of variance. Multiple group comparisons of other indicators were made using Kruskal-Wallis test. Pair-to-pair comparisons between multiple groups were made using Dunn's *post-hoc* test. The P-value was obtained by one-way analysis of variance, Kruskal-Wallis test and the Dunn's *Mpost-hoc* test. [a] Active gout compared with NCs, $P < 0.05$. [b] Inactive gout compared with NCs, $P < 0.05$.

showed that IL-38 concentrations in the three groups differed. The Dunn's *post-hoc* test showed that both active gout patients (P = 0.0013) and inactive gout patients (P = 0.0356) had lower IL-38 levels than NCs. However, no significant difference between the two groups was observed (P = 0.9667).

3.3 Correlation analysis

The correlation between the clinical data of the patients was demonstrated using Spearman's correlation analysis (Figure 3). In patients with gout, IL-38 levels was correlated with WBC counts (r = -0.2813, P = 0.031) and CR levels (r = 0.2626, P = 0.045). No correlation was found between IL-38 and UA levels (r = -0.1535, P = 0.2459). Similarly, the association between WBC counts (r = 0.2419, P = 0.0649) and CRP levels (r = 0.1140, P = 0.3899), two common indicators of inflammation, and UA levels was not statistically significant. No correlation was found between IL-38 and CRP (r = -0.07925, P = 0.5507), SAA (r = -0.06257, P = 0.6378), ESR (r = -0.08203, P = 0.5368) and other inflammatory indicators.

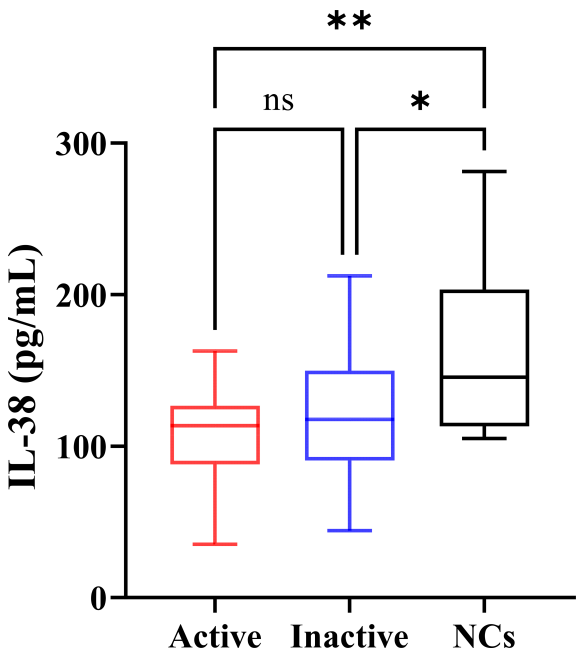

FIGURE 2
Serum IL-38 concentrations of the participants. NCs, negative controls. The *P*-values of the three groups were obtained by Kruskal-Wallis test. The *P*-value of pairwise comparison was obtained by Dunn's *post-hoc* test. *P < 0.05, **P < 0.01, ns, no significance.

3.4 ROC curve analysis

The ROC curve for evaluating the diagnostic value of gout showed that the areas under the curve (AUC) for IL-38 and UA levels were 0.7564 and 0.8339, respectively. Combined analysis of these two indicators showed that the AUC increased to 0.9034 (Figure 4).

4 Discussion

This study was conducted in Ningbo, China, and included 79 participants. Based on the ELISA results, this study is the first to identify differences in serum IL-38 levels between patients with gout and negative individuals. The serum IL-38 levels of patients with gout were lower than that of NCs, and the level of IL-38 in patients with active gout was lowest. Furthermore, correlation analysis demonstrated a negative association between IL-38 and WBC count, whereas a positive correlation was observed between IL-38

10.3389/fimmu.2024.1434738

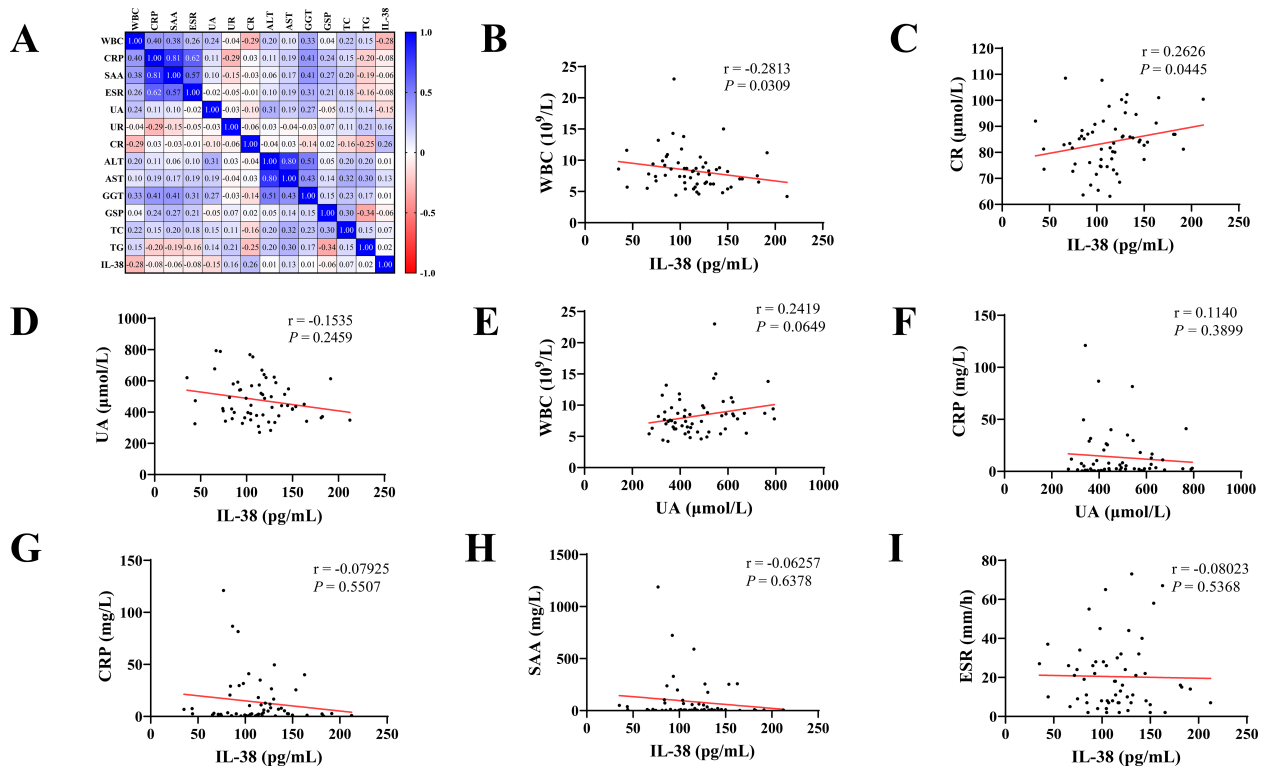

FIGURE 3
Correlation analysis of clinical indicators. **(A)** Heat map with Spearman correlation analysis of all indicators in gout patients. **(B–I)** Correlation analysis between various clinical indicators. WBC, white blood cell count; CRP, C-reactive protein; SAA, serum amyloid A; ESR, erythrocyte sedimentation rate; UA, uric acid; UR, urea; CR, creatinine; ALT, alanine aminotransferase; AST, aspartate aminotransferase; GGT, glutamyl transpeptidase; GSP, glycoserated serum protein; TC, total cholesterol; TG, triglyceride; IL-38, interleukin-38.

and CR. The ROC curve analysis supported the diagnostic value of IL-38.

Although the role of IL-38 in other types of arthritis, such as osteoarthritis and rheumatoid arthritis, has been gradually uncovered (15, 17), its significance in gout remains unclear. Some studies show that hyperuricemia is one of the independent risk factors for gout (1, 3, 27). We found that serum IL-38 levels were lower in patients with hyperuricemia than in healthy individuals (28). Although not all patients with hyperuricemia will eventually develop gout, the findings are valuable for this study. A previous study showed that recombinant IL-38 protein alleviated MSU-induced arthritis in mice (29). In other studies, serum IL-38 levels were found to be lower in patients with gout than in RA, which is also osteoarthritis (30). Unfortunately, studies of gout patients and healthy people or negative controls are not discussed at this time. In this study, patients with gout had lower IL-38 concentrations than NCs. Patients with active gout showed a slightly greater decrease in IL-38 levels than those with inactive gout. However, no statistical

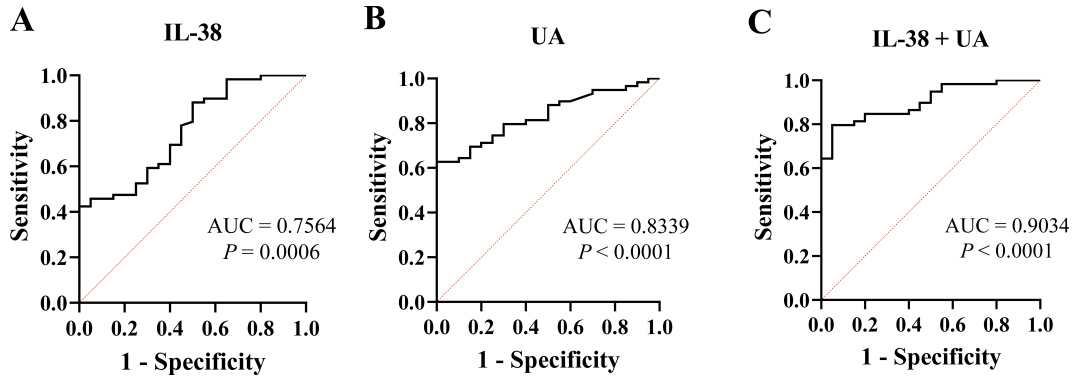

FIGURE 4
The receiver operating characteristic curve of IL-38 and UA. **(A)** IL-38 was used to diagnose gout. **(B)** UA was used for diagnose gout. **(C)** IL-38 combined with UA were used to diagnose gout. UA, uric acid; IL-38, interleukin-38; AUC, areas under the curve.

difference was observed between the two groups. These results suggest that IL-38 plays a vital role in the inflammatory response of gout. According to previous studies and existing mechanisms, the decreased levels of IL-38 in serum of patients with gout may be because IL-38 inhibits the action of IL-1β to prevent the occurrence and development of the disease (22, 29). In patients with gout, serum IL-38 failed to recover from the low level of the active period to the high level of negative individuals, suggesting that the disappearance of symptoms in patients with an inactive gout period is a temporary self-limitation and a pathogenic basis for repeated acute flares exist.

As a non-specific inflammatory indicator, the WBC count showed a negative correlation with IL-38 levels, indicating that IL-38 is related to the inflammatory response in gout. Studies on the correlation between IL-38 and CR are scarce. A correlation between CR and IL-1β in hyperuricemia has been found. Therefore, it is speculated that CR may be somewhat related to IL-38 as an intermediary variable (31). In this study, no correlation was found between UA and inflammatory markers, such as WBC and CRP, which is consistent with the results of other studies (32, 33). Probably, UA level, a gout-specific indicator, is essentially the result of the metabolic disorder; therefore, UA is not closely associated with inflammation in gout. Consequently, no correlation was expected between IL-38 and UA levels. The ROC curve analysis showed an AUC of 0.7564 for IL-38, indicating its diagnostic value for gout. Although lower than that of UA, the combined diagnostic capability of UA and IL-38 was 0.9034. Moreover, we believe that IL-38 plays a role in the inflammatory response of gout, and whether it is in the active phase has no significant influence on serum IL-38 content. However, the mechanism of IL-38 action in gout has not been fully elucidated in this study.

This pioneering study investigated differences in IL-38 levels between patients with gout and negative individuals. Additionally, we categorized the patients into active and inactive gout phases to explore the changes in serum IL-38 levels at different time points. The possible role and diagnostic value of IL-38 in gout were demonstrated using correlation and ROC curve analyses. This study has some limitations. First, as a single-center case-control study, the admission rate bias was unavoidable. Bias was controlled as much as possible using measures such as matching and objective indicators. However, we do not believe that the existence of bias will make the results unreliable. Second, the small sample size may have resulted in less stable outcomes. In a follow-up study, we will conduct a multicenter, large-sample study and animal experiments to elucidate the specific mechanism of IL-38 in the occurrence and development of gout.

In conclusion, we found, for the first time, that serum IL-38 concentration decreased in patients with gout, suggesting its potential role in gout inflammation.

Data availability statement

The raw data supporting the conclusions of this article will be made available by the authors, without undue reservation.

Ethics statement

The studies involving humans were approved by the Ethics Committee of Ningbo No. 6 Hospital Affiliated to Ningbo University. The studies were conducted in accordance with the local legislation and institutional requirements. The participants provided their written informed consent to participate in this study.

Author contributions

HH: Formal analysis, Investigation, Methodology, Writing – original draft. YZ: Data curation, Investigation, Writing – original draft. YL: Conceptualization, Formal analysis, Investigation, Methodology, Writing – original draft. HZ: Investigation, Writing – original draft. XW: Funding acquisition, Project administration, Resources, Supervision, Writing – review & editing. ML: Conceptualization, Funding acquisition, Project administration, Resources, Supervision, Writing – review & editing.

Funding

The author(s) declare financial support was received for the research, authorship, and/or publication of this article. This work was supported by the National Natural Science Foundation of China (No. 81970735), Clinical Research and Application Project of Zhejiang Health Science and Technology Program (No. 2022KY1148, No. 2024KY341, No. 2024KY1510, No. 2023KY259), and Natural Science Foundation of Ningbo (No. 2022J233, No. 2021J246).

Acknowledgments

We would like to thank Editage (www.editage.cn) for English language editing.

Conflict of interest

The authors declare that the research was conducted in the absence of any commercial or financial relationships that could be construed as a potential conflict of interest.

Publisher's note

References

1. Rock KL, Kataoka H, Lai JJ. Uric acid as a danger signal in gout and its comorbidities. *Nat Rev Rheumatol*. (2013) 9:13–23. doi: 10.1038/nrrheum.2012.143

2. Dalbeth N, Gosling AL, Gaffo A, Abhishek A. Gout. *Lancet (London England)*. (2021) 397:1843–55. doi: 10.1016/s0140-6736(21)00569-9

3. Dehlin M, Jacobsson L, Roddy E. Global epidemiology of gout: prevalence, incidence, treatment patterns and risk factors. *Nat Rev Rheumatol*. (2020) 16:380–90. doi: 10.1038/s41584-020-0441-1

4. Dalbeth N, Merriman TR, Stamp LK. Gout. *Lancet (London England)*. (2016) 388:2039–52. doi: 10.1016/s0140-6736(16)00346-9

5. Keith MP, Gilliland WR. Updates in the management of gout. *Am J Med*. (2007) 120:221–4. doi: 10.1016/j.amjmed.2006.02.044

6. Shields GE, Beard SM. A systematic review of the economic and humanistic burden of gout. *PharmacoEconomics*. (2015) 33:1029–47. doi: 10.1007/s40273-015-0288-5

7. So AK, Martinon F. Inflammation in gout: mechanisms and therapeutic targets. *Nat Rev Rheumatol*. (2017) 13:639–47. doi: 10.1038/nrrheum.2017.155

8. Dumusc A, So A. Interleukin-1 as a therapeutic target in gout. *Curr Opin Rheumatol*. (2015) 27:156–63. doi: 10.1097/bor.0000000000000143

9. Klück V, Liu R, Joosten LAB. The role of interleukin-1 family members in hyperuricemia and gout. *Joint Bone Spine*. (2021) 88:105092. doi: 10.1016/j.jbspin.2020.105092

10. Clavel G, Thiolat A, Boissier MC. Interleukin newcomers creating new numbers in rheumatology: IL-34 to IL-38. *Joint Bone Spine*. (2013) 80:449–53. doi: 10.1016/j.jbspin.2013.04.014

11. Xu WD, Huang AF. Role of interleukin-38 in chronic inflammatory diseases: A comprehensive review. *Front Immunol*. (2018) 9:1462. doi: 10.3389/fimmu.2018.01462

12. Xie L, Huang Z, Li H, Liu X, Zheng S, Su W. IL-38: A new player in inflammatory autoimmune disorders. *Biomolecules*. (2019) 9:345. doi: 10.3390/biom9080345

13. Bensen JT, Dawson PA, Mychaleckyj JC, Bowden DW. Identification of a novel human cytokine gene in the interleukin gene cluster on chromosome 2q12-14. *J Interferon Cytokine Res*. (2001) 21:899–904. doi: 10.1089/107999001753289505

14. Han Y, Huard A, Mora J, da Silva P, Brüne B, Weigert A. IL-36 family cytokines in protective versus destructive inflammation. *Cell Signalling*. (2020) 75:109773. doi: 10.1016/j.cellsig.2020.109773

15. Han MM, Yuan XR, Shi X, Zhu XY, Su Y, Xiong DK, et al. The pathological mechanism and potential application of IL-38 in autoimmune diseases. *Front Pharmacol*. (2021) 12:732790. doi: 10.3389/fphar.2021.732790

16. Rudloff I, Godsell J, Nold-Petry CA, Harris J, Hoi A, Morand EF, et al. Brief report: interleukin-38 exerts antiinflammatory functions and is associated with disease activity in systemic lupus erythematosus. *Arthritis Rheumatol (Hoboken NJ)*. (2015) 67:3219–25. doi: 10.1002/art.39328

17. Boutet MA, Bart G, Penhoat M, Amiaud J, Brulin B, Charrier C, et al. Distinct expression of interleukin (IL)-36α, β and γ, their antagonist IL-36Ra and IL-38 in psoriasis, rheumatoid arthritis and Crohn's disease. *Clin Exp Immunol*. (2016) 184:159–73. doi: 10.1111/cei.12761

18. Lea WI, Lee YH. The associations between interleukin-1 polymorphisms and susceptibility to ankylosing spondylitis: a meta-analysis. *Joint Bone Spine*. (2012) 79:370–4. doi: 10.1016/j.jbspin.2011.06.010

19. Chu M, Chu IM, Yung EC, Lam CW, Leung TF, Wong GW, et al. Aberrant expression of novel cytokine IL-38 and regulatory T lymphocytes in childhood asthma. *Molecules (Basel Switzerland)*. (2016) 21:933. doi: 10.3390/molecules21070933

20. Mora J, Schlemmer A, Wittig I, Richter F, Putyrski M, Frank AC, et al. Interleukin-38 is released from apoptotic cells to limit inflammatory macrophage responses. *J Mol Cell Biol*. (2016) 8:426–38. doi: 10.1093/jmcb/mjw006

21. Lai M, Peng H, Wu X, Chen X, Wang B, Su X. IL-38 in modulating hyperlipidemia and its related cardiovascular diseases. *Int Immunopharmacol*. (2022) 108:108876. doi: 10.1016/j.intimp.2022.108876

22. Xu Z, Yuan X, Gao Q, Li Y, Li M. Interleukin-38 overexpression prevents bleomycin-induced mouse pulmonary fibrosis. *Naunyn-Schmiedeberg's Arch Pharmacol*. (2021) 394:391–9. doi: 10.1007/s00210-020-01920-3

23. The E, de Graaf DM, Zhai Y, Yao Q, Ao L, Fullerton DA, et al. Interleukin 38 alleviates aortic valve calcification by inhibition of NLRP3. *Proc Natl Acad Sci United States Am*. (2022) 119:e2202577119. doi: 10.1073/pnas.2202577119

24. Neogi T, Jansen TL, Dalbeth N, Fransen J, Schumacher HR, Berendsen D, et al. 2015 Gout classification criteria: an American College of Rheumatology/European League Against Rheumatism collaborative initiative. *Ann Rheumatic Dis*. (2015) 74:1789–98. doi: 10.1136/annrheumdis-2015-208237

25. Felson D. Defining remission in rheumatoid arthritis. *Ann Rheumatic Dis*. (2012) 71 Suppl 2:i86–8. doi: 10.1136/annrheumdis-2011-200618

26. Pascual E, Andrés M, Sivera F. Is remission a valid target for gout? *J Rheumatol*. (2020) 47:4–5. doi: 10.3899/jrheum.190386

27. Zhang Y, Chen S, Yuan M, Xu Y, Xu H. Gout and diet: A comprehensive review of mechanisms and management. *Nutrients*. (2022) 14:3525. doi: 10.3390/nu14173525

28. Huang G, Jin Q, Li M, Tian X, Mao Y, Li Y. The potential value of low-level serum interleukin-38 for the clinical diagnosis and risk prediction of hyperuricemia. *Int Immunopharmacol*. (2022) 110:109069. doi: 10.1016/j.intimp.2022.109069

29. de Graaf DM, Maas RJA, Smeekens SP, Eisenmesser E, Redzic JS, Helsen MM, et al. Human recombinant interleukin-38 suppresses inflammation in mouse models of local and systemic disease. *Cytokine*. (2021) 137:155334. doi: 10.1016/j.cyto.2020.155334

30. Xu WD, Su LC, He CS, Huang AF. Plasma interleukin-38 in patients with rheumatoid arthritis. *Int Immunopharmacol*. (2018) 65:1–7. doi: 10.1016/j.intimp.2018.09.028

31. Di Y, Wang J, Chen Y, Sun N, Wu L, Dai X, et al. Elevated interleukin 1β and interleukin 6 levels in the serum of children with hyperuricemia. *J Clin Rheumatol*. (2018) 24:65–9. doi: 10.1097/rhu.0000000000000611

32. Jeena J, Manhas S, Prasad R, Prasad S, Gupta R. Direct relationship between uric acid and C-reactive protein and its implication in the chronic kidney disease. *Indian J Clin Biochem: IJCB*. (2022) 37:365–9. doi: 10.1007/s12291-020-00942-1

33. Kojima S, Uchiyama K, Yokota N, Tokutake E, Wakasa Y, Hiramitsu S, et al. C-reactive protein levels and cardiovascular outcomes after febuxostat treatment in patients with asymptomatic hyperuricemia: post-hoc analysis of a randomized controlled study. *Cardiovasc Drugs Ther*. (2023) 37:965–74. doi: 10.1007/s10557-022-07347-7

frontiers | Frontiers in Endocrinology

TYPE Original Research
PUBLISHED 04 November 2024
DOI 10.3389/fendo.2024.1402369

OPEN ACCESS

EDITED BY
Jixin Zhong,
Huazhong University of Science and Technology, China

REVIEWED BY
Hongrui Li,
University of North Carolina at Chapel Hill, United States
Jia Peng,
University of Kentucky, United States
Min Zhang,
University of Kentucky, United States, in collaboration with reviewer JP

*CORRESPONDENCE
Kun Lin
jornbar@126.com

RECEIVED 23 April 2024
ACCEPTED 15 October 2024
PUBLISHED 04 November 2024

CITATION
He Y, Chen X, Ma Z, Wang J and Lin K (2024) Association of oxidative balance score with hyperuricemia and gout: NHANES 2009-2018.
Front. Endocrinol. 15:1402369.
doi: 10.3389/fendo.2024.1402369

Association of oxidative balance score with hyperuricemia and gout: NHANES 2009-2018

Yiting He[1], Xiaojing Chen[1], Zeming Ma[1], Jingsa Wang[1] and Kun Lin[2*]

[1]College of Medicine, Shantou University, Shantou, China, [2]Department of Endocrinology and Metabolism, First Affiliated Hospital of Shantou University Medical College, Shantou, China

Introduction: Oxidative stress plays a crucial role in the development and progression of hyperuricemia/gout. This study aims to explore the relationship between the Oxidative Balance Score (OBS) and hyperuricemia/gout.

Methods: The study utilized complete data from adult participants in the National Health and Nutrition Examination Survey (NHANES) spanning from 2009 to 2018. OBS, composed of scores for 20 dietary and lifestyle factors, served as the exposure variable. Multivariable linear regression model was applied to evaluate the association between OBS and uric acid (UA). Multivariable logistic regression, subgroup analyses, and restricted cubic spline (RCS) regression were conducted to explore the relationship between OBS and hyperuricemia/gout.

Results: A total of 18,998 participants were included. In the fully adjusted model, compared to the lowest quartile, the highest quartiles of OBS, dietary OBS, and lifestyle OBS were negatively correlated with UA (β=-0.31 (-0.36,-0.25), β=-0.18 (-0.24,-0.12), and β=-0.64 (-0.69,-0.59), respectively) and hyperuricemia (OR=0.63 (0.55,0.71), OR=0.76 (0.67,0.86), OR=0.37 (0.33,0.42), respectively). Moreover, the highest quartiles of OBS and lifestyle OBS exhibited a negative correlation with gout (OR=0.72(0.58,0.91), OR=0.54 (0.43,0.67), respectively). Subgroup analyses revealed differences in the negative association between OBS and hyperuricemia concerning hypertension (p for interaction =0.002) and diabetes (p for interaction= 0.004), while gender-related disparities were observed in the negative association between OBS and gout (p for interaction =0.008). RCS analysis demonstrated a linear negative association between hyperuricemia and OBS (p for non-linearity >0.05), while gout exhibited a non-linear negative association (p for non-linearity<0.05).

Conclusion: The study found that a higher OBS was associated with a decreased risk of developing hyperuricemia/gout, underscoring its potential in the prevention and management of these conditions.

KEYWORDS

oxidative balance score, hyperuricemia, gout, NHANES, antioxidants, oxidative stress

1 Introduction

Uric acid (UA), a terminal product of purine analog metabolism, plays a crucial role in the development of hyperuricemia (1). Hyperuricemia is characterized by excessive production, arising from increased endogenous purine catabolism and excessive exogenous purine intake, or by impaired plasma UA excretion (2). The manifestation of hyperuricemia occurs when UA levels surpass a defined threshold, signifying the onset of a chronic metabolic disorder. Prolonged deposition of substantial UA amounts in joints and tissues eventually progresses into gout (3), affecting individuals of all ages and genders. Gout can manifest as recurrent acute attacks accompanied by joint damage and bone erosion, leading to functional impairment in severe cases (4). Additionally, hyperuricemia emerges as an independent risk factor for various systemic diseases, including cardiovascular diseases (5), hypertension (6), diabetes (7), and chronic kidney disease (CKD) (8).

Oxidative stress is usually defined as an imbalance between reactive oxygen species (ROS) and antioxidants in our body, recognized as a leading cause of cell damage and disease development. A large body of evidence has demonstrated that oxidative stress plays a crucial role in the development and progression of hyperuricemia/gout (4, 9). The oxidative balance score (OBS) is a comprehensive indicator containing 20 distinct dietary and lifestyle components, offering a means to quantify exposure to antioxidants and pro-oxidants in diet and lifestyle, therefore reflecting the overall burden of oxidative stress (10). Generally, a higher OBS is indicative of a preference for antioxidants over pro-oxidants (11). Numerous epidemiological studies have found inverse associations between OBS and various inflammation-related diseases, including CKD (12), cardiovascular disease (13), osteoarthritis (14), and type 2 diabetes (15). Nevertheless, the existing research has yet to explore the association between OBS and hyperuricemia/gout.

Recognizing the significance of OBS and implementing timely interventions may be of great value in preventing the progression of hyperuricemia and facilitating the remission of gout. To address this knowledge gap, we employ the well-established OBS in a nationally representative survey, the National Health and Nutrition Examination Survey (NHANES), to investigate its impact on hyperuricemia and gout for the first time.

2 Method

2.1 Source of data and study population

The NHANES conducted a national cross-sectional study to assess the health and nutrition status of both adults and children within the U.S. population. Employing a "stratified multistage probability sampling" method, the study gathered information through interviews, examinations, dietary questionnaires, and laboratory measurements. A total of 18998 participants were chosen from 2009 to 2018. Exclusion criteria were as follows: age of participants was <20 years, participants without serum UA and gout data, participants without OBS components' data, and variables with missing values (Figure 1). All participants provided signed written informed consent, and the study conformed to ethical standards.

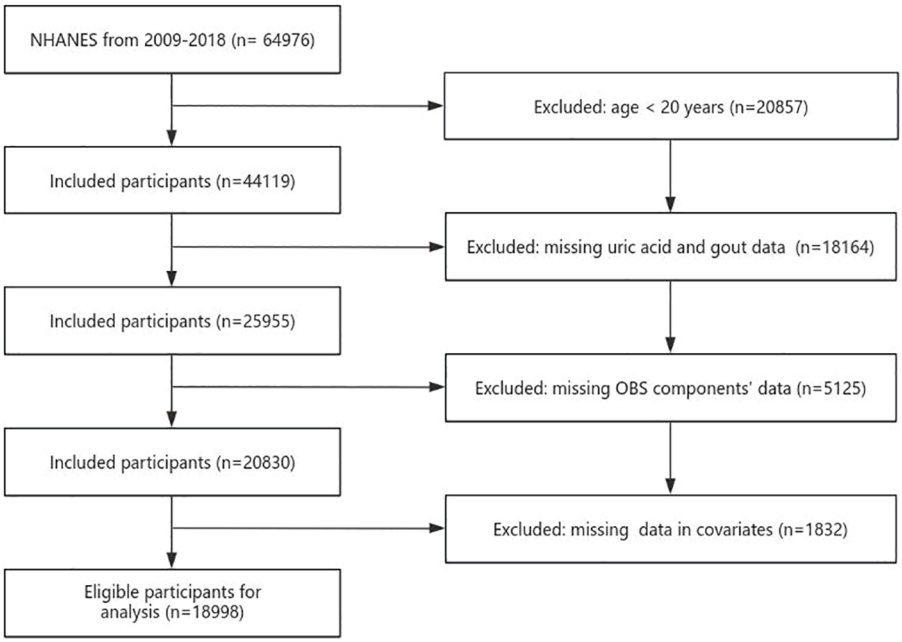

FIGURE 1
Flowchart of the sample selection from NHANES 2009–2018.

2.2 Calculation of OBS

The construction of OBS in this study was based on both prior research findings and experiential insights (16). The OBS incorporated 16 nutrients and 4 lifestyle factors. These 20 components were further classified into pro-oxidants (total fat, iron, alcohol intake, BMI, and cotinine) and antioxidants (dietary fiber, β-carotene, vitamin B2, niacin, vitamin B6, total folate, vitamin B12, vitamin C, vitamin E, calcium, magnesium, zinc, copper, selenium, and physical activity). The mean of the two 24-hour for diet and dietary supplements represented dietary and dietary supplement intake, and the intake of each nutrient was the sum of diet and dietary supplements (if available). Due to the absence of supplementation data for vitamin E and β-carotene from dietary supplements in NHANES, only dietary data were used for these two nutrients. Following Zhang et al. (16)'s method for calculating OBS, alcohol consumption was stratified into three groups, heavy drinkers (≥15 g/d for women and ≥30 g/d for men), non-heavy drinkers (0-15 g/d for women and 0-30 g/d for men), and nondrinkers, who were assigned 0, 1, and 2 points, respectively. Subsequently, the other components were categorized based on gender and further divided into three groups according to their tertile distributions. Antioxidants were assigned scores of 0-2 in groups 1-3, while pro-oxidants were assigned scores of 2-0 in groups 1-3, respectively (Supplementary Table 1). The total OBS score was the sum of scores for each component, where a higher OBS indicated a greater predominance of antioxidant exposure.

2.3 Evaluation of hyperuricemia and gout

Hyperuricemia was defined as a level of serum UA that was ≥416 mmol/L (7 mg/dL) in men and ≥357 mmol/L (6 mg/dL) in women (17). Gout was defined based on self-reported diagnosis by physicians, ascertained through the following question: "Has a doctor or other health professional ever told you that you have gout?" (17).

2.4 Covariates

Based on available literature and clinical considerations, we identified the following covariates considered potential confounders in the associations between OBS and hyperuricemia/gout. Standardized household interviews provided demographic characteristics, including age, gender (male and female), race (non-Hispanic white, non-Hispanic black, Mexican American, and other races), educational level(below high school, high school, and above high school), marital status (never married, married or lived with a partner, and others), family poverty income ratio (PIR) and total energy intake. Hypertension, diabetes, hyperlipidemia, and CKD are recognized as significant risk factors for hyperuricemia. Consequently, these diseases were integrated into the analysis. The diagnostic criteria for hypertension included an average systolic blood pressure ≥140 mmHg or average diastolic blood pressure ≥90 mmHg after at least three measurement, the use of antihypertensive drugs, and a physician-reported diagnosis of hypertension (18). Diabetes was diagnosed based on glycated hemoglobin (HbA1c) >6.5%, fasting glucose ≥7.0 mmol/L, use of diabetes medication or insulin and a previous diagnosis of diabetes by a physician (19). Hyperlipidemia was determined by total cholesterol levels ≥200 mg/dL, triglyceride levels ≥150 mg/dl, high-density lipoprotein-cholesterol ≤40 mg/dL in men and ≤50 mg/dL in women, and low-density lipoprotein-cholesterol ≥130 mg/dL (20). An albumin-to-creatinine ratio (ACR) ≥30 mg/g (3 mg/mmol) and estimated glomerular filtration rate (eGFR) <60 ml/min/1.73 m^2 were adopted as diagnostic criteria for CKD (21). we utilized the Chronic Kidney Disease Epidemiology Collaboration formulate to evaluate eGFR (22).

2.5 Statistical analysis

OBS was treated as a continuous variable. OBS group (quartile conversion) was considered a categorical variable. Continuous variables are presented as median (interquartile range (IQR)), and categorical variables are presented as frequency (percentage). Baseline characteristics were compared using the chi-square test for categorical variables and the Kruskal-Wallis test for continuous variables. To evaluate the association between OBS and UA, coefficient (β) and 95% confidence intervals (CI) were calculated using multivariable linear regression models. To explore the relationship between OBS and hyperuricemia/gout, odds ratio (OR) and 95% CI were calculated using multivariable logistic regression. The crude model was not adjusted for any covariates. Model 1 was adjusted for age, gender, and race. Model 2 was further adjusted for education level, family PIR, marital status, hypertension, diabetes, hyperlipidemia, CKD and energy. Heterogeneity between OBS (as a continuous variable) and hyperuricemia/gout was assessed through interaction and subgroup analyses for the following variables, including gender, age groups, education, race, marital status, family PIR, hypertension, hyperlipidemia, diabetes and CKD. Restricted cubic spline (RCS) analysis with four knots was applied to evaluate non-linear associations between OBS/dietary OBS/lifestyle OBS and hyperuricemia/gout risk. All statistical analyses were performed using R Statistical Software (Version 4.2.2, http://www.R-project.org, The R Foundation) and the Free Statistics analysis platform (Version 1.9, Beijing, China). Alpha was set at <0.05 for statistical significance, and all analyses were two-sided, considering a two-sided *p*-value <0.05 as statistically significant.

3 Results

3.1 Baseline characteristics

Baseline characteristics of individuals grouped by OBS quartiles are shown in Table 1. The median age of subjects was 49 years, with 52.3% being female. The majority of participants were non-Hispanic white (43.5%), and the overall prevalence of hyperuricemia and gout in the entire U.S. population was 20.1% and 4.7%, respectively. Compared to the lowest OBS quartile (Q1), individuals in the highest OBS quartile (Q4) had higher age, higher education levels, greater wealth, higher total energy intake, lower UA levels, were married or partnered, and

TABLE 1 The baseline characteristics by quartiles of the OBS: National Health and Nutrition Examination.

Characteristic	Total	Q1	Q2	Q3	Q4	*P* value
	n = 18998	n = 4983	n = 4614	n = 5288	n = 4113	
Gender, n (%)						0.259
Male	9071 (47.7)	2325 (46.7)	2241 (48.6)	2521 (47.7)	1984 (48.2)	
Female	9927 (52.3)	2658 (53.3)	2373 (51.4)	2767 (52.3)	2129 (51.8)	
Age, Median (IQR)	49.0 (35.0, 63.0)	49.0 (34.0, 63.0)	47.0 (33.0, 62.0)	49.0 (35.0, 63.0)	53.0 (38.0, 66.0)	< 0.001
Race, n (%)						< 0.001
Non-Hispanic White	8260 (43.5)	1866 (37.4)	1889 (40.9)	2352 (44.5)	2153 (52.3)	
Non-Hispanic Black	3918 (20.6)	1525 (30.6)	970 (21)	898 (17)	525 (12.8)	
Mexican American	2625 (13.8)	652 (13.1)	694 (15)	800 (15.1)	479 (11.6)	
Others	4195 (22.1)	940 (18.9)	1061 (23)	1238 (23.4)	956 (23.2)	
Education level, n (%)						< 0.001
< High school	3891 (20.5)	1407 (28.2)	1026 (22.2)	937 (17.7)	521 (12.7)	
High school	4267 (22.5)	1367 (27.4)	1074 (23.3)	1103 (20.9)	723 (17.6)	
> High school	10840 (57.1)	2209 (44.3)	2514 (54.5)	3248 (61.4)	2869 (69.8)	
Marry, n (%)						< 0.001
Never married	3429 (18.0)	1073 (21.5)	875 (19)	891 (16.8)	590 (14.3)	
Married or Living with partner	11417 (60.1)	2670 (53.6)	2757 (59.8)	3324 (62.9)	2666 (64.8)	
Others	4152 (21.9)	1240 (24.9)	982 (21.3)	1073 (20.3)	857 (20.8)	
Family PIR, Median (IQR)	2.1 (1.1, 4.1)	1.6 (0.9, 3.0)	2.0 (1.1, 3.8)	2.4 (1.2, 4.5)	3.0 (1.5, 5.0)	< 0.001
Hypertension, n (%)	9050 (47.6)	2521 (50.6)	2098 (45.5)	2449 (46.3)	1982 (48.2)	< 0.001
Diabetes, n (%)	3401 (17.9)	1090 (21.9)	839 (18.2)	872 (16.5)	600 (14.6)	< 0.001
Hyperlipidemia, n (%)	14171 (74.6)	3796 (76.2)	3450 (74.8)	3891 (73.6)	3034 (73.8)	0.012
CKD, n (%)	3324 (17.5)	1044 (21)	780 (16.9)	848 (16)	652 (15.9)	< 0.001
UA, Median (IQR)	5.3 (4.4, 6.3)	5.5 (4.5, 6.5)	5.4 (4.4, 6.4)	5.3 (4.4, 6.3)	5.2 (4.3, 6.1)	< 0.001
Hyperuricemia, n (%)	3817 (20.1)	1198 (24)	959 (20.8)	998 (18.9)	662 (16.1)	< 0.001
Gout, n (%)	886 (4.7)	280 (5.6)	187 (4.1)	237 (4.5)	182 (4.4)	0.002
Energy, Median (IQR)	1923.4 (1479.1, 2475.5)	1509.0 (1151.0, 1926.2)	1892.0 (1508.2, 2342.0)	2137.2 (1683.0, 2712.6)	2270.5 (1780.5, 2880.5)	< 0.001

PIR, poverty income ratio.
CKD, chronic kidney disease.
UA, uric acid.

were non-Hispanic white or of other races. The prevalence of hyperuricemia and gout, along with their comorbidities, including hypertension, diabetes, hyperlipidemia, and CKD, gradually decreased as OBS increased.

3.2 Association between OBS and UA

Linear regression was employed to assess the association between OBS and plasma UA. The data presented in Table 2 reveals a negative correlation between OBS and plasma UA ($p < 0.05$). In the fully adjusted model (Model 2), the highest quartile of OBS exhibited a stronger negative association with UA levels compared to the lowest quartile of OBS (β=-0.31 (-0.36, -0.25), $p < 0.001$), and this association remained relatively stable across models. We further explored the impact of dietary OBS and lifestyle OBS on UA using linear regression models. In Model 2, both dietary OBS and lifestyle OBS in the highest quartile group (Q4) were significantly associated with decreased uric acid levels compared to the lowest quartile (Q1) (β=-0.18 (-0.24, -0.12), $p < 0.001$, β=-0.64 (-0.69, -0.59), $p < 0.001$, respectively) (Table 2). The trend test indicated a statistically significant downward trend (p for trend < 0.001). These findings underscore the inverse relationship between OBS and plasma UA, highlighting the potential role of oxidative balance in modulating UA levels.

TABLE 2 Beta coefficient (95% CI) for serum UA by OBS/dietary OBS/lifestyle OBS quartiles.

Variable	Crude model		Model 1		Model 2	
	Beta coefficient 95%CI	*P* value	Beta coefficient 95%CI	*P* value	Beta coefficient 95%CI	*P* value
OBS						
Q1	0 (Ref)		0 (Ref)		0 (Ref)	
Q2	-0.11 (-0.17, -0.05)	<0.001	-0.11 (-0.16, -0.06)	<0.001	-0.08 (-0.13, -0.03)	0.002
Q3	-0.21 (-0.26, -0.15)	<0.001	-0.2 (-0.25, -0.15)	<0.001	-0.16 (-0.21, -0.11)	<0.001
Q4	-0.34 (-0.39, -0.28)	<0.001	-0.37 (-0.43, -0.32)	<0.001	-0.31 (-0.36, -0.25)	<0.001
P for trend	-0.11 (-0.13, -0.09)	<0.001	-0.12 (-0.14, -0.1)	<0.001	-0.1 (-0.12, -0.08)	<0.001
Dietary OBS						
Q1	0 (Ref)		0 (Ref)		0 (Ref)	
Q2	-0.05 (-0.1, 0.01)	0.096	-0.05 (-0.1, 0)	0.052	-0.02 (-0.07, 0.04)	0.541
Q3	-0.15 (-0.21, -0.1)	<0.001	-0.14 (-0.19, -0.09)	<0.001	-0.09 (-0.14, -0.03)	0.002
Q4	-0.21 (-0.27, -0.16)	<0.001	-0.25 (-0.3, -0.2)	<0.001	-0.18 (-0.24, -0.12)	<0.001
P for trend	-0.07 (-0.09, -0.06)	<0.001	-0.08 (-0.1, -0.07)	<0.001	-0.06 (-0.08, -0.04)	<0.001
Lifestyle OBS						
Q1	0 (Ref)		0 (Ref)		0 (Ref)	
Q2	-0.29 (-0.34, -0.23)	<0.001	-0.28 (-0.33, -0.23)	<0.001	-0.25 (-0.3, -0.2)	<0.001
Q3	-0.49 (-0.55, -0.44)	<0.001	-0.48 (-0.53, -0.43)	<0.001	-0.41 (-0.46, -0.36)	<0.001
Q4	-0.69 (-0.75, -0.64)	<0.001	-0.74 (-0.79, -0.69)	<0.001	-0.64 (-0.69, -0.59)	<0.001
P for trend	-0.23 (-0.25, -0.21)	<0.001	-0.24 (-0.26, -0.23)	<0.001	-0.21 (-0.23, -0.19)	<0.001

Crude model: unadjusted model.
Model 1: adjusted for sex, age and race.
Model 2: adjusted for sex, age, race, education level, family PIR, marital status, hypertension, diabetes, hyperlipidemia, CKD and energy.

3.3 Association between OBS and hyperuricemia

As shown in Table 3, logistic regression analysis revealed a significant negative association between OBS and hyperuricemia. The risk of hyperuricemia gradually decreased with increasing quartiles in all models (p for trend <0.001). In the fully adjusted model (Model 2), participants in Q4 of OBS showed a lower risk of hyperuricemia compared to the reference Q1 (OR = 0.63 (0.55, 0.71), $p < 0.001$), and this association remained consistent across models. Furthermore, in Model 2, both dietary OBS and lifestyle OBS in Q4 compared with Q1 reduced the risk of hyperuricemia (OR = 0.76 (0.67, 0.9), $p < 0.001$; OR = 0.37 (0.33, 0.42), $p < 0.001$, respectively) (Table 3). The trend test indicated a statistically significant downward trend (p for trend < 0.001).

3.4 Association between OBS and gout

As shown in Table 4, logistic regression analysis found a significant negative association between OBS and gout. In the fully adjusted model (Model 2), OBS was associated with a lower risk of gout in Q4 compared to Q1 (OR = 0.72 (0.58, 0.91), $p = 0.005$), and this association maintained relative stability across models. The trend test indicated a statistically significant downward trend (p for trend=0.014). When examining lifestyle OBS, individuals in Q4 exhibited a decreased risk of gout (OR = 0.54 (0.43, 0.67), $p < 0.001$). However, the associations between dietary OBS and gout were not statistically significant in Q3 and Q4 compared to Q1 after adjusting for all confounders. Only participants in Q2 of dietary OBS exhibited a statistically significant decrease in the risk of gout compared to Q1 (OR=0.75 (0.62, 0.92), $p = 0.006$) in Model 2.

3.5 Subgroup analysis

Subgroup analyses and interaction tests, stratified by sex, age, education level, race, family PIR, hypertension, diabetes, hyperlipidemia, and CKD, were conducted to identify potential variations across different populations. In hyperuricemia, as shown in Figure 2, statistical significance was found in hypertension and diabetes subgroups (P for interaction =0.002, P for interaction =0.004, respectively). The negative association effect of OBS with hyperuricemia was significantly greater in participants without hypertension (OR=0.96 (0.95, 0.97)) than in those with hypertension (OR = 0.98 (0.97, 0.99)). Similarly, the negative association effect of OBS was significantly greater in participants without diabetes

TABLE 3 Odds Ratio (95% CI) for hyperuricemia by OBS/dietary OBS/lifestyle OBS quartiles.

Variable	Crude model		Model 1		Model 2	
	OR 95%CI	*P* value	OR 95%CI	*P* value	OR 95%CI	*P* value
OBS						
Q1	1 (Ref)		1 (Ref)		1 (Ref)	
Q2	0.83 (0.75, 0.91)	<0.001	0.86 (0.78, 0.94)	0.002	0.88 (0.8, 0.98)	0.019
Q3	0.73 (0.67, 0.81)	<0.001	0.74 (0.68, 0.82)	<0.001	0.79 (0.71, 0.88)	<0.001
Q4	0.61 (0.55, 0.67)	<0.001	0.58 (0.52, 0.64)	<0.001	0.63 (0.55, 0.71)	<0.001
P for trend	0.85 (0.82, 0.88)	<0.001	0.84 (0.81, 0.87)	<0.001	0.86 (0.83, 0.9)	<0.001
Dietary OBS						
Q1	1 (Ref)		1 (Ref)		1 (Ref)	
Q2	0.9 (0.82, 0.99)	0.035	0.93 (0.85, 1.03)	0.158	0.97 (0.88, 1.08)	0.582
Q3	0.79 (0.71, 0.87)	<0.001	0.8 (0.72, 0.89)	<0.001	0.86 (0.77, 0.96)	0.007
Q4	0.73 (0.66, 0.81)	<0.001	0.69 (0.63, 0.77)	<0.001	0.76 (0.67, 0.86)	<0.001
P for trend	0.9 (0.87, 0.93)	<0.001	0.88 (0.86, 0.91)	<0.001	0.91 (0.88, 0.95)	<0.001
Life OBS						
Q1	1 (Ref)		1 (Ref)		1 (Ref)	
Q2	0.68 (0.62, 0.75)	<0.001	0.68 (0.62, 0.75)	<0.001	0.72 (0.65, 0.79)	<0.001
Q3	0.5 (0.46, 0.55)	<0.001	0.51 (0.46, 0.56)	<0.001	0.56 (0.51, 0.62)	<0.001
Q4	0.31 (0.28, 0.34)	<0.001	0.32 (0.28, 0.35)	<0.001	0.37 (0.33, 0.42)	<0.001
P for trend	0.69 (0.66, 0.71)	<0.001	0.69 (0.67, 0.72)	<0.001	0.73 (0.7, 0.75)	<0.001

Crude model: unadjusted model.
Model 1: adjusted for sex, age and race.
Model 2: adjusted for sex, age, race, education level, family PIR, marital status, hypertension, diabetes, hyperlipidemia, CKD and energy.

(OR = 0.97 (0.96, 0.98)) than in those with diabetes (OR = 0.99 (0.98, 1.01)). In the analysis of gout prevalence (Figure 3), statistical significance was found in gender subgroups (*P* for interaction =0.008). A considerably stronger negative association between OBS and the prevalence of gout was observed in females (OR=0.97 (0.95, 0.99)) compared to males (OR=0.99 (0.98, 1)). Despite some inconsistent effect values in certain subgroups, our findings suggest that the negative association between OBS and hyperuricemia/gout was consistently maintained across all subgroups.

3.6 RCS analysis

From RCS analysis based on multivariable logistic regression adjusting for all covariates, a linear association was observed between OBS, dietary OBS, and lifestyle OBS and the prevalence of hyperuricemia (all *p* for non–linear > 0.05) (Figures 3A–C). A significant nonlinear relationship was identified between OBS and the risk of gout (*p* for non-linear < 0.05, Figure 4A). Figures 4B, C display that dietary OBS and lifestyle OBS were negatively and linearly associated with the risk of gout (*p* for non-linear > 0.05). These findings indicate that higher OBS is related to a lower prevalence of hyperuricemia and gout.

4 Discussion

To illuminate the relationship between OBS and hyperuricemia/gout, we conducted a cross-sectional analysis of 18998 individuals in the NHANES cohort. Our study found that total OBS was negatively associated with the levels of UA and the prevalence of hyperuricemia/gout. In addition, both dietary and lifestyle components exhibited independent associations with UA and hyperuricemia. Besides, the risk of gout was observed with higher OBS in lifestyle components. These associations remained significant even after adjusting for potential confounders, suggesting that increased exposure to antioxidants and decreased exposure to pro-oxidants, as indicated by a higher OBS, could potentially reduce the risk of hyperuricemia/gout. To the best of our knowledge, our research is the first comprehensive retrospective study to investigate the association between OBS and hyperuricemia/gout prevalence. It may be considered a good indicator of hyperuricemia/gout prevalence. These findings may provide some potential theoretical reference for the prevention of hyperuricemia/gout through oxidative stress.

The pathogenesis of hyperuricemia/gout is multifactorial and complex, involving a mix of genetic, environmental, and dietary factors (9). Mechanistically, oxidative stress is essentially due to an imbalance between pro-oxidants and antioxidants in the body,

TABLE 4 Odds Ratio (95% CI) for gout by OBS/dietary OBS/lifestyle OBS quartiles.

Variable	Crude model		Model 1		Model 2	
	OR 95%CI	*P* value	OR 95%CI	*P* value	OR 95%CI	*P* value
OBS						
Q1	1 (Ref)		1 (Ref)		1 (Ref)	
Q2	0.71 (0.59, 0.86)	<0.001	0.74 (0.61, 0.9)	0.002	0.75 (0.61, 0.92)	0.005
Q3	0.79 (0.66, 0.94)	0.009	0.78 (0.65, 0.94)	0.008	0.82 (0.67, 1)	0.052
Q4	0.78 (0.64, 0.94)	0.01	0.67 (0.55, 0.82)	<0.001	0.72 (0.58, 0.91)	0.005
P for trend	0.93 (0.87, 0.99)	0.016	0.89 (0.83, 0.95)	<0.001	0.91 (0.85, 0.98)	0.014
Dietary OBS						
Q1	1 (Ref)		1 (Ref)		1 (Ref)	
Q2	0.72 (0.6, 0.87)	0.001	0.75 (0.62, 0.91)	0.003	0.75 (0.62, 0.92)	0.006
Q3	0.86 (0.71, 1.03)	0.099	0.86 (0.71, 1.04)	0.127	0.9 (0.73, 1.11)	0.332
Q4	0.88 (0.73, 1.05)	0.158	0.76 (0.63, 0.92)	0.005	0.8 (0.64, 1)	0.051
P for trend	0.97 (0.91, 1.03)	0.308	0.93 (0.87, 0.99)	0.019	0.95 (0.88, 1.02)	0.162
Lifestyle OBS						
Q1	1 (Ref)		1 (Ref)		1 (Ref)	
Q2	0.81 (0.68, 0.96)	0.016	0.75 (0.63, 0.9)	0.002	0.84 (0.71, 1.01)	0.065
Q3	0.64 (0.53, 0.76)	<0.001	0.61 (0.51, 0.74)	<0.001	0.71 (0.59, 0.87)	0.001
Q4	0.43 (0.35, 0.53)	<0.001	0.41 (0.33, 0.51)	<0.001	0.54 (0.43, 0.67)	<0.001
P for trend	0.77 (0.72, 0.81)	<0.001	0.76 (0.71, 0.81)	<0.001	0.82 (0.77, 0.88)	<0.001

Crude model: unadjusted model.
Model 1: adjusted for sex, age and race.
Model 2: adjusted for sex, age, race, education level, family PIR, marital status, hypertension, diabetes, hyperlipidemia, CKD and energy.

which is considered a major contributor to cellular damage and disease progression (23). Existing evidence indicates that UA has complex chemical and biological actions, featuring antioxidant properties with potential protective effects (2). However, it can also act as a pro-oxidant, contributing to the development of diseases such as hypertension, metabolic syndrome, and cardiovascular diseases (2). The exact role of UA in oxidative stress is not fully elucidated and may depend on its chemical microenvironment (2, 23). Increasing evidence suggests that some of the harmful intracellular effects induced by UA are mediated by oxidative stress. For instance, during the UA metabolism process, xanthine oxidoreductase (XOR) catalyzes the hydroxylation of hypoxanthine to xanthine, inducing the generation of ROS, subsequently resulting in an imbalance in redox signaling (24). Additionally, animal experiments have indicated that hyperuricemia-induced renal oxidative stress promotes mitochondrial dysfunction and reduced ATP levels in rats (25). Furthermore, a study conducted by Sánchez-Lozada et al. demonstrated that an elevated UA concentration exacerbates intracellular ROS production through the activation of nicotinamide adenine dinucleotide phosphate (NADPH) oxidase (26). Our research results indicate that a high OBS exerts a protective effect against the development of hyperuricemia/gout, aligning with the current understanding of the role of oxidative stress in the pathogenesis of hyperuricemia/gout.

A longitudinal study has revealed that individuals with high genetic risk, who adhere to a healthy diet and lifestyle, experience a 40% reduction in the risk of developing hyperuricemia compared to those with unhealthy dietary and living habits (27). Similarly, maintaining a healthy diet and lifestyle is associated with a nearly one-third reduction in the risk of gout related to genetic factors (28). Regarding dietary factors, some studies propose that supplementing dietary antioxidants, such as dietary fiber (29), vitamin B2 (30), vitamin E (31), vitamin C (32), folate (33, 34), carotenoids (35), calcium (30), and zinc (34), may contribute to lower UA levels. Conversely, pro-oxidants, exemplified by fat (30) and iron (36) intake, are linked to elevated UA levels. In our study, the OBS incorporates various dietary and lifestyle factors to comprehensively assess an individual's antioxidant and pro-oxidant status. The findings indicate that certain specific antioxidants within the OBS are significantly associated with a reduced risk of hyperuricemia and gout. Dietary fiber plays an important role in OBS. An experimental study has demonstrated that dietary fiber can reduce oxidative stress and inflammatory responses in hyperuricemic mice by regulating the Toll-like receptor 4/NF-κB signaling pathway. Additionally, dietary fiber shows potential in alleviating hyperuricemic by modulating the gut microbiota and metabolites (37). Vitamin E is also a potent antioxidant. It protects cell membranes from oxidative damage by

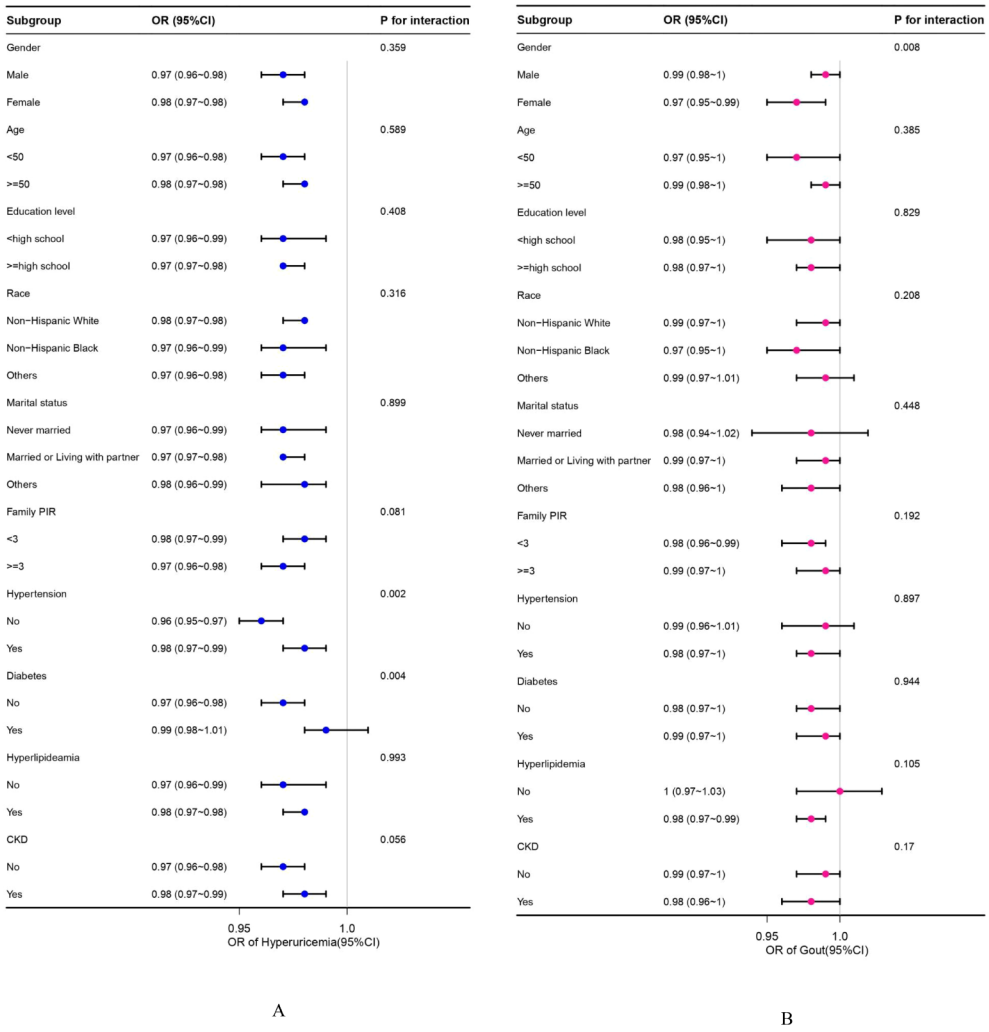

FIGURE 2
(A, B) Subgroup analyses between OBS and hyperuricemia/gout. **(A)** Hyperuricemia; **(B)** Gout. OR values are based on different population stratifications, estimated using a multivariable logistic regression model to assess the OR and 95% CI between OBS and hyperuricemia/gout. *P* for interaction values pertains to the significance of models considering interaction terms between OBS and various variables (sex, age, race, education level, family PIR, marital status, hypertension, diabetes, hyperlipidemia, and CKD) except for the stratification component itself. OBS, oxidative balance score; OR, odds ratio; CI, confidence intervals; CKD, chronic kidney disease.

inhibiting free radical production and reducing oxidative stress. Research has shown that higher vitamin E intake is associated with a lower risk of hyperuricemia (31). This suggests that vitamin E may mitigate the negative impact of oxidative stress on uric acid metabolism, thereby lowering the risk of hyperuricemia. Lifestyle factors also play a significant role, wherein an elevated body mass index (BMI) increases the risk of hyperuricemia, while physical activity lowers the risk (38). A study (39) has indicated that men with a BMI over 27.5 kg/m^2 have a 16-fold higher risk of gout compared to those with a BMI below 20 kg/m^2, and a 4-fold higher risk compared to those with a BMI under 25 kg/m^2. The impact of alcohol consumption on hyperuricemia/gout remains controversial (40), with some studies suggesting that moderate wine consumption may enhance endogenous UA clearance and prevent gout attacks, attributed to the presence of antioxidants and phytoestrogens in wine. In contrast, others argue occasional alcohol intake is associated with increased UA secretion and gout attacks (40). Considering the pro-oxidant nature of alcohol, in conjunction with our research findings, and taking into account other health issues associated with alcohol, we recommend limiting alcohol intake, especially for individuals with gout or those at risk. Interestingly, certain studies have reported that smokers exhibit significantly lower serum UA levels. This is attributed to prolonged exposure to cigarette smoke, which leads to a reduction in the production of endogenous UA with antioxidant defense capabilities (41). However, conflicting findings have been reported, suggesting higher UA levels in smokers (42).

Recognizing the potential antagonistic and synergistic effects of pro-oxidants or antioxidants, we employed the OBS as a comprehensive assessment of individual oxidative balance for the first time to study its impact on hyperuricemia/gout. Our research indicated that the OBS in the non-hyperuricemia/gout group was markedly higher than that in the hyperuricemia/gout group. Notably, we found that lifestyle OBS was more effective in

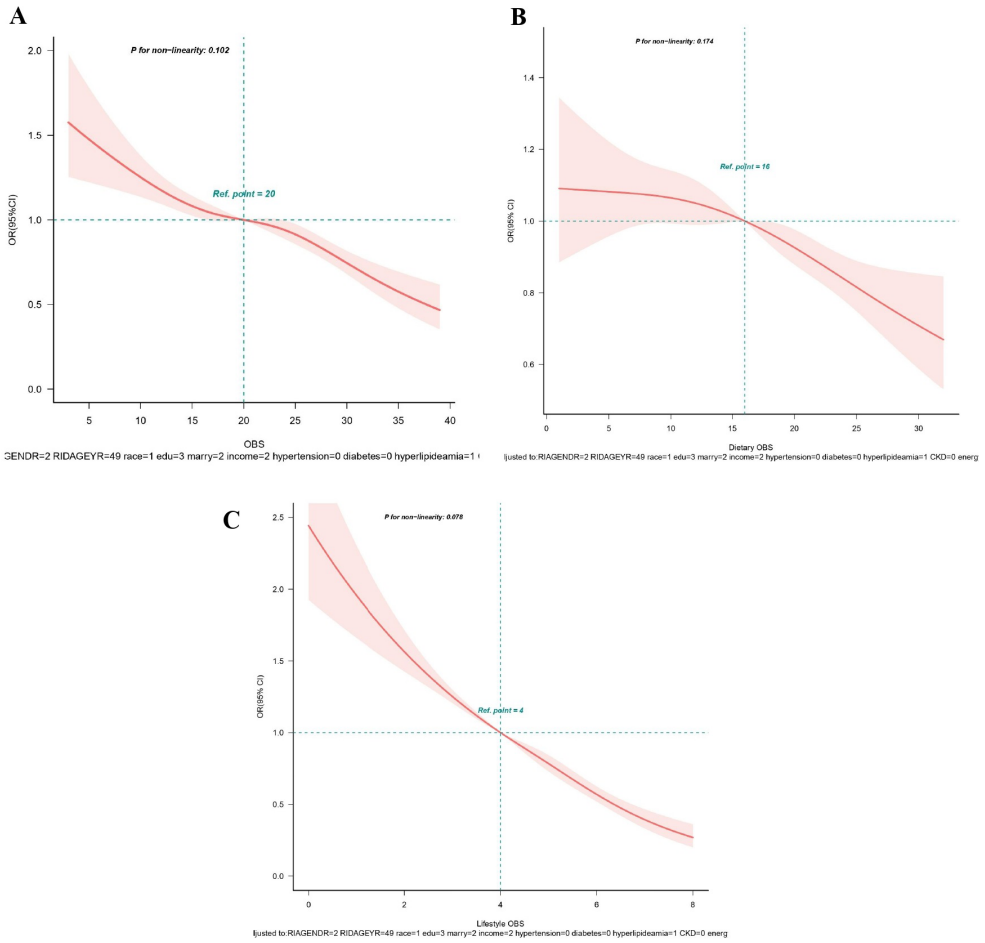

FIGURE 3
(A-C) Restricted spline curves for the associations between all OBS and hyperuricemia. **(A)** OBS; **(B)** Dietary OBS; **(C)** Lifestyle OBS. Red lines represent the OR and red transparent areas represent the 95% CI. OR (95% CI) were all adjusted according to Model 2. OBS, oxidative balance score; OR, odds ratio; CI, confidence intervals.

reducing the risk of hyperuricemia compared to dietary OBS. According to NHANES III data (43), 44%, 9%, and 8% of the risk of hyperuricemia in the general adult population may be attributed to obesity, unhealthy diet, and alcohol consumption, respectively. A study suggests that dietary habits exert a greater impact on the likelihood of developing hyperuricemia in males, while lifestyle factors related to physical activity have a more significant impact on females (44). Surprisingly, an unexpected finding in our study was a seemingly insignificant correlation between dietary OBS and gout. The underlying mechanism remains unclear, possibly because gout is a multifactorial metabolic disease, and its pathogenesis should not rely solely on hyperuricemia or monosodium urate (MSU) crystal formation (45). However, a study using NHANES data indicated a negative correlation between a comprehensive dietary antioxidant index(CDAI), evaluated with zinc, selenium, carotenoids, and vitamins A, C, and E, and the prevalence of gout in U.S. adults (46). Therefore, future high-quality prospective studies are needed to further explore the relevant mechanisms.

In the subgroup analysis, our study indicated a significant impact of diabetes and hypertension on the relationship between OBS and hyperuricemia. A prospective investigation revealed an elevated risk of developing hyperuricemia in individuals with diabetes or hypertension at baseline (47). The potential influences of insulin resistance and renal sodium handling on the renal clearance rate of UA might contribute to explaining the increased prevalence of hyperuricemia in individuals with diabetes and hypertension (48). Consequently, we speculate that the protective effect of OBS against hyperuricemia may not be as pronounced in participants with these chronic diseases. In addition, our research suggested a notable gender influence on the correlation between OBS and gout. Specifically, in females, there is a significantly stronger negative correlation between OBS and the incidence of gout. It may be attributed to the differing roles of sex hormones in oxidative stress and uric acid metabolism. Estrogen, which is more prevalent in females, has been shown to have antioxidant properties that can enhance the body's defense against oxidative stress. This hormone may reduce the production of ROS and increase the activity of antioxidant enzymes, thereby lowering oxidative damage and potentially reducing uric acid levels (49). A study has demonstrated that postmenopausal hormone therapy, whether estrogen alone or in combination with progestin, moderately reduces the risk of gout (50). In contrast, androgens, which are

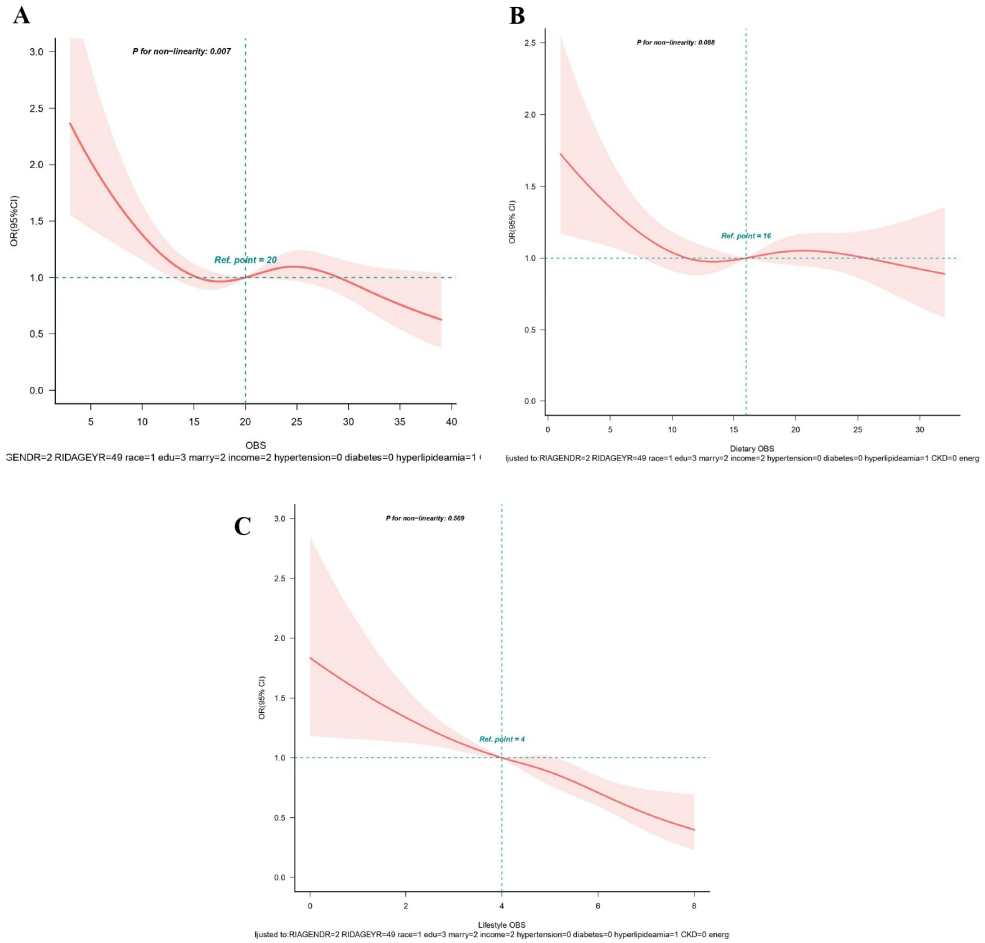

FIGURE 4
(A-C) Restricted spline curves for the associations between all OBS and gout. **(A)** OBS; **(B)** Dietary OBS; **(C)** Lifestyle OBS. Red lines represent the OR and red transparent areas represent the 95% CI. OR (95% CI) were all adjusted according to Model 2. OBS, oxidative balance score; OR, odds ratio; CI, confidence intervals.

more prevalent in males, have been associated with increased oxidative stress and higher uric acid levels (50). These differences in hormone profiles could explain why females might experience a more pronounced protective effect from a high OBS, leading to a stronger association with reduced gout risk. Future research should explore whether different antioxidant interventions differ in effectiveness between men and women. Specifically, studies could investigate if tailored antioxidant supplementation or lifestyle modifications based on hormonal profiles could optimize the reduction of uric acid levels and prevent gout more effectively in each gender.

This study suggests that the OBS may be a valuable tool for managing hyperuricemia and gout. Clinicians could use OBS in dietary and lifestyle counseling by encouraging patients to increase antioxidant-rich foods, such as fruits and vegetables, while reducing pro-oxidative factors like processed foods, potentially lowering the risk of these conditions. However, implementing OBS-based interventions in clinical practice presents challenges. Calculating OBS requires detailed dietary and lifestyle information, which can be difficult to collect and interpret. Additionally, patients' adherence may also vary, especially with significant lifestyle changes. Integrating OBS into clinical workflows may require additional training for healthcare providers and the development of supportive tools.

While antioxidants generally protect against oxidative stress, certain antioxidants may exhibit pro-oxidative effects at high doses, known as the "antioxidant paradox." For example, high doses of vitamin C may generate ROS instead of neutralizing them (51). Similarly, high concentrations of synthetic vitamin E can exacerbate oxidative stress (52). The threshold at which antioxidants shift from protective to harmful effects varies depending on factors such as the specific antioxidant, the presence of metal ions, and the redox status of the cellular environment. These threshold effects are critical for interpreting our study's findings. The OBS reflects the balance between pro-oxidative and antioxidative factors, with higher scores suggesting a more favorable oxidative balance. However, at high doses, antioxidants may become pro-oxidative, indicating this balance is not linear. Individuals with very high antioxidant intake may experience diminished or even adverse effects, which could complicate the relationship between OBS and disease risk. While our study supports the general protective role of antioxidants, future research should explore dose-dependent effects, identify conditions where antioxidants become pro-oxidative, and

determine optimal intake levels to maximize benefits and minimize risks.

This study employed a nationally representative population-based investigation, ensuring the universality and representativeness of our findings. Additionally, we incorporated potential covariates based on previous research, significantly reducing the impact of confounding factors. Finally, the robustness and stability of our study results were underscored through stratified analysis and sensitivity analysis. However, inherent limitations do exist in our study. Firstly, due to its cross-sectional nature, establishing causation is not feasible. Secondly, although averaging the data from two 24-hour dietary recalls enhanced representativeness, it may not fully capture long-term dietary habits, considering potential recall bias and the limited variety of foods considered. Thirdly, the study did not account for potential threshold effects of antioxidants, as some antioxidants have demonstrated potential pro-oxidative activity at high doses or under specific conditions. Therefore, the results obtained are merely the outcome of statistical analysis, and future prospective research is needed to address these limitations and provide further insights.

5 Conclusion

In conclusion, this nationally representative cross-sectional study revealed that a higher OBS was associated with a decreased risk of developing hyperuricemia/gout. The finding underscores the importance of adhering to an antioxidant-rich diet and lifestyle, contributing to the prevention and treatment of hyperuricemia/gout. However, further research is necessary in future studies to investigate the causal relationship and precise mechanisms underlying the association between OBS and hyperuricemia/gout.

Data availability statement

The original contributions presented in the study are included in the article/Supplementary Material. Further inquiries can be directed to the corresponding authors.

Ethics statement

The studies involving humans were approved by The National Center for Health Statistics (NCHS) Ethics Review Board. The studies were conducted in accordance with the local legislation and institutional requirements. The participants provided their written informed consent to participate in this study.

Author contributions

YH: Conceptualization, Writing – review & editing, Writing – original draft. XC: Writing – original draft, Visualization. ZM: Writing – original draft, Formal Analysis. JW: Data curation, Writing – original draft. KL: Supervision, Writing – review & editing, Writing – original draft.

Funding

The author(s) declare that no financial support was received for the research, authorship, and/or publication of this article.

Acknowledgments

We express our gratitude to the participants and staff of the NHANES for their invaluable contributions to this study.

Conflict of interest

The authors declare that the research was conducted in the absence of any commercial or financial relationships that could be construed as a potential conflict of interest.

Publisher's note

Supplementary material

The Supplementary Material for this article can be found online at: https://www.frontiersin.org/articles/10.3389/fendo.2024.1402369/full#supplementary-material

References

1. Steunou A-S, Babot M, Durand A, Bourbon M-L, Liotenberg S, Miotello G, et al. Discriminating susceptibility of xanthine oxidoreductase family to metals. *Microbiol Spectr*. 11:e04814–22. doi: 10.1128/spectrum.04814-22

2. So A, Thorens B. Uric acid transport and disease. *J Clin Invest*. (2010) 120 (6):1791–1799. doi: 10.1172/JCI42344

3. Richette P, Doherty M, Pascual E, Barskova V, Becce F, Castaneda J, et al. 2018 updated European League Against Rheumatism evidence-based recommendations for the diagnosis of gout. *Ann Rheum Dis*. (2020) 79:31–8. doi: 10.1136/annrheumdis-2019-215315

4. McQueen FM, Chhana A, Dalbeth N. Mechanisms of joint damage in gout: evidence from cellular and imaging studies. *Nat Rev Rheumatol*. (2012) 8:173–81. doi: 10.1038/nrrheum.2011.207

5. Tseng W-C, Chen Y-T, Ou S-M, Shih C-J, Tarng D-C. U-shaped association between serum uric acid levels with cardiovascular and all-cause mortality in the

elderly: the role of malnourishment. *J Am Heart Assoc*. (2018) 7:e007523. doi: 10.1161/JAHA.117.007523

6. Kanbay M, Segal M, Afsar B, Kang D-H, Rodriguez-Iturbe B, Johnson RJ. The role of uric acid in the pathogenesis of human cardiovascular disease. *Heart*. (2013) 99:759–66. doi: 10.1136/heartjnl-2012-302535

7. Dehghan A, van Hoek M, Sijbrands EJG, Hofman A, Witteman JCM. High serum uric acid as a novel risk factor for type 2 diabetes. *Diabetes Care*. (2008) 31:361–2. doi: 10.2337/dc07-1276

8. Madero M, Sarnak MJ, Wang X, Greene T, Beck GJ, Kusek JW, et al. Uric acid and long-term outcomes in CKD. *Am J Kidney Dis*. (2009) 53:796–803. doi: 10.1053/j.ajkd.2008.12.021

9. Wu Z-D, Yang X-K, He Y-S, Ni J, Wang J, Yin K-J, et al. Environmental factors and risk of gout. *Environ Res*. (2022) 212:113377. doi: 10.1016/j.envres.2022.113377

10. Goodman M, Bostick RM, Dash C, Flanders WD, Mandel JS. Hypothesis: oxidative stress score as a combined measure of pro-oxidant and antioxidant exposures. *Ann Epidemiol*. (2007) 17:394–9. doi: 10.1016/j.annepidem.2007.01.034

11. Lakkur S, Bostick RM, Roblin D, Ndirangu M, Okosun I, Annor F, et al. Oxidative balance score and oxidative stress biomarkers in a study of Whites, African Americans, and African immigrants. *Biomarkers*. (2014) 19:471–80. doi: 10.3109/1354750X.2014.937361

12. Ilori TO, Sun Ro Y, Kong SY, Gutierrez OM, Ojo AO, Judd SE, et al. Oxidative balance score and chronic kidney disease. *Am J Nephrol*. (2015) 42:320–7. doi: 10.1159/000441623

13. Ilori TO, Wang X, Huang M, Gutierrez OM, Narayan KMV, Goodman M, et al. Oxidative balance score and the risk of end-stage renal disease and cardiovascular disease. *Am J Nephrol*. (2017) 45:338–45. doi: 10.1159/000464257

14. Lee J-H, Joo YB, Han M, Kwon SR, Park W, Park K-S, et al. Relationship between oxidative balance score and quality of life in patients with osteoarthritis: Data from the Korea National Health and Nutrition Examination Survey (2014-2015). *Med (Baltimore)*. (2019) 98:e16355. doi: 10.1097/MD.0000000000016355

15. Golmohammadi M, Ayremlou P, Zarrin R. Higher oxidative balance score is associated with better glycemic control among Iranian adults with type-2 diabetes. *Int J Vitam Nutr Res*. (2021) 91:31–9. doi: 10.1024/0300-9831/a000596

16. Zhang W, Peng S-F, Chen L, Chen H-M, Cheng X-E, Tang Y-H. Association between the oxidative balance score and telomere length from the national health and nutrition examination survey 1999-2002. *Oxid Med Cell Longev*. (2022) 2022:1345071. doi: 10.1155/2022/1345071

17. Chen-Xu M, Yokose C, Rai SK, Pillinger MH, Choi HK. Contemporary prevalence of gout and hyperuricemia in the United States and decadal trends: the national health and nutrition examination survey, 2007-2016. *Arthritis Rheumatol*. (2019) 71:991–9. doi: 10.1002/art.40807

18. Elliott WJ. Systemic hypertension. *Curr Probl Cardiol*. (2007) 32:201–59. doi: 10.1016/j.cpcardiol.2007.01.002

19. Wu C, Ren C, Song Y, Gao H, Pang X, Zhang L. Gender-specific effects of oxidative balance score on the prevalence of diabetes in the US population from NHANES. *Front Endocrinol (Lausanne)*. (2023) 14:1148417. doi: 10.3389/fendo.2023.1148417

20. National Cholesterol Education Program (NCEP) Expert Panel on Detection, Evaluation, and Treatment of High Blood Cholesterol in Adults (Adult Treatment Panel III). Third Report of the National Cholesterol Education Program (NCEP) Expert Panel on Detection, Evaluation, and Treatment of High Blood Cholesterol in Adults (Adult Treatment Panel III) final report. *Circulation*. (2002) 106:3143–421. doi: 10.1161/circ.106.25.3143

21. Kidney Disease: Improving Global Outcomes (KDIGO) Glomerular Diseases Work Group. KDIGO 2021 clinical practice guideline for the management of glomerular diseases. *Kidney Int*. (2021) 100:S1–S276. doi: 10.1016/j.kint.2021.05.021

22. Levey AS, Stevens LA, Schmid CH, Zhang YL, Castro AF, Feldman HI, et al. A new equation to estimate glomerular filtration rate. *Ann Intern Med*. (2009) 150:604–12. doi: 10.7326/0003-4819-150-9-200905050-00006

23. Liu N, Xu H, Sun Q, Yu X, Chen W, Wei H, et al. The role of oxidative stress in hyperuricemia and xanthine oxidoreductase (XOR) inhibitors. *Oxid Med Cell Longevity*. (2021) 2021:e1470380. doi: 10.1155/2021/1470380

24. Krishnan E. Inflammation, oxidative stress and lipids: the risk triad for atherosclerosis in gout. *Rheumatol (Oxford)*. (2010) 49:1229–38. doi: 10.1093/rheumatology/keq037

25. Cristóbal-García M, García-Arroyo FE, Tapia E, Osorio H, Arellano-Buendía AS, Madero M, et al. Renal oxidative stress induced by long-term hyperuricemia alters mitochondrial function and maintains systemic hypertension. *Oxid Med Cell Longev*. (2015) 2015:535686. doi: 10.1155/2015/535686

26. Sánchez-Lozada LG, Soto V, Tapia E, Avila-Casado C, Sautin YY, Nakagawa T, et al. Role of oxidative stress in the renal abnormalities induced by experimental hyperuricemia. *Am J Physiol Renal Physiol*. (2008) 295:F1134–1141. doi: 10.1152/ajprenal.00104.2008

27. Zhang T, Gu Y, Meng G, Zhang Q, Liu L, Wu H, et al. Genetic risk, adherence to a healthy lifestyle, and hyperuricemia: the TCLSIH cohort study. *Am J Med*. (2023) 136:476–483.e5. doi: 10.1016/j.amjmed.2023.01.004

28. Zhang Y, Yang R, Dove A, Li X, Yang H, Li S, et al. Healthy lifestyle counteracts the risk effect of genetic factors on incident gout: a large population-based longitudinal study. *BMC Med*. (2022) 20:138. doi: 10.1186/s12916-022-02341-0

29. Koguchi T, Tadokoro T. Beneficial effect of dietary fiber on hyperuricemia in rats and humans: A review. *Int J Vitam Nutr Res*. (2019) 89:89–108. doi: 10.1024/0300-9831/a000548

30. Zykova SN, Storhaug HM, Toft I, Chadban SJ, Jenssen TG, White SL. Cross-sectional analysis of nutrition and serum uric acid in two Caucasian cohorts: the AusDiab Study and the Tromsø study. *Nutr J*. (2015) 14:49. doi: 10.1186/s12937-015-0032-1

31. Zhang L, Shi X, Yu J, Zhang P, Ma P, Sun Y. Dietary vitamin E intake was inversely associated with hyperuricemia in US adults: NHANES 2009-2014. *Ann Nutr Metab*. (2020) 76:354–60. doi: 10.1159/000509628

32. Juraschek SP, Miller ER, Gelber AC. Effect of oral vitamin C supplementation on serum uric acid: a meta-analysis of randomized controlled trials. *Arthritis Care Res (Hoboken)*. (2011) 63:1295–306. doi: 10.1002/acr.20519

33. Qin X, Li Y, He M, Tang G, Yin D, Liang M, et al. Folic acid therapy reduces serum uric acid in hypertensive patients: a substudy of the China Stroke Primary Prevention Trial (CSPPT). *Am J Clin Nutr*. (2017) 105:882–9. doi: 10.3945/ajcn.116.143131

34. Sun X, Wen J, Guan B, Li J, Luo J, Li J, et al. Folic acid and zinc improve hyperuricemia by altering the gut microbiota of rats with high-purine diet-induced hyperuricemia. *Front Microbiol*. (2022) 13:907952. doi: 10.3389/fmicb.2022.907952

35. Ford ES, Choi HK. Associations between concentrations of uric acid with concentrations of vitamin A and beta-carotene among adults in the United States. *Nutr Res*. (2013) 33:995–1002. doi: 10.1016/j.nutres.2013.08.008

36. Wang Y, Yang Z, Wu J, Xie D, Yang T, Li H, et al. Associations of serum iron and ferritin with hyperuricemia and serum uric acid. *Clinical Rheumatology*. (2020) 39 (12):3777–3785. doi: 10.1007/s10067-020-05164

37. Wang Y, Miao F, Wang J, Zheng M, Yu F, Yi Y. The ameliorative and neuroprotective effects of dietary fibre on hyperuricaemia mice: a perspective from microbiome and metabolome. *Br J Nutr*. (2024) 132(3):275–88. doi: 10.1017/S0007114524001211

38. Zhou J, Wang Y, Lian F, Chen D, Qiu Q, Xu H, et al. Physical exercises and weight loss in obese patients help to improve uric acid. *Oncotarget*. (2017) 8:94893–9. doi: 10.18632/oncotarget.22046

39. Williams PT. Effects of diet, physical activity and performance, and body weight on incident gout in ostensibly healthy, vigorously active men. *Am J Clin Nutr*. (2008) 87:1480–7. doi: 10.1093/ajcn/87.5.1480

40. Nieradko-Iwanicka B. The role of alcohol consumption in pathogenesis of gout. *Crit Rev Food Sci Nutr*. (2022) 62:7129–37. doi: 10.1080/10408398.2021.1911928

41. Haj Mouhamed D, Ezzaher A, Neffati F, Douki W, Gaha L, Najjar MF. Effect of cigarette smoking on plasma uric acid concentrations. *Environ Health Prev Med*. (2011) 16:307–12. doi: 10.1007/s12199-010-0198-2

42. Jang YS, Nerobkova N, Yun I, Kim H, Park E-C. Association between smoking behavior and serum uric acid among the adults: Findings from a national cross-sectional study. *PloS One*. (2023) 18:e0285080. doi: 10.1371/journal.pone.0285080

43. Choi HK, McCormick N, Lu N, Rai SK, Yokose C, Zhang Y. Population impact attributable to modifiable risk factors for hyperuricemia. *Arthritis Rheumatol*. (2020) 72:157–65. doi: 10.1002/art.41067

44. Liu L, Lou S, Xu K, Meng Z, Zhang Q, Song K. Relationship between lifestyle choices and hyperuricemia in Chinese men and women. *Clin Rheumatol*. (2013) 32:233–9. doi: 10.1007/s10067-012-2108-z

45. Zhang W-Z. Why does hyperuricemia not necessarily induce gout? *Biomolecules*. (2021) 11:280. doi: 10.3390/biom11020280

46. Hu W, Ye Z, Li T, Shi Z. Associations between composite dietary antioxidant index and gout: national health and nutrition examination survey 2007-2018. *Biol Res Nurs*. (2024) 26:150–9. doi: 10.1177/10998004231198166

47. McAdams-DeMarco MA, Law A, Maynard JW, Coresh J, Baer AN. Risk factors for incident hyperuricemia during mid-adulthood in African American and white men and women enrolled in the ARIC cohort study. *BMC Musculoskelet Disord*. (2013) 14:347. doi: 10.1186/1471-2474-14-347

48. Perez-Ruiz F, Aniel-Quiroga MA, Herrero-Beites AM, Chinchilla SP, Erauskin GG, Merriman T. Renal clearance of uric acid is linked to insulin resistance and lower excretion of sodium in gout patients. *Rheumatol Int*. (2015) 35:1519–24. doi: 10.1007/s00296-015-3242-0

49. Chainy GBN, Sahoo DK. Hormones and oxidative stress: an overview. *Free Radic Res*. (2020) 54:1–26. doi: 10.1080/10715762.2019.1702656

50. Hak AE, Curhan GC, Grodstein F, Choi HK. Menopause, postmenopausal hormone use and risk of incident gout. *Ann Rheum Dis*. (2010) 69:1305–9. doi: 10.1136/ard.2009.109884

51. Buettner GR. The pecking order of free radicals and antioxidants: lipid peroxidation, α-tocopherol, and ascorbate. *Arch Biochem Biophysics*. (1993) 300:535–43. doi: 10.1006/abbi.1993.1074

52. Traber MG, Atkinson J. Vitamin E, antioxidant and nothing more. *Free Radic Biol Med*. (2007) 43:4–15. doi: 10.1016/j.freeradbiomed.2007.03.024

frontiers | Frontiers in Medicine

TYPE Original Research
PUBLISHED 06 November 2024
DOI 10.3389/fmed.2024.1455164

OPEN ACCESS

EDITED BY
Lihua Duan,
Jiangxi Provincial People's Hospital, China

REVIEWED BY
Xintian Cai,
People's Hospital of Xinjiang Uygur Autonomous Region, China
Chenghao Zhanghuang,
Kunming Children's Hospital, China
Dorin Ionescu,
Carol Davila University of Medicine and Pharmacy, Romania

*CORRESPONDENCE
Jingxiu Fan
✉ fanjingxiu@scu.edu.cn

RECEIVED 26 June 2024
ACCEPTED 29 October 2024
PUBLISHED 06 November 2024

CITATION
Wang X and Fan J (2024) Association between life's essential 8 and hyperuricemia among adults in the United States: insights from NHANES 2005–2018.
Front. Med. 11:1455164.
doi: 10.3389/fmed.2024.1455164

Association between life's essential 8 and hyperuricemia among adults in the United States: insights from NHANES 2005–2018

Xiaolan Wang[1,2] and Jingxiu Fan[3]*

[1]Department of Critical Care Medicine, West China Hospital, Sichuan University, Chengdu, China, [2]West China School of Nursing, Sichuan University, Chengdu, China, [3]Department of Cardiovascular Surgery, West China School of Medicine, West China Hospital, Sichuan University, Chengdu, Sichuan Province, China

Background: Hyperuricemia is a significant risk factor for various metabolic and cardiovascular conditions. Life's Essential 8 (LE8), a comprehensive measure of cardiovascular health promoted by the American Heart Association, may have a protective role against hyperuricemia. This study aims to evaluate the association between LE8 scores and hyperuricemia in a representative sample of US adults.

Methods: We conducted a cross-sectional study using data from the National Health and Nutrition Examination Survey (NHANES) 2005–2018, encompassing 26,885 adults. LE8 scores were calculated based on diet, physical activity, nicotine exposure, sleep health, body mass index, blood lipids, blood glucose, and blood pressure. Hyperuricemia was defined as serum uric acid levels ≥7.0 mg/dL in men and ≥ 6.0 mg/dL in women. Logistic regression and generalized additive models (GAMs) were used to analyze the relationship between LE8 scores and hyperuricemia, adjusting for potential confounders.

Results: Higher LE8 scores were significantly associated with lower odds of hyperuricemia (OR per 10-point increase: 0.73, 95% CI: 0.72–0.75, $p < 0.001$). Stratified analyses revealed consistent protective effects across subgroups defined by sex, age, race/ethnicity, PIR (poverty income ratio), education level, drinking status, eGFR, and CVD status. Logistic regression and GAM analyses both confirmed a linear relationship between increasing LE8 scores and reduced hyperuricemia risk. For example, in males, the OR was 0.81 (95% CI: 0.78–0.84), and in females, it was 0.66 (95% CI: 0.64–0.68).

Conclusion: The findings suggest that higher LE8 scores are robustly associated with lower odds of hyperuricemia in US adults. These results support the promotion of comprehensive cardiovascular health behaviors encapsulated by LE8 to mitigate hyperuricemia risk. Further studies are needed to explore the causal pathways and potential interventions.

KEYWORDS

hyperuricemia, life's essential 8, cardiovascular health, NHANES (National Health and nutrition examination survey), cross-sectional study

1 Introduction

Hyperuricemia, characterized by elevated serum uric acid levels, is a significant precursor to gout and is associated with several metabolic and cardiovascular diseases (CVDs) (1). The prevalence of hyperuricemia has been rising globally (2, 3), correlating with increased rates of obesity, hypertension, and other lifestyle-related conditions (4, 5). Given its multifactorial etiology, addressing hyperuricemia requires a comprehensive approach that includes lifestyle modification and management of underlying risk factors.

Recently, the American Heart Association introduced Life's Essential 8 (LE8), an updated framework for cardiovascular health that emphasizes a holistic approach to health behaviors and factors (6). LE8 includes eight critical components: diet, physical activity, nicotine exposure, sleep health, body mass index (BMI), blood lipids, blood glucose, and blood pressure. Each of these elements has been individually associated with hyperuricemia and related metabolic disorders (7). For instance, poor diet and physical inactivity contribute to obesity, a major risk factor for hyperuricemia (8). Similarly, smoking and inadequate sleep have been linked to higher serum uric acid levels and increased risk of gout (9, 10). By integrating these components, LE8 offers a comprehensive framework for evaluating and improving overall health, which could potentially mitigate the risk of hyperuricemia.

Previous studies have shown an inverse relationship between LE8 and hyperuricemia, but there are still several limitations. Research conducted in non-U.S. populations has limited generalizability, while studies using U.S. data often lack comprehensive adjustments for key confounders such as socioeconomic status, alcohol consumption, kidney function, and CVD (11–13). Moreover, while some studies have used advanced models to explore non-linear trends, they did not assess the individual contributions of LE8 components to hyperuricemia risk (14). This study addresses these gaps by using a large, representative U.S. dataset, adjusting for a wide range of confounders, and analyzing both overall LE8 scores and individual components, offering a more detailed and precise understanding of LE8's impact on hyperuricemia.

This study seeks to address this gap by utilizing the National Health and Nutrition Examination Survey (NHANES) data to evaluate the relationship between LE8 scores and hyperuricemia in U.S. adults. Specifically, we assess the combined effects of all LE8 components, offering new insights into the link between comprehensive cardiovascular health and metabolic disorders.

2 Materials and methods

2.1 Study design and participants

The data from the NHANES 2005–2018 were utilized in this cross-sectional study. NHANES is a program of studies designed to assess the health and nutritional status of adults and children in the United States. It combines interviews and physical examinations to provide a comprehensive dataset. For this analysis, we included adults aged 18 years and older with complete data on serum uric acid levels and LE8 components. Participants with missing data on key variables were excluded, resulting in a final analytical sample of 26,885 individuals.

2.2 Demographic characteristics

The demographic characteristics collected in this study included a wide array of variables such as age, sex, race/ethnicity, poverty income ratio (PIR), and education level. Lifestyle factors were also assessed, including smoking status and alcohol consumption. Physical examination data covered measurements of height, waist circumference (WC), blood pressure, and BMI, which was calculated from height and weight. Laboratory data included serum uric acid levels and estimated glomerular filtration rate (eGFR). Additionally, self-reported health information related to CVD history was recorded, encompassing conditions like heart attack, congestive heart failure, coronary heart disease, angina, and stroke. The PIR was calculated by dividing the household income by the poverty threshold, classifying participants into three income groups: low (less than 1.3), medium (1.3 to 3.5), and high (greater than 3.5). Alcohol intake was categorized into five groups: current drinking groups include heavy (defined as consuming 3 or more drinks per day for females, 4 or more drinks per day for males, or engaging in binge drinking on 5 or more days per month), moderate (2 or more drinks per day for females, 3 or more drinks per day for males, or binge drinking on 2 or more days per month), and mild (up to 1 drink per day for females and up to 2 drinks per day for males). Additionally, individuals classified as never drinkers are those who have had less than 12 drinks in their lifetime, while former drinkers are defined as individuals who had 12 or more drinks in 1 year but did not drink in the previous year, or those who did not drink in the previous year but had 12 or more drinks in their lifetime. The eGFR was calculated using the 2009 Chronic Kidney Disease Epidemiology Collaboration (CKD-EPI) formula based on serum creatinine levels (15).

2.3 Measurement of LE8

LE8, as defined by the American Heart Association, includes eight components: diet, physical activity, nicotine exposure, sleep health, BMI, blood lipids, blood glucose, and blood pressure (6). Each component is assigned a score based on predefined values, ranging from 0 to 100, with higher scores indicating better health status (Supplementary Table S1). The overall LE8 score is calculated as the arithmetic mean of the scores for these eight components. Based on the overall score, LE8 scores are categorized into three levels: low (below 50), moderate (ranging from 50 to 79), and high (80 or above) (6).

Dietary intake was assessed using the Healthy Eating Index 2015 (HEI-2015), which evaluates diet quality based on key food and nutrient components (Supplementary Table S2) (16). Physical activity was measured in minutes per week of moderate to vigorous activity. Nicotine exposure was determined based on self-reported smoking status and exposure to secondhand smoke. Sleep health was assessed by self-reported average hours of sleep per night. BMI was calculated as weight in kilograms divided by height in meters squared. Blood lipids were measured using non-high-density lipoprotein (HDL) cholesterol. Blood glucose levels were assessed using fasting blood glucose or hemoglobin A1c (HbA1c). Blood pressure was measured using standard procedures during the physical examination.

2.4 Measurements and definition of hyperuricemia

Hyperuricemia was defined as serum uric acid levels ≥7.0 mg/dL for men and ≥6.0 mg/dL for women, consistent with established clinical thresholds (17). Serum uric acid was measured using a biochemical analyzer with enzymatic methods. Blood samples were collected and processed following standardized NHANES protocols to ensure accuracy and reliability.

2.5 Statistical analysis

Descriptive statistics were used to summarize baseline characteristics of the study population. Continuous variables were reported as means and standard deviations, while categorical variables were presented as frequencies and percentages. Logistic regression models were employed to examine the association between LE8 scores and hyperuricemia, adjusting for potential confounders. Three models were constructed: Model 1 was unadjusted, Model 2 was adjusted for age and sex, and Model 3 was further adjusted for race/ethnicity, PIR, education level, alcohol consumption, eGFR, and CVD. We utilized generalized additive models (GAMs) to explore potential non-linear relationships between LE8 scores and hyperuricemia. GAMs offer greater flexibility than traditional linear regression models by allowing for smooth, non-parametric functions of predictor variables. This flexibility helps reduce the risk of model misspecification, particularly when the relationship between predictors and outcomes is complex or unknown (18). GAMs were fitted using the mgcv package in R, with smoothing splines for LE8 scores to capture the trend across its entire range. We selected the degree of smoothness using restricted maximum likelihood (REML) to avoid overfitting. Stratified analyses were conducted to verify the consistency of associations across subgroups defined by sex, age, race/ethnicity, PIR, education level, drinking status, eGFR, and CVD status. Missing data were handled using Multiple Imputation by Chained Equations (MICE) to reduce potential bias and improve estimate precision (19, 20). We generated 5 imputed datasets (m = 5) with 50 iterations (maxit = 50) to ensure stable imputation. A random seed (seed = 500) was set to allow reproducibility. The imputation process was performed using the mice() function, which assesses convergence implicitly by monitoring parameter stability across iterations. A maximum of 50 iterations (maxit = 50) was allowed to ensure convergence. A p-value of less than 0.05 was considered statistically significant. Statistical analyses were conducted utilizing R software (version 4.2.0) and EmpowerStats.[1]

3 Results

3.1 Participant selection and categorization

The initial dataset from NHANES 2005–2018 included 70,190 participants. After excluding 43,204 participants with missing LE8 score data, the sample size was reduced to 26,986 participants. Further exclusion of 101 participants with missing uric acid data resulted in an analytical sample of 26,885 participants. These participants were categorized based on their LE8 scores into three groups: 3,498 participants with a low LE8 score, 18,195 participants with a moderate LE8 score, and 5,192 participants with a high LE8 score (Figure 1).

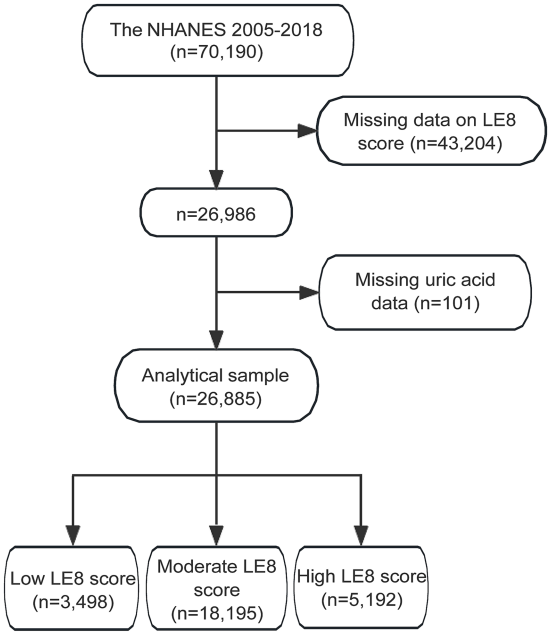

FIGURE 1
Flowchart of study participants selection from NHANES 2005–2018. NHANES, the National Health and Nutrition Examination Survey; LE8, Life's Essential 8.

3.2 Baseline demographic characteristics

The study population comprised 26,885 participants from the NHANES 2005–2018 dataset, divided into 21,465 individuals without hyperuricemia and 5,420 with hyperuricemia. Significant differences were observed between these groups. Participants with hyperuricemia were older, with a mean age of 54.28 years compared to 48.87 years in the non-hyperuricemia group ($p < 0.001$). Gender distribution also showed a higher proportion of males in the hyperuricemia group (54.74%) than in the non-hyperuricemia group (47.23%), indicating a significant difference ($p < 0.001$). Racial disparities were evident, with a higher percentage of Non-Hispanic Black people in the hyperuricemia group (24.54% vs. 19.53%) and fewer Mexican Americans (10.74% vs. 16.18%) compared to the non-hyperuricemia group ($p < 0.001$). PIR categories revealed that a larger proportion of hyperuricemia participants were in the medium PIR category (39.93%) compared to the non-hyperuricemia group (37.83%; $p = 0.015$). Additionally, education levels showed a higher percentage of high school graduates among the hyperuricemia group (24.50% vs. 22.69%; $p = 0.018$). Drinking habits also differed significantly, with more former drinkers in the hyperuricemia group ($p < 0.001$).

Anthropometric and health measures further highlighted the differences between the groups. Participants with hyperuricemia had higher mean BMI (32.42 kg/m^2 vs. 28.37 kg/m^2), WC (108.12 cm vs. 97.37 cm), systolic blood pressure (SBP; 127.80 mmHg vs. 122.55 mmHg), and diastolic blood pressure (DBP; 71.03 mmHg vs. 70.24 mmHg; $p < 0.001$ for all). The eGFR was significantly lower in the hyperuricemia group (81.25 mL/min/1.73 m^2 vs. 96.12 mL/min/1.73 m^2; $p < 0.001$). Furthermore, the prevalence of CVD was markedly higher among those with hyperuricemia (17.79% vs. 9.38%; $p < 0.001$; Table 1).

1 http://www.EmpowerStats.com

TABLE 1 Baseline characteristics of the study population.

Characteristics	Total *n* = 26,885	Non-hyperuricemia *n* = 21,465	Hyperuricemia *n* = 5,420	*p*-value
Age (years)	49.96 ± 17.58	48.87 ± 17.36	54.28 ± 17.77	<0.001
Sex (n, %)				<0.001
Male	13,105 (48.74%)	10,138 (47.23%)	2,967 (54.74%)	
Female	13,780 (51.26%)	11,327 (52.77%)	2,453 (45.26%)	
Race/ethnicity (n, %)				<0.001
Non-Hispanic White	12,150 (45.19%)	9,548 (44.48%)	2,602 (48.01%)	
Non-Hispanic Black	5,522 (20.54%)	4,192 (19.53%)	1,330 (24.54%)	
Mexican American	4,055 (15.08%)	3,473 (16.18%)	582 (10.74%)	
Others	5,158 (19.19%)	4,252 (19.81%)	906 (16.72%)	
PIR (n, %)				0.015
Low	8,061 (29.98%)	6,465 (30.12%)	1,596 (29.45%)	
Medium	10,284 (38.25%)	8,120 (37.83%)	2,164 (39.93%)	
High	8,540 (31.76%)	6,880 (32.05%)	1,660 (30.63%)	
Education level (n, %)				0.018
Less than high school	6,074 (22.59%)	4,865 (22.66%)	1,209 (22.31%)	
High school	6,199 (23.06%)	4,871 (22.69%)	1,328 (24.50%)	
More than high school	14,612 (54.35%)	11,729 (54.64%)	2,883 (53.19%)	
Drinking (n, %)				<0.001
Never	3,704 (13.78%)	3,011 (14.03%)	693 (12.79%)	
Former	4,486 (16.69%)	3,471 (16.17%)	1,015 (18.73%)	
Mild	9,109 (33.88%)	7,327 (34.13%)	1782 (32.88%)	
Moderate	4,307 (16.02%)	3,478 (16.20%)	829 (15.30%)	
Heavy	5,279 (19.64%)	4,178 (19.46%)	1,101 (20.31%)	
Smoking (n, %)				<0.001
Never	14,843 (55.21%)	12,066 (56.21%)	2,777 (51.24%)	
Former	6,729 (25.03%)	5,031 (23.44%)	1,698 (31.33%)	
Now	5,313 (19.76%)	4,368 (20.35%)	945 (17.44%)	
Height (cm)	167.32 ± 10.11	167.11 ± 10.04	168.16 ± 10.31	<0.001
BMI (kg/m^2)	29.19 ± 6.84	28.37 ± 6.37	32.42 ± 7.61	<0.001

(Continued)

10.3389/fmed.2024.1455164

TABLE 1 (Continued)

Characteristics	Total n = 26,885	Non-hyperuricemia n = 21,465	Hyperuricemia n = 5,420	p-value
WC (cm)	99.54 ± 16.37	97.37 ± 15.58	108.12 ± 16.60	<0.001
SBP (mmHg)	123.61 ± 18.30	122.55 ± 17.90	127.80 ± 19.23	<0.001
DBP (mmHg)	70.40 ± 11.81	70.24 ± 11.47	71.03 ± 13.02	<0.001
eGFR (mL/min/1.73 m^2)	93.12 ± 23.61	96.12 ± 21.93	81.25 ± 26.13	<0.001
CVD (n, %)	2,977 (11.07%)	2013 (9.38%)	964 (17.79%)	<0.001
Uric acid (mg/dL)	5.46 ± 1.43	4.95 ± 1.02	7.46 ± 1.02	<0.001
LE8	66.45 ± 14.47	67.91 ± 14.34	60.69 ± 13.53	<0.001

PIR, poverty income ratio; BMI, body mass index; WC, waist circumference; SBP, systolic blood pressure; DBP, diastolic blood pressure; eGFR, estimated glomerular filtration rate; CVD, cardiovascular disease; LE8, life's essential 8.

Analysis of the LE8 components revealed significant disparities between the hyperuricemia and non-hyperuricemia groups (Table 2). Participants with hyperuricemia scored lower across several components, including diet quality (38.49 vs. 40.16), physical activity (62.88 vs. 68.49), and sleep health (79.46 vs. 81.44), with p-values of <0.001 for each. Notably, BMI scores were substantially lower in the hyperuricemia group (44.46 vs. 63.47), reflecting a higher prevalence of obesity ($p < 0.001$). Blood lipids and glucose scores were also lower among those with hyperuricemia (57.20 vs. 66.37 and 75.89 vs. 83.63, respectively), alongside lower blood pressure scores (55.95 vs. 68.68; $p < 0.001$ for all). Despite the significant differences in these components, the nicotine exposure score was slightly higher in individuals with hyperuricemia (71.20 vs. 71.03; $p < 0.001$), indicating increased nicotine exposure among hyperuricemic individuals.

3.3 Association between LE8 and hyperuricemia

The logistic regression analysis revealed a significant inverse relationship between LE8 scores and the likelihood of hyperuricemia. In Model 1, which was unadjusted, a 10-point increase in the LE8 score corresponded to a 29% reduction in the odds of hyperuricemia (OR: 0.71, 95% CI: 0.69–0.72). This association remained robust in adjusted models: Model 2 (adjusted for age and sex) and Model 3 (further adjusted for race/ethnicity, PIR, education level, drinking, eGFR, and CVD), with ORs of 0.73 (95% CI: 0.71–0.75) and 0.73 (95% CI: 0.72–0.75), respectively (P for trend <0.001 for all models; Table 3).

When examining individual components of the LE8 score, several components showed significant associations with hyperuricemia. Higher scores in diet, physical activity, sleep health, BMI, blood lipids, blood glucose, and blood pressure were each linked to lower odds of hyperuricemia. For instance, a high physical activity score (80–100) was significantly associated with a lower likelihood of hyperuricemia compared to a low score (0–49), with an OR of 0.86 (95% CI: 0.80–0.93) in the fully adjusted model (P for trend <0.0001). Conversely, higher nicotine exposure scores were associated with increased odds of hyperuricemia, with those in the moderate category (50–79) having an OR of 1.32 (95% CI: 1.20–1.45) compared to the reference group (P for trend <0.05; Table 4).

The analysis using a GAM revealed a linear relationship between LE8 scores and the probability of hyperuricemia. Initially, the exploration aimed to identify any nonlinear associations; however, the results indicated a clear linear trend. As the LE8 score increased, the probability of hyperuricemia consistently decreased. This linear association suggests a potential protective impact of higher LE8 scores on reducing the risk of hyperuricemia (Figure 2).

3.4 Stratified analysis of the association between LE8 and hyperuricemia

Figures 3, 4 present stratified analyses to verify the association between LE8 scores and hyperuricemia across different population subgroups. Figure 3 employs logistic regression to assess interactions within various subgroups, while Figure 4 uses GAMs to further explore these associations, maintaining the same subgroup categories as in Figure 3.

TABLE 2 Comparison of each component of LE8 scores between individuals with hyperuricemia and individuals without hyperuricemia.

LE8 components	Total n = 26,885	Non-hyperuricemia n = 21,465	Hyperuricemia n = 5,420	p-value
HEI-2015 diet score	39.82 ± 31.37	40.16 ± 31.49	38.49 ± 30.88	<0.001
Physical activity score	67.36 ± 43.25	68.49 ± 42.79	62.88 ± 44.74	<0.001
Nicotine exposure score	71.06 ± 39.00	71.03 ± 39.43	71.20 ± 37.24	<0.001
Sleep health score	81.04 ± 25.71	81.44 ± 25.50	79.46 ± 26.46	<0.001
Body mass index score	59.64 ± 33.64	63.47 ± 32.75	44.46 ± 32.85	<0.001
Blood lipids score	64.52 ± 30.21	66.37 ± 29.94	57.20 ± 30.19	<0.001
Blood glucose score	82.07 ± 26.43	83.63 ± 25.90	75.89 ± 27.56	<0.001
Blood pressure score	66.12 ± 32.20	68.68 ± 31.79	55.95 ± 31.78	<0.001

LE8, life's essential 8; HEI, healthy eating index.

TABLE 3 Association of the LE8 scores with hyperuricemia.

Exposure	Model 1	Model 2	Model 3
Continuous (per 10 points)	0.71 (0.69, 0.72)	0.73 (0.71, 0.75)	0.73 (0.72, 0.75)
Categorical			
Low (0–49)	Reference	Reference	Reference
Moderate (50–79)	0.55 (0.51, 0.60)	0.58 (0.54, 0.63)	0.63 (0.58, 0.69)
High (80–100)	0.18 (0.16, 0.21)	0.22 (0.20, 0.25)	0.24 (0.21, 0.27)
P for trend	<0.001	<0.001	<0.001

Model 1: Non-adjusted. Model 2: Adjusted for age and sex. Model 3: Adjusted for age, sex, race/ethnicity, PIR, educational level, drinking, eGFR, and CVD. LE8, life's essential 8; PIR, poverty income ratio; eGFR, estimated glomerular filtration rate; CVD, cardiovascular disease.

In Figure 3, logistic regression analysis demonstrates that higher LE8 scores are consistently associated with lower odds of hyperuricemia across all subgroups, including sex, age, race/ethnicity, PIR, education level, drinking status, eGFR, and CVD status. For example, males and females both show a significant reduction in the odds of hyperuricemia with higher LE8 scores, with OR of 0.81 (95% CI: 0.78–0.84) and 0.66 (95% CI: 0.64–0.68), respectively ($p < 0.05$ for both). This pattern holds across other subgroups, indicating that the beneficial effects of higher LE8 scores on reducing hyperuricemia risk are robust and broadly applicable.

Figure 4 corroborates these findings using GAMs, revealing a linear decrease in the probability of hyperuricemia with increasing LE8 scores across the same subgroups. The analyses highlight that irrespective of demographic or health-related factors, higher LE8 scores consistently correlate with lower hyperuricemia risk.

4 Discussion

This study explored the relationship between LE8 scores and hyperuricemia among adults in the United States using data from the NHANES 2005–2018. The results revealed that higher LE8 scores are significantly associated with lower odds of hyperuricemia. Specifically, for every 10-point increase in the LE8 score, the likelihood of hyperuricemia decreased by 27%. This inverse relationship remained consistent across various subgroups, including differences in sex, age, race/ethnicity, PIR, educational level, drinking status, eGFR, and CVD status. These findings suggest that higher LE8 scores, which reflect better cardiovascular health, may lower the risk of hyperuricemia by improving metabolic status.

LE8, as an enhanced framework for assessing and promoting cardiovascular health, encompasses a comprehensive range of behavioral, psychological, and social factors (6). It has been widely demonstrated to be closely associated with cardiovascular health and mortality risk (21, 22). Concurrently, numerous studies have shown that LE8 is closely related to metabolic diseases such as diabetes mellitus, hypertension, and metabolic syndrome (MetS). Pang et al. found that higher LE8 scores were associated with lower insulin resistance (IR) ratios (OR per 10-unit increase, 0.57 [95% CI, 0.54–0.61]) in a fully adjusted model (23). Ueno et al. demonstrated that the four health behavior factors involved in LE8 can stratify the risk of diabetes and hypertension, suggesting that improving these health behaviors can help prevent these conditions in the general population (24). Tian et al.'s study also identified a negative correlation between LE8 and hypertension risk (25). Similarly, Gou et al. found that elevated LE8 scores were linked to a decreased incidence of MetS. Specifically, the high LE8 subgroup experienced a 79.73% reduction in MetS risk compared to the low LE8 subgroup (OR = 0.20 [95% CI, 0.09–0.47]) (26). Additionally, both Cao et al. and Yang et al. found a negative association between LE8 and metabolic health and the risk of cardiometabolic diseases (27, 28). Therefore, the relationship between LE8 and hyperuricemia, which is closely related to metabolic factors such as blood pressure, blood lipid, and blood glucose, warrants further study and discussion.

Recent studies have explored the association between LE8 and hyperuricemia, yet certain limitations in methodology and scope highlight the need for further investigation. Yang et al. conducted an

TABLE 4 Associations between components of LE8 scores and hyperuricemia.

Exposure	Model 1	Model 2	Model 3
HEI-2015 diet score			
Continuous (per 10 points)	0.98 (0.97, 0.99)	0.97 (0.96, 0.98)	0.98 (0.97, 0.99)
Categorical			
Low (0–49)	Reference	Reference	Reference
Moderate (50–79)	1.04 (0.97, 1.11)	0.97 (0.91, 1.05)	1.03 (0.96, 1.11)
High (80–100)	0.88 (0.81, 0.94)	0.78 (0.72, 0.84)	0.87 (0.80, 0.94)
P for trend	0.0025	<0.0001	0.0030
Physical activity score			
Continuous (per 10 points)	0.97 (0.96, 0.98)	0.98 (0.97, 0.99)	0.98 (0.98, 0.99)
Categorical			
Low (0–49)	Reference	Reference	Reference
Moderate (50–79)	0.88 (0.76, 1.02)	0.96 (0.83, 1.11)	1.02 (0.88, 1.19)
High (80–100)	0.76 (0.72, 0.81)	0.83 (0.78, 0.88)	0.86 (0.80, 0.93)
P for trend	<0.0001	<0.0001	<0.0001
Nicotine exposure score			
Continuous (per 10 points)	1.00 (0.99, 1.01)	1.00 (0.99, 1.01)	1.01 (1.01, 1.02)
Categorical			
Low (0–49)	Reference	Reference	Reference
Moderate (50–79)	1.50 (1.37, 1.63)	1.20 (1.10, 1.32)	1.32 (1.20, 1.45)
High (80–100)	1.01 (0.94, 1.09)	1.02 (0.94, 1.10)	1.15 (1.06, 1.26)
P for trend	0.0300	0.5802	0.0237
Sleep health score			
Continuous (per 10 points)	0.97 (0.96, 0.98)	0.97 (0.96, 0.98)	0.98 (0.97, 1.00)
Categorical			
Low (0–49)	Reference	Reference	Reference
Moderate (50–79)	0.87 (0.80, 0.96)	0.88 (0.80, 0.97)	0.96 (0.87, 1.06)
High (80–100)	0.81 (0.75, 0.88)	0.81 (0.75, 0.88)	0.89 (0.82, 0.96)
P for trend	<0.0001	<0.0001	0.0023
Body mass index score			
Continuous (per 10 points)	0.84 (0.84, 0.85)	0.84 (0.83, 0.84)	0.83 (0.83, 0.84)
Categorical			
Low (0–49)	Reference	Reference	Reference
Moderate (50–79)	0.50 (0.47, 0.54)	0.46 (0.43, 0.50)	0.46 (0.43, 0.50)
High (80–100)	0.24 (0.22, 0.26)	0.25 (0.22, 0.27)	0.24 (0.22, 0.27)
P for trend	<0.0001	<0.0001	<0.0001
Blood lipids score			
Continuous (per 10 points)	0.91 (0.90, 0.91)	0.92 (0.91, 0.93)	0.91 (0.90, 0.92)
Categorical			
Low (0–49)	Reference	Reference	Reference
Moderate (50–79)	0.68 (0.63, 0.74)	0.76 (0.70, 0.82)	0.78 (0.72, 0.84)
High (80–100)	0.57 (0.54, 0.61)	0.61 (0.57, 0.65)	0.56 (0.52, 0.60)
P for trend	<0.0001	<0.0001	<0.0001

(Continued)

TABLE 4 (Continued)

Exposure	Model 1	Model 2	Model 3
Blood glucose score			
Continuous (per 10 points)	0.90 (0.89, 0.91)	0.93 (0.92, 0.94)	0.94 (0.93, 0.95)
Categorical			
Low (0–49)	Reference	Reference	Reference
Moderate (50–79)	0.89 (0.81, 0.98)	0.94 (0.86, 1.03)	1.07 (0.97, 1.18)
High (80–100)	0.48 (0.44, 0.52)	0.60 (0.55, 0.65)	0.65 (0.59, 0.72)
P for trend	<0.0001	<0.0001	<0.0001
Blood pressure score			
Continuous (per 10 points)	0.89 (0.88, 0.90)	0.91 (0.90, 0.92)	0.92 (0.91, 0.93)
Categorical			
Low (0–49)	Reference	Reference	Reference
Moderate (50–79)	0.66 (0.61, 0.71)	0.76 (0.70, 0.82)	0.84 (0.77, 0.91)
High (80–100)	0.46 (0.43, 0.49)	0.59 (0.54, 0.64)	0.62 (0.57, 0.68)
P for trend	<0.0001	<0.0001	<0.0001

Model 1: Non-adjusted. Model 2: Adjusted for age and sex. Model 3: Adjusted for age, sex, race/ethnicity, PIR, educational level, drinking, eGFR, and CVD. LE8, life's essential 8; HEI, healthy eating index; PIR, poverty income ratio; eGFR, estimated glomerular filtration rate; CVD, cardiovascular disease.

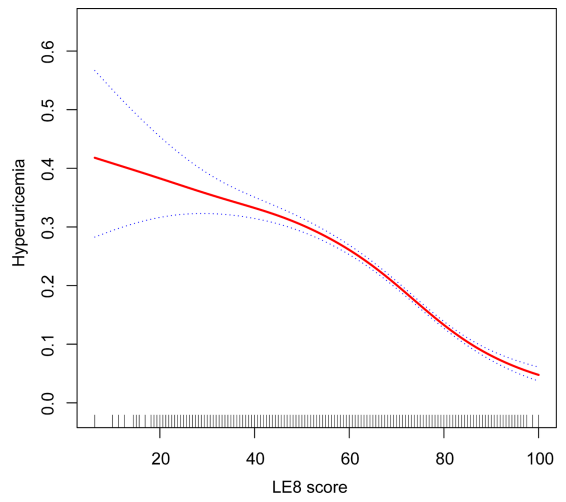

FIGURE 2
Relationship between LE8 and hyperuricemia. LE8, Life's Essential 8.

analysis of the Kailuan cohort, revealing that higher LE8 scores were associated with a lower risk of hyperuricemia (12). However, the predominantly male, middle-aged population in this study limits the generalizability of its findings to more diverse groups (29). Similarly, Wang et al. examined LE8 in a multi-ethnic Chinese cohort (CMEC), showing an inverse association with hyperuricemia, but the study was geographically restricted to China, leaving the results less applicable to non-Asian populations (11, 30). Wang and Meng extended this research by using NHANES data from 2009 to 2020 to assess the relationship between LE8 and hyperuricemia in U.S. adults (13). While their study offered valuable insights, it combined data from the 2019–2020 cycle with the 2017–2018 cycle, which may introduce methodological concerns, as the NHANES protocol combines these cycles (31). This potential duplication in the dataset could affect the robustness of their findings. Additionally, although they adjusted for some confounders, key lifestyle factors such as alcohol consumption were not fully considered, potentially impacting the accuracy of their risk estimates (32). Han et al. also investigated the association between LE8 and hyperuricemia in a U.S. cohort, utilizing restricted cubic spline models to analyze non-linear relationships (14). However, their study focused on overall LE8 scores and long-term health outcomes, such as all-cause mortality, without fully addressing the contribution of individual LE8 components, such as BMI, blood lipids, and blood glucose, to hyperuricemia risk.

Our findings are in alignment with previous research, highlighting the importance of individual components of LE8 in their association with serum uric acid levels and hyperuricemia. For instance, Fang et al. observed that patients with dyslipidemia were 1.88 times more likely to develop hyperuricemia compared to those without dyslipidemia (95% CI: 1.84–1.92) (33). Similarly, Nie et al. demonstrated that adherence to a healthy diet, as measured by the HEI-2015, significantly lowers serum uric acid levels and decreases the risk of hyperuricemia (34). Additionally, Hong et al. reported that increased physical activity correlates with reduced serum uric acid levels and a lower incidence of hyperuricemia (35). These studies support our findings, indicating that the cumulative effect of these health behaviors, as reflected by LE8 scores, offers substantial protection against hyperuricemia.

Our study also found that higher nicotine exposure scores were associated with increased odds of hyperuricemia, a finding that contrasts with some prior studies. While Wang and Krishnan reported that cigarette smoking is associated with a lower risk of incident gout, possibly due to the inactivation of xanthine oxidase by the cyanides in cigarettes (36), other studies suggest a more complex relationship. For instance, Jee et al. indicated that the association between smoking and gout risk remains controversial (37), with some studies showing decreased risk and others showing no significant association. Additionally, Gee Teng et al. highlighted the potential risk of hyperuricemia in smokers, attributing it to the oxidative stress and its

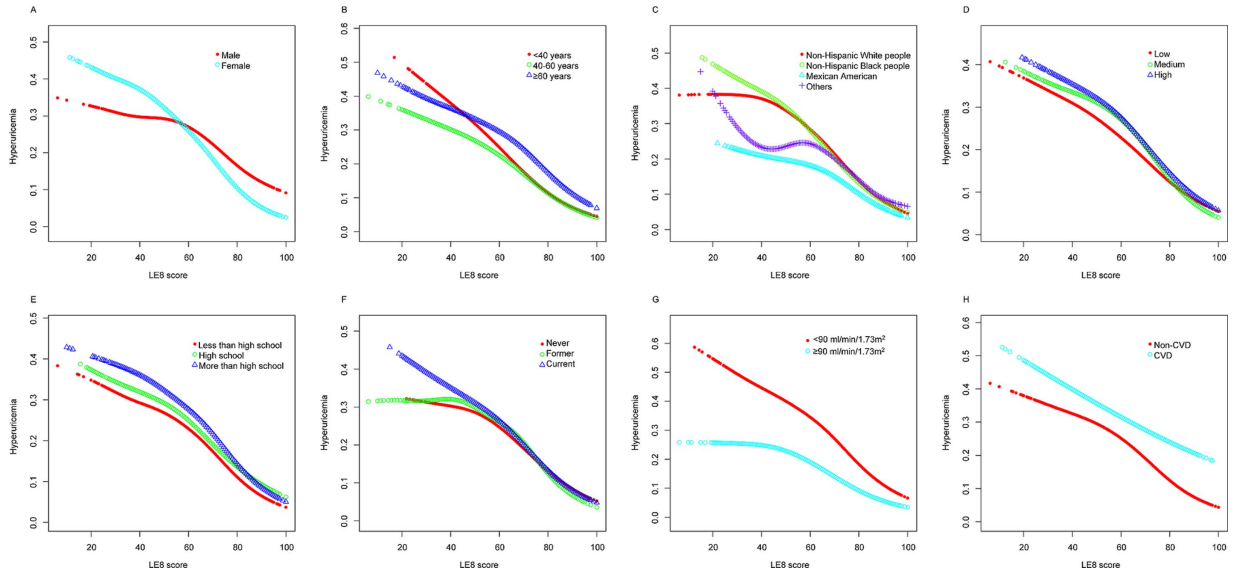

FIGURE 3
Logistic regression analysis for subgroup interaction. *Each stratification adjusted for all the factors (age, sex, race/ethnicity, PIR, educational level, drinking, eGFR, and CVD) except the stratification factor itself. OR, odds ratio; CI, confidence interval; PIR, poverty income ratio; eGFR, estimated glomerular filtration rate; CVD, cardiovascular disease.

impact on uric acid metabolism (38). These mixed findings suggest that the relationship between nicotine exposure and hyperuricemia may be influenced by various factors, including smoking intensity, duration, and concurrent health behaviors (36–39). Therefore, while some studies indicate that smoking may offer limited protection against hyperuricemia, this should not be interpreted as an endorsement of smoking, given its well-documented health risks.

In addition, some studies have reported weak or inconsistent associations between other individual lifestyle factors, such as sleep, and serum uric acid levels. For example, a cross-sectional study involving Chinese government employees examined the relationship between nighttime sleep duration and hyperuricemia risk. The findings indicated that participants sleeping less than 7 h per night had a higher risk of hyperuricemia compared to those sleeping 7–8 h (40). Conversely, other research suggested that poor sleep quality might be associated with lower serum uric acid levels, particularly in patients with Parkinson's disease (41). Additionally, some studies found no significant association between blood pressure and serum uric acid levels (42). Although many epidemiological studies have identified a strong correlation between hyperuricemia and hypertension, some evidence suggests that lowering uric acid levels does not substantially improve blood pressure control in hypertensive patients (43). Furthermore, variations in uric acid levels may interact with other metabolic factors, such as insulin resistance or dyslipidemia, contributing to the development of hypertension (44, 45). Therefore, caution is warranted when interpreting these findings, particularly given the complex interplay between uric acid and hypertension (46). Inconsistencies across studies may arise from differences in population characteristics, measurement tools, or definitions of lifestyle factors. For example, studies focusing solely on individual components of LE8 may overlook the cumulative effects of multiple behaviors, which are better captured through a composite LE8 score in our research (6). Additionally, environmental, genetic, and cultural factors across populations may influence how lifestyle affects hyperuricemia risk, highlighting the importance of validating these findings in diverse demographic contexts.

The components of LE8 play a crucial role in mitigating hyperuricemia by addressing its underlying risk factors and mechanisms. Uric acid, a metabolic byproduct of purine catabolism, frequently exhibits elevated levels in individuals with CVD due to shared risk factors, including hypertension, obesity, and insulin resistance (47, 48). By enhancing cardiovascular health, LE8 helps reduce uric acid levels by attenuating systemic inflammation, improving insulin sensitivity, and optimizing renal function, thereby promoting increased uric acid excretion. A diet rich in fiber and antioxidants helps reduce oxidative stress and inflammation, both key contributors to purine accumulation and hyperuricemia development (49, 50). Regular physical activity enhances metabolic health, aids in weight management, and improves insulin sensitivity, thereby facilitating more efficient renal clearance of uric acid (51). Furthermore, avoiding nicotine exposure diminishes systemic inflammation and supports renal function, contributing to better uric acid regulation (52). In contrast, inadequate sleep exacerbates metabolic dysfunction, oxidative stress, and chronic inflammation, thus elevating the risk of hyperuricemia (53). Therefore, improving sleep quality and duration is critical for the prevention and management of hyperuricemia. Recent research suggests that elevated plasma aldosterone concentrations (PAC) in individuals with hypertension significantly contribute to the onset of hyperuricemia and gout by impairing renal excretion of uric acid (54). Managing hypertension and optimizing blood pressure—key aspects of LE8—can help regulate aldosterone levels, mitigating its negative impact on uric acid metabolism. Additionally, dyslipidemia and hyperglycemia exacerbate metabolic dysfunction, resulting in increased uric acid production and reduced excretion (55). Effective management of lipid levels and blood glucose, both integral to LE8, supports metabolic

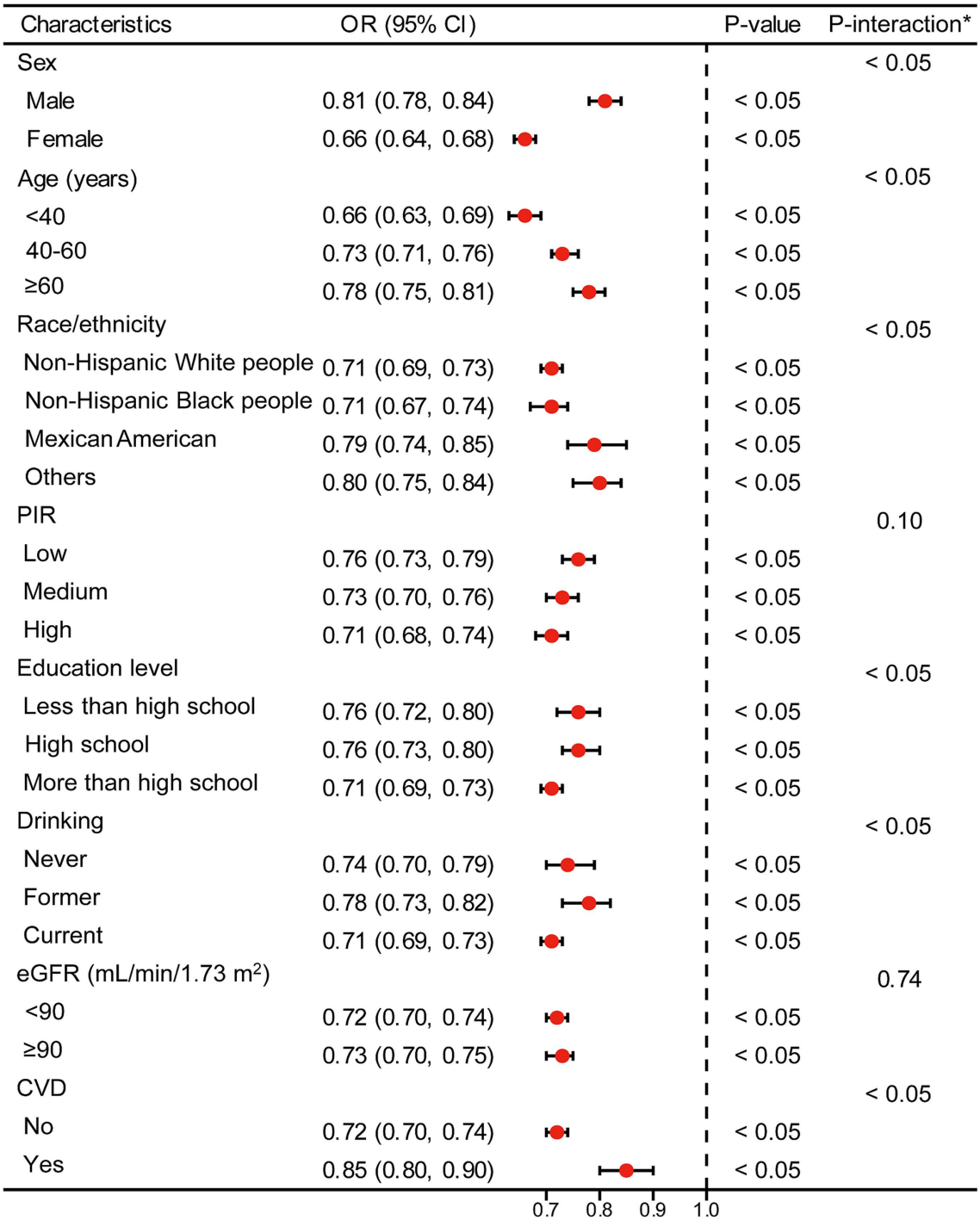

FIGURE 4
Stratified analyses [by (A) sex; (B) age; (C) race/ethnicity; (D) PIR; (E) education level; (F) drinking; (G) eGFR; (H) CVD] between LE8 and hyperuricemia using GAM. *Each generalized additive model and smooth curve fitting was adjusted for all factors, including age, sex, race/ethnicity, PIR, educational level, drinking, eGFR, and CVD, except for the stratification factor itself. PIR, poverty income ratio; eGFR, estimated glomerular filtration rate; CVD, cardiovascular disease; LE8, Life's Essential 8; GAM, generalized additive model.

health and reduces the risk of hyperuricemia. Finally, a higher BMI is associated with elevated uric acid levels due to overproduction and impaired excretion (56). Maintaining a healthy BMI, another crucial element of LE8, lowers the risk of hyperuricemia.

While our study provides valuable insights into the relationship between LE8 and hyperuricemia, several limitations should be acknowledged. First, the cross-sectional nature of NHANES data limits our ability to infer causality between LE8 scores and hyperuricemia. Longitudinal studies are needed to establish temporal relationships and causality. Second, this study relies on self-reported data for lifestyle factors, such as diet and physical activity, which introduces the possibility of recall bias.

However, this limitation is inherent in the design of the NHANES survey. Despite this, NHANES follows standardized procedures to enhance data accuracy, such as using validated questionnaires and trained interviewers. Third, one potential limitation is the presence of unmeasured confounding variables that could influence the observed relationship between LE8 scores and hyperuricemia. For instance, diet and physical activity are closely interrelated and may jointly affect serum uric acid levels. It is possible that diet acts as a mediator between physical activity and hyperuricemia, with healthier dietary habits amplifying the protective effect of physical activity. Future research could explore these potential interactions using mediation models to better understand how individual components of LE8 interact to influence hyperuricemia risk. Additionally, while we adjusted for major covariates such as age, sex, race/ethnicity, and eGFR, residual confounding by other unmeasured factors cannot be entirely ruled out. Fourth, although MICE was used to handle missing data, the method assumes that data were missing at random, which may not always be the case. Finally, although NHANES data are representative of the U.S. population, our findings may not directly apply to populations with different genetic, environmental, or cultural backgrounds.

5 Conclusion

This study underscores the importance of comprehensive cardiovascular health, as captured by LE8, in reducing hyperuricemia risk among adults. The LE8 framework, which encompasses diet, physical activity, nicotine exposure, sleep health, BMI, blood lipids, blood glucose, and blood pressure, offers a holistic approach to health that effectively mitigates metabolic disorders such as hyperuricemia. The consistent association between higher LE8 scores and lower hyperuricemia risk indicates a clear metabolic association. This underscores the importance of considering various metabolic determinants in the context of hyperuricemia and suggests potential public health implications for promoting cardiovascular health behaviors.

For future research, longitudinal studies are needed to confirm causal relationships and explore the long-term effects of LE8 adherence across diverse groups. Mediation analysis can further clarify how LE8 components interact to influence uric acid levels. Incorporating objective measures, such as wearable devices for activity tracking and dietary biomarkers, will improve data accuracy and reduce self-reporting bias.

From a public health perspective, promoting LE8 adherence in high-risk groups—such as those with obesity or hypertension—is essential. Community programs, educational campaigns, and policy efforts that improve access to healthy foods and physical activity can help drive sustainable lifestyle changes. Interventional studies in diverse populations will further guide effective prevention strategies for hyperuricemia.

Data availability statement

The raw data supporting the conclusions of this article will be made available by the authors, without undue reservation.

Ethics statement

The studies involving humans were approved by National Center for Health Statistics Institutional Ethics Review Board. The studies were conducted in accordance with the local legislation and institutional requirements. The participants provided their written informed consent to participate in this study.

Author contributions

XW: Conceptualization, Data curation, Formal analysis, Investigation, Methodology, Supervision, Validation, Writing – original draft. JF: Conceptualization, Funding acquisition, Methodology, Project administration, Resources, Software, Supervision, Validation, Visualization, Writing – original draft, Writing – review & editing.

Funding

The author(s) declare that no financial support was received for the research, authorship, and/or publication of this article.

Acknowledgments

We acknowledge the National Center for Health Statistics at the CDC, which was responsible for designing, collecting, and administering the NHANES data and making the data available for public use.

Conflict of interest

The authors declare that the research was conducted in the absence of any commercial or financial relationships that could be construed as a potential conflict of interest.

Publisher's note

Supplementary material

The Supplementary material for this article can be found online at: https://www.frontiersin.org/articles/10.3389/fmed.2024.1455164/full#supplementary-material

References

1. Borghi C, Agabiti-Rosei E, Johnson RJ, Kielstein JT, Lurbe E, Mancia G, et al. Hyperuricaemia and gout in cardiovascular, metabolic and kidney disease. *Eur J Intern Med*. (2020) 80:1–11. doi: 10.1016/j.ejim.2020.07.006

2. Liu R, Han C, Wu D, Xia X, Gu J, Guan H, et al. Prevalence of hyperuricemia and gout in mainland China from 2000 to 2014: a systematic review and Meta-analysis. *Bio Med Res Int*. (2015) 2015:1–12. doi: 10.1155/2015/762820

3. Kuo CF, Grainge MJ, Zhang W, Doherty M. Global epidemiology of gout: prevalence, incidence and risk factors. *Nat Rev Rheumatol*. (2015) 11:649–62. doi: 10.1038/nrrheum.2015.91

4. Benn CL, Dua P, Gurrell R, Loudon P, Pike A, Storer RI, et al. Physiology of hyperuricemia and urate-lowering treatments. *Front Med*. (2018) 5:160. doi: 10.3389/fmed.2018.00160

5. Li L, Zhang Y, Zeng C. Update on the epidemiology, genetics, and therapeutic options of hyperuricemia. *Am J Transl Res*. (2020) 12:3167–81.

6. Lloyd-Jones DM, Allen NB, Anderson CAM, Black T, Brewer LPC, Foraker RE, et al. Life's essential 8: updating and enhancing the American Heart Association's construct of cardiovascular health: a presidential advisory from the American Heart Association. *Circulation*. (2022) 146:e18–43. doi: 10.1161/CIR.0000000000001078

7. Choi HK, McCormick N, Yokose C. Excess comorbidities in gout: the causal paradigm and pleiotropic approaches to care. *Nat Rev Rheumatol*. (2022) 18:97–111. doi: 10.1038/s41584-021-00725-9

8. Ali N, Perveen R, Rahman S, Mahmood S, Rahman S, Islam S, et al. Prevalence of hyperuricemia and the relationship between serum uric acid and obesity: a study on Bangladeshi adults. *PLoS One*. (2018) 13:e0206850. doi: 10.1371/journal.pone.0206850

9. Nakanishi N, Yoshida H, Nakamura K, Suzuki K, Tatara K. Predictors for development of hyperuricemia: An 8-year longitudinal study in middle-aged Japanese men. *Metabolism*. (2001) 50:621–6. doi: 10.1053/meta.2001.24196

10. Qiu L, Cheng X, Wu J. Prevalence of hyperuricemia and its related risk factors in healthy adults from northern and northeastern Chinese provinces. *BMC Public Health*. (2013) 13:1–9. doi: 10.1186/1471-2458-13-664

11. Wang Y, Meng Q, Zhang X, Baima K, Chen L, Dai Y, et al. Life's essential 8, Life's simple 7 and the odds of hyperuricaemia: results from the China multi-ethnic cohort study. *Rheumatol Adv Pract*. (2023) 8:1–8. doi: 10.1093/rap/rkae009

12. Yang W, Cui L. AB1616 adherence to the LIFE'S essential 8 metrics and hyperuricemia:a cross-sectional study. *Scientific Abstracts*. (2023) 82:2042–43. doi: 10.1136/annrheumdis-2023-eular.4531

13. Wang M, Meng H. Association between cardiovascular health assessed by life's essential 8 and hyperuricemia in U.S. adults: the NHANES 2009-2020. *Front Endocrinol*. (2024) 15:15. doi: 10.3389/fendo.2024.1445787

14. Han Y, Di H, Wang Y. Exploration of the association between new "Life's essential 8" with hyperuricemia and gout among US adults. *Qual Life Res Published*. (2024) 21. doi: 10.1007/s11136-024-03777-y

15. Levey AS, Stevens LA, Schmid CH, Zhang Y(L), Castro AF III, Feldman HI, et al. A new equation to estimate glomerular filtration rate. *Ann Intern Med*. (2009) 150:604–12. doi: 10.7326/0003-4819-150-9-200905050-00006

16. Krebs-Smith SM, Pannucci TE, Subar AF. Update of the healthy eating index: HEI-2015. *J Acad Nutr Diet*. (2018) 118:1591–602. doi: 10.1016/j.jand.2018.05.021

17. Feig DI, Kang DH, Johnson RJ. Uric acid and cardiovascular risk. *N Engl J Med*. (2008) 359:1811–21. doi: 10.1056/NEJMra0800885

18. Hastie T, Tibshirani R. Generalized additive models: some applications. *J Am Stat Assoc*. (1987) 82:371–86. doi: 10.1080/01621459.1987.10478440

19. Toutenburg H, Rubin DB. Multiple imputation for nonresponse in surveys. *Stat Pap*. (1990) 31:180–0. doi: 10.1007/BF02924688

20. Sterne JAC, White IR, Carlin JB, Spratt M, Royston P, Kenward MG, et al. Multiple imputation for missing data in epidemiological and clinical research: potential and pitfalls. *BMJ*. (2009) 338:b2393. doi: 10.1136/bmj.b2393

21. Ning H, Perak AM, Siddique J, Wilkins JT, Lloyd-Jones DM, Allen NB. Association between Life's essential 8 cardiovascular health metrics with cardiovascular events in the cardiovascular disease lifetime risk pooling project. *Circ: Cardiovascular Quality and Outcomes*. (2024) 17:e010568. doi: 10.1161/CIRCOUTCOMES.123.010568

22. Song C, Cheng X, Bai Y. Association of change in cardiovascular health based on life's essential 8 with incident cardiovascular disease. *American J Preventive Cardiol*. (2024) 18:100668. doi: 10.1016/j.ajpc.2024.100668

23. Pang S, Wang Y, Sun S, Wang S, Li F, Zhao W, et al. Associations between Life's essential 8 and insulin resistance among nondiabetic adults. *JAHA*. (2024) 13:e033997. doi: 10.1161/JAHA.123.033997

24. Ueno K, Kaneko H, Okada A, Suzuki Y, Matsuoka S, Fujiu K, et al. Association of four health behaviors in Life's essential 8 with the incidence of hypertension and diabetes mellitus. *Prev Med*. (2023) 175:107685. doi: 10.1016/j.ypmed.2023.107685

25. Tian X, Feng J, Chen S, Zhang Y, Zhang X, Xu Q, et al. Baseline and longitudinal cardiovascular health using Life's essential 8 metrics with the risk of incident hypertension. *Clin Exp Hypertens*. (2023) 45:2271190. doi: 10.1080/10641963.2023.2271190

26. Gou R, Xiong S, Liang X, Wu H, Qin S, Li B, et al. Relationship between Life's essential 8 and metabolic syndrome among older Americans (NHANES, 2007–2010): navigating biological aging and inflammation. *Front Med*. (2024) 11:1380464. doi: 10.3389/fmed.2024.1380464

27. Cao Q, Li M, Qin G, Yan L, He J, Xu M, et al. Early adulthood weight change, midlife "Life's essential 8" health status and risk of cardiometabolic diseases: a chinese nationwide cohort study. *Nutr Metab (Lond)*. (2023) 20:48. doi: 10.1186/s12986-023-00765-w

28. Yang T, Yi J, Shao M, Linlin Z, Wang J, Huang F, et al. Associations between life's essential 8 and metabolic health among us adults: insights of NHANES from 2005 to 2018. *Acta Diabetol*. (2024) 61:963–74. doi: 10.1007/s00592-024-02277-2

29. Hou Q, Qi Q, Han Q, Yu J, Wu J, Yang H, et al. Association of the triglyceride-glucose index with early-onset atherosclerotic cardiovascular disease events and all-cause mortality: a prospective cohort study. *Cardiovasc Diabetol*. (2024) 23:149. doi: 10.1186/s12933-024-02249-4

30. McCormick N, Choi HK. Racial disparities in the modern gout epidemic. *J Rheumatol*. (2022) 49:443–6. doi: 10.3899/jrheum.220173

31. NHANES. (2019). NHANES questionnaires, datasets, and related documentation. Available at: https://wwwn.cdc.gov/nchs/nhanes/continuousnhanes/default.aspx?Begin (Accessed on October 20, 2024)

32. Nieradko-Iwanicka B. The role of alcohol consumption in pathogenesis of gout. *Crit Rev Food Sci Nutr*. (2022) 62:7129–37. doi: 10.1080/10408398.2021.1911928

33. Fang Y, Mei W, Wang C, Ren X, Hu J, Su F, et al. Dyslipidemia and hyperuricemia: a cross-sectional study of residents in Wuhu, China. *BMC Endocr Disord*. (2024) 24:2. doi: 10.1186/s12902-023-01528-7

34. Nie J, Deng MG, Wang K, Liu F, Xu H, Feng Q, et al. Higher HEI-2015 scores are associated with lower risk of gout and hyperuricemia: results from the national health and nutrition examination survey 2007–2016. *Front Nutr*. (2022) 9:921550. doi: 10.3389/fnut.2022.921550

35. Hong R, Huang J, Xu C, Zhang X, Mi F, Xu F, et al. Association of Sedentary Behavior and Physical Activity with Hyperuricemia and sex differences: results from the China multi-ethnic cohort study. *J Rheumatol*. (2022) 49:513–22. doi: 10.3899/jrheum.211180

36. Wang W, Krishnan E. Cigarette smoking is associated with a reduction in the risk of incident gout: results from the Framingham heart study original cohort. *Rheumatology (Oxford)*. (2015) 54:91–5. doi: 10.1093/rheumatology/keu304

37. Jee Y, Jeon C, Sull JW, Go E, Cho SK. Association between smoking and gout: a meta-analysis. *Clin Rheumatol*. (2018) 37:1895–902. doi: 10.1007/s10067-018-4118-y

38. Gee Teng G, Pan A, Yuan J, Koh W. Cigarette smoking and the risk of incident gout in a prospective cohort study. *Arthritis Care Res*. (2016) 68:1135–42. doi: 10.1002/acr.22821

39. Teramura S, Yamagishi K, Umesawa M, Hayama-Terada M, Muraki I, Maruyama K, et al. Risk factors for hyperuricemia or gout in men and women: the circulatory risk in communities study (CIRCS). *JAT*. (2023) 30:1483–91. doi: 10.5551/jat.63907

40. An Y, Li X, Ouyang F, Xiao S. Association between nocturnal sleep duration and the risk of hyperuricemia among Chinese government employees: a cross-sectional study. *Front Public Health*. (2022) 10:1055778. doi: 10.3389/fpubh.2022.1055778

41. Zhou C, Gu M, Yin L, Yin W, Liu J, Zhu Y, et al. Low serum uric acid levels may be a potential biomarker of poor sleep quality in patients with Parkinson's disease. *Sleep Med*. (2023) 105:9–13. doi: 10.1016/j.sleep.2023.03.011

42. Kuwabara M, Kodama T, Ae R, Kanbay M, Andres-Hernando A, Borghi C, et al. Update in uric acid, hypertension, and cardiovascular diseases. *Hypertens Res*. (2023) 46:1714–26. doi: 10.1038/s41440-023-01273-3

43. Piani F, Cicero AFG, Borghi C. Uric acid and hypertension: prognostic role and guide for treatment. *JCMM*. (2021) 10:448. doi: 10.3390/jcm10030448

44. Wang R, Bai Z, Zhang D, Zhang R, Yang J, Yin C, et al. Mediating effects of insulin resistance on the development of hypertension associated with elevated serum uric acid: a prospective cohort study. *J Hum Hypertens*. (2022) 36:760–6. doi: 10.1038/s41371-021-00562-z

45. Xu L, Sun H, Liu L, Zhan S, Wang S, Lv X, et al. The effects of Cardiometabolic factors on the association between serum uric acid and chronic kidney disease in Chinese middle-aged and older population: a mediation analysis. *Front Endocrinol*. (2021) 12:702138. doi: 10.3389/fendo.2021.702138

46. Kawasoe S, Kubozono T, Ojima S, Kawabata T, Miyahara H, Tokushige K, et al. J-shaped curve for the association between serum uric acid levels and the prevalence of blood pressure abnormalities. *Hypertens Res*. (2021) 44:1186–93. doi: 10.1038/s41440-021-00691-5

47. Landolfo M, Borghi C. Hyperuricaemia and vascular risk. *Curr Opin Cardiol*. (2019) 34:399–405. doi: 10.1097/HCO.0000000000000626

48. Ndrepepa G. Uric acid and cardiovascular disease. *Clin Chim Acta*. (2018) 484:150–63. doi: 10.1016/j.cca.2018.05.046

49. Lee OYA, Wong ANN, Ho CY, Tse KW, Chan AZ, Leung GPH, et al. Potentials of natural antioxidants in reducing inflammation and oxidative stress in chronic kidney disease. *Antioxidants*. (2024) 13:751. doi: 10.3390/antiox13060751

50. Wang H, Qin S, Li F, Zhang H, Zeng L. A cross-sectional study on the association between dietary inflammatory index and hyperuricemia based on NHANES 2005–2018. *Front Nutr*. (2023) 10:10. doi: 10.3389/fnut.2023.1218166

51. Zhang T, Liu W, Gao S. Exercise and hyperuricemia: an opinion article. *Ann Med*. (2024) 56:2396075. doi: 10.1080/07853890.2024.2396075

52. Jang YS, Nerobkova N, Yun I, Kim H, Park EC. Association between smoking behavior and serum uric acid among the adults: findings from a national cross-sectional study. *PLoS One*. (2023) 18:e0285080. doi: 10.1371/journal.pone.0285080

53. Yu X, Gong S, Chen J, Zhang H, Shen Z, Gu Y, et al. Short sleep duration increases the risk of hyperuricemia among Chinese adults: findings from the China health and nutrition survey. *Sleep Med*. (2021) 84:40–5. doi: 10.1016/j.sleep.2021.05.014

54. Song S, Cai X, Hu J, Zhu Q, Shen D, Ma H, et al. Plasma aldosterone concentrations elevation in hypertensive patients: the dual impact on hyperuricemia and gout. *Front Endocrinol*. (2024) 15:1424207. doi: 10.3389/fendo.2024.1424207

55. Sharaf El Din UAA, Salem MM, Abdulazim DO. Uric acid in the pathogenesis of metabolic, renal, and cardiovascular diseases: a review. *J Adv Res*. (2017) 8:537–48. doi: 10.1016/j.jare.2016.11.004

56. Weinstein S, Maor E, Bleier J, Kaplan A, Hod T, Leibowitz A, et al. Non-interventional weight changes are associated with alterations in serum uric acid levels. *JCMM*. (2024) 13:2314. doi: 10.3390/jcm13082314

frontiers | Frontiers in Immunology

TYPE Original Research
PUBLISHED 14 November 2024
DOI 10.3389/fimmu.2024.1468810

OPEN ACCESS

EDITED BY
Lihua Duan,
Jiangxi Provincial People's Hospital, China

REVIEWED BY
Shui Lian Yu,
The Second Affiliated Hospital of Guangzhou Medical University, China
Eloi Franco-Trepat,
IrsiCaixa, Spain

*CORRESPONDENCE
Tianwang Li
litian-wang@163.com

RECEIVED 22 July 2024
ACCEPTED 29 October 2024
PUBLISHED 14 November 2024

CITATION
Huang Z, Zhong X, Zhang Y, Li X, Liu M, Huang Y, Yue J, Yi G, Liu H, Yuan B, Chen X, Zheng S and Li T (2024) A targeted proteomics screen reveals serum and synovial fluid proteomic signature in patients with gout.
Front. Immunol. 15:1468810.
doi: 10.3389/fimmu.2024.1468810

A targeted proteomics screen reveals serum and synovial fluid proteomic signature in patients with gout

Zhengping Huang[1,2,3], Xiaoyan Zhong[1,2], Yuexi Zhang[2], Xinjian Li[2], Meng Liu[2], Yukai Huang[2], Jian Yue[2], Guanqun Yi[2], Hongji Liu[2], Bingyan Yuan[2], Xu Chen[2], Shaoling Zheng[2] and Tianwang Li[1,2,3]*

[1]The Second School of Clinical Medicine, Southern Medical University, Guangzhou, China, [2]Department of Rheumatology and Immunology, The Affiliated Guangdong Second Provincial General Hospital of Jinan University, Guangzhou, China, [3]Department of Rheumatology and Immunology, Zhaoqing Central People's Hospital, Zhaoqing, China

Objective: To characterize the inflammatory proteome in both serum and synovial fluid (SF) of patients with gout, in comparison to healthy controls and individuals with osteoarthritis (OA), by utilizing a high-quality, high-throughput proteomic analysis technique.

Methods: Using the Olink Target 48 Inflammation panel, we measured serum concentrations of 45 inflammatory proteins in gout, OA, and healthy controls. We analyzed protein levels in SF samples from gout and OA, performed ROC curve analyses to identify diagnostic biomarkers, evaluate efficacy, and set cut-off values. Additionally, A protein-protein interaction (PPI) network was used to study protein relationships and significance.

Results: We have delineated the proteomic landscape of gout and identified 20 highly differentially expressed proteins (DEPs) in the serum of gout patients in comparison to that of healthy controls, which included VEGF-A, MMP-1, TGF-α, and OSM with corresponding area under the curve (AUC) values of 0.95, 0.95, 0.92, and 0.91 respectively. For the analysis of synovial fluid, 6 proteins were found to be elevated in gout in contrast to osteoarthritis (OA), among which IP-10, VEGF-A, IL-8, and MIP-3β had corresponding AUC values of 0.78, 0.78, 0.76, and 0.75 respectively. The protein-protein interaction (PPI) network analysis identified significantly prominent pathways in gout.

Conclusion: This research marks a significant advancement in elucidating the inflammatory profile present in the serum and synovial fluid of individuals suffering from gout. Our discoveries have identified several novel proteins in both serum and synovial fluid that are potential biomarkers for diagnostic purposes and are believed to have critical roles as pathogenic factors in the pathophysiology of gout.

KEYWORDS

crystal arthropathies, osteoarthritis, biomarkers, synovial fluid analysis, proteomics, cytokines and inflammatory mediators

Introduction

Gout is among the most prevalent forms of arthritis, defined by an innate immune response that is activated due to hyperuricemia. This condition is aggravated by the build-up of monosodium urate crystals (MSU) within joints and surrounding connective tissues (1). Epidemiological research conducted recently has highlighted a swift and widespread rise in the incidence of both primary gout and hyperuricemia on a global scale (2). Specifically, in China, the adjusted prevalence rate for gout stands at 3.2%, with hyperuricemia impacting a significant 17.7% of the population (3).

The accumulation of monosodium urate (MSU) crystals in the joint triggers an innate immune reaction, where these crystals are recognized as foreign bodies by the immune system (4). This recognition leads to the activation of neutrophils, a type of white blood cell. Central to the cellular inflammatory cascade initiated by MSU crystals is the NLRP3 inflammasome (5). Once activated, the NLRP3 inflammasome promotes the secretion of pro-inflammatory cytokines, including interleukin-1 beta (IL-1β) and interleukin-18 (IL-18). Among these, IL-1β is a crucial factor in mediating the inflammatory cascade characteristic of gout (6). The secretion of these cytokines initiates the recruitment of additional immune cells, setting off an inflammatory cascade. This cascade manifests as the hallmark symptoms of gout, such as intense pain, redness, swelling, and heat in the affected joint. While the activation of the NLRP3 inflammasome is recognized as a critical event, the exact mechanisms driving gout remain incompletely understood. It is thought that a complex interplay of multiple regulatory pathways contributes to the diverse clinical manifestations observed in gouty inflammation.

The Proximity Extension Assay (PEA) represents a cutting-edge proteomics approach, meticulously quantifying even the most minute protein concentrations within biological fluids, including as little as 1μl of plasma or serum (7). Utilizing the PEA technology, Olink reagents employ a set of 45 antibody probe pairs, each labeled with oligonucleotides and specifically designed to bind to their corresponding target proteins within the sample (8). This method is further enhanced by PCR-based signal amplification, which markedly boosts sensitivity and facilitates the detection of proteins at ultra-low levels.

To our knowledge, this study is the first to delineate the inflammatory profile of both serum and synovial fluid (SF) in gout patients by examining a comprehensive panel of 45 inflammatory proteins via PEA technology. Our objective was to map the inflammatory proteome of gout patient serum and SF, with the goal of identifying novel proteins that could serve as potential biomarkers for diagnosis, as well as to identify proteins that may play significant roles in the underlying mechanisms of gout pathogenesis.

Methods

Human subjects

Research was granted ethical approval by the Ethics Committee of Guangdong Second Provincial General Hospital under the protocol number 2024-KY-KZ-285-01. Informed consent was obtained from all participants prior to the collection of research samples. Clinical data were gathered through a retrospective review of medical records. Gout patients were selected based on the 2015 American College of Rheumatology (ACR)/European League Against Rheumatism (EULAR) classification criteria for gout, while osteoarthritis (OA) patients were classified according to the clinical criteria established by the ACR (9, 10). All patients, both with gout and OA, exhibited active disease as indicated by elevated C-reactive protein (CRP) levels, clinical symptoms, and findings from a physical examination conducted by a rheumatologist. Serum and SF samples were collected from patients with active gout and osteoarthritis (OA) during their inpatient or outpatient visits to the Department of Rheumatology and Clinical Immunology. Healthy control serum samples were obtained from volunteer participants. All collected samples were stored at -80°C and were thawed immediately prior to assay preparation.

PEA

We utilized the Olink Target 48 Cytokine Panel to analyze 45 analytes in plasma and serum samples, adhering to the

10.3389/fimmu.2024.1468810

manufacturer's protocol. Each assay run involved processing forty samples on a 48 × 48 integrated fluidic circuit (IFC). The samples were incubated with 1 µl of plasma or serum and antibodies for 18 hours. Following hybridization, DNA tags were extended and preamplified using a Bio-Rad T100 Thermocycler (Hercules, CA). The preamplified samples, along with primers, were then loaded onto a primed IFC, and quantitative PCR (qPCR) amplification was performed for 40 cycles on an Olink Signature Q-100 instrument. To maintain accuracy, each run included internal controls and calibrators. Data analysis and quality control were performed using the Olink NPX Signature software, which also facilitated the conversion of NPX-values to protein concentrations in standard units (pg/mL) by fitting them to a standard curve.

Bioinformatics and statistical analysis

For the generation of PCA, heatmap, dotplot, ggplot, and volcano plots, the seurat package (version 4.0.1), complexheatmap package (version 2.6.2), ggrepel package (version 0.9.2), and ggplot2 package (version 3.3.3) were utilized within the R programming environment (version 4.1.2). Additionally, STRING (Search Tool for the Retrieval of Interacting Genes/Proteins) functional protein association networks and signal analysis were created using the STRING online tool (http://string-db.org/, accessed on 10 July 2024). Independent samples were analyzed using T-tests or the Mann–Whitney U tests. For contingency analysis involving more than two groups, one-way independent analysis of variance or Kruskal–Wallis tests were conducted for continuous variables. A P-value of less than 0.05 was deemed statistically significant, unless indicated otherwise. For differentially expressed proteins (DEPs) between two groups, A p-value of less than 0.05 and an absolute log2 fold change greater than 1 were defined as criteria for significant differential expression. Receiver Operating Characteristic (ROC) curve analysis was employed to assess the sensitivity and specificity of potential biomarkers across a range of threshold values. All statistical analyses, including ROC curve evaluations, were carried out using Prism 8.0 software (GraphPad Software, La Jolla, CA).

Results

Overall proteomic signature

In total, serum samples were collected from 8 gout patients (GS), 8 OA patients (OS), and 8 healthy controls (HS). Additionally, synovial fluid (SF) was collected from 14 gout patients (GJ) and 13 OA patients (OJ) (Supplementary Table S1). Subsequently, the Olink Target 48 Cytokine Panel, which measures 45 proteins such as cytokines, chemokines, and growth factors, was used (Table 1). The key steps of PEA are illustrated in Figure 1A. To depict the overall population structure and variance of the samples, Principal Component Analysis (PCA) was utilized. PCA of serum proteins revealed distinct clustering patterns among gout, OA, and healthy controls (HC), effectively segregating them into their respective groups (Figure 1B). The PCA plot demonstrated a high level of consistency within the protein profiles of the healthy controls, while the protein profiles of gout serum samples exhibited significant heterogeneity. PCA analysis of SF proteins indicated substantial overlap between gout and OA, suggesting a similarity in proteomic signatures within these groups (Figure 1C). A heatmap was then used to show the expression levels of various proteins among the groups. In GS, several proteins displayed different expression levels compared to HS, with some proteins exhibiting significantly higher levels (Figure 1D). Similarly, there were notable differences in protein levels between the GJ and HS groups. In the SF analysis, GJ did not show many significantly higher levels of proteins compared to OJ, which aligned with the results from the PCA plot (Figure 1E).

TABLE 1 45 inflammatory proteins in the Olink Target 48 Inflammation panel.

VEGF-A	M-CSF	IL-1β
TWEAK	MCP-4	IL-18
TSLP	MCP-3	IL-17F
TRAIL	MCP-2	IL-17C
TNF-β	MCP-1	IL-17A)
TNF-α	LOX-1	IL-15
TGF-α	I-TAC	IL-13
SDF-1α	IP-10	IL-10
OSM	IL-8	IFN-γ
MMP-12	IL-7	HGF
MMP-1	IL-6	GM-CSF
MIP-3β	IL-4	G-CSF
MIP-1β	IL-33	FLT3L
MIP-1α	IL-27	Eotaxin
MIG	IL-2	EGF

Profiling of gout versus controls samples

In order to elucidate the expression patterns of inflammatory proteins among individuals with gout and to compare these with cytokine levels in different groups, we conducted an analysis of protein levels across the groups. A comparative analysis between GS and HS revealed that 20 proteins are markedly increased in GS, including IL-8, MCP-3, IL-1β, IL-6, EGF, OSM, LOX-1, MIP-1α, MMP-1, TGF-α, VEGF-A, MIP-1β, IL-7, MMP-12, MCP-2, MCP-1, GM-CSF, IL-2, HGF and I-TAC (Figure 2A). Most of these proteins were also observed to be significantly higher in OS compared to HS, except for IL-2, HGF, and MCP-1 (Figure 2B). In the comparison between GJ and OJ, the levels of IL-8, IL-6, IP-10, IL-17F, MIP-3β, and VEGF-A were found to be elevated in GJ (Figure 2C). When comparing GJ to GS, a distinct pattern of protein

10.3389/fimmu.2024.1468810

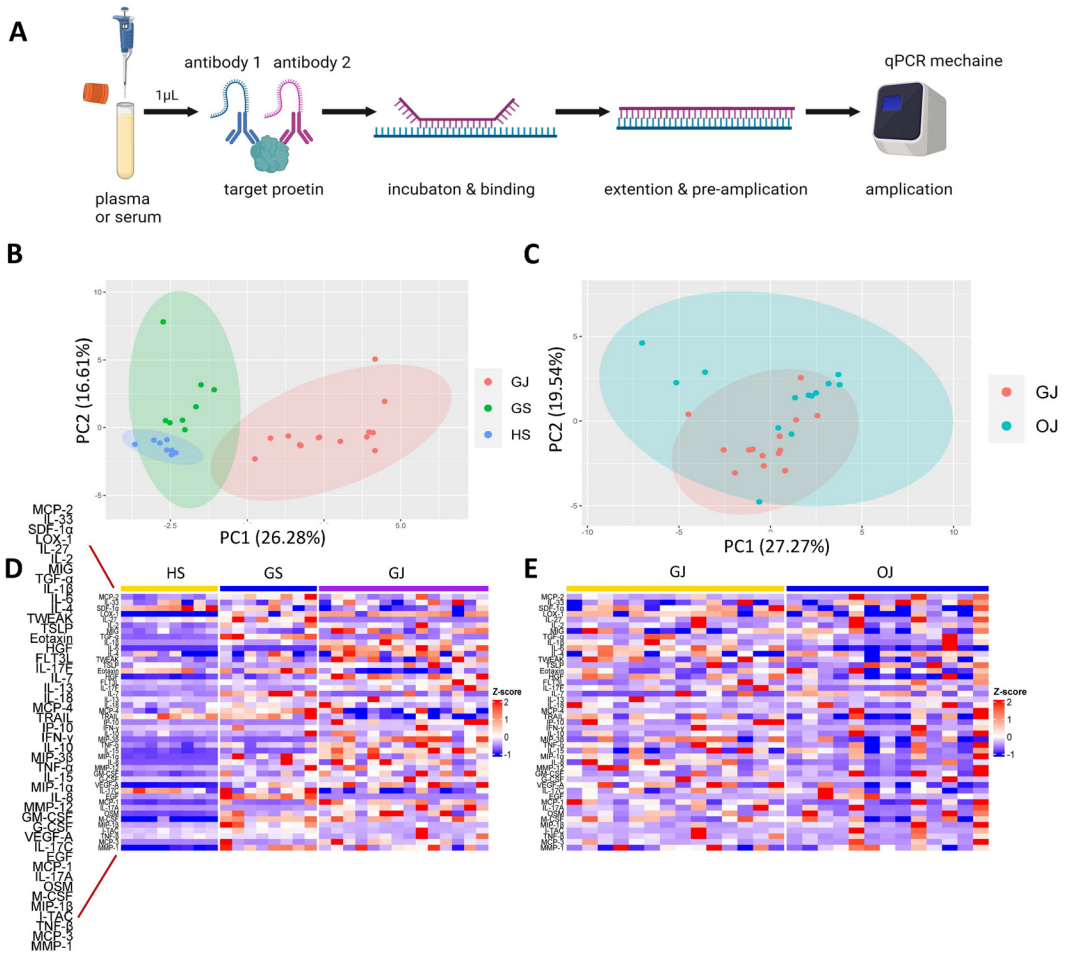

FIGURE 1
Comprehensive proteomic profile of gout. **(A)** Schematic representation of the key steps in PEA. **(B)** PCA of serum proteins in groups GS, GJ, and HS. Each data point corresponds to a sample, with PC1 represented on the vertical axis and PC2 on the horizontal axis. **(C)** PCA of serum proteins in groups GJ and OJ. Each data point represents a sample, with PC1 shown on the vertical axis and PC2 on the horizontal axis. **(D)** Heatmap depicting serum protein expression levels in groups GS, GJ, and HS, where blue indicates lower expression and red indicates higher expression. **(E)** Heatmap illustrating serum protein expression levels in groups GJ and OJ, with blue indicating lower expression and red indicating higher expression.

expression was observed. A set of proteins, including IL-17A, IL-6, MIP-3β, IP-10, IL-17F, IL-15, IL-1β, HGF, TSLP, MIG, and MCP-1, were found to be significantly higher in GJ. In contrast, the levels of IL-17C, Eotaxin, MCP-2, TRAIL, TGF-α, IL-7, MIP-1β, IL-27, and EGF were significantly higher in GS (Figure 2D).

To further assess the effectiveness of these proteins in distinguishing gout from OA and healthy controls, we performed ROC curve analysis. The proteins that were identified to be highly expressed in GS and GJ than in the control group were selected for inclusion in the ROC analysis. In the serum samples, the proteins which showed higher expression levels in GS compared with OS and HS samples included VEGF-A, MMP-1, TGF-α, and OSM, with the corresponding area under the curve (AUC) values of 0.95, 0.95, 0.92, and 0.91 respectively (Figure 3). The determined cut-off values for VEGF-A, MMP-1, TGF-α, and OSM were 674.1 pg/mL, 2169 pg/L, 25.83 pg/L, and 13.23 pg/L. In the synovial fluid (SF) samples, the proteins presenting elevated expression in GJ as opposed to OJ samples were IP-10, VEGF-A, IL-8, and MIP-3β, with the AUC values of 0.78, 0.78, 0.76, and 0.75 respectively (Figure 4). The identified cut-off values for IP-10, VEGF-A, IL-8, and MIP-3β were 226.0 pg/mL, 2387.0 pg/L, 148.6 pg/L, and 587.1 pg/L.

Protein-protein interaction and pathway enrichment analysis

To understand the functional relationships and biological significance of proteins in gout. A protein-protein interaction (PPI) network was constructed using the STRING (Search Tool for the Retrieval of Interacting Genes/Proteins) online tool (http://string-db.org/, accessed on 20 June 2024) was used to analyze the protein interaction network. Inputting proteins (Supplementary Table S2) that show higher expression in GS compared to HS revealed that most of these proteins participate in forming a densely interconnected PPI network (Figure 5A). Notably, only one protein (MYDGF) is not part of this network. The resulting network comprises 21 nodes connected by 145 edges, with an average node degree of 13.8 and an average local clustering coefficient of

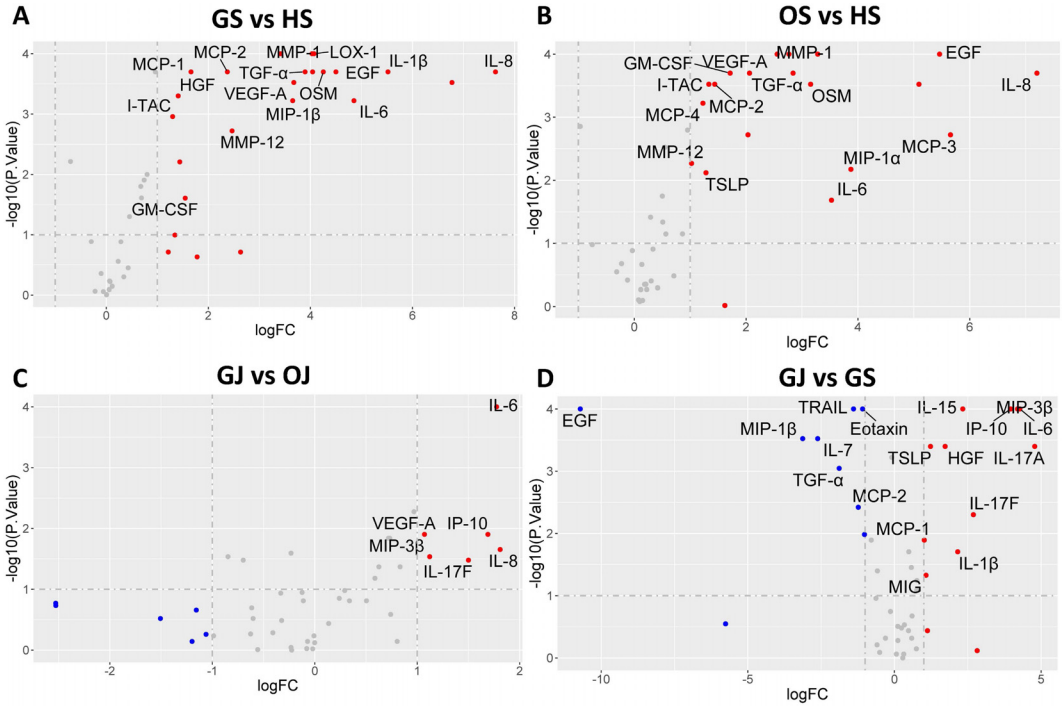

FIGURE 2
Volcano plot illustrating differential protein levels between two subject groups. **(A)** DEPs in serum between gout patients and healthy controls. **(B)** DEPs in serum between OA patients and healthy controls. **(C)** DEPs in SF between gout patients and healthy controls. **(D)** DEPs between serum and SF in gout patients. Each data point corresponds to a protein, with the horizontal axis representing the protein's fold change magnitude on a log2 scale. The vertical axis indicates significance, presented as the -log10 transformation of the P value. Proteins located on the right side of the plot indicate higher levels in the respective group's samples.

0.836. The number of edges in this network exceeds what would be expected by random associations, indicating a significantly higher number of interactions than expected. This network is characterized by a PPI enrichment p-value of < 10e−16, underscoring the substantial enrichment of interactions (Figure 5A). These findings suggest that the majority of proteins with differential expression in GS can interact with each other effectively within this internal PPI network. To clarify the function of differentially expressed proteins in the comparison between GS and HS, a KEGG pathways enrichment analysis was performed. The analysis identified 53 significantly enriched pathways, with the most prominent KEGG pathways visualized in bubble plot (Figure 5B). The bubble plot effectively visualizes the most significantly enriched pathways, highlighting key processes such as "Cytokine-cytokine receptor interaction", "Chemokine signaling pathway", "IL-17 signaling pathway", "Toll-like receptor signaling pathway", "JAK-STAT signaling pathway" and "PI3K-AKT signaling pathway". These significantly enriched pathways offer valuable insights into the underlying biological mechanisms of gout. In particular, the "Cytosolic DNA-sensing pathway" exhibit smaller dot sizes but remain statistically significant, suggesting their potential relevance to gout.

Subsequently, we examined proteins (Supplementary Table S2) that exhibit higher expression in GJ compared to OJ. The data revealed that these proteins are primarily involved in forming a densely interconnected PPI network (Figure 5C). The resulting network consists of 11 nodes connected by 38 edges, with an average node degree of 6.91 and an average local clustering coefficient of 0.848. The number of edges in this network surpasses what would be anticipated by random associations, indicating a significantly higher number of interactions than expected. This network is distinguished by a PPI enrichment p-value of 1.11e-15, highlighting the substantial enrichment of interactions. These findings suggest that the majority of proteins with differential expression in GJ can effectively interact with each other within this internal PPI network. Additionally, KEGG pathway enrichment analysis was also conducted using proteins that exhibited higher expression in GJ compared to OJ. The bubble plot provides a clear visualization of the most significantly enriched pathways in GJ (Figure 5D). Many of these pathways were also identified in GS compared to HS, including "Cytokine-cytokine receptor interaction," "IL-17 signaling pathway," and "Toll-like receptor signaling pathway." Additionally, pathways such as "Cytosolic DNA-sensing pathway" and "AGE-RAGE signaling pathway" were found to be associated with GJ. These enriched pathways offer valuable insights into the underlying biological mechanisms of arthritis in gout.

Discussion

Gout is characterized by both acute and chronic inflammatory responses. Cytokines and chemokines play crucial roles in the

10.3389/fimmu.2024.1468810

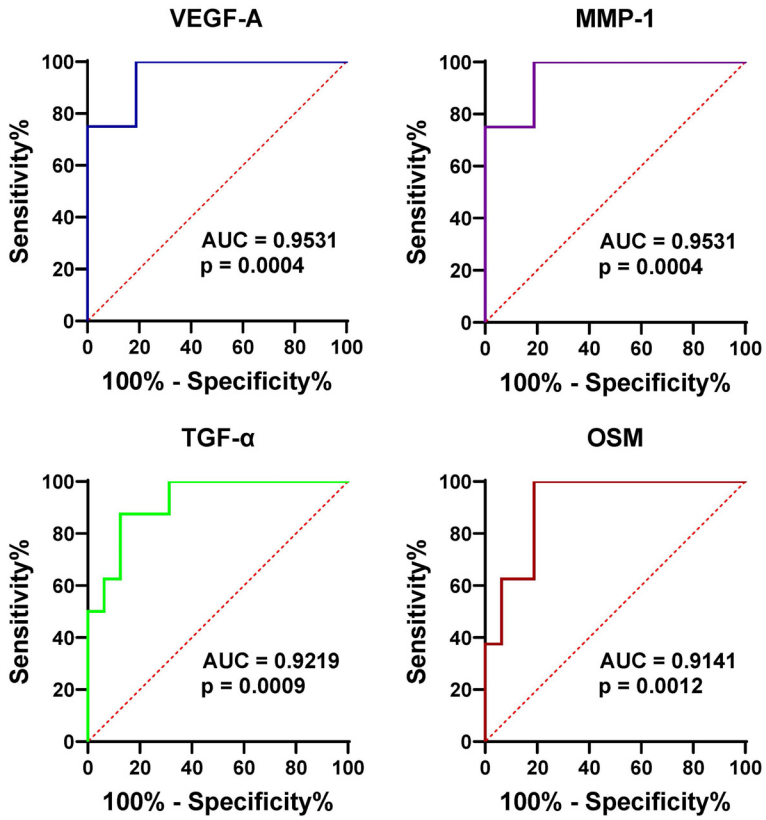

FIGURE 3
ROC curve analysis assessing the diagnostic potential of serum VEGF-1, MMP-1, TGF-α, and OSM in differentiating gout from OA and healthy controls. This figure presents ROC curves for the four proteins (VEGF-1, MMP-1, TGF-α, and OSM) in serum, demonstrating their ability to distinguish gout patients from those with OA and healthy controls. The AUC values are provided for each protein, indicating their diagnostic accuracy.

pathogenesis of arthritis by regulating inflammation, immune responses, immune cells migration and tissue repair within the joints (11). These signaling molecules are key mediators of the complex inflammatory processes involved in various forms of arthritis, including gout. Chemokines such as CCL2 (MCP-1), CCL5 (RANTES), and CXCL8 (IL-8) are involved in recruiting monocytes, T cells, and neutrophils to the synovium, contributing to the perpetuation of inflammation and tissue damage (12–14). In osteoarthritis (OA), TGF-β plays a role in maintaining cartilage homeostasis and promoting chondrocyte proliferation and matrix synthesis (15). However, dysregulation of TGF-β signaling can lead to cartilage degradation and OA progression (15, 16).

It is now widely acknowledged that the proteome offers profound insights into the pathophysiology of inflammatory arthritis, serving as a pivotal resource for the discovery of novel biomarkers (17). PEA, pioneered by Olink Proteomics, stands out as an effective method for the simultaneous identification and quantification of a multitude of biomarkers within a single sample. Here, we utilized high-fidelity protein quantification through PEA to investigate proinflammatory mediators in gout and controls. The PCA plot revealed a high degree of consistency in the protein profiles of the healthy controls. In contrast, the protein profiles of the gout serum samples showed significant heterogeneity. Additionally, the PCA analysis of SF proteins indicated a substantial overlap between gout and OA, suggesting a resemblance in proteomic signatures within these groups. Furthermore, Olink revealed 20 proteins that are highly differentially expressed (DEPs) in the serum of gout patients relative to healthy controls. Notably, VEGF-A, MMP-1, TGF-α, and OSM were identified with high discriminative power by ROC. These high AUC values suggest that these proteins could be strong candidates for biomarkers in gout diagnostics. In addition, our analysis of synovial fluid revealed a distinct pattern in gout, with IP-10, VEGF-A, IL-8, and MIP-3β showing elevated levels compared to OA.

VEGF-A, a central mediator that regulates angiogenesis, plays a critical role in angiogenic, inflammatory, and bone-destructive processes in rheumatoid arthritis (RA) (18). Consequently, it may also contribute to inflammation in gout by increasing vascular permeability and recruiting inflammatory cells to the affected area. VEGFA can induce MMP-1 and other MMPs, which promote angiogenesis by degrading the extracellular matrix and enabling the migration of new cells within the synovium and the proliferation of new blood vessels (19). TGF-α belongs to the EGF family and promotes proliferation and differentiation in epidermal and epithelial cells (20). OSM is a versatile cytokine that participates in various inflammatory responses, including wound healing (21). Interferon Gamma-induced Protein 10 (IP-10) serves as a crucial biomarker in numerous diseases. It is a chemokine released in reaction to IFN-γ and plays a key role in the inflammatory response (22). IL-8 is a key mediator of the inflammatory response which acts

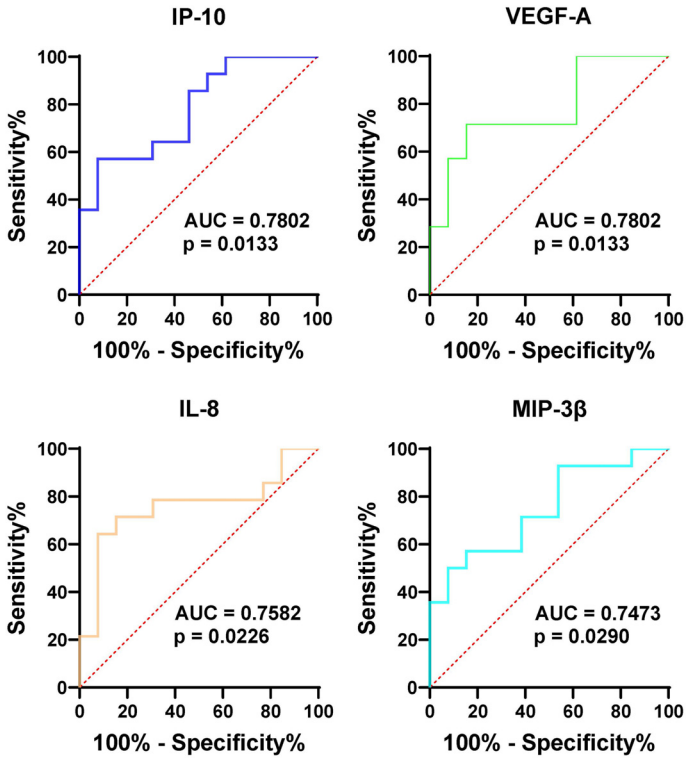

FIGURE 4
ROC curve analysis assessing the diagnostic potential of SF VEGF-1, MMP-1, TGF-α, and OSM in differentiating gout from OA and healthy controls. Similar to Figure 3, this figure shows ROC curves for the four proteins in synovial fluid (SF), indicating their potential as diagnostic markers for distinguishing gout from OA and healthy controls. The AUC values are provided for each protein, reflecting their diagnostic performance.

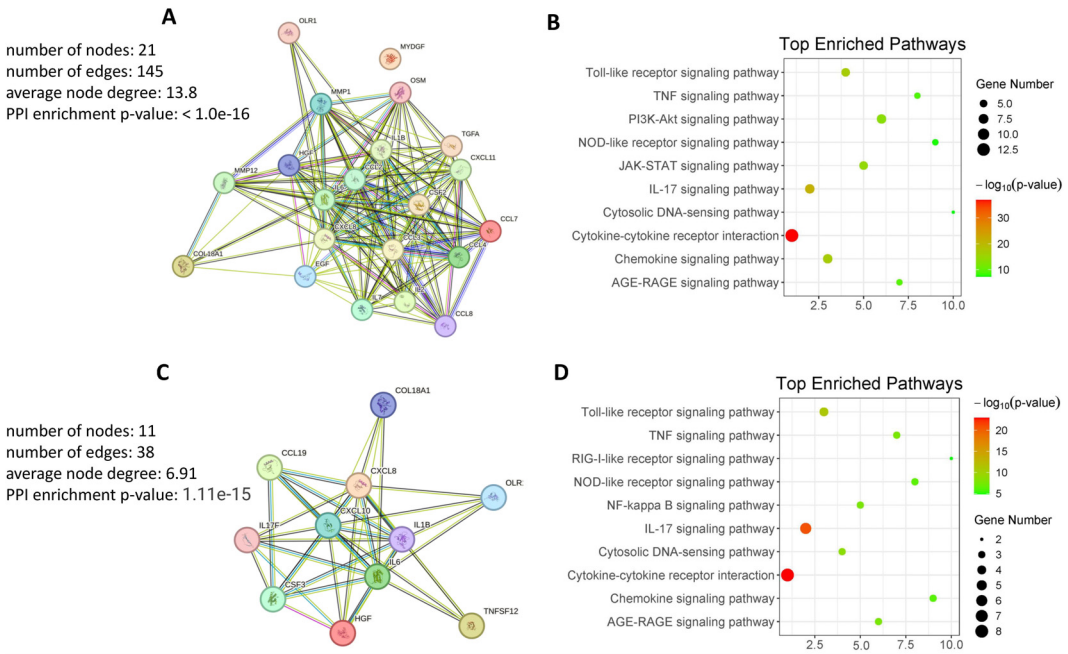

FIGURE 5
Protein-protein interaction and pathway enrichment analysis. **(A)** Protein-Protein Interaction Network of DEPs in GS compared to HS. The network visualizes interactions among DEPs, highlighting key nodes and pathways. **(B)** KEGG Pathway Enrichment Analysis of Highly DEPs in GS compared to HS. The analysis identifies enriched pathways, providing insights into the biological processes involved. **(C)** Protein-Protein Interaction Network of Highly DEPs in GJ compared to OJ. The network visualizes interactions among DEPs, highlighting key nodes and pathways. **(D)** KEGG Pathway Enrichment Analysis of Highly DEPs in GJ compared to OJ. The analysis identifies enriched pathways, providing insights into the biological processes involved.

as a chemoattractant and a potent angiogenic factor (23). MIP - 3β is a member of the chemokine family and plays a crucial role in the initiation, progression, and resolution of inflammatory responses.

The clinical implications of our findings are multifaceted. Firstly, the proteins identified as differentially expressed between gout and healthy controls, such as VEGF-A, MMP-1, TGF-α, and OSM, show high discriminative power and may serve as potential biomarkers for gout diagnosis. Elevated levels of these proteins in gout serum and synovial fluid suggest their involvement in the inflammatory process and tissue damage associated with the disease. The use of these biomarkers could aid in early detection and monitoring of disease progression, potentially leading to improved patient outcomes. Secondly, the similarity in proteomic signatures between gout and OA highlights the need for more specific biomarkers to differentiate between these conditions. The distinct patterns observed in gout, particularly with respect to IP-10, VEGF-A, IL-8, and MIP-3β, indicate their potential as differential diagnostic markers. These findings could facilitate more accurate diagnosis and personalized treatment strategies.

PPI on proteins with elevated expression levels in both gout serum and synovial fluid (SF) had revealed significant enrichment of pathways that are characteristic of gout. This approach underscores the complex interplay of these proteins in the pathogenesis of the disease and may provide insights into potential therapeutic targets. There is no doubt that the "Cytokine-cytokine receptor interaction" and "Chemokine signaling pathway" pathways were significantly enriched in gout. We also discovered that the "IL-17 signaling pathway" and "JAK-STAT signaling pathway" were enriched in gout. IL-17, a pro-inflammatory cytokine, plays a crucial role in mediating inflammation and immune responses, including arthritis. Studies have demonstrated that the IL-17A neutralizing antibody regulates monosodium urate crystal-induced gouty inflammation (24). Certain cytokines and molecules involved in the JAK-STAT signaling pathway may be overactivated or malfunctioning, leading to the excessive production of inflammatory mediators and the subsequent development and progression of gout symptoms (25). During gout flare-ups, the JAK2/STAT3 signaling pathway is activated, leading to increased expression of cytokines such as IL-6, IL-1β, and TNF-α in both the kidneys and joints (25). Interestingly, the "Cytosolic DNA-sensing pathway" and "AGE-RAGE signaling pathway" were also enriched in both serum and SF of gout. The "Cytosolic DNA-sensing pathway" plays a significant role in inflammation and arthritis. This pathway is involved in detecting the presence of cytosolic DNA, which can be released from damaged cells or pathogens, leading to the activation of immune responses (26). AGEs are formed through non-enzymatic reactions between sugars and proteins, and their accumulation in tissues can lead to chronic inflammation and tissue damage (27).

Based on the pathway enrichment analyses, several potential therapeutic targets emerge. For instance, the "Cytokine-cytokine receptor interaction" and "Chemokine signaling pathway" pathways are significantly enriched in gout. Targeting key components of these pathways, such as IL-17A and its receptors, has shown promise in preclinical models and clinical trials for rheumatoid arthritis and may also be beneficial for gout management (24, 28). The "IL-17 signaling pathway" and "JAK-STAT signaling pathway" are also enriched in both serum and synovial fluid in gout. Given the role of IL-17 and the JAK-STAT pathway in driving inflammation, inhibitors of these pathways represent potential therapeutic options. For example, targeting the JAK2/STAT3 signaling pathway could reduce the expression of pro-inflammatory cytokines like IL-6, IL-1β, and TNF-α, thereby alleviating gout symptoms and slowing disease progression. The "Cytosolic DNA-sensing pathway" is enriched in the serum of gout patients, suggesting that targeting components of this pathway, such as cGAS-STING signaling, could dampen excessive inflammation. Similarly, the "AGE-RAGE signaling pathway" is prominent in the synovial fluid of gout patients, indicating that inhibiting AGE formation or blocking the interaction between AGEs and RAGE could mitigate chronic inflammation and tissue damage.

One limitation of the present study is the relatively small cohort size, which could have led to an underestimation of the differences in protein levels between the gout and OA groups, given the stringent FDR correction applied. In reality, it is difficult to include a large number of patients with severe gout and OA with synovial fluid in basic science studies. Functional validation will be essential to identify the specific proteins and predicted pathways that play a role in the pathogenesis of gout. Another limitation of our study is that we only collected samples from patients with active gout, without including samples from different stages of gout, including stable gout. In future research, we plan to characterize the inflammatory profiles of gout at various phases, including stable gout, to provide a more comprehensive understanding of the disease.

Overall, this study provides a detailed exploration of the serum and SF proteomic signature in the context of gout, offering insights into the molecular mechanisms and potential therapeutic avenues for the condition. Further research is warranted to validate these findings and explore their clinical implications.

Data availability statement

The raw data supporting the conclusions of this article will be made available by the authors, without undue reservation.

Ethics statement

The studies involving humans were approved by the Ethics Committee of Guangdong Second Provincial General Hospital (2023-KY-KZ-285-01). The studies were conducted in accordance with the local legislation and institutional requirements. The participants provided their written informed consent to participate in this study.

Author contributions

ZH: Conceptualization, Data curation, Formal analysis, Funding acquisition, Investigation, Methodology, Project administration, Resources, Software, Validation, Visualization, Writing – original draft, Writing – review & editing. XZ: Methodology, Writing – review & editing. YZ: Investigation, Methodology, Resources, Writing

– review & editing. XL: Data curation, Formal analysis, Resources, Writing – original draft. ML: Data curation, Validation, Visualization, Writing – review & editing. YH: Data curation, Software, Validation, Writing – review & editing. JY: Data curation, Investigation, Methodology, Writing – review & editing. GY: Investigation, Project administration, Writing – review & editing. HL: Writing – review & editing, Methodology. BY: Writing – review & editing, Methodology. XC: Investigation, Writing – review & editing, Supervision. SZ: Writing – review & editing. TL: Methodology, Writing – review & editing, Funding acquisition, Investigation, Supervision.

Funding

The author(s) declare financial support was received for the research, authorship, and/or publication of this article. ZH received funding from the National Natural Science Foundation of China (No. 82302025), Young Talent Support Project of Guangzhou Association for Science and Technology (QT-2024-032) and Guangzhou Science and Technology Plan Projects (2024A03J0773). TL received funding from Guangzhou Science and Technology Plan Projects (No. 202102080321).

Conflict of interest

The authors declare that the research was conducted in the absence of any commercial or financial relationships that could be construed as a potential conflict of interest.

Publisher's note

Supplementary material

The Supplementary Material for this article can be found online at: https://www.frontiersin.org/articles/10.3389/fimmu.2024.1468810/full#supplementary-material

References

1. Dalbeth N, Choi HK, Joosten LA, Khanna PP, Matsuo H, Perez-Ruiz F, et al. Gout (primer). *Nat Reviews: Dis Primers*. (2019) 5:69. doi: 10.1038/s41572-019-0115-y

2. Dehlin M, Jacobsson L, Roddy E. Global epidemiology of gout: prevalence, incidence, treatment patterns and risk factors. *Nat Rev Rheumatol*. (2020) 16:380–90. doi: 10.1038/s41584-020-0441-1

3. Song J, Jin C, Shan Z, Teng W, Li J. Prevalence and risk factors of hyperuricemia and gout: A cross-sectional survey from 31 provinces in mainland China. *J Trans Internal Med*. (2022) 10:134–45. doi: 10.2478/jtim-2022-0031

4. Martillo MA, Nazzal L, Crittenden DB. The crystallization of monosodium urate. *Curr Rheumatol Rep*. (2014) 16:1–8. doi: 10.1007/s11926-013-0400-9

5. Kingsbury SR, Conaghan PG, McDermott MF. The role of the NLRP3 inflammasome in gout. *J Inflammation Res*. (2011) 2011:39–49. doi: 10.2147/JIR.S11330

6. Mitroulis I, Kambas K, Ritis K. Neutrophils, IL-1β, and gout: is there a link? *Semin immunopathology*. (2013) 35:501–12. doi: 10.1007/s00281-013-0361-0

7. Wik L, Nordberg N, Broberg J, Björkesten J, Assarsson E, Henriksson S, et al. Proximity extension assay in combination with next-generation sequencing for high-throughput proteome-wide analysis. *Mol Cell Proteomics*. (2021) 20. doi: 10.1016/j.mcpro.2021.100168

8. Jabbari E, Woodside J, Guo T, Magdalinou NK, Chelban V, Athauda D, et al. Proximity extension assay testing reveals novel diagnostic biomarkers of atypical parkinsonian syndromes. *J Neurology Neurosurg Psychiatry*. (2019) 90:768–73. doi: 10.1136/jnnp-2018-320151

9. Peat G, Thomas E, Duncan R, Wood L, Hay E, Croft P. Clinical classification criteria for knee osteoarthritis: performance in the general population and primary care. *Ann Rheum Dis*. (2006) 65:1363–7. doi: 10.1136/ard.2006.051482

10. Neogi T, Jansen TLTA, Dalbeth N, Fransen J, Schumacher HR, Berendsen D, et al. 2015 Gout classification criteria: an American College of Rheumatology/European League Against Rheumatism collaborative initiative. *Ann Rheumatic Dis*. (2015) 74:1789–98. doi: 10.1136/annrheumdis-2015-208237

11. Ea HK, Kischkel B, Chirayath TW, Klück V, Aparicio C, Loeung HU, et al. Systemic inflammatory cytokine profiles in patients with gout during flare, intercritical and treat-to-target phases: TNFSF14 as new biomarker. *Ann Rheum Dis*. (2024) 83:945–56. doi: 10.1136/ard-2023-225305

12. Cambier S, Gouwy M, Proost P. The chemokines CXCL8 and CXCL12: molecular and functional properties, role in disease and efforts towards pharmacological intervention. *Cell Mol Immunol*. (2023) 20:217–51. doi: 10.1038/s41423-023-00974-6

13. Agere SA, Akhtar N, Watson JM, Ahmed S. RANTES/CCL5 induces collagen degradation by activating MMP-1 and MMP-13 expression in human rheumatoid arthritis synovial fibroblasts. *Front Immunol*. (2017) 8:1341. doi: 10.3389/fimmu.2017.01341

14. Deshmane SL, Kremlev S, Amini S, Sawaya BE. Monocyte chemoattractant protein-1 (MCP-1): an overview. *J Interferon Cytokine research: Off J Int Soc Interferon Cytokine Res*. (2009) 29:313–26. doi: 10.1089/jir.2008.0027

15. Shen J, Li S, Chen D. TGF-β signaling and the development of osteoarthritis. *Bone Res*. (2014) 2:14002. doi: 10.1038/boneres.2014.2

16. van der Kraan PM. Differential role of transforming growth factor-beta in an osteoarthritic or a healthy joint. *J Bone Metab*. (2018) 25:65–72. doi: 10.11005/jbm.2018.25.2.65

17. Cuesta-López L, Escudero-Contreras A, Hanaee Y, Pérez-Sánchez C, Ruiz-Ponce M, Martínez-Moreno JM, et al. Exploring candidate biomarkers for rheumatoid arthritis through cardiovascular and cardiometabolic serum proteome profiling. *Front Immunol*. (2024) 15:1333995. doi: 10.3389/fimmu.2024.1333995

18. Kim HR, Kim KW, Kim BM, Cho ML, Lee SH. The effect of vascular endothelial growth factor on osteoclastogenesis in rheumatoid arthritis. *PloS One*. (2015) 10:e0124909. doi: 10.1371/journal.pone.0124909

19. Cabău G, Gaal O, Badii M, Nica V, Mirea AM, Hotea I, et al. Hyperuricemia remodels the serum proteome toward a higher inflammatory state. *iScience*. (2023) 26:107909. doi: 10.1016/j.isci.2023.107909

20. Huang Y, Chen Z, Lu T, Bi G, Li M, Liang J, et al. HIF-1α switches the functionality of TGF-β signaling via changing the partners of smads to drive glucose metabolic reprogramming in non-small cell lung cancer. *J Exp Clin Cancer research: CR*. (2021) 40:398. doi: 10.1186/s13046-021-02188-y

21. Wolf CL, Pruett C, Lighter D, Jorcyk CL. The clinical relevance of OSM in inflammatory diseases: a comprehensive review. *Front Immunol*. (2023) 14:1239732. doi: 10.3389/fimmu.2023.1239732

22. Lev S, Gottesman T, Sahaf Levin G, Lederfein D, Berkov E, Diker D, et al. Observational cohort study of IP-10's potential as a biomarker to aid in inflammation regulation within a clinical decision support protocol for patients with severe COVID-19. *PloS One*. (2021) 16:e0245296. doi: 10.1371/journal.pone.0245296

23. Nishimoto-Kakiuchi A, Sato I, Nakano K, Ohmori H, Kayukawa Y, Tanimura H, et al. A long-acting anti-IL-8 antibody improves inflammation and fibrosis in endometriosis. *Sci Trans Med*. (2023) 15:eabq5858. doi: 10.1126/scitranslmed.abq5858

24. Raucci F, Iqbal AJ, Saviano A, Minosi P, Piccolo M, Irace C, et al. IL-17A neutralizing antibody regulates monosodium urate crystal-induced gouty inflammation. *Pharmacol Res*. (2019) 147:104351. doi: 10.1016/j.phrs.2019.104351

25. Sun X, Yang L, Sun H, Sun Y, Wei S, Han Y, et al. TCM and related active compounds in the treatment of gout: the regulation of signaling pathway and urate transporter. *Front Pharmacol*. (2023) 14:1275974. doi: 10.3389/fphar.2023.1275974

26. Yu L, Liu P. Cytosolic DNA sensing by cGAS: regulation, function, and human diseases. *Signal Transduction Targeted Ther*. (2021) 6:170. doi: 10.1038/s41392-021-00554-y

27. Basta G, Schmidt AM, De Caterina R. Advanced glycation end products and vascular inflammation: implications for accelerated atherosclerosis in diabetes. *Cardiovasc Res*. (2004) 63:582–92. doi: 10.1016/j.cardiores.2004.05.001

28. Taams LS. Interleukin-17 in rheumatoid arthritis: Trials and tribulations. *J Exp Med*. (2020) 217. doi: 10.1084/jem.20192048

Frontiers in Immunology

Explores novel approaches and diagnoses to treat immune disorders.

The official journal of the International Union of Immunological Societies (IUIS) and the most cited in its field, leading the way for research across basic, translational and clinical immunology.

Discover the latest Research Topics

See more →

Frontiers

Avenue du Tribunal-Fédéral 34
1005 Lausanne, Switzerland
frontiersin.org

Contact us

+41 (0)21 510 17 00
frontiersin.org/about/contact